Paper I

ChemPubSoc Europe

DOI: 10.1002/chem.201503552

CHEMISTRY A European Journal Full Paper

Kinases

# Addressing the Glycine-Rich Loop of Protein Kinases by a Multi-Facetted Interaction Network: Inhibition of PKA and a PKB Mimic

Birgit S. Lauber,[a] Leo A. Hardegger,[a] Alam K. Asraful,[b] Bjarte A. Lund,[b] Oliver Dumele,[a] Michael Harder,[a] Bernd Kuhn,[c] Richard A. Engh,*[b] and François Diederich*[a]

*Dedicated to Professor Donald Hilvert on the occasion of his 60th birthday*

**Abstract:** Protein kinases continue to be hot targets in drug discovery research, as they are involved in many essential cellular processes and their deregulation can lead to a variety of diseases. A series of 32 enantiomerically pure inhibitors was synthesized and tested towards protein kinase A (PKA) and protein kinase B mimic PKAB3 (PKA triple mutant). The ligands bind to the hinge region, ribose pocket, and glycine-rich loop at the ATP site. Biological assays showed high potency against PKA, with $K_i$ values in the low nanomolar range. The investigation demonstrates the significance of targeting the often neglected glycine-rich loop for gaining high binding potency. X-ray co-crystal structures revealed a multi-facetted network of ligand–loop interactions for the tightest binders, involving orthogonal dipolar contacts, sulfur and other dispersive contacts, amide–$\pi$ stacking, and H-bonding to organofluorine, besides efficient water replacement. The network was analyzed in a computational approach.

## Introduction

Protein kinases, with their function to phosphorylate other proteins as a core mechanism of cellular signal transduction, constitute one of the most important enzyme classes. The "prototype" for the class, protein kinase A (PKA), was first described in 1968 by Krebs and co-workers as a mediator for the second messenger cyclic adenosine monophosphate (cAMP).[1] Because its phosphotransferase activity occurs after dissociation into a single and constitutively active catalytic domain, PKA is well suited as the prototype for mechanistic studies of protein kinases. Its kinetic properties and the crystal structure of its apoenzyme provided detailed insight into the signaling pathway, including the activation and deactivation mechanisms and the constitution of the active site.[2–5] These data have proven invaluable for understanding the mechanisms of the other protein kinases in the human genome, numbering more than 500 when considering sequence alone, making up approximately 2% of human genes.[6]

The large number of kinases, a high degree of sequence conservation, and the competition with millimolar concentrations of adenosine triphosphate (ATP) in cells make the kinases challenging targets in drug discovery. However, HA1077 (Fasudil) was approved as a ROCK1 inhibitor in Japan in 1995, and imatinib (Glivec or Gleevec) was approved as an ABL kinase inhibitor in 2001, initiating an era of rapidly growing investment into pharmaceutical research, now with some 30 drugs on the market.[7]

Among the protein kinase signaling proteins and drug targets, protein kinase B (PKB, also known as Akt) has a central role in regulatory pathways, including cell survival, metabolism, motility, transcription, and cell-cycle progression. It is a downstream target in the phosphoinositide (PI) 3-kinase signaling pathway, and it has been shown that cells with dysregulated PKB-production, for example, knockout or over-expression, may cause cardiac or skeletal muscle hypertrophy, tumors, and a disordered insulin secretory pathway.[8–11] This highly conserved enzyme belongs to the AGC subfamily (together with PKA and several other subgroups) and consists of three isoforms, PKB$\alpha$, PKB$\beta$, and PKB$\gamma$ (Akt1, Akt2, and Akt3, respectively). The three isoforms are encoded by distinct genes but share a highly conserved structure across species. The architecture of the kinases consists of three functional domains, a C-terminal regulatory domain with the hydrophobic motive (HM), the N-terminal pleckstrin-homology domain (PH), and a central kinase domain.

As mentioned above, PKA is one of the best studied kinases and is closely related to PKB, sharing a sequence identity of

[a] Dr. B. S. Lauber, Dr. L. A. Hardegger, O. Dumele, Dr. M. Harder, Prof. Dr. F. Diederich
Laboratorium für Organische Chemie, ETH Zürich
Vladimir-Prelog-Weg 3, 8093 Zürich (Switzerland)
Fax: (+41) 44-632-11-09
E-mail: diederich@org.chem.ethz.ch

[b] A. K. Asraful, B. A. Lund, Prof. Dr. R. A. Engh
Department of Chemistry, University of Tromsø
Forskningsparken 3, Sykehusvegen 23, 9037 Tromsø (Norway)
E-mail: richard.engh@uit.no

[c] Dr. B. Kuhn
Small Molecule Research, Roche Innovation Center Basel
F. Hoffmann-La Roche, Grenzacherstrasse 124, 4070 Basel (Switzerland)

Supporting information for this article is available on the WWW under http://dx.doi.org/10.1002/chem.201503552.

45% in the catalytic domain, rising up to 80% in the active pocket.[12] Although they share high sequence similarity in their catalytic domains, PKA and PKB are involved in different signaling pathways, making their feasibility as drug targets dependent on the ability to achieve selectivity for their inhibition.

At the ATP binding sites of PKA (PKA$\alpha$) and PKB (PKB$\alpha$/PKB$\gamma$), as few as three amino acids need to be mutated in one kinase to mimic the binding pocket of the other.[13] In the PKA triple mutant enzyme PKAB3 used herein, two mutations mimic the parent active pocket of the enzyme PKB (V123A and L173M). A third mutation (Q181K) is required to prevent a rotamer conformation of Q181, enabled by the V123A mutation, that can occlude the ATP site.[13] A fourth site of possible mutation, V104T, may play a role especially for polar interaction networks that are not the focus of this work. It has been shown by Engh and co-workers that PKAB3 works as a PKB surrogate, features similar enzyme kinetics, and is generally more suitable for enzyme crystallization than PKB.[13] Further, comparative studies of ligand–enzyme interactions using point mutants allow increased focus on the effects of individual interactions, removing spurious indirect effects from enzyme differences elsewhere.

Herein, we report the structure-based design and synthesis of a series of ligands for inhibition of PKA and PKAB3 and the subsequent in vitro evaluation. We present a series of novel PKA/PKAB3 selective inhibitors and an SAR analysis of their binding to the glycine-rich loop supported by several X-ray co-crystal structures. This motif, with the general sequence GxGxxG, is adjacent to the phosphate groups of bound ATP and also forms a hydrophobic "lid" over the adenine ring of ATP and the typically heteroaromatic moieties of inhibitors binding to the protein kinase hinge. This fact and the slightly different sequence highlights the significant difference to the so called Walker-motif (GxxxxGKT/S) of ATP binding proteins.[14,15]

We aimed primarily to synthesize highly potent, low-molecular-weight inhibitors and evaluate their binding mode and in particular their interactions with the glycine-rich loop. In contrast to the hinge region, the adenine pocket with the gatekeeper residues, the ribose pocket, the DFG (Asp-Phe-Gly) loop, and apolar back pockets, the glycine-rich loop has largely not been addressed in protein kinase inhibitor design. The experimental $K_i$ values, the SAR analysis, and several X-ray analyses have been used to obtain structural information to explain new potent binding motifs to the glycine-rich loop involving a highly diverse set of weak intermolecular interactions. To complete the analysis, a computational treatment of the cooperative interaction network was performed, revealing multiple interactions and hotspot atoms.

## Results and Discussion

### Inhibitor Design

Molecular modeling was performed with the program MOLOC[16] using the MAB force field. The X-ray co-crystal structure of PKAB3 (PDB ID: 2uw0)[17] was used with the ligand removed for modeling and the enzyme kept rigid during energy minimization. We designed ligands based on a potential gain of selectivity for PKB over PKA and to investigate the ligand-binding properties of the glycine-rich loop. Our initial design targeted the L173M substitution, which was hoped to deliver selectivity of PKB over PKA through sulfur–aromatic interactions (Figure 1).[18]

The design of the new inhibitors followed the binding mode of ATP in the hinge region, with two hydrogen bonds formed between the quinazolinone (as an adenine substitute) and the backbone NH of Ala123 and the backbone C=O of Glu121 (Figure 1a). In PKAB3, the quinazolinone ring was expected to be sandwiched between the side chains of Val57 and Met173, engaging in sulfur–aromatic interactions at optimal distances of 3.4–3.8 Å (Figure 1b).[18]

The ribose pocket was addressed with a protonated pyrrolidine ring, which was hoped to engage in ionic hydrogen bonds to Glu127 and the backbone carbonyl of Glu170 (Figure 1c). The glycine-rich loop was targeted by incorporating different halogenated benzoyl or carbothienyl substituents, as shown for ligand (+)-**1i** in Figure 1c (see Table 1 for all ligands **1a**–**p**). The organohalogens should interact with the glycine-rich loop by orthogonal dipolar C–X···C=O interactions.[19,20] According to the modeling studies, only the (3*R*,4*S*)-enantiomer was expected to strongly bind into the active pockets of PKA and PKAB3.

**Table 1.** $K_i$ values [nM] of quinazolinone-based inhibitors determined by the multi-component spectrophotometric Cook assay. The reported values are the average of three repeated measurements. Inhibitor (+)-**1e** decomposed over time and is marked with *. n.a: $K_i$ value over 2000 nM and/or inhibition did not show a characteristic inhibition curve. clog*D* and clog*P* values were calculated with the ACD Labs program[a] at pH 7.4.

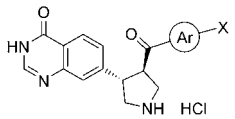


| | Ar | X | clog*P* | clog*D* | $K_i$(PKA) [nM] (+) | (−) | $K_i$(PKAB3) [nM] (+) | (−) |
|---|---|---|---|---|---|---|---|---|
| **1a** | Ph | H | 0.98 | −0.43 | 30 | n.a | 70 | n.a |
| **1b** | Ph | 3-F | 1.22 | −0.02 | 10 | 1600 | 80 | 400 |
| **1c** | Ph | 3-Cl | 1.67 | 0.04 | 300 | 200 | 1500 | 500 |
| **1d** | Ph | 3-Br | 1.77 | 0.55 | 80 | 1800 | n.a | n.a |
| **1e*** | Ph | 3-I | 2.17 | 0.95 | 80 | 200 | 740 | 400 |
| **1f** | Ph | 3-$CF_3$ | 1.83 | 0.46 | 200 | 200 | n.a | n.a |
| **1g** | Ph | 3-$OCF_3$ | 2.33 | 1.14 | 400 | 500 | n.a | n.a |
| **1h** | Ph | 4-F | 1.46 | 0.23 | 70 | n.a | 50 | 1200 |
| **1i** | Ph | 4-Cl | 1.73 | 0.54 | 3 | 400 | 70 | 1300 |
| **1j** | Ph | 4-Br | 1.73 | 0.54 | 3 | 600 | 20 | 1900 |
| **1k** | Ph | 4-I | 2.20 | 1.00 | 5 | 700 | 20 | n.a |
| **1l** | Ph | 4-$CF_3$ | 1.91 | 0.67 | 2 | 400 | 80 | n.a |
| **1m** | Ph | 4-$OCF_3$ | 2.20 | 1.02 | 12 | 1100 | 370 | n.a |
| **1n** | 2-thienyl | H | 0.74 | −0.5 | 170 | n.a | 1600 | 1600 |
| **1o** | 2-thienyl | 5-Cl | 1.60 | 0.44 | 23 | n.a | 80 | 1500 |
| **1p** | 2-thienyl | 5-Br | 1.77 | 0.62 | 0.9 | 500 | 40 | 1000 |

[a] ACD/Structure Elucidator, Version 15.01, Advanced Chemistry Development, Inc., Toronto, ON, Canada, www.acdlabs.com, **2015**.

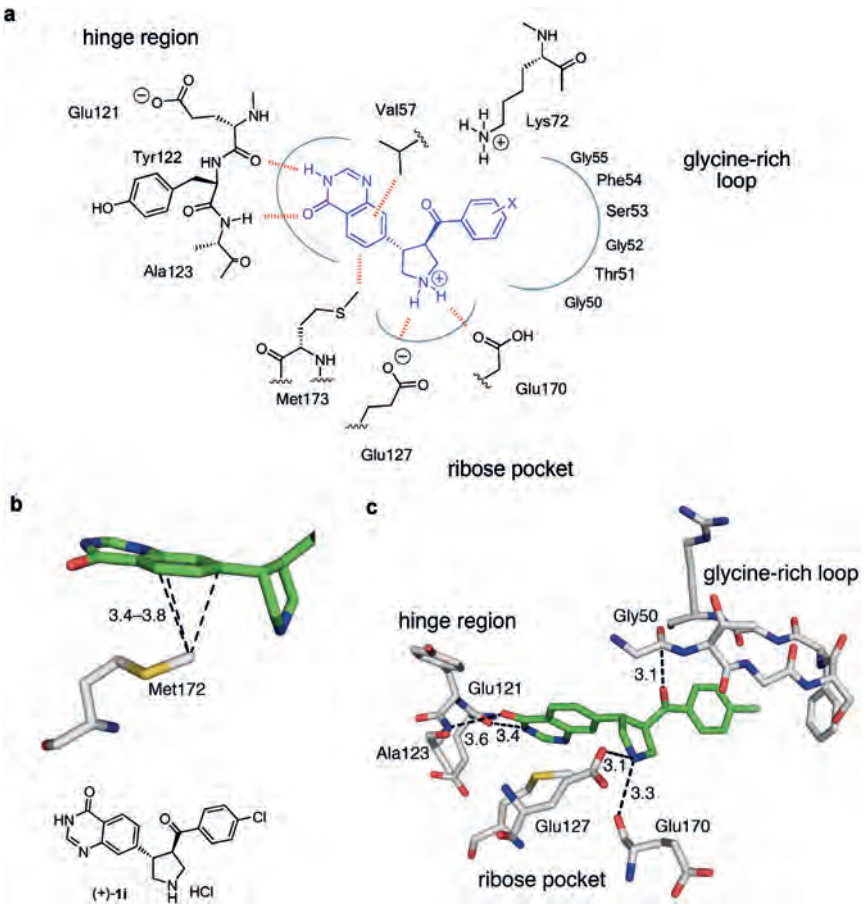


**Figure 1.** Design of inhibitors for the triple mutant PKAB3. a) Schematic representation of the active site of PKAB3. Inhibitor (+)-**1** (blue) is shown in the binding mode proposed by MOLOC.[16] Favorable interactions are highlighted with red dashed lines. The orthogonal C=O···C=O interaction to Gly50 is omitted for clarity. b) Close-up view of the targeted sulfur–aromatic interactions between Met173 and the quinazolinone moiety of the ligand. c) Proposed binding mode of ligand (+)-**1i** to PKAB3 (2.00 Å resolution, PDB ID: 2uw0) as predicted by MOLOC. The expected orthogonal C=O···C=O interaction to Gly50 is shown. Pictures generated using PyMOL (The PyMOL Molecular Graphics System, Version 1.7.4 Schrödinger, LLC). Distances are given in Å, and interactions are shown as dashed lines. Color code: $C_{enzyme}$ gray, $C_{ligand}$ green, N blue, O red, S yellow, Cl limon.

## Synthesis

The synthetic route is based on a Horner–Wadsworth–Emmons reaction to generate activated (*E*)-olefins, followed by a 1,3-dipolar cycloaddition with azomethine ylides to afford the central pyrrolidine ring. The synthesis of protected, 3,4-disubstituted pyrrolidines by a similar route had been reported previously,[21] however the protocol had to be altered so that unprotected variants could be accessed instead.[22] Furthermore, as only the 3*R*,4*S*-enantiomer was expected to be active according to the modeling, conditions for HPLC enantiomer separation by HPLC on a chiral stationary phase had to be identified.

In this route, esters **2a**–**p** which were either commercially available or produced from their corresponding acids (**3b**/**c**/**d**/**i**/**h**/**m**) following well-established procedures,[23] were transformed to β-ketophosphonates **4a**–**p** with diethyl methylphosphonate at −78 °C in good yields (Scheme 1).

Aldehyde **5** was synthesized starting from 2-aminoterephthalate **6** in a cyclization reaction to afford quinazolinone **7**, which was converted to the Me-protected quinazolinone **8** *via* its chlorinated intermediate in two steps (Scheme 2). Reduction with $LiAlH_4$ to **9**, followed by oxidation with PCC, yielded aldehyde **5**.[24]

β-Ketophosphonates **4a**–**p** were coupled to aldehyde **5** to afford alkenes **10a**–**p** in moderate to good yields with (*E*/*Z*) ratios between 97:3 and 83:17.[25,26] The use of KO*t*Bu instead of NaH as base led to increased (*E*) selectivities.[21] Purification by HPLC afforded diastereoisomerically pure products, but upon concentration, the alkenes showed limited stability as indicated by LCMS chromatography and $^1$H NMR spectroscopy.

In a first step, the reaction conditions for the 1,3-dipolar cycloaddition with azomethine ylides generated from glycine and *para*-formaldehyde to afford unprotected pyrrolidines were optimized. The protocol for the synthesis of protected pyrrolidines (Bn or Me protecting groups) is well-established,[21] but there is only one example present in the literature in which 3,4-disubstituted unprotected pyrrolidines were obtained through a 1,3-dipolar cycloaddition.[22] Trapping of the water formed in the course of the reaction was crucial for the formation of the unprotected pyrrolidines. For this purpose, a layer of $MgSO_4$ or $Na_2SO_4$ was installed on top of the flask containing the reaction mixture at reflux. Yields for this key

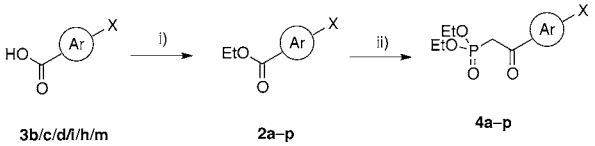


| compound | Ar | X |
|---|---|---|
| **a** | Ph | H |
| **b** | Ph | 3-F |
| **c** | Ph | 3-Cl |
| **d** | Ph | 3-Br |
| **e** | Ph | 3-I |
| **f** | Ph | 3-$CF_3$ |
| **g** | Ph | 3-$OCF_3$ |
| **h** | Ph | 4-F |
| **i** | Ph | 4-Cl |
| **j** | Ph | 4-Br |
| **k** | Ph | 4-I |
| **l** | Ph | 4-$CF_3$ |
| **m** | Ph | 4-$OCF_3$ |
| **n** | 2-$C_4H_2S$ | H |
| **o** | 2-$C_4H_2S$ | 5-Cl |
| **p** | 2-$C_4H_2S$ | 5-Br |

**Scheme 1.** Synthesis of β-ketophosphonates **4a–p**. i) $H_2SO_4$, EtOH, 80 °C, 4–30 h, quant.; ii) diethyl methylphosphonate, *n*BuLi, THF, −78 to 22 °C, 1.5–6 h, 62–100%.

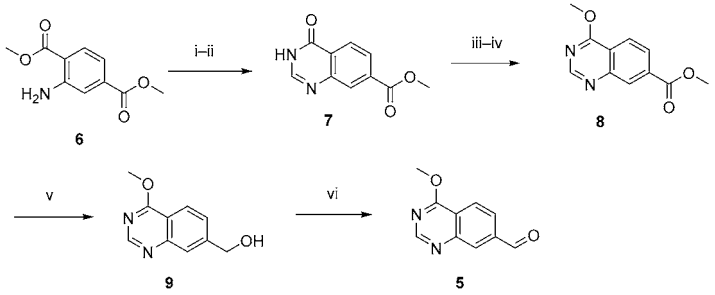


**Scheme 2.** Synthesis of aldehyde **5**. i) $H_4NHCO_2$, $HCO_2H$, 100 °C, 19 h, 63%; ii) $NH_4HCO_2$, formamide, 140 °C, 7 h, 51%; iii) $POCl_3$, DBU, toluene, 120 °C, 2.5 h; iv) NaOMe, 0 to 22 °C, 1 h, 42%; v) $LiAlH_4$, THF, 0 to 22 °C, 2 h; vi) PCC, $CH_2Cl_2$, 0 °C, 2 h, 75%. DBU = 1,8-diazabicyclo[5.4.0]undec-7-ene; PCC = pyridinium chlorochromate.

step ranged from low to moderate (14–45%), most probably due to the decreased stability of the olefins. In contrast, by employing the same reaction conditions, *para*-formaldehyde, glycine, and the dipolarophile *trans*-chalcone (1,3-diphenylprop-2-en-one; **11**) afforded, after Boc-protection, the corresponding pyrrolidine (**12**) in 83% yield over two steps (for the structures of **11** and **12**, see the Supporting Information, Scheme S1).

The olefins **10a–p** were directly subjected to cyclization reactions with *para*-formaldehyde and glycine to afford the corresponding pyrrolidines, which were subsequently *N*-protected ($Boc_2O$) to afford the respective carbamates (±)-**13a–p** in moderate overall yields (Scheme 3). The *tert*-butylcarbamate group greatly facilitated the optical resolution of (±)-**13a–p** by chiral HPLC to obtain (+)-**13a–p** and (−)-**13a–p**, respectively, in enantiomerically pure form. Removal of the protecting group by treatment with 2 M aq. HCl in THF afforded the target compounds (+)-**1a–p** and (−)-**1a–p** which were isolated as HCl salts.[27] The absolute configuration of (+)-**1c** was assigned by modeling the optical rotatory dispersion (ORD) of (3*S*,4*R*)-(+)-**1c**, employing density functional theory methods. The calculated $[\alpha]_D$ value of +47.7° for chlorine derivative (+)-**1c** in the four lowest-energy conformations is in acceptable agreement with the measured $[\alpha]_D^{20}$ of +77.5° ($c = 0.1$ in MeOH) (see the Supporting Information, Section S2.1).[28] Ultimate proof of the absolute configurations of (+)-**1b,c,e,l,p** was later obtained by the X-ray co-crystal structures of these inhibitors with PKA.

### Biological affinities and X-ray co-crystal structures

Both enantiomers of ligands **1a–p** were evaluated for their in vitro affinities against PKA and PKAB3 *via* the activity-based ATP-regenerative NADH (nicotinamide adenine dinucleotide)-consuming Cook-assay (for details see the Supporting Information, Section S4).[29] Assay interference tests were done to exclude any undesired interactions of the inhibitors. Neither adding ADP instead of ATP to mimic the effects of ADP production by the protein kinase, with and without inhibitor, or measuring the production of ADP by spontaneous hydrolysis of ATP (with and without inhibitor) showed any side effects.

The velocity was measured at different inhibitor concentrations, allowing the determination of $K_i$ values for the different ligands. Using the Cheng–Prusoff equation with the known $K_M$ values of ATP, the $K_i$ values were obtained as summarized in Table 1. Herein, we focus on the $K_i$ values of the (+)-**1a–p** enantiomers, as they were significantly more active, strongly supporting our modeling studies.

The majority of the optically pure inhibitors displayed nanomolar affinity ($K_i$ values) against PKA, while being significantly less active against PKAB3 (Table 1). We obtained X-ray co-crystal structures of inhibitors (+)-**1b,c,e,l,p** with PKA and two structures of (+)-**1c,p** with PKAB3. All X-ray co-crystal structures with PKA were loaded to the PDB database ((+)-**1b** (PDB ID: 4UJB, 1.95 Å), (+)-**1c** (PDB ID: 4UJ1, 1.76 Å), (+)-**1e** (PDB ID: 4UJ2, 2.02 Å), (+)-**1l** (PDB ID: 4UJ9, 1.87 Å) and (+)-**1p** (PDB ID: 4UJA, 1.95 Å)), as well as with PKAB3 ((+)-**1c** (PDB ID: 4Z84, 1.55 Å), (+)-**1p** (PDB ID: 4Z83, 1.80 Å)). In addition to the observed biological affinities, they form the basis of our analysis and are discussed below.

### Binding mode

All bound inhibitors observed in the X-ray co-crystal structures of PKA superimpose well, and adopt a similar binding mode

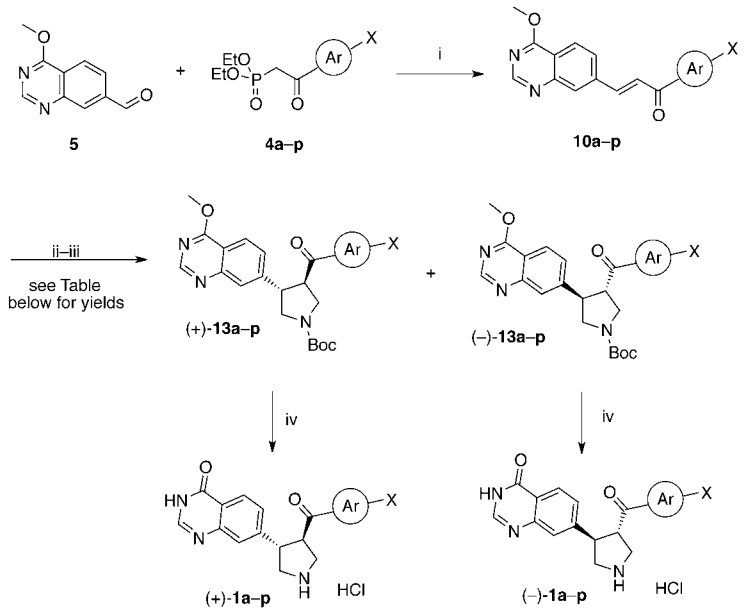


| compound | Ar | X | Yield [%] for pyrrolidine synthesis (+) / (–) |
|---|---|---|---|
| **a** | Ph | H | 7 / 7 |
| **b** | Ph | 3-F | 10 / 10 |
| **c** | Ph | 3-Cl | 8 / 8 |
| **d** | Ph | 3-Br | 7 / 7 |
| **e** | Ph | 3-I | 11 / 10 |
| **f** | Ph | 3-$CF_3$ | 7 / 7 |
| **g** | Ph | 3-$OCF_3$ | 7 / 10 |
| **h** | Ph | 4-F | 25 / 20 |
| **i** | Ph | 4-Cl | 21 / 21 |
| **j** | Ph | 4-Br | 19 / 20 |
| **k** | Ph | 4-I | 23 / 23 |
| **l** | Ph | 4-$CF_3$ | 8 / 9 |
| **m** | Ph | 4-$OCF_3$ | 9 / 13 |
| **n** | 2-$C_4H_2S$ | H | 10 / 10 |
| **o** | 2-$C_4H_2S$ | 5-Cl | 17 / 17 |
| **p** | 2-$C_4H_2S$ | 5-Br | 7 / 7 |

**Scheme 3.** 1,3-Dipolar cycloaddition to pyrrolidines **1a–p**. i) NaH or *t*BuOK, THF, 0 to 22 °C, 5–29 h, 50–100 %; ii) $(H_2CO)_n$, glycine, toluene, 120 °C, 1–4 h; iii) $Boc_2O$, MeOH, 0 to 22 °C, 1.5–24 h, chiral HPLC, 14–45 %; iv) 2 M aq. HCl, THF, 0 to 22 °C, 1–2 d, 15–98 %. Boc = *tert*-butyloxycarbonyl.

within the hinge region and in the ribose pocket, in good agreement with the modeling predictions. Their phenyl/thienyl vectors reach into the glycine-rich loop region (Figure 2a). In the X-ray co-crystal structure of (+)-**1b** bound to PKA (Figure 2b), the fluorinated inhibitor is anchored with two hydrogen bonds to the hinge region ($d(N_{ligand}\cdots O_{Glu121})$ = 2.6 Å, $d(O_{ligand}\cdots N_{Val123})$ = 3.2 Å) and by an additional hydrogen bond to the gatekeeper residue Thr183 ($d(N_{ligand}\cdots O_{Thr183})$ = 2.8 Å). The flat quinazolinone moiety is intercalated between the hydrophobic side chains of Ala70 and Val57 on one side and Leu173 on the other, at distances ranging from 3.2 to 4.2 Å. The central, most probably protonated pyrrolidinium ring is perfectly orientated to reach into the ribose pocket where it forms an ionic hydrogen bond to the backbone C=O of Glu170 ($d(N_{ligand}\cdots O_{Glu170})$ = 3.0 Å) and a salt-bridge-type hydrogen bond to the side chain of Asp184 ($d(N_{ligand}\cdots O_{Asp184})$ = 2.7 Å) (Figure 2c). Additional longer contacts exist between the pyrrolidinium N-atom and the side chains of Glu127 and Asn171. An orthogonal dipolar C=O···C=O interaction of the benzoyl C=O group of the inhibitor to the C=O of Gly50, at a distance of 3.0 Å and an angle C···C=O of 96° (Figure 2b) completes the interaction pattern observed in all X-ray co-crystal structures which guides the different aromatic substituents into the glycine-rich loop. Similar interactions and a nearly identical alignment of the quinazolinone-pyrrolidine moiety in all inhibitor series allowed a comparison of the PKA and PKAB3 binding modes and a comprehensive SAR analysis of the interactions with the glycine-rich loop.

## Selectivity of the inhibitors

The tested inhibitors were more active against PKA than PKAB3 (Table 1). Comparison between two X-ray co-crystal structures of the thienyl inhibitor (+)-**1p** with PKA and PKAB3,

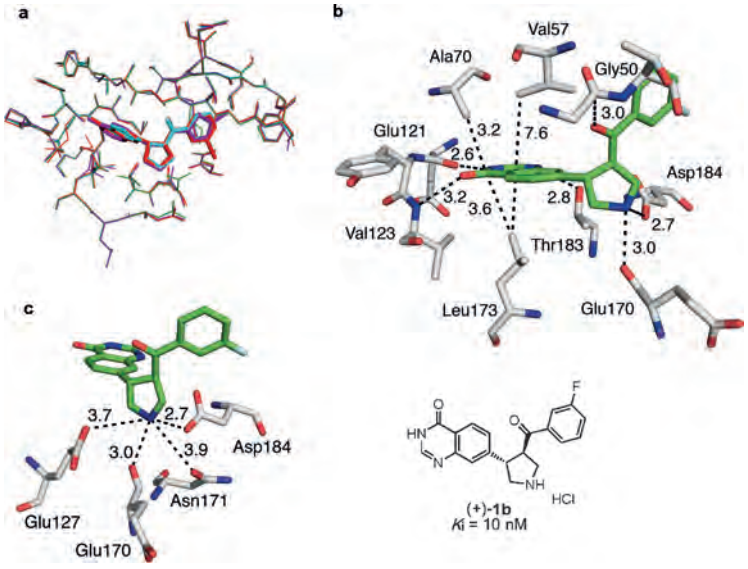


**Figure 2.** a) Overlay of the X-ray co-crystal structures of inhibitors (+)-**1b** (1.95 Å resolution, PDB ID: 4UJB), (+)-**1e** (2.02 Å resolution, PDB ID: 4UJ2), (+)-**1l** (1.87 Å resolution, PDB ID: 4UJ9), and (+)-**1p** (1.93 Å resolution, PDB ID: 4UJA) bound to PKA. Color code: $(\mathbf{1b})_{ligand/enzyme}$ red, $(\mathbf{1e})_{ligand/enzyme}$ blue, $(\mathbf{1l})_{ligand/enzyme}$ green, $(\mathbf{1p})_{ligand/enzyme}$ magenta. The four inhibitors show a nearly identical binding mode to the active site of PKA. b) Binding mode of inhibitor (+)-**1b**. c) Detailed view of the binding mode in the ribose pocket. Distances are given in Å and interactions are shown as dashed lines. Color code: $C_{enzyme}$ gray, $C_{ligand}$ green, N blue, O red, S yellow, F light blue.

respectively, reveals the origin of this difference in binding affinity. Modeling with MOLOC had predicted that the ligand (magenta in Figure 3) undergoes a salt-bridge-type hydrogen bond to the carboxylate side chain of Glu127 ($d$(N···O) = 2.9 Å). In the X-ray co-crystal structures (Figure 3, green ligand in PKA and blue ligand in PKAB3 shown with the protein environment of PKAB3), the pyrrolidine ring of the inhibitor reaches deeper into the ribose pocket to form an ionic hydrogen bond with the backbone C=O of Glu170 ($d$(N···O) = 2.8 Å (PKAB3) and 2.9 Å (PKA)) and a salt bridge with Asp184 ($d$(N···O) = 2.7 Å (PKAB3) and 2.5 Å (PKA)). As a consequence, the methyl group of Met173 in PKAB3 is forced to an outwards orientation in an energetically less favored gauche conformation. In the inward, *anti* orientation (see Figure 1b) a steric clash with the C-atom $\alpha$ to the pyrrolidine ring N-atom would occur, at a modeled, strongly repulsive distance of $d(H_3C_{Met173}\cdots C(2)_{pyrrolidine}) = 2.3$ Å. As a result of this conformational flip, Met173 in PKAB3 interacts less favorably with the quinazolinone ring of the inhibitor. The deeper positioning of the pyrrolidine ring in the ribose pocket, on the other hand, does not affect the favorable location of the shorter Leu173 side chain in PKA. The outward gauche conformation of Met173 was found in both X-ray co-crystal structures obtained for PKAB3 with inhibitor (+)-**1c** and (+)-**1p**. Overall, the flip of the methionine side chain to a less favorable conformation, together with the reduced interactions with the quinazolinone ring, might contribute to the lower affinity of the inhibitors towards PKAB3.

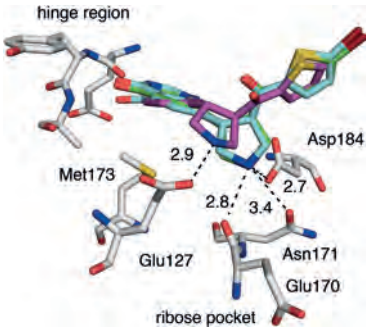


**Figure 3.** Overlay of inhibitor (+)-**1p** modeled in PKAB3 (PDB ID: 2uw0; magenta) and in the X-ray co-crystal structures of (+)-**1p** bound to PKA (green, 1.93 Å resolution, PDB ID: 4UJA) and PKAB3 (blue, 1.80 Å resolution, PDB ID: 4Z83). The protein surrounding shown is PKAB3 (PDB ID: 4Z83). Distances for inhibitor (+)-**1p** bound to PKAB3 (PDB ID: 4Z83) and the modeled inhibitor are given in Å, and interactions are shown as dashed lines. Color code: $C_{enzyme}$ gray, $C_{ligand,X-ray}$ green and blue, $C_{ligand,\ modeled}$ magenta, N blue, O red, S yellow, Br dark red.

## SAR analysis

With a plausible explanation for the differences in selectivity, the inhibitors were analyzed for their binding with PKA. As they all display the same binding pattern, a meaningful comparative analysis of their contacts with the glycine-rich loop became possible. The following discussion proceeds from the weaker ligands with a *meta*-substituted phenyl ring, to the stronger ligands with *para*-substituted phenyl rings, and to the thienyl derivatives.

## Interactions of *meta*-substituted phenyl rings with the glycine-rich loop

The *meta*-substituted inhibitors are generally less active than their *para*-substituted analogues and do not possess as many favorable interactions with the glycine-rich loop (Figure 4). X-ray co-crystal structures of inhibitors (+)-**1b**, (+)-**1c**, and even (+)-**1e** with PKA were obtained. The iodide derivative (+)-**1e** slowly decomposes at ambient conditions, leading to unreliable $K_i$ values; yet an X-ray co-crystal structure could be solved.

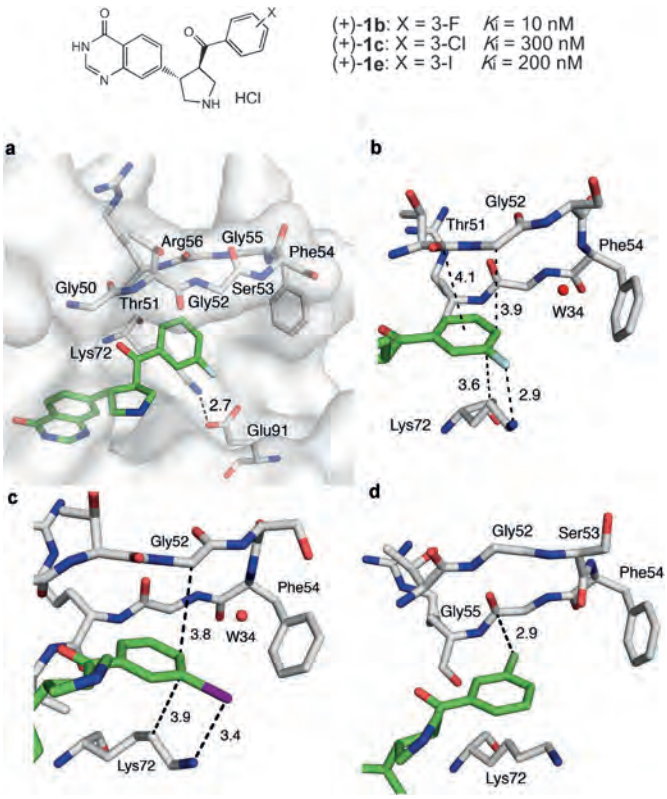


**Figure 4.** X-ray co-crystal structures of *meta*-aryl-substituted inhibitors (+)-**1b** (1.95 Å resolution, PDB ID: 4UJB), (+)-**1c** (1.76 Å resolution, PDB ID: 4UJ1) and (+)-**1e** (2.02 Å resolution, PDB ID: 4UJ2) bound to PKA. a) Surface (grey) of the active site with bound fluorinated inhibitor (+)-**1b**. b) Closer look into the interactions of the fluorophenyl ring with the glycine-rich loop. c) Binding mode of iodo-substituted inhibitor (+)-**1e** in the glycine-rich loop region. d) Interactions of chloro-substituted inhibitor (+)-**1c** with the glycine-rich loop, with the ligand-induced flip of the peptide bond Ser53-Phe54. Distances are given in Å, and interactions are shown as dashed lines. Color code: $C_{enzyme}$ gray, O red, N blue, $C_{ligand}$ green, F light blue, I violet, Cl limon. Water molecules are shown as red spheres.

Remarkably, all substituents in *meta*-position, with the exception of fluorine in (+)-**1b**, reduce binding affinity with respect to the unsubstituted phenyl derivative (+)-**1a** (Table 1). The glycine-rich loop is rather open on the side approached by the aromatic ring (Figure 4a), and the *meta*-substituents can orient in different ways. The halogenated aromatic ring of (+)-**1b** and (+)-**1c** is sandwiched between the peptide bond Thr51–Gly52 of the loop and the hydrophobic side chain of

Lys72, which occupies a conserved position in all co-crystal structures due to a salt bridge with the side chain of Glu91 (Figure 4a, $d$(N···O) = 2.7 Å). The organofluorine in (+)-**1b** favorably interacts with the $NH_3^+$ terminus of Lys72 at a distance $d$(F···N) of 2.9 Å (Figure 4b). A similar interaction is also seen for organoiodine in (+)-**1e** ($d$(I···N) of 3.4 Å, Figure 4c); however, due to the reduced polarization of the C–I bond, as compared to C–F, a gain in ligand binding strength is not observed. The organochlorine in (+)-**1c** takes a different orientation, pointing inwards towards Gly55 to engage in an orthogonal dipolar interaction ($d$(Cl···C=$O_{Gly55}$) = 2.9 Å, $\alpha$(Cl···C=$O_{Gly55}$) = 92°), however without identifiable gain in binding strength. This orientation of the chlorine apparently disturbs the geometry of the loop as seen by a complete flip of the peptide bond between Ser53 and Phe54 (Figure 4d). Stacking interactions of the chlorophenyl ring with the loop are nearly eliminated, which presumably explains the lowest binding affinity in the *meta*-halophenyl series.

A high degree of solvation is observed in the X-ray co-crystal structures. Particularly one water molecule (W34, Figure 4b and c), located on the aromatic face of Phe54 in the structures of fluoride (+)-**1b** (Figure 4b) and iodide (+)-**1e** (Figure 4c), needs to be considered in the energetics of protein–ligand binding (see below). Its major interaction with the protein is a short H-bond ($d$(O···N) = 2.7 Å) to the backbone N–H of Phe54; additionally O–H···π H-bonding to the phenyl ring of Phe54 may be assumed. It further interacts with one water molecule in a larger water cluster. Compared to bulk water, the solvation of W34 is clearly reduced, and therefore, it can be most probably considered as enthalpically strained.[20,30]

### Interactions of *para*-substituted phenyl rings with the glycine-rich loop

The binding affinities of the *para*-substituted inhibitors, except fluorine derivative (+)-**1h**, are greatly increased, by up to an order of magnitude in $K_i$ value, with respect to the unsubstituted phenyl derivative **1a**. The co-crystal structure of (+)-**1l** bound to PKA ($K_i$ = 2 nM) was solved and revealed an extended interaction network[31] between the *para*-$F_3$C-phenyl ring and the loop. An obvious first advantage of the *para*-series, compared to the *meta*-series, is the absence of different conformations of the substituted ring, which again is sandwiched between the loop ($d$($C_{Phe}$···$C_{Thr51}$) = 3.9 Å) and the side chain of Lys72 ($d$($C_{Phe}$···$C_{Lys72}$) = 4.2 Å). The total spacing in the sandwich (8.1 Å) is somewhat larger than needed for the intercalation of an aromatic ring (6.8–7.2 Å), which is favorable to minimize binding-induced losses in conformational entropy ("wiggling") of the phenyl substituent and the flexible loop (see Figure S1 in the Supporting Information).

The $CF_3$ substituent displaces the previously mentioned water molecule W34 into the bulk solvent (Figure 5a). The favorable energetics of this water replacement contribute to the difference between the $K_i$ value of the *para*-fluoro-inhibitor (+)-**1h** (70 nM) and those of (+)-**1i**–**l** (2–3 nM) with bulkier substituents (Table 1). Most probably, the F-atom is too small, as compared to the larger substituents, to efficiently displace W34; additionally for steric reasons, it can geometrically engage less well in attractive interactions with the loop.

The interactions of the $F_3$C-phenyl ring of (+)-**1l** with the loop are indeed extensive (Figure 5b). Besides the mentioned sandwiching of the phenyl ring, which involves the parallel-slipped stacking of the ring with the peptide bond Thr51-Gly52,[32] the $CF_3$ substituent engages in multiple favorable contacts. The complete set of interactions is shown in the Supporting Information, Figure S2. The $CF_3$ group undergoes three orthogonal dipolar C–F···C=O interactions with the loop backbone,[33] to the backbone C=O of Gly55 ($d$(F···C) = 3.3 Å, $\alpha$(F···C=O) = 93°), of Phe54 ($d$(F···C) = 3.6 Å, $\alpha$(F···C=O) = 106°), and Gly52 ($d$(F···C) = 3.6 Å, $\alpha$(F···C=O) = 127°) (Figure 5b). Additionally, several favorable C–F···H–N contacts are observed, such as with Lys72 ($d$(F···N) = 3.7 Å) and Ser53 ($d$(F···N) = 3.5 Å (see the Supporting Information, Figure S2). The $CF_3$ group further interacts at short F···C distances around 3.1–3.2 Å with the H–$C_\alpha$ bonds of loop residues Gly55 and Gly52, and maintains other C-F···H-C contacts to the side chains of Phe54 and Leu74. Clearly, the $CF_3$ group is embedded into a truly fluorophilic environment.[19b,34]

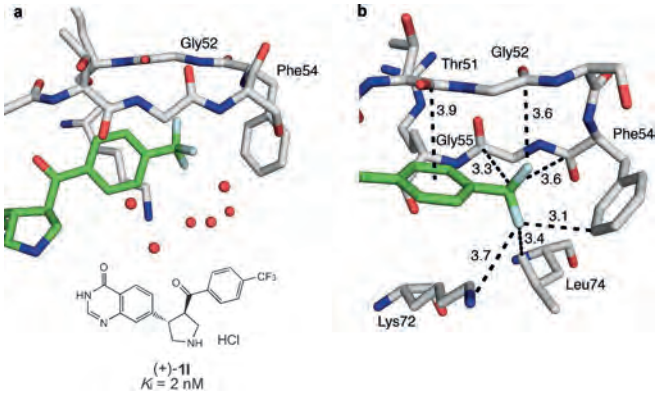


**Figure 5.** X-ray co-crystal structure of compound (+)-**1l** bound to PKA (1.78 Å resolution, PDB ID: 4UJ9). a) Structure of (+)-**1l** and a closer look into the glycine-rich loop, where the water molecule W34 is replaced. b) Contacts between the $F_3$C-phenyl ring in the glycine-rich loop region. Distances are given in Å, and interactions are shown as dashed lines. Color code: $C_{enzyme}$ gray, $C_{ligand}$ green, O red, N blue, F light blue. Water molecules are shown as red spheres.

The experimental finding that the water molecule W34, seen in the co-crystal structures of the *meta*-series, had been displaced by the *para*-$CF_3$ group of (+)-**1l** led us to perform a PDB search (see the Supporting Information, Section 3) to obtain further evidence for the presence of a conserved water molecule at this position. This analysis showed that the active pocket of PKA is highly solvated and that solvation extends to the glycine-rich loop. Most interestingly, the water molecule W34 was found in eight of the thirteen analyzed structures with a loop conformation similar to the one seen in our study. Engh and co-workers had previously shown that the glycine-rich loop is quite flexible[3] (see Supporting Information, Figure S1); therefore only a small number of structures were incorporated into the analysis. Still this investigation gave us fur-

ther evidence for the hypothesis, that the *para*-substituted inhibitors gain energy by replacing that water molecule.[35] As the water molecule W34 seems to be energetically frustrated[20,30] (see above), the replacement is expected to be favorable. A water score analysis further supports this hypothesis. In this analysis, we used a geometric scoring similar to the Rank score developed by Kellogg and co-workers, by exploring the coordination of structural water to neighboring water molecules as well as to the protein.[36]

### Interactions of the thienyl inhibitors with the glycine-rich loop

A sharp increase in binding affinity was observed upon adding halides in *ortho*-position to the sulfur atom of the thiophene substituent. While the parent thiophene ligand (+)-**1n** ($K_i$ = 170 nM) is less potent than the phenyl compound (+)-**1a** ($K_i$ = 30 nM), addition of a chlorine enhances binding to a $K_i$ value of 23 nM and bromination afforded the most potent inhibitor of all three series, (+)-**1p**, with a $K_i$ value of 0.9 nM, Figure 6). Gratifyingly, a co-crystal structure of (+)-**1p** with PKA was obtained. In this structure, some electron density is observed in proximity of Phe54, which is attributed to a bromine atom, derived from radiation damage, rather than the conservation of a water molecule. The close proximity of the inhibitor to the phenyl ring (4.6 Å) further supports this.[37]

The very strong binding is again a result of an extensive interaction network in the complex. The thiophene inhibitor adopts the expected *cis* conformation, enforced by an intramolecular chalcogen bonding interaction of one of the two σ*-orbitals of the divalent sulfur atom with the lone pair of the C=O oxygen atom.[18c,38–41] The conformational preorganization through this intramolecular 1,4-S···O interaction[18c] ($d$(S···O) = 3.0 Å) directs the bromothienyl ring into the glycine-rich loop (Figure 6). Here, the highly polarizable and apparently ideally sized bromine atom of (+)-**1p** finds a perfect environment for multiple dispersive and orthogonal dipolar interactions.

The thiophene sulfur atom undergoes additional interactions with neighboring backbone C=O groups in the loop ($d$(S···C=$O_{Thr51}$) = 3.4 Å, $d$(S···C=$O_{Gly55}$) = 4.1 Å and $d$(S···C=$O_{Arg56}$) = 3.9 Å; Figure 6a), which presumably are mostly dispersive.[18c,38–41] Dunitz and co-workers had previously analyzed the geometries for nonbonded atomic contacts of divalent sulfur with electrophiles and nucleophiles.[42]

The bromine is surrounded by the glycine-rich loop and undergoes similarly favorable interactions to those discussed before for the $CF_3$ group of inhibitor (+)-**1l** (Figure 6b). Halogen bonding was not observed as the interaction distances and angles do not fulfill the rigorous geometric requirements.[43]

An additional contribution to binding affinity could originate from the favorable dipolar alignment of the bromothienyl ring and the peptide bond Gly52–Thr51 in the loop, which undergo parallel-shifted amide–π stacking at a distance of 3.9–4.1 Å. Harder et al. reported a computational study which revealed that the energetics of this stacking interaction is strongest if strong dipoles are aligned in an antiparallel fashion.[44] The best inhibitors (+)-**1p** and (+)-**1l** exhibit substantial local dipole moments in their aromatic rings (3.6 and 2.4 Debye) with favorable alignment angles of 139° and 163°, respectively (see Supporting Information, Figure S5).

The numerous weak intermolecular interactions of (+)-**1p** with the glycine-rich loop are indeed remarkable and result in the nearly sub-nanomolar inhibition ($K_i$ value) of PKA. Although the contribution of each isolated contact cannot be quantified on its own, their simultaneous presence is important for the high inhibitory activity of the bromothienyl ligand.

### Computational analysis of the interaction network

To further decipher the impact of multiple interactions observed in the binding of ligand (+)-**1p** to PKA, an enzyme-ligand network interaction analysis, as developed by Kuhn et al., was performed.[31] It specifically identifies networks of favorable enzyme–ligand interactions and categorizes close enzyme–ligand contacts to distinct classes of interactions, which allows an advanced analysis of binding modes and provides a rational for biological activity.

A large number of favorable contacts are detected around the carbonylbromothienyl moiety (Figure 7b; for the full network see the Supporting Information, Figure S3). In this analysis, the ligand C=O interacts with the polarized Cα of Gly50 by

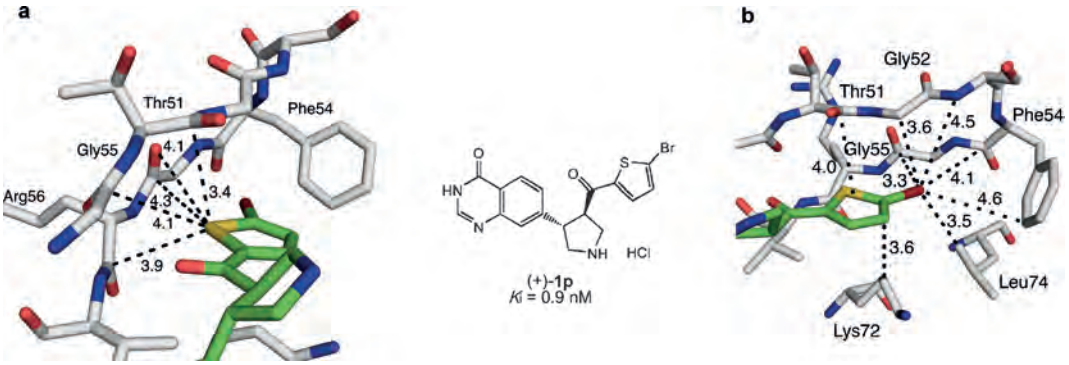


**Figure 6.** X-ray co-crystal structure of inhibitor (+)-**1p** bound to PKA (1.93 Å resolution, PDB ID: 4UJA). a) S···C=O contacts. b) Contacts between the Br atom and the glycine-rich loop. The amide–π stacking distance is also shown. Distances are given in Å. Color code: $C_{enzyme}$ gray, $C_{ligand}$ green, O red, N blue, S yellow, Br dark red.

a weak hydrogen bond ($d = 3.0$ Å). The thiophene moiety undergoes several dispersive interactions with the glycine-rich loop, and π–π stacking with the backbone amide moiety is detected. Finally, the bromine atom is suitably embedded in an environment with three close apolar contacts to the enzyme ($d$(Br···enzyme) = 3.3–3.6 Å). The more quantitative network contribution analysis reveals six ligand atoms with remarkably high scores (≥ 1.0), suggesting that these may act as binding hot-spots (Figure 7 a). They comprise three atoms of the hinge-binding quinazolinone heterocycle, the pyrrolidine nitrogen atom in the ribose pocket, and the thienyl sulfur and bromine atoms of the loop-binding substituent. According to the network analysis, the interactions of the 5-bromothienyl moiety with the glycine-rich loop clearly make an important contribution to the excellent ligand binding affinity of (+)-**1 p**.

## Conclusion

We described design, synthesis, and biological evaluation of a new family of enantiopure inhibitors for protein kinase A (PKA) and its mutant PKAB3 as mimic of PKB. The ligands bind to the ATP site of the proteins, with a quinazolinone ring interacting with the hinge, a most probably protonated pyrrolidine ring filling the ribose pocket, and substituted aromatic rings (phenyl, thienyl) binding to the glycine-rich loop, the ATP-triphosphate binding site. Depending on the nature and substitution of these aromatic vectors, binding affinities down to $K_i$ values in the single-digit nanomolar range were measured. The inhibitors exhibited a preference for binding to PKA over PKAB3, the origin of which could be elucidated by X-ray co-crystal structure determination. A total of seven co-crystal structures revealed a conserved binding mode, which allowed establishment of an SAR, with a focus on the interactions of the ligands with the glycine-rich loop. This loop has not been addressed in most protein kinase inhibitor design, but this work shows that proper ligand interactions with the loop can greatly enhance binding potency. The data suggest that the glycine-rich loop is best addressed by an intricate network of dispersive contacts and dipolar interactions. In addition, favorable water replacement by the ligand in the loop region contributes to binding strength. The aromatic rings of the inhibitors interact with the loop by undergoing amide–π stacking interactions. The loop was best addressed with *para*-$CF_3$-phenyl and 5-bromothienyl rings which both feature in the co-crystal structures a remarkable network of weak interactions, including orthogonal dipolar contacts and dispersive interactions. While the energetic contribution of each contact cannot be quantified on its own, the ensemble of weak interactions with the loop is key to high inhibitory activity. The interaction network was analyzed computationally for the bromothienyl-substituted ligand, and both the sulfur and bromine atoms were identified as interaction hotspots. In summary, this work strongly validates binding to the glycine-rich ring as a promising strategy in the development of potent inhibitors of protein kinases.

## Experimental Section

**Materials and methods**: For detailed descriptions of the chemical analytical equipment, see the Supporting Information S5. This Section provides general procedures for the pyrrolidine ring synthesis and deprotection, and reports the preparation of inhibitor (+)-**1 j**. All other synthetic protocols, analytical data, and the co-crystal structure analyses are included in the Supporting Information, Section S5.

**General procedure A (GP-A) for the phosphonate synthesis**

A solution of diethyl methylphosphonate (1.5 equiv) in THF (10 or 20 mL) was treated at −78 °C dropwise with a 1.6 M *n*BuLi solution in hexane (1.5 equiv), stirred for 10 min, treated with a solution of the halogenated ethyl-benzoate (**2**) (1 equiv) in THF (10 or 20 mL), stirred for 2 h, and diluted with sat. aq. $NH_4Cl$ solution (200 mL). The aqueous phase was extracted with EtOAc (3 × 200 mL), and the combined organic phases were dried over $MgSO_4$, filtered, and evaporated.

**General procedure B (GP-B) for the olefin synthesis**

1) A suspension of 60wt% NaH on mineral oil (1 equiv) in THF (1.5 mL) was treated with a solution of the corresponding phosphonate **4** (1 equiv) in THF (3.0 mL) at 0 °C. The mixture was stirred at 0 °C for 10 min, treated with aldehyde **5** (1 equiv), stirred for 30 min at 0 °C, warmed to 22 °C, and stirred for additional 0.25–

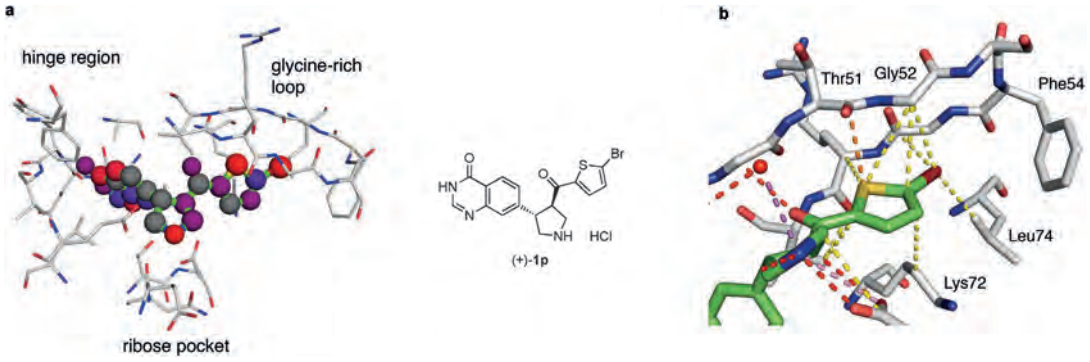


**Figure 7.** Interaction network analysis of inhibitor (+)-**1 p** bound to PKA (1.93 Å resolution, PDB ID: 4UJA). a) Atom-based score contributions in a blue to red color scheme, with gray indicating no interactions. Binding hot spots (contribution score ≥ 1) are shown in red with the highest scores for: Br 1.7, S 2.2, $N_{pyrrolidine}$ 1.6, $N_{quinazolinone}$ 1.2, $O_{quinazolinone}$ 1.0, and $C_{quinazolinone}$ 1.0 b) Illustration of the favorable interaction network around the Gly-rich loop. Color code: $C_{enzyme}$ gray, $C_{ligand}$ green, O red, N blue, S yellow, Br dark red. Interactions are shown as dashed lines. The color code for interactions is hydrogen bond: red, dispersive: yellow, ionic: pink, cation-dipole: magenta, π···π: orange.

22 h before being diluted with a sat. aq. $NH_4Cl$ solution (50 mL). The aqueous phase was extracted with $CH_2Cl_2$ (3×50 mL). The combined organic phases were dried over $MgSO_4$, filtered, and evaporated.

2) A suspension of KO*t*Bu (1 equiv) in THF (1.5 mL) was treated with a solution of the corresponding phosphonate **4** (1 equiv) in THF (3.5 mL) at 0 °C, stirred for 30 min, treated with aldehyde **5** (1 equiv), stirred for 20 min at 0 °C, for 5–22 h at 22 °C, and diluted with sat. aq. $NH_4Cl$ (50 mL). The aqueous phase was extracted with $CH_2Cl_2$ (3×50 mL). The combined organic phases were dried over $MgSO_4$, filtered, and evaporated.

**General procedure C (GP-C) for the pyrrolidine synthesis**

A solution of alkene **10** (1 equiv) in toluene (6 mL) at 100 °C or 120 °C (with $Na_2SO_4$ in a frit above) was simultaneously treated with *para*-formaldehyde (6 equiv) and glycine (2 equiv), stirred at 120 °C for 2 h, treated with additional *para*-formaldehyde (6 equiv) and glycine (2 equiv), stirred for 2 h at 120 °C, cooled to 22 °C, and the solvent was removed under reduced pressure. A solution of the crude intermediate in MeOH (6 mL) was treated with $Boc_2O$ (1.2 equiv), stirred at 22 °C overnight, and the solvent was removed under reduced pressure.

**General procedure D (GP-D) for the deprotection of pyrrolidines**

A solution of pyrrolidine **13** (1 equiv) in THF (1 mL) at 0 °C was treated with 2 M aq. HCl (1 mL) and stirred for 1–48 h at 22 °C, until LCMS showed complete conversion. The mixture was evaporated, triturated with $Et_2O$ (2 mL), and evaporated. HPLC (amino phase: LiChrospher 100 $NH_2$ (5 μm); 15 mL min$^{-1}$, MeOH/$CHCl_3$ 10:90), evaporation, treatment with 1.25 M HCl in MeOH (1 mL) at 0 °C, evaporation, precipitation from $Et_2O$, and drying under HV afforded the pyrrolidines as HCl salts.

**Diethyl [2-(4-bromophenyl)-2-oxoethyl]phosphonate (4j)**: GP-A (10 mL THF) starting from ethyl 4-bromobenzoate (346 μL, 2.07 mmol). FC ($SiO_2$; EtOAc/heptane 4:1) gave phosphonate **4j** (614 mg, quant.) as a colorless oil. $R_f$ = 0.26 ($SiO_2$; EtOAc/heptane 4:1); $^1$H NMR (400 MHz, $CDCl_3$): $\delta$ = 1.30 (td, $J$ = 7.1 Hz, $^4J$(H,P) = 2.1 Hz, 6H; 2 $OCH_2CH_3$), 3.60 (d, $^2J$(H,P) = 22.8 Hz, 2H; H-C(1)), 4.09–4.19 (m, 4H; 2 $OCH_2CH_3$), 7.63, 7.90 ppm (AA′MM′, $J$ = 9.1 Hz, 4H; $C_6H_4$); $^{13}$C NMR (100 MHz, $CDCl_3$): $\delta$ = 16.26 (d, $^3J$(C,P) = 6.2 Hz, 2 C; 2 $OCH_2CH_3$), 38.67 (d, $^1J$(C,P) = 128.4 Hz, 1 C; C(1)), 62.74 (d, $^2J$(C,P) = 6.4 Hz, 2 C; 2 $OCH_2CH_3$), 129.07 (C(4′)), 130.51 (2 C; C(2′)), 131.94 (2 C; C(3′)), 135.24 (d, $^3J$(C,P) = 1.7 Hz, 1 C; C(1′)), 190.95 ppm (d, $^2J$(C,P) = 6.5 Hz, 1 C; C=O); $^{31}$P NMR (162 MHz, $CDCl_3$): $\delta$ = 19.33 ppm (tquint., $^2J$(P,H) = 24.1 Hz, $^3J$(P,H) = 8.1 Hz, 1 P; $PO_3$); IR (ATR): = 2982 (w), 2932 (w), 1679 (m), 1585 (m), 1568 (w, sh), 1484 (w), 1443 (w), 1395 (w), 1248 (s), 1200 (w), 1163 (w), 1098 (w), 1052 (s, sh), 1019 (s), 998 (s), 956 (s), 872 (w), 802 (s), 738 (m), 704 cm$^{-1}$ (w); HR-MS (ESI): *m/z* (%): 337.0027 (100, $[M+H]^+$, calcd for $C_{12}H_{17}{}^{81}BrO_4P^+$: 337.0022), 335.0044 (88, $[M+H]^+$, calcd for $C_{12}H_{17}{}^{79}BrO_4P^+$: 335.0042).

**(2*E*)-1-(4-Bromophenyl)-3-(4-methoxyquinazolin-7-yl)prop-2-en-1-one (10j)**: GP-B1 starting from phosphonate **4j** (110 mg, 0.33 mmol); 20 h at 22 °C. MPLC (80 g $SiO_2$; 120 mL min$^{-1}$, MeOH/$CH_2Cl_2$ 0:100 → 2:98) gave impure alkene **10j** (77 mg, 64%; (*E*/*Z*) 99:1) as an off-white solid, of which a small amount was purified by HPLC (Reprosil; 15 mL min$^{-1}$, hexane/*i*PrOH/$CHCl_3$ 72:3:25) to afford alkene **10j** as an off-white solid. The compound appears to react upon concentration and was therefore used for the next step without further purification. $R_f$ = 0.38 ($SiO_2$; MeOH/$CH_2Cl_2$ 1:19); m.p. 203–206 °C; $^1$H NMR (400 MHz, $CDCl_3$): $\delta$ = 4.23 (s, 3H; OMe), 7.69 (d, $J$ = 15.8 Hz, 1H; CH=C*H*-C=O), 7.70, 7.95 (AA′MM′, $J$ = 8.4 Hz, 4H; $C_6H_4Br$), 7.84 (dd, $J$ = 8.5, 1.6 Hz, 1H; H-C(6)), 7.97 (d, $J$ = 15.6 Hz, 1H; C*H*=CH-C=O), 8.17 (d, $J$ = 1.2 Hz, 1H; H-C(8)), 8.22 (d, $J$ = 8.8 Hz, 1H; H-C(5)), 8.87 ppm (s, 1H; H-C(2)); $^{13}$C NMR (100 MHz, $CDCl_3$): $\delta$ = 54.52 (OMe), 117.48 (C(4a)), 124.35, 124.38, 125.73 (C(5)), 128.36 (CH=*C*H-C=O), 128.41 (C(4′)), 130.10 (2 C; C(2′)), 132.11 (2 C; C(3′)), 136.52 (C(1′)), 139.64 (C(7)), 143.58 (*C*H=CH-C=O), 151.22 (C(8a)), 155.30 (C(2)), 166.98 (C(4)), 188.84 ppm (C=O); IR (ATR): = 2923 (w), 2853 (w), 1658 (m), 1619 (w), 1586 (m), 1574 (s), 1495 (m), 1455 (m), 1397 (w), 1380 (s), 1361 (s), 1322 (m), 1276 (m), 1209 (m), 1168 (m), 1096 (m), 1071 (m), 1025 (m), 993 (s), 977 (m), 906 (w), 875 (m), 862 (m), 813 (s), 784 (s), 764 (w), 745 (m), 732 (m), 682 (m), 673 (m), 629 cm$^{-1}$ (m); HR-MS (ESI): *m/z* (%): 371.0211 (63, $[M+H]^+$, calcd for $C_{18}H_{14}{}^{81}BrN_2O_2^+$: 371.0213), 369.0230 (67, $[M+H]^+$, calcd for $C_{18}H_{14}{}^{79}BrN_2O_2^+$: 369.0233), 177.1271 (96), 150.0367 (100).

**(+)- and (−)-*tert*-Butyl (3,4-*trans*)-3-(4-bromobenzoyl)-4-(4-methoxyquinazolin-7-yl)pyrrolidine-1-carboxylate ((+)-13 and (−)-13)**: GP-C starting from alkene **10j** (67 mg, 0.18 mmol). FC ($SiO_2$; MeOH/$CH_2Cl_2$ 1:99 → 2.5:97.5) and chiral HPLC (Reprosil; 15 mL min$^{-1}$, hexane/*i*PrOH/$CHCl_3$ 75:3:22) gave pyrrolidines (+)-**13j** (18 mg, 19%) and (−)-**13j** (19 mg, 20%) as colorless waxes.

Data of (+)-**13j**: $R_f$ = 0.33 ($SiO_2$; MeOH/$CH_2Cl_2$ 1:19); $t_R$ (prep. HPLC) = 40 min (Reprosil; 15 mL min$^{-1}$, hexane/*i*PrOH/$CHCl_3$ 75:3:22); $[a]_D^{20}$ = +23.2 ($c$ = 0.1 in $CHCl_3$); $^1$H NMR (400 MHz, $CDCl_3$; approx. 1:1 mixture of diastereoisomers, assignment based on HSQC and HMBC spectra of (+)-**13j**): $\delta$ = 1.51 (s, 9H; $C(CH_3)_3$), 3.60 (dd, $J$ = 10.5, 7.9 Hz, 1H; $H_a$-C(2 or 5)), 3.64–3.71 (m, 1H; $H_a$-C(2 or 5)), 3.96–4.26 (m, 4H; $H_b$-C(2), H-C(3), H-C(4), $H_b$-C(5)), 4.18 (s, 3H; $CH_3$), 7.49 (dd, $J$ = 8.5, 1.4 Hz, 1H; H-C(6″)), 7.57, 7.74 (AA′MM′, $J$ = 8.6 Hz, 4H; H-C(2′), H-C(3′)), 7.82 (br. s, 1H; H-C(8″)), 8.11 (d, $J$ = 8.5 Hz, 1H; H-C(5″)), 8.80 ppm (s, 1H; H-C(2″)); $^{13}$C NMR (100 MHz, $CDCl_3$; approx. 1:1 mixture of diastereoisomers): $\delta$ = 28.48, 46.43 and 46.74, 49.39, 51.91 and 51.97, 52.20 and 52.60, 54.36, 80.11, 115.72, 124.26, 125.57, 127.10, 129.13, 129.87, 132.17, 134.70, 146.16 and 146.34, 151.13, 153.97 and 154.03, 154.88, 166.95, 196.93 ppm; IR (ATR): = 2974 (w), 2937 (w), 2876 (w), 1682 (s), 1624 (m), 1581 (m), 1567 (m), 1496 (m), 1454 (m), 1377 (s), 1256 (w), 1167 (m), 1121 (m), 1098 (m), 1070 (m), 1007 (m), 976 (w), 877 (m), 839 (m), 796 (m), 769 (m), 749 (m), 688 cm$^{-1}$ (m); HR-ESI-MS: *m/z* (%): 514.1168 (69, $[M+H]^+$, calcd for $C_{25}H_{27}{}^{81}BrN_3O_4^+$: 514.1160), 512.1183 (73, $[M+H]^+$, calcd for $C_{25}H_{27}{}^{79}BrN_3O_4^+$: 512.1179), 458.0540 (99), 456.0556 (100).

Data of (−)-**13j**: $t_R$ (prep. HPLC) = 58 min; $[a]_D^{20}$ = −23.1 ($c$ = 0.1 in $CHCl_3$); $^1$H NMR and HR-ESI-MS data consistent with (+)-**13j**.

**(+)-(3*R*,4*S*)-3-(4-Bromobenzoyl)-4-(4-oxo-3,4-dihydroquinazolin-7-yl)pyrrolidinium Chloride ((+)-1j)**: GP-D starting from pyrrolidine (+)-**13j** (18 mg, 0.04 mmol) gave pyrrolidinium (+)-**1j** (11 mg, 72%) as a white solid. M.p. 147 °C (decomp.); $[a]_D^{20}$ = +66.2 ($c$ = 0.1 in MeOH); $^1$H NMR (400 MHz, $(CD_3)_2SO$): $\delta$ = 3.36–3.50 (m, 2H; $H_a$-C(2), $H_a$-C(5)), 3.75–3.96 (m, 2H; $H_b$-C(2), $H_b$-C(5)), 3.91 (dd, $J$ = 17.2, 10.0 Hz, 1H; H-C(4)), 4.62 (t, $J$ = 8.9 Hz, 1H; H-C(3)), 7.60 (dd, $J$ = 8.4, 2.0 Hz, 1H; H-C(6″)), 7.68, 7.74 (AA′MM′, $J$ = 8.4 Hz, 4H; $C_6H_4Br$), 7.68 (d, $J$ = 1.6 Hz, 1H; H-C(8″)), 8.07 (d, $J$ = 8.2 Hz, 1H; H-C(5″)), 8.25 (s, 1H; H-C(2″)), 9.60 and 9.86 (2 br. s, 2H; $H_2N^+$), 12.0–13.0 ppm (br. s, 1H; H-N(3″)); $^{13}$C NMR (100 MHz, $(CD_3)_2SO$, signal of C(2) not visible due to fast exchange, assignment based on HSQC and HMBC spectra of (−)-**1i**): $\delta$ = 46.79 (C(4)), 47.80 (C(2 or 5)), 51.05 (C(2 or 5)), 51.45 (C(3)), 122.02 (C(4a″)), 125.90 (C(8″)), 127.00 (C(5″)), 127.17 (C(6″)), 128.67 (C(4′)), 130.84 (2 C; C(2′)), 132.39 (2 C; C(3′)), 135.07 (C(1′)), 145.44 (C(7″)), 146.84 (C(8a″)), 160.61 (C(4″)), 197.80 ppm (C=O); IR (ATR): = 3600–2200 (m, with 3359 (w), 3030 (m), 2900 (m), 2864 (m), 2709 (m), 2595 (m)), 1713 (s), 1680 (s), 1652 (s), 1621 (m, sh), 1581 (m), 1498 (w), 1463 (w), 1397 (m), 1287 (m), 1244 (m), 1069 (m), 1005 (m), 839 (m), 781 (m), 734 (w), 689 cm$^{-1}$ (m); HR-ESI-MS: *m/z* (%): 426.9491 (100),

400.0486 (69, $[M+H]^+$, calcd for $C_{19}H_{17}{}^{81}BrN_3O_2{}^+$: 400.0479), 398.0501 (68, $[M+H]^+$, calcd for $C_{19}H_{17}{}^{79}BrN_3O_2{}^+$: 398.0499).

## Acknowledgements

This work was supported by a grant from the ETH Research Council and by F. Hoffmann-La Roche, Basel. O.D. thanks the German Fonds der Chemischen Industrie for a Kekulé fellowship. We acknowledge Dr. Alexander Pflug who initiated the measurements at the Norwegian Structural Biology Centre, Tromsø.

**Keywords:** glycine-rich loop · interaction networks · kinases · molecular recognition · pyrrolidines · water replacement

[1] D. A. Walsh, J. P. Perkins, E. G. Krebs, *J. Biol. Chem.* **1968**, *243*, 3763 – 3765.
[2] S. S. Taylor, J. Wang, J. Wu, N. M. Haste, E. Radzio-Andzelm, G. Anand, *Biochim. Biophys. Acta Proteins Proteomics* **2004**, *1697*, 259 – 269.
[3] a) E. Åberg, B. Lund, A. Pflug, O. A. B. S. M. Gani, U. Rothweiler, T. M. de Oliveira, R. A. Engh, *Biol. Chem.* **2012**, *393*, 1121 – 1129; b) T. M. de Oliveira, R. Ahmad, R. A. Engh, *J. Phys. Chem. A* **2011**, *115*, 3895 – 3904.
[4] P. Akamine, Madhusudan, J. Wu, N.-H. Xuong, L. F. Ten Eyck, S. S. Taylor, *J. Mol. Biol.* **2003**, *327*, 159 – 171.
[5] S. S. Taylor, *J. Biol. Chem.* **1989**, *264*, 8443 – 8446.
[6] G. Manning, D. B. Whyte, R. Martinez, T. Hunter, S. Sudarsanam, *Science* **2002**, *298*, 1912 – 1934.
[7] a) P. Cohen, D. R. Alessi, *ACS Chem. Biol.* **2013**, *8*, 96 – 104; b) http://www.brimr.org/PKI/PKIs.htm.
[8] S. S. Staal, J. W. Hartley, W. P. Rowe, *Proc. Natl. Acad. Sci. USA* **1977**, *74*, 3065 – 3067.
[9] D. P. Brazil, Z.-Z. Yang, B. A. Hemmings, *Trends Biochem. Sci.* **2004**, *29*, 233 – 242.
[10] K.-M. V. Lai, M. Gonzalez, W. T. Poueymirou, W. O. Kline, E. Na, E. Zlotchenko, T. N. Stitt, A. N. Economides, G. D. Yancopoulos, D. J. Glass, *Mol. Cell. Biol.* **2004**, *24*, 9295 – 9304.
[11] Z.-Z. Yang, O. Tschopp, M. Hemmings-Mieszczak, J. Feng, D. Brodbeck, E. Perentes, B. A. Hemmings, *J. Biol. Chem.* **2003**, *278*, 32124 – 32131.
[12] T. G. Davies, M. L. Verdonk, B. Graham, S. Saalau-Bethell, C. C. F. Hamlett, T. McHardy, I. Collins, M. D. Garrett, P. Workman, S. J. Woodhead, H. Jhoti, D. Barford, *J. Mol. Biol.* **2007**, *367*, 882 – 894.
[13] M. Gaßel, C. B. Breitenlechner, P. Rüger, U. Jucknischke, T. Schneider, R. Huber, D. Bossemeyer, R. A. Engh, *J. Mol. Biol.* **2003**, *329*, 1021 – 1034.
[14] J. E. Walker, M. Saraste, M. J. Runswick, N. J. Gay, *EMBO J.* **1982**, *1*, 945 – 951.
[15] a) A. K. H. Hirsch, F. Fischer, F. Diederich, *Angew. Chem. Int. Ed.* **2007**, *46*, 338 – 352; *Angew. Chem.* **2007**, *119*, 342 – 357; b) S. S. Taylor, A. P. Kornev, *Trends Biochem. Sci.* **2011**, *36*, 65 – 77.
[16] P. R. Gerber, K. Müller, *J. Comput-Aided Mol. Des.* **1995**, *9*, 251 – 268.
[17] A. Donald, T. McHardy, M. G. Rowlands, L.-J. K. Hunter, T. G. Davies, V. Berdini, R. G. Boyle, G. W. Aherne, M. D. Garrett, I. Collins, *J. Med. Chem.* **2007**, *50*, 2289 – 2292.
[18] a) E. A. Meyer, R. K. Castellano, F. Diederich, *Angew. Chem. Int. Ed.* **2003**, *42*, 1210 – 1250; *Angew. Chem.* **2003**, *115*, 1244 – 1287; b) L. Salonen, M. Ellermann, F. Diederich, *Angew. Chem. Int. Ed.* **2011**, *50*, 4808 – 4842; *Angew. Chem.* **2011**, *123*, 4908 – 4944; c) B. R. Beno, K.-S. Yeung, M. D. Bartberger, L. D. Pennington, N. A. Meanwell, *J. Med. Chem.* **2015**, *58*, 4383 – 4438.
[19] a) R. Paulini, K. Müller, F. Diederich, *Angew. Chem. Int. Ed.* **2005**, *44*, 1788 – 1805; *Angew. Chem.* **2005**, *117*, 1820 – 1839; b) K. Müller, C. Fäh, F. Diederich, *Science* **2007**, *317*, 1881 – 1886.
[20] E. Persch, O. Dumele, F. Diederich, *Angew. Chem. Int. Ed.* **2015**, *54*, 3290 – 3327; *Angew. Chem.* **2015**, *127*, 3341 – 3382.
[21] J. E. Davoren, D. L. Gray, A. R. Harris, D. M. Nason, W. Xu, *Synlett* **2010**, *16*, 2490 – 2492.
[22] M. Joucla, J. Mortier, *J. Chem. Soc. Chem. Commun.* **1985**, 1566 – 1567.
[23] G. Solladié, N. Wilb, C. Bauder, C. Bonini, L. Viggiani, L. Chiummiento, *J. Org. Chem.* **1999**, *64*, 5447 – 5452.
[24] C. E. F. Rickard, W. R. Roper, F. Tutone, S. D. Woodgate, L. J. Wright, *J. Organomet. Chem.* **2001**, *619*, 293 – 298.
[25] Z. E. Wilson, J. G. Hubert, M. A. Brimble, *Eur. J. Org. Chem.* **2011**, 3938 – 3945.
[26] N. Ghavtadze, R. Narayan, B. Wibbeling, E.-U. Würthwein, *J. Org. Chem.* **2011**, *76*, 5185 – 5197.
[27] Enantiomers (+)-**1a**–**p** and (−)-**1a**–**p** were further purified on an amino phase HPLC column, treated with 1.2 M HCl in MeOH, and subsequently precipitated from $Et_2O$ as the mono-HCl salts; see: A. Thaqi, A. McCluskey, J. L. Scott, *Tetrahedron Lett.* **2008**, *49*, 6962 – 6964.
[28] E. Giorgio, M. Roje, K. Tanaka, Z. Hamersak, V. Sunjic, K. Nakanishi, C. Rosini, N. Berova, *J. Org. Chem.* **2005**, *70*, 6557 – 6563.
[29] P. F. Cook, M. E. Neville, Jr., K. E. Vrana, E. Kent, F. T. Hartl, R. Roskoski Jr., *Biochemistry* **1982**, *21*, 5794 – 5799.
[30] a) F. Biedermann, W. M. Nau, H.-J. Schneider, *Angew. Chem. Int. Ed.* **2014**, *53*, 11158 – 11171; *Angew. Chem.* **2014**, *126*, 11338 – 11352; b) S. G. Krimmer, M. Betz, A. Heine, G. Klebe, *ChemMedChem* **2014**, *9*, 833 – 846.
[31] B. Kuhn, J. E. Fuchs, M. Reutlinger, M. Stahl, N. R. Taylor, *J. Chem. Inf. Model.* **2011**, *51*, 3180 – 3198.
[32] M. Harder, M. A. Carnero Corrales, N. Trapp, B. Kuhn, F. Diederich, *Chem. Eur. J.* **2015**, *21*, 8455 – 8463.
[33] Orthogonal dipolar interactions with the DFG-loop of the Bcr-Abl kinase have previously been observed in the X-ray co-crystal structure with the inhibitor Nilotinib (PDB ID: 3CS9); E. Weisberg, P. W. Manley, W. Breitenstein, J. Brüggen, S. W. Cowan-Jacob, A. Ray, B. Huntly, D. Fabbro, G. Fendrich, E. Hall-Meyers, A. L. Kung, J. Mestan, G. Q. Daley, L. Callahan, L. Catley, C. Cavazza, A. Mohammed, D. Neuberg, R. D. Wright, D. G. Gilliland, J. D. Griffin, *Cancer Cell* **2005**, *7*, 129 – 141.
[34] a) J. Olsen, D. W. Banner, P. Seiler, B. Wagner, T. Tschopp, U. Obst-Sander, M. Kansy, K. Müller, F. Diederich, *ChemBioChem* **2004**, *5*, 666; b) T. Vogt, M. Salwicek, B. Koksch in "Fluorine in Pharmaceutical and Medicinal Chemistry" (Eds.: V. Gouverneur, K. Müller), Imperial College Press, London, **2012**, Chapter 2, pp. 33 – 90.
[35] S. Riniker, L. J. Barandun, F. Diederich, O. Krämer, A. Steffen, W. F. van Gunsteren, *J. Comput. Aided Mol. Des.* **2012**, *26*, 1293 – 1309.
[36] A. Amadasi, J. A. Surface, F. Spyrakis, P. Cozzini, A. Mozzarelli, G. E. Kellogg, *J. Med. Chem.* **2008**, *51*, 1063 – 1067.
[37] For a report on a similar radiation damage in the co-crystal structure of a protein-bound aryl halide ligand, see: C. Koch, A. Heine, G. Klebe, *J. Synchrotron Radiat.* **2011**, *18*, 782 – 789.
[38] K. A. Brameld, B. Kuhn, D. C. Reuter, M. Stahl, *J. Chem. Inf. Model.* **2008**, *48*, 1 – 24.
[39] H. V. Le, D. D. Hawker, R. Wu, E. Doud, J. Widom, R. Sanishvili, D. Liu, N. L. Kelleher, R. B. Silverman, *J. Am. Chem. Soc.* **2015**, *137*, 4525 – 4533.
[40] G. E. Garrett, G. L. Gibson, R. N. Straus, D. S. Seferos, M. S. Taylor, *J. Am. Chem. Soc.* **2015**, *137*, 4126 – 4133.
[41] C. Bleiholder, D. B. Werz, H. Köppel, R. Gleiter, *J. Am. Chem. Soc.* **2006**, *128*, 2666 – 2674.
[42] R. E. Rosenfield, R. Parthasarathy, J. D. Dunitz, *J. Am. Chem. Soc.* **1977**, *99*, 4860 – 4862.
[43] L. A. Hardegger, B. Kuhn, B. Spinnler, L. Anselm, R. Ecabert, M. Stihle, B. Gsell, R. Thoma, J. Diez, J. Benz, J.-M. Plancher, G. Hartmann, D. W. Banner, W. Haap, F. Diederich, *Angew. Chem. Int. Ed.* **2011**, *50*, 314 – 318; *Angew. Chem.* **2011**, *123*, 329 – 334.
[44] M. Harder, B. Kuhn, F. Diederich, *ChemMedChem* **2013**, *8*, 397 – 404.

Received: September 5, 2015
Published online on ■■ ■■, 0000

# FULL PAPER

**Kinases**

*B. S. Lauber, L. A. Hardegger, A. K. Asraful, B. A. Lund, O. Dumele, M. Harder, B. Kuhn, R. A. Engh,* F. Diederich**

■■ – ■■

## Addressing the Glycine-Rich Loop of Protein Kinases by a Multi-Facetted Interaction Network: Inhibition of PKA and a PKB Mimic

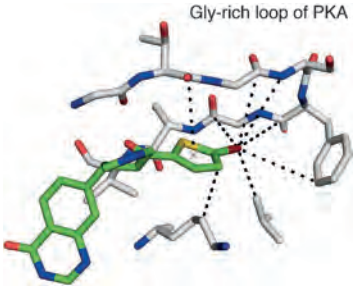


**The forgotten pocket**: A new family of enantiopure inhibitors for protein kinase A (PKA) is reported. They complex to the ATP site, with inhibitory activities ($K_i$) down to the low single-digit nanomolar range. Besides binding to the hinge and the ribose pocket, the ligands also interact in a multi-facetted interaction network with the glycine-rich loop, which has been neglected in kinase inhibitor design. This network of orthogonal dipolar interactions, dispersive contacts, amide–π stacking, together with water replacement makes an important contribution to the overall ligand binding affinity.

CHEMISTRY
A European Journal

Supporting Information

# Addressing the Glycine-Rich Loop of Protein Kinases by a Multi-Facetted Interaction Network: Inhibition of PKA and a PKB Mimic

Birgit S. Lauber,[a] Leo A. Hardegger,[a] Alam K. Asraful,[b] Bjarte A. Lund,[b] Oliver Dumele,[a] Michael Harder,[a] Bernd Kuhn,[c] Richard A. Engh,*[b] and François Diederich*[a]

chem_201503552_sm_miscellaneous_information.pdf

**Supporting Information**

***Chemistry – A European Journal***

# Addressing the Glycine-Rich Loop of Protein Kinases by a Multi-Facetted Interaction Network: Inhibition of PKA and a PKB Mimic

Birgit S. Lauber,[a] Leo A. Hardegger,[a] Alam K. Asraful,[b] Bjarte A. Lund,[b] Oliver Dumele,[a] Michael Harder,[a] Bernd Kuhn,[c] Richard A. Engh,[b]* François Diederich*[a]

[a] B. S. Lauber, Dr. L. A. Hardegger, O. Dumele, Dr. M. Harder, Prof. Dr. F. Diederich
Laboratorium für Organische Chemie, ETH Zurich
Vladimir-Prelog-Weg 3, CH-8093 Zurich (Switzerland)
Fax: (+41) 44 632 11 09
E-mail: diederich@org.chem.ethz.ch

[b] A. K. Asraful, L. B. Aarmo, Prof. Dr. R. A. Engh
Department of Chemistry, University of Tromsø
Forskningsparken 3, Sykehusvegen 23, NO-9037 Tromsø (Norway)
E-mail: richard.engh@uit.no

[c] Dr. B. Kuhn
Small Molecule Research, Roche Innovation Center Basel, F. Hoffmann-La Roche, Grenzacherstrasse 124, 4070 Basel (Switzerland)
E-mail: bernd.kuhn@roche.com

**Table of Contents**

# S1. Schemes, Figures, and X-ray Co-Crystal Structures

**Scheme S1.** Test reaction for the azomethine ylide 1,3 dipolar cycloaddition. *Trans*-chalcone (**11**) afforded the Boc-protected pyrrolidine (±)-**12** in good yields. Reaction conditions: i) $(H_2CO)_n$, glycine, toluene, 90 °C, 7.5 h. ii) $Boc_2O$, MeOH, 22 °C, 1 h; 83%.

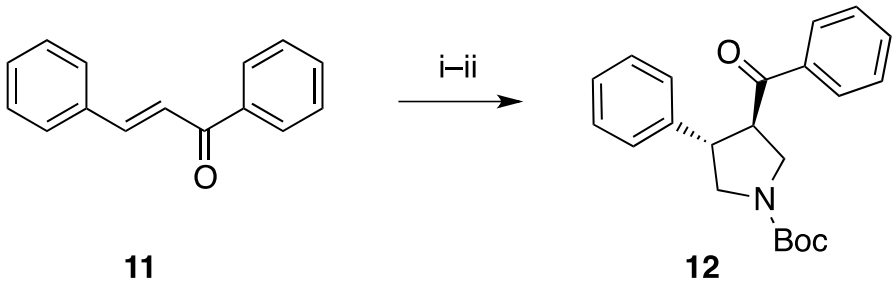


**11** **12**

**Figure S1.** Superposition of 78 individual catalytic domains of 69 PKA entries in the PDB as done by Engh and co-workers[1] with a close-up of the glycine-rich loop. The data are taken from the original publication and slightly adjusted; for details see.[1] The enzyme backbones are shown as thin sticks and the ligand AMP-PNP (PDB code: 1CDK)[2] is shown as stick representation; the substrate mimic peptide PKI is removed. Color code: Enzyme = rainbow (from dark blue at the N-terminus to red at the C-terminus), $C_{ligand}$ gray, $P_{ligand}$ orange, $O_{ligand}$ red, $P_{ligand}$ blue. The overlay shows the "swinging" of the glycine-rich loop (blue) compared to the other secondary structural elements of the enzymes.

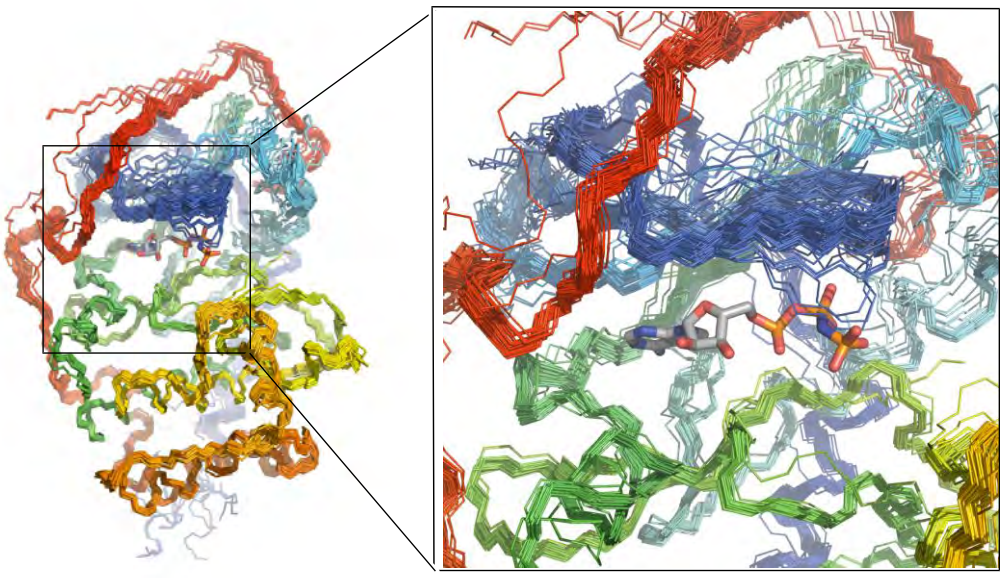

**Figure S2.** X-ray co-crystal structure of compound (+)-**1l** bound to PKA (1.76 Å resolution, PDB ID: 4UJ9). Closer look into the glycine-rich loop with the $CF_3$ contacts. All three F atoms were found to engage in a) F···C b) F···H–C, and c) F···H–N contacts. Distances are given in Å and shown as dashed lines. Color code: $C_{enzyme}$ gray, $C_{ligand}$ green, O red, N blue, F light blue.

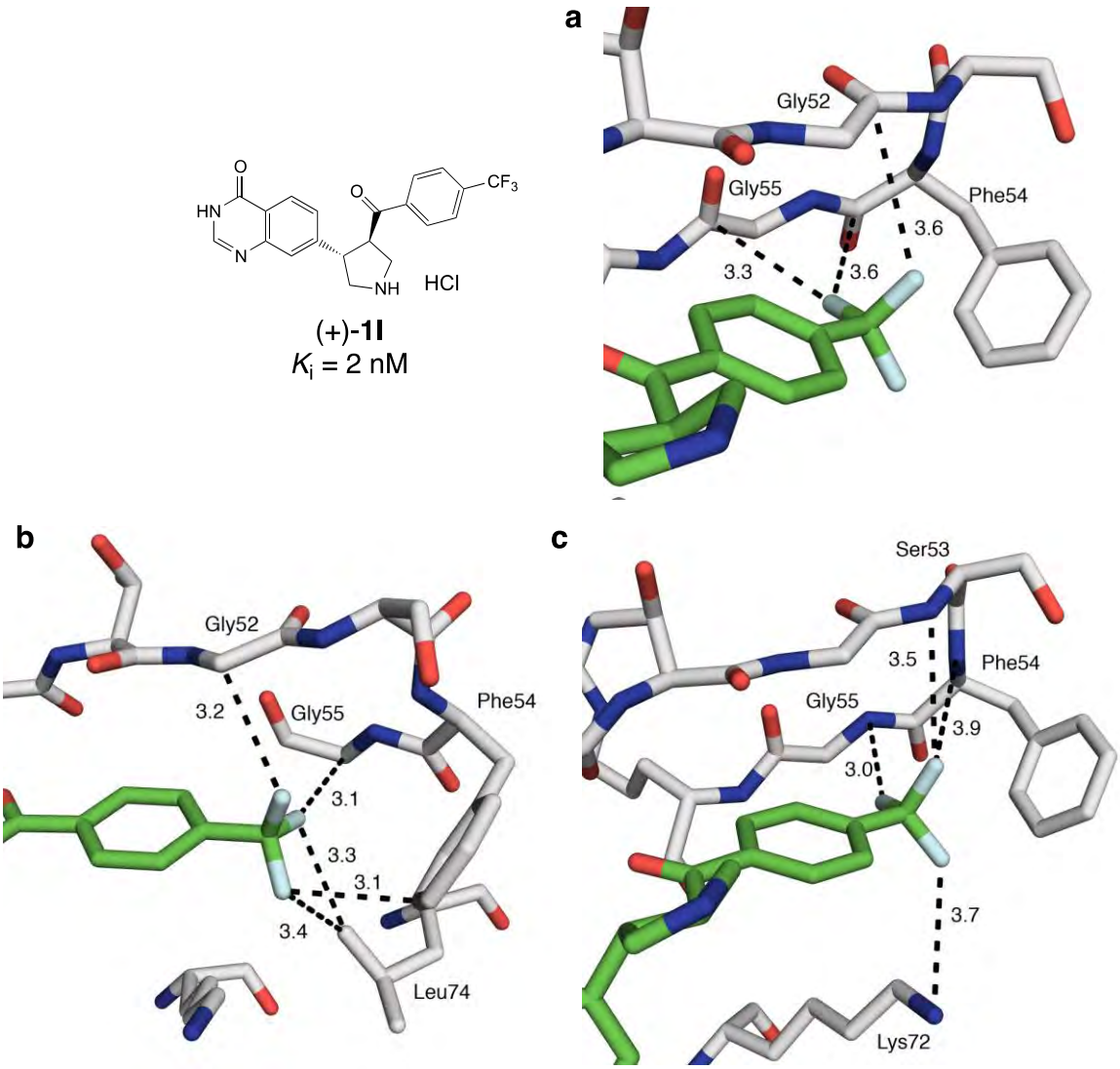

**Figure S3.** Interaction network analysis of inhibitor (+)-**1p** bound to PKA (1.93 Å resolution, PDB ID: 4UJA). a) Hinge region. b) Ribose pocket. c) Glycine-rich loop. d) Atom-based score contributions. Color code: $C_{enzyme}$ gray, $C_{ligand}$ green, O red, N blue, S yellow, Br dark red. The favorable contacts are shown as dashed lines with the following color code: hydrogen bond red, dispersive yellow, ionic pink, cation-dipole dark pink, π··· π orange.

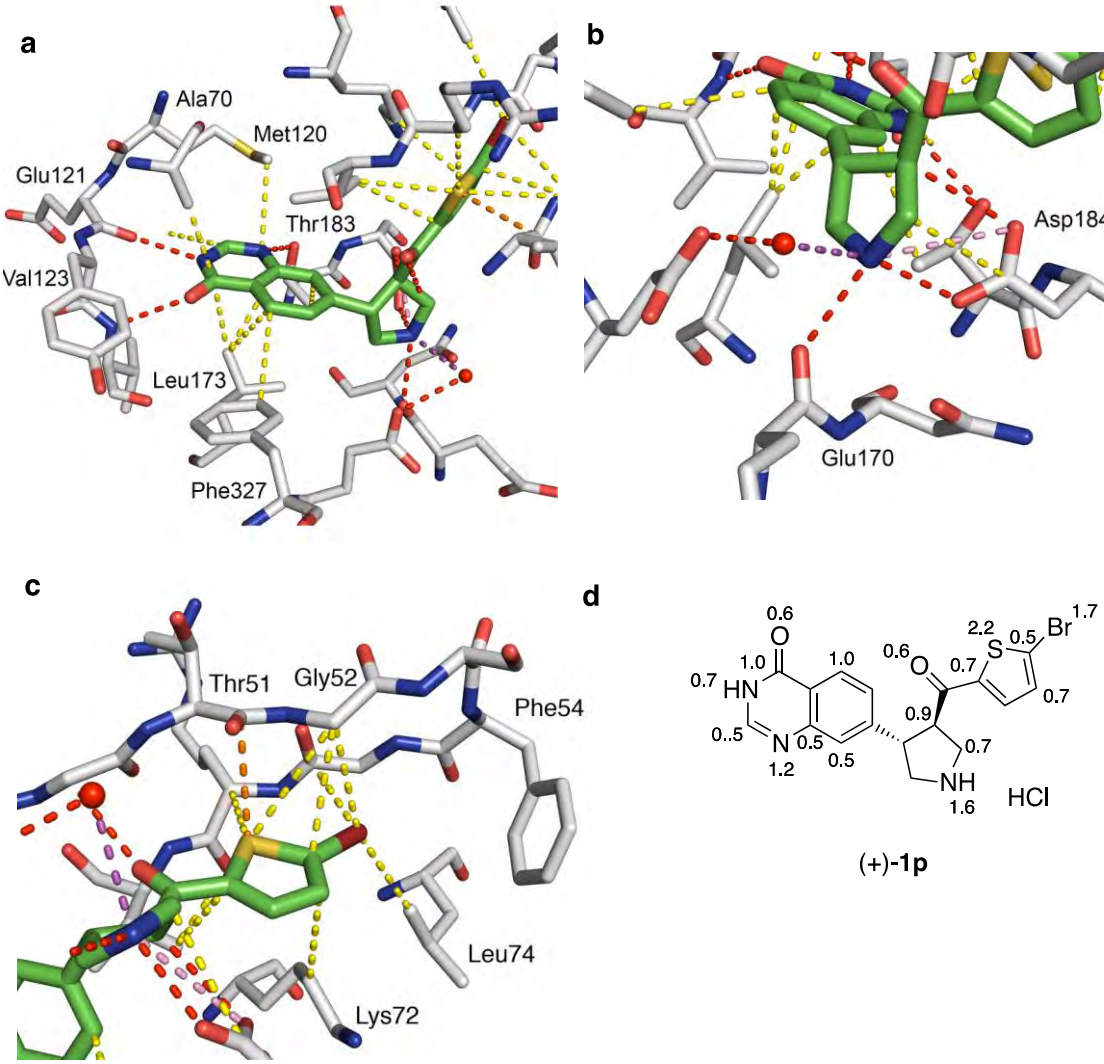

# S2. Theoretical Calculations

## S2.1. Calculation of Optical Rotations of (3*S*/4*R*)-1c·H$^+$ at Specific Frequencies

Conformational searches were performed using a Monte Carlo Multiple Minimum (MCMM) algorithm, employing the OPLS-2005 force field (using a solvation continuum model in water) as implemented in MacroModel 9.7.[3] A maximum of $10^6$ iterations employing a PRCG gradient with a convergence criteria of 0.005 was allowed to sample 2000 structures with 60 steps per rotatable bond at an enhanced torsional sampling MCMM level. The energy window was set to 3 kcal mol$^{-1}$ above the global minimum, allowing a limit of 200 structures to be saved.

The results of these conformational searches were manually analyzed. Four groups of conformers **c1**–**c4** were identified to cover the conformational space. For each group, one representative geometry was considered for further optimization at the DFT level (see Figure S4). All DFT calculations were performed using the Gaussian 09 program package.[4] The B3LYP/6-31G(d) (gas phase) level of theory was applied for pre-optimizations of the selected conformers obtained from the MCMM force field results. On these structures, the hybrid functional B3LYP was utilized with Grimme's dispersion with the original D3 damping function and Ahlrich's cc-pVDZ double-zeta basis set.[5] All structures are ground-state minima according to the analysis of their harmonic vibrational analytical frequencies computed at the same level, which show no imaginary frequencies. All energies reported are zero-point corrected electronic energies ($\Delta E$).

Optical rotations were computed with frequency-dependent polarizabilities and hyperpolarizabilities at 589 nm at the DFT//CAM-B3LYP/6-31+G(d) level of theory using PCM solvation in methanol.

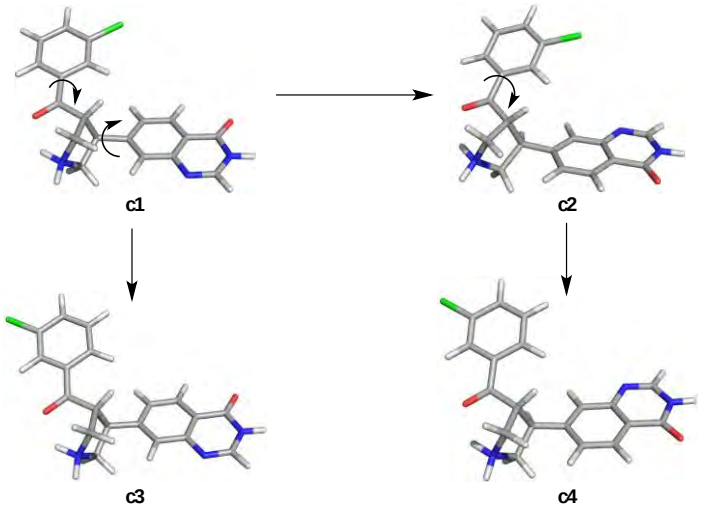


**Figure S4.** Conformer space of (3*S*/4*R*)-**1c**·H$^+$. Conformers **c1–c4** represent the conformational space of a 3 kcal mol$^{-1}$ energy threshold. Shown are the B3LYP-D3/cc-pVDZ optimized geometries.

**Table S1.** Calculated optical rotations of the four lowest energy conformations of (3*S*/4*R*)-**1c**·H$^+$. Experimental value $[\alpha]_{589\ nm,\ methanol} = 77.5°$.

| **Conformer** | $[\alpha]_{589\ nm}$ / ° | $\Delta E_{rel.}$ / kcal mol$^{-1}$ |
|---|---|---|
| 1 | +41.7 | 0 |
| 2 | +57.3 | 0.405 |
| 3 | +175.1 | 0.526 |
| 4 | +297.8 | 0.889 |

As shown in Table S1, the calculated optical rotations $[\alpha]_{589\ nm}$ of all conformers are positive, with a predicted value of +47.7° for the lowest energy conformer **c1**. These results fit the measured experimental magnitude well and allow the assignment of the absolute configuration of ligand (+)-**1c**·H$^+$.

## Cartesian Coordinates of Optimized Geometries

**c1**: DFT//B3LYP/cc-pVDZ

| | | | |
|---|---|---|---|
| C | 2.51492900 | -1.56289000 | -0.25061200 |
| C | 3.25670000 | -0.29258400 | -0.17613100 |
| Cl | 2.54812900 | 3.66166400 | -0.40644900 |
| C | 4.72630000 | 2.08222200 | 0.04450400 |
| C | 5.36130700 | 0.84565400 | 0.20324400 |
| O | 3.05192300 | -2.64652200 | 0.00648100 |
| C | -1.06432700 | -0.73076800 | 0.65748200 |
| C | -3.37112300 | -0.47495400 | -0.09215400 |
| C | -5.52834100 | -0.30823900 | -0.80302000 |
| C | -4.52642000 | 1.72507300 | 0.12306600 |
| O | -4.62991200 | 2.90074400 | 0.41521100 |
| C | -3.33280000 | 0.88212700 | 0.30539100 |
| C | -2.17076200 | 1.42129600 | 0.87635800 |
| C | 0.03397500 | -3.02849900 | 1.14114900 |
| H | 0.53740100 | -3.32354600 | 2.06847400 |
| C | 1.01677800 | -1.55344400 | -0.56987600 |
| H | 0.73283700 | -0.70936500 | -1.20350500 |
| C | 0.59922200 | -2.87785800 | -1.20116600 |
| H | 1.27693500 | -3.25266100 | -1.97753300 |
| H | -0.43275500 | -2.85221400 | -1.57155400 |
| C | 0.21758000 | -1.52959800 | 0.78860500 |
| H | 0.83969800 | -1.05294700 | 1.55723800 |
| C | -2.21834000 | -1.26576000 | 0.09276900 |
| H | -2.29955400 | -2.30765400 | -0.22237000 |
| C | -1.04833100 | 0.62513100 | 1.05316200 |
| H | -0.14960600 | 1.04596700 | 1.50915200 |
| C | 4.63646300 | -0.33754100 | 0.10267500 |
| H | 5.11558500 | -1.30717000 | 0.23445900 |
| H | 5.28725500 | 3.01337900 | 0.12732300 |
| H | 6.43178000 | 0.81595000 | 0.41108100 |
| H | -6.44116200 | -0.72350900 | -1.24067200 |
| H | -2.18142000 | 2.46895900 | 1.17941500 |
| H | -1.02112700 | -3.31784900 | 1.19678300 |
| C | 3.35372300 | 2.12314500 | -0.22214200 |
| C | 2.61448400 | 0.94891100 | -0.34375000 |
| H | 1.54902600 | 1.02657900 | -0.55241200 |
| N | -5.59261500 | 1.01133100 | -0.45059500 |
| H | -6.44964000 | 1.53914100 | -0.59988700 |
| N | -4.49070900 | -1.07026500 | -0.65639700 |
| H | 0.26873700 | -4.71792000 | -0.15365000 |
| N | 0.67104600 | -3.78740100 | -0.00372100 |
| H | 1.70156800 | -3.85138700 | 0.17142000 |

**c2**: DFT//B3LYP/cc-pVDZ

| | | | |
|---|---|---|---|
| C | 2.79318600 | -1.18000400 | -0.14453400 |
| C | 3.07709100 | 0.26391600 | -0.10295100 |
| Cl | 1.16171400 | 3.75286900 | -0.69149600 |
| C | 3.66954700 | 2.99541900 | 0.06845800 |
| C | 4.64776800 | 2.04375700 | 0.37711000 |
| O | 3.60055300 | -2.01949400 | 0.26946100 |
| C | -0.90752700 | -1.33097300 | 0.40304200 |
| C | -2.57106300 | 0.42968200 | 0.68466300 |
| C | -4.08375900 | 2.10408300 | 0.98891900 |
| C | -4.79644800 | 0.24003400 | -0.42849700 |
| O | -5.64980200 | -0.28115700 | -1.12141900 |
| C | -3.45661300 | -0.30007300 | -0.14287700 |
| C | -3.06758600 | -1.53244200 | -0.68859600 |
| C | 0.62345500 | -3.31697000 | 1.03735700 |
| H | 0.93128500 | -3.48440800 | 2.07567100 |
| C | 1.42452900 | -1.67433200 | -0.62234200 |
| H | 0.97169900 | -1.00754800 | -1.36055600 |
| C | 1.54557300 | -3.09638500 | -1.16502300 |
| H | 2.42773500 | -3.27417600 | -1.79122900 |
| H | 0.63661300 | -3.42826000 | -1.68144300 |
| C | 0.50334500 | -1.81974500 | 0.65230100 |
| H | 0.92978700 | -1.21145800 | 1.45998300 |
| C | -1.29356200 | -0.10973400 | 0.94562100 |
| H | -0.62530800 | 0.46667300 | 1.58805700 |
| C | -1.80683900 | -2.04482700 | -0.42134200 |
| H | -1.52735300 | -3.00746800 | -0.85540200 |
| C | 4.35829700 | 0.68517100 | 0.30226700 |
| H | 5.10626700 | -0.06734900 | 0.55014900 |
| H | 3.88847700 | 4.06167000 | 0.12985300 |
| H | 5.64119300 | 2.37602200 | 0.68158900 |
| H | -4.39839400 | 3.06306000 | 1.41157300 |
| H | -3.78076000 | -2.06448000 | -1.31932200 |
| H | -0.30323400 | -3.87005300 | 0.84246500 |
| C | 2.39441900 | 2.57275000 | -0.32137600 |
| C | 2.09038000 | 1.21696100 | -0.41912500 |
| H | 1.08346800 | 0.93123400 | -0.71856100 |
| N | -5.01090100 | 1.47552200 | 0.20299200 |
| H | -5.92133900 | 1.90198900 | 0.04628200 |
| N | -2.89969000 | 1.65118800 | 1.25390500 |
| H | 1.64767000 | -4.88729700 | 0.00841300 |
| N | 1.68749700 | -3.86882300 | 0.11839700 |
| H | 2.63354500 | -3.57467100 | 0.45805600 |

**c3**: DFT//B3LYP/cc-pVDZ

| | | | |
|---|---|---|---|
| C | -2.13125600 | 1.27229700 | -0.28022400 |
| C | -2.85141500 | -0.01112700 | -0.33236400 |
| Cl | -6.66767400 | -1.16581900 | 0.21889600 |
| C | -4.31164300 | -2.39991000 | -0.36730700 |
| C | -2.93789200 | -2.41615100 | -0.61757400 |
| O | -2.69390800 | 2.32076100 | 0.05795000 |
| C | 1.44836500 | 0.47479600 | 0.65082000 |
| C | 3.76828100 | 0.29725600 | -0.08105800 |
| C | 5.93646900 | 0.20378300 | -0.77190600 |
| C | 4.97341600 | -1.88094300 | 0.07750500 |
| O | 5.10076800 | -3.06304900 | 0.33239000 |
| C | 3.75844800 | -1.07226200 | 0.27346100 |
| C | 2.60410700 | -1.65623500 | 0.81499100 |
| C | 0.29732600 | 2.72128600 | 1.23308100 |
| H | -0.21249600 | 2.95289600 | 2.17488400 |
| C | -0.62837000 | 1.32171300 | -0.57247600 |
| H | -0.31030600 | 0.52523000 | -1.24975100 |
| C | -0.24187300 | 2.69435100 | -1.11765500 |
| H | -0.92069900 | 3.09509400 | -1.88006400 |
| H | 0.79477900 | 2.72167100 | -1.47484800 |
| C | 0.14840300 | 1.24049800 | 0.79691700 |
| H | -0.47827700 | 0.71168400 | 1.52665900 |
| C | 2.59524700 | 1.05443100 | 0.11620800 |
| H | 2.65467500 | 2.10761900 | -0.16431300 |
| C | 1.46091600 | -0.89281300 | 1.00338600 |
| H | 0.56691300 | -1.34730200 | 1.43589300 |
| C | -2.20393700 | -1.23094700 | -0.60739000 |
| H | -1.13254500 | -1.27235500 | -0.80132400 |
| H | -4.89171900 | -3.32295800 | -0.38108000 |
| H | -2.44090700 | -3.36437800 | -0.82623200 |
| H | 6.84382000 | 0.65403000 | -1.18565800 |
| H | 2.63835300 | -2.71196300 | 1.08689000 |
| H | 1.34572300 | 3.03094100 | 1.30594500 |
| C | -4.95216100 | -1.18309900 | -0.09514600 |
| C | -4.23539300 | 0.00750700 | -0.07037700 |
| H | -4.72805800 | 0.95411900 | 0.14622300 |
| N | 6.02845900 | -1.12458600 | -0.46041400 |
| H | 6.89945200 | -1.62697400 | -0.61648300 |
| N | 4.87935900 | 0.93604000 | -0.61362700 |
| H | 0.01350300 | 4.47811600 | 0.04273100 |

| | | | |
|---|---|---|---|
| N | -0.35609300 | 3.52638500 | 0.13109300 |
| H | -1.39092800 | 3.54030900 | 0.29986400 |

**c4**: DFT//B3LYP/cc-pVDZ

| | | | |
|---|---|---|---|
| C | -2.16118200 | 1.36580100 | -0.26524600 |
| C | -2.68257600 | -0.00701800 | -0.36904300 |
| Cl | -6.23153400 | -1.77215900 | 0.33038600 |
| C | -3.75988900 | -2.58880000 | -0.47131200 |
| C | -2.42007200 | -2.37649400 | -0.80253500 |
| O | -2.84738700 | 2.29267200 | 0.18187300 |
| C | 1.51657900 | 0.96649900 | 0.45219100 |
| C | 2.94062300 | -1.01252700 | 0.53009400 |
| C | 4.22478000 | -2.89023400 | 0.64049900 |
| C | 5.26001000 | -0.92492000 | -0.38785300 |
| O | 6.22181000 | -0.40959700 | -0.92539400 |
| C | 3.96985500 | -0.27535200 | -0.10189100 |
| C | 3.77000600 | 1.06817100 | -0.45000700 |
| C | 0.16060200 | 3.03021000 | 1.23353500 |
| H | -0.27271700 | 3.13133700 | 2.23489700 |
| C | -0.70249000 | 1.66115800 | -0.62843100 |
| H | -0.31426400 | 0.97928800 | -1.38908600 |
| C | -0.55497400 | 3.11660200 | -1.06407500 |
| H | -1.33894300 | 3.47537600 | -1.74167600 |
| H | 0.43711500 | 3.32898700 | -1.48039500 |
| C | 0.15079500 | 1.57508200 | 0.69590900 |
| H | -0.37948300 | 0.93361300 | 1.41106000 |
| C | 1.71643600 | -0.36588400 | 0.80003200 |
| H | 0.93716700 | -0.94843300 | 1.29503500 |
| C | 2.55743400 | 1.68519400 | -0.17818900 |
| H | 2.43170800 | 2.73476000 | -0.45269500 |
| C | -1.87671100 | -1.09332000 | -0.76035400 |
| H | -0.82673100 | -0.95672200 | -1.01739900 |
| H | -4.19155700 | -3.58920700 | -0.50910100 |
| H | -1.79850900 | -3.22257600 | -1.09811900 |
| H | 4.39271500 | -3.93678300 | 0.91226800 |
| H | 4.58923800 | 1.60323500 | -0.93180600 |
| H | 1.16530500 | 3.46835600 | 1.23175900 |
| C | -4.55884300 | -1.50375300 | -0.08489200 |
| C | -4.03206000 | -0.21902500 | -0.02529200 |
| H | -4.64658400 | 0.62521300 | 0.28325900 |
| N | 5.28085300 | -2.26295100 | 0.03779400 |
| H | 6.14856800 | -2.76800200 | -0.12771500 |
| N | 3.07986100 | -2.34264900 | 0.89974300 |
| H | -0.47642100 | 4.81605700 | 0.24014400 |
| N | -0.69257400 | 3.81443700 | 0.26209900 |
| H | -1.70282200 | 3.65739800 | 0.49487500 |

## S2.2. Computational Network Calculation

We used the Scorpion software from DesertSci (www.desertsci.com) with default program settings to calculate the interaction diagrams and atom-based score contributions for the complex of PKA with inhibitor (+)-**1p**. Details of the computational network analysis are described in the publication by Kuhn *et al*.[6]

## S2.3. Calculation of the Dipoles

The molecular electronic dipoles were calculated at the DFT:B3LYP/6-31G(d,p) level of theory in the gas phase on the molecular geometries optimized at the same level of theory.

**Figure S5.** Dipole moments aligned as seen in the X-ray co-crystal structures. Top-view on the amide···π-stacking of the fragment *N*-methylacetamide (NMAC) and the acetophenone moieties of inhibitors (+)-**1p** (I), (+)-**1l** (II), (+)-**1b** (III), and (+)-**1f** (IV). Level of theory: DFT:B3LYP/6-31G(d,p).

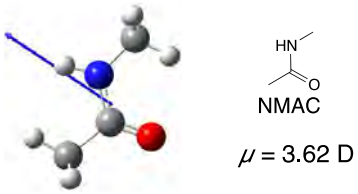


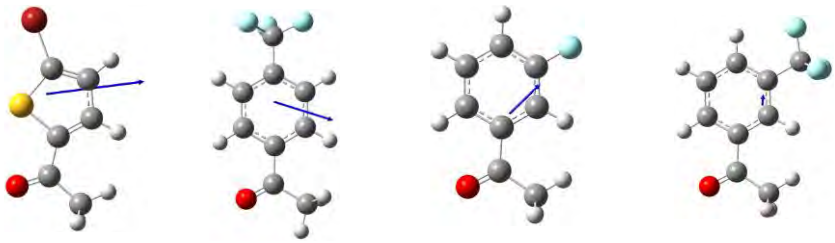

| | I | II | III | IV |
|---|---|---|---|---|
| $K_i$ / nM | 0.9 | 2 | 70 | 400 |
| $\mu$ / D | 3.56 | 2.40 | 1.47 | 0.42 |
| $<(\mu_1,\mu_2)$ / ° | 139 | 163 | 72 | 117 |

## S3. PDB Search

All Protein Data Bank (PDB) files, containing X-ray co-crystal structures with the proteins PKA, PKB, or PKA mutants (PKAB3/4/8) from *human* or *bos taurus* with a resolution ≤ 2.20 Å, were downloaded from www.rcsb.org. This yielded over 400 PDB structures. These structures were manually sorted for an open glycine-rich loop configuration and short inhibitors, which do not fully fill this pocket (allowing for a water molecule). Further criteria were the orientation of Phe54 inwards the loop and a maximal C···C (backbone) distance between the different entries in the glycine-rich loop of the different entries of 1.9 Å. These restrictions yielded 13 entries, providing a good idea about structural water molecules in this loop.

We observed in 8 of these 13 structures a water molecule face to the Phe54 ring which, taken together with our structures, give evidence for a conserved structural water molecule at this position. Figure S5 shows an overlay of some of them and the observed water molecules.

The structures analyzed were (the ones containing the W34 water were signed with *): 1JLU[7] (2.20 Å) 1Q8T[8] (2.00 Å), 1YDR[9] (2.20 Å), 2C1B[10]* (1.95 Å), 2C1A[10]* (1.95 Å), 2UW0[11]* (2.0 Å), 2UW3[12]* (1.95 Å), 2UW5[12]* (1.95 Å), 2UW7[12]* (1.95 Å), 2VO0[13]* (1.95 Å), 2VNW[13] (1.94 Å), 3OOG[14] (1.95 Å), 4AXA[15]* (1.90 Å).

**Figure S6.** Overlay of different structures analyzed from the PDB-databank. Shown in a ribbon representation are the enzymes with the following PDB ID: 2C1A[10] red, 2C1B[10] blue, 2UWO[11] green and 4AXA[15] cyan. The water molecules front to Phe54 of the corresponding entries are shown as red dots.

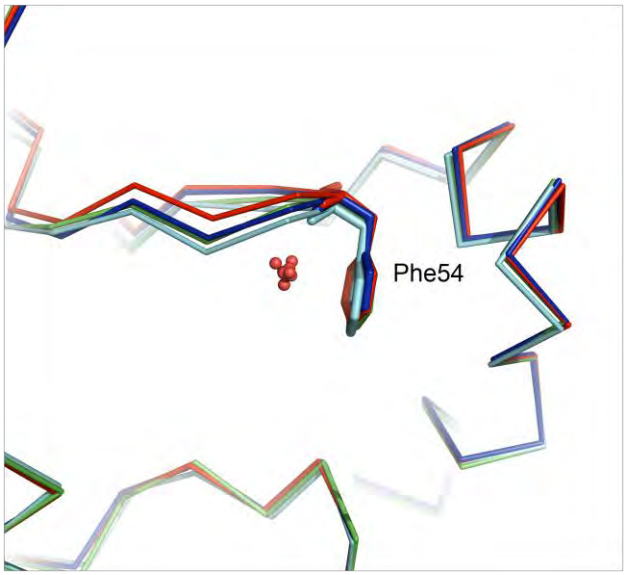

# S4. Biological Parameters

## S4.1 Assay for Affinity towards PKA and PKAB3

The Cook assay[16] was performed in 96-well microtiter plate at room temperature with a final volume of 100 µL. The assay (pH = 6.8) contains two different solutions, a reaction mixture with potassium chloride (KCl, 0.1 M), magnesium chloride ($MgCl_2$, 10 mM), phosphoenolpyruvate (1 mM), kemptide (LRRASLG, 0.1 mM), β-mercaptoethanol (1 mM), lactate dehydrogenase (15 U $mL^{-1}$), pyruvate kinase (10 U $mL^{-1}$), NADH (0.21 mM), and an enzyme mixture, containing potassium chloride (KCl, 0.1 M), MOPS (pH = 6.8), water and PKA or PKAB3 (20 nM). To this mixture, ATP (20 µM) was added to start the measurements. U = 1 µmol $min^{-1}$.

Affinities and enzyme kinetics were determined in 96-well microtiter plate in triplicate. $IC_{50}$ values were determined from the time-dependent change in absorption at λ= 340 nm during 10–15 minutes in a SpectraMax M2e microtiter plate photometer from *Molecular Devices* until there was a stable decrease over 10 minutes. Measurements with different inhibitor concentrations (10 to 14 different dilutions) were performed for the determination of the median inhibitory concentration ($IC_{50}$), and the data thus obtained were analyzed with GraphPad Prism 5 using the sigmoidal dose-response-function. $K_i$ values were calculated from their $IC_{50}$ values using the Cheng-Prusoff equation (Equation 1).[17]

$$K_i = IC_{50}/[1+([S]/K_{M,ATP})] \qquad \text{(Equation 1)}$$

Where $K_{M,ATP}$ is the Michaelis-Menten constant for ATP, identified at different concentrations; $K_{M,ATP}$(PKA) = 4 µmol and $K_{M,ATP}$(PKAB3) = 6.5 µmol and the substrate S is ATP. For Michaelis-Menten kinetics, $K_M = (k_1' + k_2) / k_1$, where $k_1$ is the rate for the formation

of the enzyme-substrate complex, $k_1$' the rate constant for the back reaction, and $k_2$ the rate constant for the catalytic process according to Equation 2.

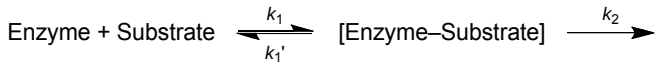

(Equation 2)

## S4.2. Protein Expression and Purification of PKA and PKAB3

The $His_6$-tagged Cα subunit of bovine PKA in pET 28b was expressed in *E.coli* (BL21(DE3)-pRARE). The cultures were grown at 37 °C in TB media containing 50 μg $mL^{-1}$ ampicillin and 34 μg $mL^{-1}$ chloramphenicol and induced at 0.7 (OD600) by adding 0.5 mM isopropyl β-D-1-thiogalactopyranoside. The Cα subunit of bovine PKA and PKAB3 were expressed in the vector pT7-7 in *E. coli* BL21(DE3)RIL cells. Cultures were grown at 37 °C in 2YT media containing 100 μg $mL^{-1}$ ampicillin and 34 μg $mL^{-1}$ chloramphenicol and induced by at 0.7 (OD600) by adding 0.5 mM isopropyl β-D-1-thiogalactopyranoside. The cultures were grown for 16 h at 23 °C. The $His_6$-tagged Cα subunit of bovine PKA pellet lysed by using binding buffer (50 mM Tris-HCl, 500 mM NaCl, pH 7.5) and purified by using an imidazole elution buffer (50 mM Tris-HCl, 500 mM NaCl, 1M imidazole, pH 7.5). The hexahistidine tag was removed by TEV digestion overnight at 4 °C. The PKAB3 and PKA phosphorylations and purification followed the procedure described by Gaßel *et al*.[18]

## S4.3. Crystallization

The catalytic domains of PKA and PKB3 with their ligands were crystallized at 4 °C in hanging drops. The droplets, containing 16 mg/ml protein 25 mM Bis-Tris-HCl, pH 7.0, 150 mM KCl, 1.5 mM octanoyl-*N*-methylglucamide and 0.8 mM PKI peptide, were equilibrated against 12–26 % (v/v) methanol. The crystals were frozen in 30 % MPD.

## S4.4. Data collection and structure determination

The crystal diffraction data were collected at the 14.1 beamline at Berlin Electron Storage Ring Society for Synchrotron Radiation (BESSY, Berlin) and at the European Synchrotron Radiation Facility (ESRF, Grenoble, France). The diffraction data were integrated and scaled by using either XDS and XSCALE[19] or with MOSFILM[20] and SCALA.[21] The molecular replacement and structure refinement were done by MOLREP, REFMAC5 and Pheoenix.[21] Coordinate and molecular topology files for ligands were created with PRODRG.[22]

## S4.5. Refinement statistic for X-ray co-crystal structures

**Table S2.** Data collection and refinement statistics of PKA complexed with (+)-**1b**, **c**, **e**, **l,** and **p**

| **Parameters** | (+)-**1c** | (+)-**1e** | (+)-**1b** | (+)-**1l** | (+)-**1p** |
|---|---|---|---|---|---|
| X-ray source | BESSY | BESSY | BESSY | ESRF | ESRF |
| Resolution (Å) | 1.76 | 2.02 | 1.95 | 1.87 | 1.93 |
| Wavelength (Å) | 0.92 | 0.92 | 0.92 | 0.87 | 0.98 |
| Space group | $P2_12_12_1$ | $P2_12_12_1$ | $P2_12_12_1$ | $P2_12_12_1$ | $P2_12_12_1$ |
| Unit cell | 72.4 75.4 80.2 90 90 90 | 71.8 74.8 79.1 90 90 90 | 72.6 75.4 80.4 90 90 90 | 72.7 75.2 80.3 90 90 90 | 72.2 74.9 80.0 90 90 90 |
| Total reflections | 554293 | 103631 | 168919 | 239220 | 57306 |
| Unique reflections | 42975 | 25822 | 32724 | 36790 | 30034 |
| Multiplicity (last shell) | 12.9 (10.1) | 4.0 (4.0) | 5.2 (5.1) | 6.5 (6.3) | 1.9 (1.9) |
| Completeness % (last shell) | 98.55 (87.24) | 90.19 (90.94) | 99.49 (98.36) | 99.21 (93.28) | 90.13 (92.18) |
| Mean I/ σ (I) | 9.5 | 5.4 | 10.2 | 4.6 | 5.5 |
| Wilson B ($Å^2$) | 23.3 | 33.8 | 23.4 | 23.5 | 25.3 |
| $R_{merge}$ (%) | 9.5 | 5.4 | 10.2 | 4.9 | 5.5 |
| $R_{meas}$ (%) | 9.9 | 6.1 | 11.3 | 5.2 | 7.8 |
| $R_{work}$ (%) | 16.7 | 16.1 | 15.5 | 16.5 | 16.4 |
| $R_{free}$ (%) | 20.1 | 20.9 | 19.0 | 20.6 | 20.1 |
| Number of non-hydrogen atoms | 3327 | 3132 | 3467 | 3448 | 3264 |
| macromolecules | 2937 | 2912 | 3006 | 2937 | 2937 |
| ligands | 33 | 33 | 41 | 56 | 33 |
| water | 357 | 187 | 420 | 455 | 294 |
| Protein residues | 357 | 357 | 357 | 360 | 358 |
| RMS-bond lengths (Å) | 0.020 | 0.008 | 0.007 | 0.018 | 0.030 |
| RMS-bond angles (°) | 1.76 | 1.03 | 0.94 | 1.71 | 1.25 |
| Ramachandran-favored (%) | 97 | 97 | 97 | 98 | 97 |
| Ramachandran-outliers (%) | 0 | 0.28 | 0.27 | 0 | 0 |
| Clashscore | 2.90 | 5.71 | 3.84 | 6.97 | 5.63 |
| Average B factor ($Å^2$) | 27.30 | 39.40 | 29.60 | 23.80 | 29.10 |
| PDB ID code | 4UJ1 | 4UJ2 | 4UJB | 4UJ9 | 4UJA |

**Table S3.** Data collection and refinement statistics of PKAB3 complexed with (+)-**1c** and **p**

| **Parameters** | (+)-**1c** | (+)-**1p** |
|---|---|---|
| X-ray source | BESSY | BESSY |
| Resolution (Å) | 1.55 | 1.80 |
| Wavelength (Å) | 0.92 | 0.92 |
| Space group | $P2_12_12_1$ | $P2_12_12_1$ |
| Unit cell | 61.9 78.4 79.5<br>90 90 90 | 82.6 61.5 79.0<br>90 90 90 |
| Total reflections | 177136 | 145987 |
| Unique reflections | 51523 | 37443 |
| Multiplicity<br>(last shell) | 3.4 (1.9) | 3.9 (3.9) |
| Completeness %<br>(last shell) | 91.5 (53.0) | 98.6 (97.1) |
| Mean I/ σ (I) | 5.94 | 10.78 |
| Wilson B (Å$^2$) | 20.78 | 26.10 |
| $R_{merge}$ (%) | 12.7 | 8.6 |
| $R_{meas}$ (%) | 14.9 | 9.9 |
| $R_{work}$ (%) | 20.9 | 18.0 |
| $R_{free}$ (%) | 23.6 | 21.8 |
| Number of non-hydrogen atoms | 3378 | 3294 |
| macromolecules | 2892 | 2885 |
| ligands | 29 | 34 |
| water | 457 | 375 |
| Protein residues | 357 | 357 |
| RMS-bond lengths (Å) | 0.010 | 0.026 |
| RMS-bond angles (°) | 1.11 | 1.01 |
| Ramachandran-favored (%) | 97 | 97 |
| Ramachandran-outliers (%) | 0 | 0 |
| Clashscore | 2.99 | 6.99 |
| Average B factor (Å$^2$) | 27.00 | 31.40 |
| PDB ID code | 4Z84 | 4Z83 |

# S5. Synthesis

## S5.1 Materials and General Procedures

Commercially available chemicals were purchased from *Aldrich*, *Acros*, *Fluka*, *ABCR*, and *Strem* and used without further purification. Solvents for extraction or flash column chromatography (FC) were of technical quality and distilled before use. Dry solvents (DMF, $CH_2Cl_2$, 1,4-dioxane, THF and toluene) for reactions were purified by a solvent drying system from *LC Technology Solutions Inc. SP-105* under nitrogen atmosphere ($H_2O$ content < 10 ppm as determined by *Karl-Fischer* titration). Other solvents were purchased in *p.a* quality. All reactions were carried out under argon or nitrogen atmosphere and in oven-dried glassware unless otherwise stated. All products were dried under high vacuum ($10^{-2}$ Torr) before analytical characterization. Analytical thin-layer chromatography (TLC) was conducted on glass sheets coated with $SiO_2$-60 $UV_{254}$ obtained from *Merck* and visualized with a UV lamp (245 nm) or by staining with $KMnO_4$ solution ($KMnO_4$ (1.5g), $K_2CO_3$ (10g), 5% NaOH (2.5mL) in $H_2O$ (150 mL)). Flash chromatography (FC) was carried out using $SiO_2$-60 (particle size 0.040–0.063 mm, 230–400 mesh) from *Fluka* with a head pressure of 0.1–0.4 bar. The eluent are reported in parentheses for each compound. Liquid chromatography/mass spectrometry (LC/MS) for reaction control was performed on a *Ultimate 3000* series LC instrument combined with a MSQ Plus mass spectrometer from *Dionex*, using *Zorbax Eclipse Plus C18* columns (30 x 3; 3.5µm pore size) from *Agilent*. Medium-pressure liquid chromatography (MPLC) was carried out using $SiO_2$ *RediSep Rf columns* (particle size 0.040–0.063mm, 230–400 mesh) from *Teledyne ISCO* on a Combiflash Rf 200 from *Teledyne ISCO*. High-pressure column chromatography (HPLC) was run on a *Merck-Hitachi L-6250* Intelligent Pump equipped with a *Merck-Hitachi L-4000* UV detector on either a chiral Reprosil column (Reprosil Chiral-NR 8µm, 250 x 20 mm; *Dr. Maisch GmbH*) or an amino phase column (LiChrospher HiBar, 250 x 25 mm, 100 NH2 (5~µm); *Merck*). Melting points (m.p.) were determined in open capillaries on a *Büchi B-540* capillary

melting point apparatus and are uncorrected. IR Spectra were recorded on a *Perkin-Elmer FT-IR 1600* spectrometer (*ATR-unit, Attenuated Total Reflection*). The spectra were measured between 4000–600~$cm^{-1}$, and absorption bands are reported in wavenumbers ($cm^{-1}$). NMR spectra (1H, 13C, 10F and 31 P) were measured on a *Varian Gemini-300*, *Mercury-300*, *Bruker ARX-300*, *AV-400*, *DRX-400, DRX-500* or *AV-600* spectrometer at 298~K using the solvent peak as an internal reference. Chemical shifts are reported in ppm, and the coupling constants (*J*) are given in Hz. The resonance multiplicity is described as s (singlet), d (doublet), t (triplet), q (quartet), quint. (quintet), m (multiplet) and br. (broad). High-resolution mass spectroscopy spectra were measured on a *Bruker maXis ESI-Q-TOF* (HR-MS (ESI)) spectrometer. The relevant signals are reported in *m/z* units and relative intensities given in parenthesis. Elemental analyses were performed by the Mikrolabor at the Laboratorium für Organische Chemie, ETH Zurich. Nomenclature follows the suggestions of the computer program *ACD/Name* version 12.5 *(Advanced Chemistry Development Inc*.).

## S5.2 Synthetic Procedures

**(3*R*,4*S*)-3-Benzoyl-4-(4-oxo-3,4-dihydroquinazoline-7-yl)pyrrolidinium Chloride ((+)-1a).**

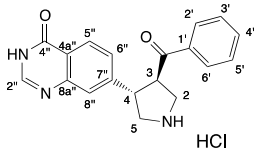


GP-D starting from pyrrolidine (+)-**13a** (10 mg, 0.027 mmol) gave pyrrolidinium salt (+)-**1a** (6 mg, 70%) as a yellow solid.

Prep. HPLC: $t_R$ = 10 min (amino phase: LiChrospher 100 $NH_2$ (5 □m); 15 mL $min^{-1}$, MeOH/$CHCl_3$ 10:90); m.p. 164 °C (decomp.); $[a]_D^{20}$ = +83.3 (*c* = 0.05 in MeOH); $^1$H NMR (600 MHz, $(CD_3)_2SO$); assignment based on HSQC and HMBC spectra): $\delta$ = 3.38–3.48 (m, 2 H; $H_a$–C(2), $H_a$–C(5) (overlay with the $(CD_3)_2SO$-signal), 3.78–3.84 and 3.85–3.91 (2 m, 3 H; $H_b$–C(2), $H_b$–C(5)), 3.91 (q, *J* = 9.5 Hz, 1 H; H–C(4)), 4.63 (q, *J* = 9.1 Hz, 1 H; H–C(3)), 7.45–7.48 (m, 2 H; H–C(3')), 7.55 (dd, *J* = 8.3, 1.7 Hz, 1 H; H–C(6")), 7.61 (tt, *J* = 7.7, 1.2 Hz, 1 H; H–C(4')), 7.68 (d, *J* = 1.7, 1 H; H–C(8")), 7.82 (dd, *J* = 8.5, 1.2 Hz, 2 H; H–C(2')), 8.05 (d, *J* = 8.2, 1 H; H–C(5")), 8.11 (s, 1 H; H–C(2")), 9.38 and 9.57 (2 br. s, 2 H; $H_2N$), 12.29 ppm (br. s, 1 H; H–N(3)); $^{13}$C NMR (150 MHz, $(CD_3)_2SO$); assignment based on HSQC and HMBC spectra): $\delta$ = 46.38 (C(4)), 47.58 (C(2)), 50.77 (C(5)), 50.79 (C(3)), 121.70 (C(4a")), 126.04 (C(8")), 126.40 (C(5")), 126.53 (C(6")), 128.45 (C(3')), 128.85 (C(2')), 134.02 (C(4')), 135.47(C(1')), 144.84 (C(2")), 145.97 (C(7")), 148.67 (C(8a")), 160.32 (C(4")), 197.35 ppm (C=O). IR (ATR): $\tilde{n}$ = 3357 (br.), 3037 (m), 2919 (m), 2850 (m), 2738 (br.), 1715 (s), 1671 (s), 1656 (s), 1618 (s), 1594 (m), 1575 (m), 1497 (w), 1447 (m), 1355 (w), 1243 (m), 1060 (w), 1000 (w), 851 (m), 781 (m), 689 $cm^{-1}$ (s); HR-MS (ESI) *m/z* (%): 320.1394 (100, $[M + H]^+$, calcd for $C_{19}H_{18}N_3O_2^+$: 320.1394).

**(3*S*,4*R*)-3-Benzoyl-4-(4-oxo-3,4-dihydroquinazoline-7-yl)pyrrolidinium Chloride ((–)-1a).**

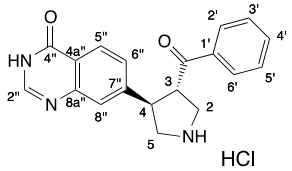


GP-D starting from pyrrolidine (–)-**13a** (10 mg, 0.027 mmol) gave pyrrolidinium salt (–)-**1a** (6 mg, 70%) as a yellow solid.

$[a]_D^{20}$ = –85.5 (*c* = 0.05 in MeOH); $^1$H NMR and HR-MS (ESI) data consistent with (+)-**1a**.

**(3*S*,4*R*)-3-(3-Fluorobenzoyl)-4-(4-oxo-3,4-dihydroquinazolin-7-yl)pyrrolidinium Chloride ((–)-1b).**

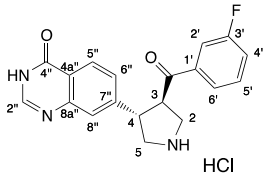


GP-D starting from pyrrolidine (–)-**13b** (10 mg, 0.022 mmol) gave pyrrolidinium salt (–)-**1b** (6 mg, 70%) as a yellow solid.

Prep. HPLC: $t_R$ = 11 min (amino phase: LiChrospher 100 $NH_2$ (5 □m); 15 mL min$^{-1}$, MeOH/$CHCl_3$ 10:90); m.p. 192 °C (decomp.); $[a]^D_{20}$ = –74.9 (*c* = 0.05 in MeOH); $^1$H NMR (600 MHz, $(CD_3)_2SO$): $\delta$ = 3.38–3.51 (m, 2 H; $H_a$–C(4) $H_a$–C(5)), 3.77–3.91 (m, 3 H; H–C(2), $H_b$–C(4), $H_b$–C(5)), 4.62 (q, *J* = 9.2 Hz, 1 H; H–C(3)), 7.47 (tdd, $^3J$(H,F) = 8.4 Hz, *J* = 2.6, 1.1 Hz, 1 H; H–C(4')), 7.50 (td, $^4J$(H,F) = 2.4 Hz, *J* = 7.5 Hz, 1 H; H–C(5')), 7.56 (dd, *J* = 8.2, 1.8 Hz, 1 H; H–C(6")), 7.57 (ddd, $^3J$(H,F) = 9.8 Hz, *J* = 2.5, 1.5 Hz, 1 H; H–C(2')), 7.65 (dt, *J* = 7.6, 1.3 Hz, 1 H; H–C(6')), 7.68 (d, *J* = 1.7, 1 H; H–C(8")), 8.04 (d, *J* = 8.2 Hz, 1 H; H–C(5")), 8.14 (s, 1 H; H–C(2")), 9.48 and 9.68 (2 br. s, 2 H; $H_2N^+$), 12.29 ppm (br. s, 1 H; HN(3)); $^{13}$C NMR (150

MHz, $(CD_3)_2SO$): $\delta$ = 46.35 (C(4)), 47.34 (C(2)), 50.74 (C(5)), 51.12 (C(3)), 114.97 (d, $^2J$(C,F) = 22.6 Hz; C(4')), 120.85 (d, $^2J$(C,F) = 21.3 Hz; C(2')), 121.67 (C(4a")), 124.65 (d, $^4J$(C,F) = 2.3 Hz; C(6')), 125.92 (C(8")), 126.42 (C(5")), 126.60 (C(6")), 131.06 (d, $^3J$ C,F) = 7.8 Hz; C(5')), 137.74 ($^3J$(C,F) = 6.3 Hz; C(1')), 144.74 (C(7")), 146.08 (C(2")), 148.40 (C(8a")), 160.27 (C(4")), 162.05 ($^1J$(C,F) = 245.7 Hz; C(3')), 196.39 ppm (C=O); $^{19}$F NMR (376 MHz; $(CD_3)_2SO$): $\delta$ = (–112.05)–(–112.10) ppm (m, 1 F); IR (ATR): $\tilde{\eta}$ = 3367 (br.), 3040 (m), 2607 (br.), 1714 (s), 1672 (s), 1655 (s), 1619 (m), 1573 (m),1499 (w), 1446 (m), 1355 (w), 1300 (m), 1245 (m), 995 (w), 886 (m), 781 (m), 688 cm$^{-1}$ (s); HR-MS (ESI) m/z (%): 339.1326 (30, [$M$ + H]$^+$, calcd for $C_{19}H_{17}FN_3O_2^+$: 339.1321), 338.1294 (100, [$M$ + H]$^+$, calcd for $C_{19}H_{17}FN_3O_2^+$: 338.1299).

**(3*R*,4*S*)-3-(3-Fluorobenzoyl)-4-(4-oxo-3,4-dihydrocquinazolin-7-yl)pyrrolidinium Chloride ((+)-1b).**

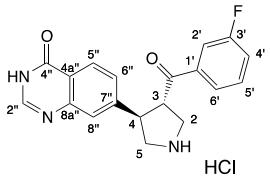


GP-D starting from pyrrolidine (+)-**13b** (10 mg, 0.022 mmol) gave pyrrolidinium salt (+)-**1b** (6 mg, 70%) as a yellow solid.

$[a]^D_{20}$ = +70.7 ($c$ = 0.05 in MeOH); $^1$H NMR and HR-MS (ESI) data consistent with (–)-**1b**.

**(3*S*,4*R*)-3-(3-Chlorobenzoyl)-4-(4-oxo-3,4-dihydroquinazolin-7-yl)pyrrolidinium Chloride ((–)-1c).**

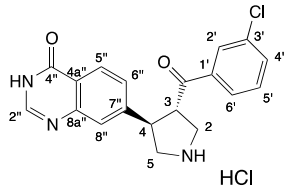


GP-D starting from pyrrolidine (–)-**13c** (10 mg, 0.021 mmol) gave pyrrolidinium salt (–)-**1c** (7 mg, 89%) as a white solid.

Prep. HPLC: $t_R$ = 10 min (amino phase: LiChrospher 100 $NH_2$ (5 □m); 15 mL $min^{-1}$, MeOH/$CHCl_3$ 10:90); m.p. 204 °C (decomp.); $[a]^D_{20}$ = –70.5 (*c* = 0.05 in MeOH); $^1$H NMR (600 MHz, $(CD_3)_2SO$); assignment based on HSQC and HMBC spectra): $\delta$ = 3.47–3.54 (m, 2 H; $H_a$–C(2), $H_a$–C(5)), 3.75–3.89 (m, 3 H; $H_b$–C(2), $H_b$–C(5), H–C(4)), 4.62 (q, *J* = 9.0 Hz, 1 H; H–C(3)), 7.48 (t, *J* = 7.9 Hz, 1 H; H–C(5')), 7.54 (dd, *J* = 8.3, 1.8 Hz, 1 H; H–C(6")), 7.65 (ddd, *J* = 8.0, 2.2, 1.0 Hz, 1 H; H–C(4')), 7.68 (d, *J* = 1.8 Hz, 1 H; H–C(8")), 7.70 (t, *J* = 1.9 Hz, 1 H; H–C(2')), 7.74 (dt, *J* = 7.8, 1.3 Hz, 1 H; H–C(6')), 8.05 (d, *J* = 8.2 Hz, 1 H; H–C(5")), 8.13 (s, 1 H; H–C(2")), 9.44 and 9.63 (2 br. s, 2 H; $H_2N^+$), 12.31 ppm (br. s, 1 H; H–N(3'')); $^{13}$C NMR (150 MHz, $(CD_3)_2SO$); assignment based on HSQC and HMBC spectra): $\delta$ = 46.53 (C(4)), 47.24 (C(2)), 50.81 (C(5)), 51.25 (C(3)), 121.76 (C(4a")), 126.02 (C(6')), 126.42 (C(8")), 126.60 (C(5")), 126.98 (C(6")), 128.25 (C(4')), 130.76 (C(5')), 133.52, 133.65, 137.37, 144.71 (C(7")), 146.04 (C(2")), 148.50 (C(8a")), 160.30 (C(4")), 196.40 ppm (C=O); IR (ATR): $\tilde{n}$ = 3355 (br.), 3037 (w), 2920 (m), 2851 (m), 2607 (br.), 1714 (s), 1678 (s), 1654 (s), 1619 (s), 1595 (m), 1573 (m), 1498 (w), 1447 (w), 1355 (w), 1299 (m), 1239 (m), 1060 (w), 100 (w), 851 (w), 781 (m), 688 (s), 635 $cm^{-1}$ (w); HR-MS (ESI) *m/z* (%): 356.0980 (37, $[M + H]^+$, calcd for $C_{19}H_{17}{}^{37}ClN_3O_2^+$: 356.0980), 354.1004 (100, $[M + H]^+$, calcd for $C_{19}H_{17}{}^{35}ClN_3O_2^+$: 354.1004).

**(3*R*,4*S*)-3-(3-Chlorobenzoyl)-4-(4-oxo-3,4-dihydroquinazolin-7-yl)pyrrolidinium Chloride ((+)-1c).**

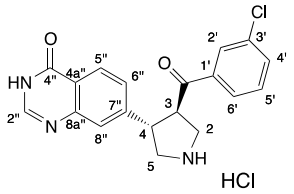


GP-D starting from pyrrolidine (+)-**13c** (10 mg, 0.021 mmol) gave pyrrolidinium salt (+)-**1c** (7 mg, 89%) as a white solid.

$[a]^{D}_{20}$ = +77.5 (*c* = 0.05 in MeOH); $^{1}$H NMR and HR-MS (MALDI) data consistent with (–)-**1c**.

**(3*R*,4*S*)-3-(3-Bromobenzoyl)-4-(4-oxo-3,4-dihydroquinazoline-7-yl)pyrrolidinium Chloride ((+)-1d).**

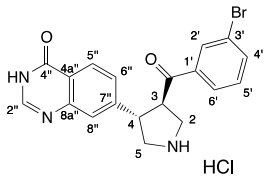


GP-D starting from pyrrolidine (+)-**13d** (10 mg, 0.020 mmol) gave pyrrolidinium salt (+)-**1d** (6 mg, 70%) as a yellow solid.

Prep. HPLC: $t_R$ = 12 min (amino phase: LiChrospher 100 $NH_2$ (5 □m); 15 mL min$^{-1}$, MeOH/$CHCl_3$ 10:90); m.p. 181 °C (decomp.); $[a]_D^{20}$ = +73.9 (*c* = 0.05 in MeOH); $^{1}$H NMR (600 MHz, $(CD_3)_2SO$); assignment based on HSQC and HMBC spectra): $\delta$ = 3.38 (q, *J* = 7.0 Hz, 1 H; H–C(4)), 3.72–3.90 (m, 4 H; $H_a$–C(2), $H_a$–C(5)), 4.61 (q, *J* = 8.7 Hz, 1 H; H–C(3)), 7.41 (td, *J* = 7.8, 0.6 Hz, 1 H; H–C(5')), 7.53 (dd, *J* = 8.3, 1.8 Hz, 1 H; H–C(6")), 7.68 (d, *J* = 1.7, 1 H; H–C(8")), 7.74–7.81 (m, 3 H; H–C(2'), H–C(4'), H–C(6')), 8.04 (dd, *J* = 8.2, 0.5 Hz, 1 H; H–C(5")), 8.12 (s, 1 H; H–C(2")), 9.43 and 9.61 (2 br. s, 2 H; $H_2N^+$), 12.31 ppm (br. s, 1 H; H–N(3'')); $^{13}$C NMR (150 MHz, $(CD_3)_2SO$); assignment based on HSQC and HMBC spectra): $\delta$ = 46.59 (C(4)), 47.21 (C(2)), 50.83 (C(5)), 51.26 (C(3)), 121.80 (C(4a")), 122.04 (C(3')), 126.04 (C(8")),

126.41 (C(5")), 126.57 (C(6")), 127.29 (C(5')), 130.95 (C(6')), 131.16 (C(2')), 136.37 (C(4')), 137.53 (C(1')), 144.68 (C(2")), 146.00 (C(7")), 148.58 (C(8a")), 160.30 (C(4")), 196.34 ppm (C=O); IR (ATR): $\tilde{n}$ = 3357 (br.), 3037 (m), 2922 (m), 2852 (m), 2719 (br.), 1714 (s), 1682 (s), 1654 (s), 1618 (s), 1567 (s),1498 (w), 1464 (m), 1422 (m), 1355 (w), 1299 (m), 1237 (m), 1212 (m), 1061 (w), 996 (w), 886 (m), 781 (m), 723 (w), 688 $cm^{-1}$ (s); HR-MS (ESI) m/z (%): 400.0479 (90, $[M + H]^+$, calcd for $C_{19}H_{17}{}^{81}BrN_3O_2^+$: 400.0479), 398.0497 (100, $[M + H]^+$, calcd for $C_{19}H_{17}{}^{79}BrN_3O_2^+$: 398.0499).

**(3*S*,4*R*)-3-(3-Bromobenzoyl)-4-(4-oxo-3,4-dihydroquinazolin-7-yl)pyrrolidinium Chloride ((–)-1d).**

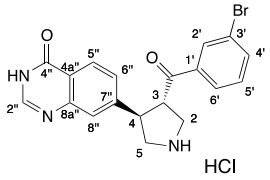


GP-D starting from pyrrolidine (–)-**13d** (10 mg, 0.020 mmol) gave pyrrolidinium salt (–)-**1d** (6 mg, 70%) as a yellow solid.

$[a]^{D}_{20}$ = –78.0 (*c* = 0.05 in MeOH); $^1$H NMR and HR-MS (ESI) data consistent with (+)-**1d**.

**(3*R*,4*S*)-3-(3-Iodobenzoyl)-4-(4-oxo-3,4-dihydroquinazolin-7-yl)pyrrolidinium Chloride ((+)-1e).**

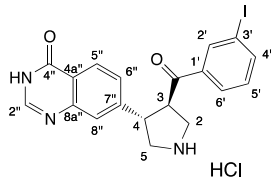


GP-D starting from pyrrolidine (+)-**13e** (10 mg, 0.018 mmol) gave pyrrolidinium salt (+)-**1e** (8 mg, 92%) as a yellow solid. This compound is unstable and shows impurities in the spectra. Prep. HPLC: $t_R$ = 16 min (amino phase: LiChrospher 100 $NH_2$ (5 □m); 15 mL $min^{-1}$, MeOH/$CHCl_3$ 10:90); $[a]_D^{20}$ = +67.5 ($c$ = 0.1 in MeOH); $^1$H NMR (600 MHz, $(CD_3)_2SO$): $\delta$ = 3.38–3.55 (m, 2 H), 3.75–3.94 (m, 2 H), 4.55–4.66 (m, 2 H), 7.24 (t, $J$ = 7.8 Hz, 1 H), 7.46 (br. t, $J$ = 7.5 Hz, 2 H), 7.51 (dd, $J$ = 8.3, 1.7 Hz, 1 H), 7.55 (dd, $J$ =8.3, 1.8 Hz, 1 H), 7.61 (t, $J$ = 7.4 Hz, 1 H), 7.68 (br. t, $J$ = 7.4 Hz, 1 H), 7.79 (ddd, $J$ = 7.9, 1.7, 1.0 Hz, 1 H), 7.80–7.84 (m, 2 H), 7.89–7.94 (m, 2 H), 8.05 (d, $J$ = 8.3 Hz, 2 H), 8.12 (d, $J$ =1.3 Hz, 1 H), 9.39 (br. s, 1 H), 9.52 (br. s, 1 H), 12.30 ppm (br. s, 1 H); HR-MS (MALDI) *m/z* (%): 446.0360 (100, $[M + H]^+$, calcd for $C_{19}H_{17}IN_3O_2^+$: 446.0360).

**(3*S*,4*R*)-3-(3-Iodobenzoyl)-4-(4-oxo-3,4-dihydroquinazolin-7-yl)pyrrolidinium Chloride ((–)-1e).**

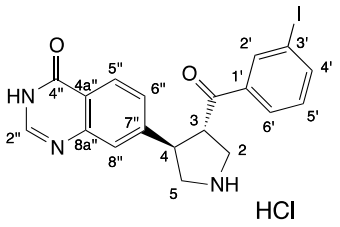


GP-D starting from pyrrolidine (–)-**13e** (10 mg, 0.018 mmol) gave pyrrolidinium salt (–)-**1e** (9 mg, 94%) as a yellow solid. This compound is unstable and shows impurities in the spectra. $[a]_D^{20}$ = –64.3 ($c$ = 0.1 in MeOH); $^1$H NMR and HR-MS (ESI) data consistent with (–)-**1e**.

**(3*R*,4*S*)-3-[(3-Trifluoromethoxy)benzoyl]-4-(4-oxo-3,4-dihydroquinazolin-7-yl)pyrrolidinium Chloride ((–)-1f).**

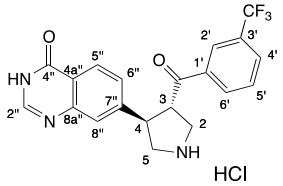


GP-D starting from pyrrolidine (–)-**13f** (6 mg, 0.012 mmol) gave pyrrolidinium salt (–)-**1f** (6 mg, 70%) as a yellow solid.

Prep. HPLC: $t_R$ = 20 min (amino phase: LiChrospher 100 $NH_2$ (5 □m); 15 mL min$^{-1}$, MeOH/$CHCl_3$ 10:90); m.p. 178 °C (decomp.); $[a]^D_{20}$ = –48.7 ($c$ = 0.05 in MeOH); $^1$H NMR (600 MHz, $(CD_3)_2SO$); assignment based on HSQC and HMBC spectra): $\delta$ = 3.56–3.70 (m, 2 H; $H_a$–C(2), $H_a$–C(5)), 3.78–3.86 (m, 3 H; $H_b$–C(2), $H_b$–C(5), H–C(4)), 4.61 (q, $J$ = 8.5 Hz, 1 H; H–C(3)), 7.51 (dd, $J$ = 8.3, 1.8 Hz, 1 H; H–C(6")), 7.68 (d, $J$ = 1.8 Hz, 1 H; H–C(8")), 7.69 (t, $J$ = 7.8 Hz, 1 H; H–C(5')), 7.83 (br. s, 1 H; H–C(2')), 7.92 (br. d, $J$ = 7.9 Hz, 1 H; H–C(4')), 8.01 (d, $J$ = 8.3 Hz, 1 H; H–C(5")), 8.06 (br. d, $J$ = 8.0 Hz, 1 H; H–C(6')), 8.09 (s, 1 H; H–C(2")), 9.40

and 9.56 (2 br. s, 2 H; $H_2N^+$), 12.26 ppm (br. s, 1 H; H–N(3'')); $^{13}$C NMR (150 MHz, $(CD_3)_2SO$); assignment based on HSQC and HMBC spectra): $\delta$ = 46.89 (C(4)), 47.13 (C(2)), 50.70 (C(5)), 51.44 (C(3)), 121.81 (C(4a")), 123.49 (q, $^1J$(C,F) = 272.2 Hz, $CF_3$), 124.95 (q, $^3J$(C,F) = 3.7 Hz; C(2')), 126.22 (C(8")), 126.37 (C(5")), 126.49 (C(6")), 129.23 (q, $^2J$(C,F) = 32.2 Hz; C(3')), 130.07 (q, $^3J$(C,F) = 3.4 Hz; C(4')), 130.07 (C(5')), 132.19 (C(6')), 136.32 (C(1')), 144.54 (C(2")), 145.87 (C(7")), 148.83 (C(8a")), 160.31 (C(4")), 196.56 ppm (C=O); $^{19}$F NMR (376 MHz, $(CD_3)_2SO$): $\delta$ = –61.78 ppm (s, 3 F; $CF_3$); IR (ATR): $\tilde{\nu}$ = 3363 (br.), 2919 (m), 2850 (m), 2719 (br.), 1716 (s), 1687 (s), 1655 (s), 1612 (s), 1573 (m),1499 (w), 1435 (m), 1329 (s), 1234 (w), 1167 (m), 1122 (s), 1072 (s), 891 (w), 851 (m), 814 (m), 782 (w), 732 (w), 691 cm$^{-1}$ (s); HR-MS (MALDI): 388.1267 (37, $[M + H]^+$, calcd for $C_{20}H_{17}F_3N_3O_2^+$: 388.1267).

**(3*S*,4*R*)-3-[(3-Trifluoromethoxy)benzoyl]-4-(4-oxo-3,4-dihydroquinazolin-7-yl)pyrrolidinium Chloride ((+)-1f)**.

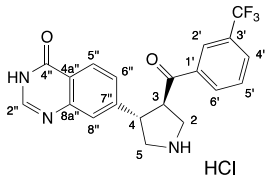


GP-D starting from pyrrolidine (+)-**13f** (6 mg, 0.012 mmol) gave pyrrolidinium (+)-**1f** (6 mg, 70%) as a yellow solid.

$[a]^D_{20}$ = +49.6 ($c$ = 0.05 in MeOH); $^1$H NMR and HR-MS (MALDI) data consistent with (–)-**1f**.

**(3*R*,4*S*)-3-[(3-Trifluormethoxy)benzoyl]-4-(4-oxo-3,4-dihydroquinazolin-7-yl)pyrrolidinium Chloride ((–)-1g).**

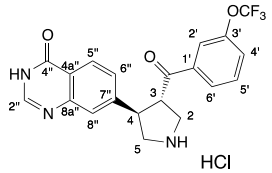


GP-D starting from pyrrolidine (–)-**13g** (10 mg, 0.019 mmol) gave pyrrolidinium (–)-**1g** (8 mg, quant.) as a yellow solid.

Prep. HPLC: $t_R$ =20 (amino phase: LiChrospher 100 $NH_2$ (5 □m); 15 mL $min^{-1}$, MeOH/$CHCl_3$ 10:90); m.p. 178 °C (decomp.); $[a]^D_{20}$ = –78.2 (*c* = 0.05 in MeOH); $^1$H NMR (400 MHz, $(CD_3)_2SO$): $\delta$ = 3.40–3.57 (m, 2 H; $H_a$–C(2), $H_a$–C(5)), 3.82–3.89 (m, 3 H; $H_b$–C(2), $H_b$–C(5), H–C(4)), 4.64 (q, *J* = 8.8 Hz, 1 H; H–C(3)), 7.55 (dd, *J* = 8.3, 1.8 Hz, 1 H; H–C(6")), 7.59–7.62 (m, 3 H; H–C(2'), H–C(4'), H–C(5')), 7.69 (d, *J* = 1.7 Hz, 1 H; H–C(8")), 7.78–7.85 (m, 1 H; H–C(6')), 8.01 (d, *J* = 8.2 Hz, 1 H; H–C(5")), 8.13 (s, 1 H; H–C(2")), 9.47 and 9.67 (2 br. s, 2 H; $H_2N^+$), 12.30 ppm (br. s, 1 H; H–N(3'')); $^{13}$C NMR (150 MHz, $(CD_3)_2SO$): $\delta$ = 46.63 (C(4)), 47.29 (C(2)), 50.81 (C(5)), 51.29 (C(3)), 119.65, 120.62, 121.72, 122.87, 125.95, 130.67, 131.06, 137.63, 144.63, 146.01, 148.45, 160.25, 196.37 ppm (C=O); IR (ATR): $\tilde{n}$ = 3374 (br.), 2920 (m), 2851 (m), 2744 (br.), 1716 (s), 1686 (s), 1655 (s), 1620 (m), 1573 (m), 1442 (w), 1358 (w), 1246 (s), 1209 (s), 1155 (s), 1058 (w), 1013 (w), 889 (m), 849 (w), 782 (m), 733 (w), 690 (m), 632 $cm^{-1}$ (w); HR-MS (MALDI): 404.1216 (100, $[M + H]^+$, calcd for $C_{20}H_{17}F_3N_3O_3^+$: 404.1217).

**(3*S*,4*R*)-3-[(3-Trifluoromethoxy)benzoyl]-4-(4-oxo-3,4-dihydroquinazolin-7-l)pyrrolidinium Chloride ((+)-1g).**

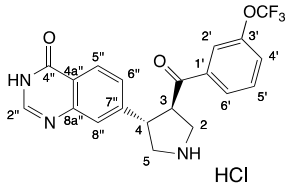


GP-D starting from pyrrolidine (+)-**13g** (10 mg, 0.019 mmol) gave pyrrolidinium salt (+)-**1g** (6 mg, 70%) as a yellow solid.

$[a]^{D}_{20}$ = +76.9 (*c* = 0.05 in MeOH); $^{1}$H NMR and HR-MS (MALDI) data consistent with (–)-**1g**.

**(3*R*,4*S*)-3-(4-Fluorobenzoyl)-4-(4-oxo-3,4-dihydroquinazolin-7-yl)pyrrolidinium Chloride ((+)-1h).**

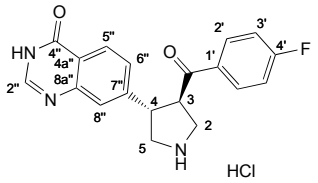


GP-D starting from pyrrolidine (+)-**13h** (30 mg, 0.07 mmol) gave pyrrolidinium salt (+)-**1h** (12 mg, 48%) as a white solid.

Prep. HPLC: $t_R$ = 25 (amino phase: LiChrospher 100 $NH_2$ (5 □m); 15 mL $min^{-1}$, MeOH/$CHCl_3$ 10:90); m.p. 138 °C (decomp.); $[a]_D^{20}$ = +86.4 (*c* = 0.1 in MeOH); $^{1}$H NMR (400 MHz, $(CD_3)_2SO$; assignment based on HSQC and HMBC spectra of (+)-**1h**): $\delta$ = 3.31–3.54 (m, 2 H; $H_a$–C(4), $H_a$–C(5)), 3.76–3.98 (m, 2 H; $H_b$–C(2), $H_b$–C(5)), 3.94 (dd, *J* = 18.0, 10.4 Hz, 1 H; H–C(4)), 4.66 (q, *J* = 9.0 Hz, 1 H; H–C(3)), 7.31 (t and higher order splittings, *J* = 8.8 Hz, $^{3}J$(H,F) = 8.8 Hz, 2 H; H–C(3')), 7.66 (dd, *J* = 8.3, 1.7 Hz, 1 H; H–C(6'')), 7.72 (d, *J* = 1.6 Hz, 1 H; H–C(8'')), 7.92 (dd and higher order splittings, *J* = 9.0 Hz, $^{4}J$(H,F) = 5.4 Hz, 2 H; H–C(2')), 8.08 (d, *J* = 8.3 Hz, 1 H; H–C(5'')), 8.42 (s, 1 H; H–C(2'')), 9.78 and 10.07 (2 br. s, 2 H; $H_2N^+$), 12.1–13.5 ppm (br. s, 1 H; H–N(3'')); $^{13}$C NMR (100 MHz, $(CD_3)_2SO$; assignment based on HSQC and HMBC spectra of (+)-**1h**): $\delta$ = 46.78 (C(4)), 47.84 (C(2 or 5)), 50.88 (C(2 or 5)),

51.42 (C(3)), 116.44 (d, $^{2}J$(C,F) = 21.9 Hz; C(3')), 121.77 (C(4a'')), 124.95 (C(8'')), 127.15 (C(5'')), 127.46 (C(6'')), 132.00 (d, $^{3}J$(C,F) = 9.7 Hz; C(2')), 132.83 (d, $^{4}J$(C,F) = 2.7 Hz; C(1')), 145.78 (C(7'')), 146.54 (C(2'')), 147.37 (C(8a'')), 160.36 (C(4'')), 165.84 (d, $^{1}J$(C,F) = 251.8 Hz; C(4')), 196.22 ppm (C=O); $^{19}$F NMR (376 MHz, $(CD_3)_2SO$): $\delta$ = –104.52 ppm (tt, $^{3}J$(F,H) = 8.6 Hz, $^{4}J$(F,H) = 5.3 Hz, 1 F; F–C(4')); IR (ATR): $\tilde{n}$ = 3600–2200 (m), 3379 (w), 3038 (m), 2900 (m), 2709 (m), 2640 (m), 2601 (m)), 1712 (s), 1679 (s), 1655 (s), 1595 (s), 1572 (s), 1505 (m), 1463 (w), 1411 (m), 1355 (m), 1299 (m), 1231 (m), 1157 (m), 1058 (w), 1035 (w), 846 (s), 782 (m), 735 (w), 689 cm$^{-1}$ (m); HR-MS (ESI): *m/z* (%): 338.1300 (100, $[M + H]^+$, calcd for $C_{19}H_{17}FN_3O_2^+$: 338.1299).

**(3*S*,4*R*)-3-(4-Fluorobenzoyl)-4-(4-oxo-3,4-dihydroquinazolin-7-yl)pyrrolidinium Chloride ((–)-1h).**

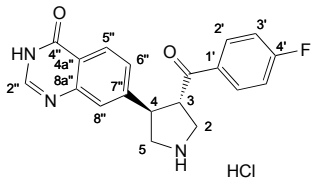


GP-D starting from pyrrolidine (–)-**13h** (24 mg, 0.05 mmol) gave pyrrolidinium salt (–)-**1h** (19 mg, 91%) as a white solid.

$[a]_D^{20}$ = –80.2 (*c* = 0.1 in MeOH); $^{1}$H NMR and HR-MS (ESI) data consistent with (+)-**1h**

**(3*R*,4*S*)-3-(4-Chlorobenzoyl)-4-(4-oxo-3,4-dihydroquinazolin-7-yl)pyrrolidinium Chloride ((+)-1i).**

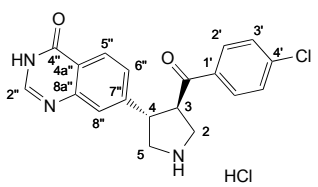

GP-D starting from pyrrolidine (+)-**13i** (20 mg, 0.04 mmol) gave pyrrolidinium salt (+)-**1i** (12 mg, 72%) as a white solid.

$[a]_D^{20}$ = +77.5 ($c$ = 0.1 in MeOH); $^1$H NMR and HR-MS (ESI) data consistent with (–)-**1i**.

**(3*S*,4*R*)-3-(4-Chlorobenzoyl)-4-(4-oxo-3,4-dihydroquinazolin-7-yl)pyrrolidinium Chloride ((–)-1i).**

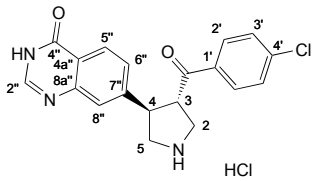


GP-D starting from pyrrolidine **13i** (20 mg, 0.04 mmol) gave pyrrolidinium salt (–)-**1i** (8 mg, 48%) as a white solid.

Prep. HPLC: $t_R$ = 16 min (amino phase: LiChrospher 100 $NH_2$ (5 □m); 15 mL min$^{-1}$, MeOH/$CHCl_3$ 10:90); m.p. 177 °C (decomp.); $[a]_D^{20}$ = –86.1 ($c$ = 0.1 in MeOH); $^1$H NMR (400 MHz, $(CD_3)_2SO$; assignment based on HSQC and HMBC spectra): $\delta$ = 3.36–3.49 (m, 2 H; $H_a$–C(2), $H_a$–C(5)), 3.75–3.97 (m, 3 H; $H_b$–C(2), H–C(4), $H_b$–C(5)), 4.64 (dd, $J$ = 17.6, 8.8 Hz, 1 H; H–C(3)), 7.54, 7.83 (AA'MM', $J$ = 8.4 Hz; 4 H; $C_6H_4Cl$), 7.62 (dd, $J$ = 8.3, 1.7 Hz, 1 H; H–C(6'')), 7.69 (d, $J$ = 1.6 Hz, 1 H; H–C(8'')), 8.08 (d, $J$ = 8.2 Hz, 1 H; H–C(5'')), 8.30 (s, 1 H; H–C(2'')), 9.66 and 9.94 (2 s, 2 H; $H_2N^+$), 11.8–13.2 ppm (br. s, 1 H; H–N(3'')); $^{13}$C NMR (100 MHz, $(CD_3)_2SO$, signal of C(2) not visible due to fast exchange, assignment based on HSQC and HMBC spectra): $\delta$ = 46.79 (C(4)), 47.80 (C(2 or 5)), 50.99 (C(2 or 5)), 51.48 (C(3)), 121.93 (C(4a'')), 125.59 (C(8'')), 127.06 (C(5'')), 127.27 (C(6'')), 129.44 (C(3')), 130.78 (C(2')), 134.75 (C(1')), 139.40 (C(4')), 145.54 (C(7'')), 147.02 (C(8a'')), 160.53 (C(4'')), 196.81 ppm (C=O); IR (ATR): $\tilde{n}$ = 3600–2200 (m, with 3379 (w), 3034 (m), 2904 (m), 2864 (m), 2709 (m), 2599 (m)), 1713 (s), 1680 (s), 1652 (s), 1621 (m), 1586 (s), 1571 (s), 1401 (m), 1287 (m), 1245

(m), 1090 (m), 1009 (m), 842 (m), 781 (m), 689 $cm^{-1}$ (m); HR-MS (ESI): *m/z* (%): 356.0974 (28, $[M + H]^+$, calcd for $C_{19}H_{17}{}^{37}ClN_3O_2^+$: 356.0975), 354.0998 (100, $[M + H]^+$, calcd for $C_{19}H_{17}{}^{35}ClN_3O_2^+$: 354.1004).

**(3*R*,4*S*)-3-(4-Bromobenzoyl)-4-(4-oxo-3,4-dihydroquinazolin-7-yl)pyrrolidinium Chloride ((+)-1j).**

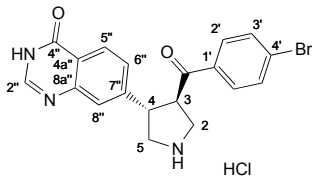


GP-D1 starting from pyrrolidine (+)-**13j** (18 mg, 0.04 mmol) gave pyrrolidinium salt (+)-**1j** (11 mg, 72%) as a white solid.

$[a]_D^{20}$ = +66.2 ($c$ = 0.1 in MeOH); $^1$H NMR and HR-MS (ESI) data consistent with (–)-**1j**.

**(3*S*,4*R*)-3-(4-Bromobenzoyl)-4-(4-oxo-3,4-dihydroquinazolin-7-yl)pyrrolidinium Chloride ((–)-1j).**

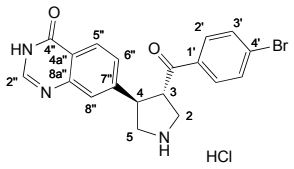


GP-D starting from pyrrolidine (–)-**13j** (19 mg, 0.04 mmol) gave pyrrolidinium salt (–)-**1j** (11 mg, 68%) as a white solid.

Prep. HPLC: $t_R$ = 13 min (amino phase: LiChrospher 100 $NH_2$ (5 □m); 15 mL $min^{-1}$, MeOH/$CHCl_3$ 10:90); m.p. 147 °C (decomp.); $[a]_D^{20}$ = –64.0 ($c$ = 0.1 in MeOH); $^1$H NMR (400 MHz, $(CD_3)_2SO$; assignment based on HSQC and HMBC spectra): $\delta$ = 3.36–3.50 (m, 2 H; $H_a$–C(2), $H_a$–C(5)), 3.75–3.96 (m, 2 H; $H_b$–C(2), $H_b$–C(5)), 3.91 (dd, $J$ = 17.2, 10.0 Hz, 1 H; H–C(4)), 4.62 (t, $J$ = 8.9 Hz, 1 H; H–C(3)), 7.60 (dd, $J$ = 8.4, 2.0 Hz, 1 H; H–C(6'')), 7.68, 7.74 (AA'MM', $J$ = 8.4 Hz, 4 H; $C_6H_4Br$), 7.68 (d, $J$ = 1.6 Hz, 1 H; H–C(8'')), 8.07 (d, $J$ = 8.2 Hz, 1 H; H–C(5'')), 8.25 (s, 1 H; H–C(2'')), 9.60 and 9.86 (2 br. s, 2 H; $H_2N^+$), 12.0–13.0 ppm (br. s, 1 H; H–N(3'')); $^{13}$C NMR (100 MHz, $(CD_3)_2SO$, signal of C(2) not visible due to fast exchange, assignment based on HSQC and HMBC spectra): $\delta$ = 46.79 (C(4)), 47.80 (C(2 or 5)), 51.05 (C(2 or 5)), 51.45 (C(3)), 122.02 (C(4a'')), 125.90 (C(8'')), 127.00 (C(5'')), 127.17 (C(6'')), 128.67 (C(4')), 130.84 (C(2')), 132.39 (C(3')), 135.07 (C(1')), 145.44 (C(7'')), 146.84 (C(8a'')), 160.61 (C(4'')), 197.80 ppm (C=O); IR (ATR): $\tilde{\eta}$ = 3600–2200 (m, with 3359 (w), 3030 (m), 2900 (m), 2864 (m), 2709 (m), 2595 (m)), 1713 (s), 1680 (s), 1652 (s), 1621 (m, sh), 1581 (m), 1498 (w), 1463 (w), 1397 (m), 1287 (m), 1244 (m), 1069 (m), 1005 (m), 839 (m), 781 (m), 734 (w), 689 $cm^{-1}$ (m); HR-MS (ESI): *m/z* (%): 426.9491 (100), 400.0486 (69, $[M + H]^+$, calcd for $C_{19}H_{17}{}^{81}BrN_3O_2^+$: 400.0479), 398.0501 (68, $[M + H]^+$, calcd for $C_{19}H_{17}{}^{79}BrN_3O_2^+$: 398.0499).

**(3*R*,4*S*)-3-(4-Iodobenzoyl)-4-(4-oxo-3,4-dihydroquinazolin-7-yl)pyrrolidinium Chloride ((+)-1k).**

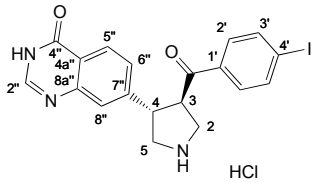


GP-D starting from pyrrolidine (+)-**13k** (15 mg, 0.03 mmol) gave pyrrolidinium salt (+)-**1k** (8 mg, 62%) as a white solid.

$[a]_D^{20}$ = +54.7 ($c$ = 0.1 in MeOH); $^1$H NMR and HR-MS (ESI) data consistent with (–)-**1k**.

**(3*S*,4*R*)-3-(4-Iodobenzoyl)-4-(4-oxo-3,4-dihydroquinazolin-7-yl)pyrrolidinium Chloride ((–)-1k).**

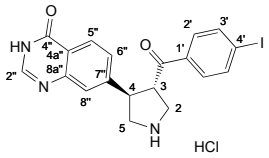


GP-D starting from pyrrolidine (–)-**13k** (20 mg, 0.04 mmol) gave pyrrolidinium salt (–)-**1k** (3 mg, 15%) as a yellow solid.

Prep. HPLC: $t_R$ = 16 min (amino phase: LiChrospher 100 $NH_2$ (5 □m); 15 mL min$^{-1}$, MeOH/$CHCl_3$ 10:90); m.p. 191 °C (decomp.); $[a]_D^{20}$ = –57.5 ($c$ = 0.1 in MeOH); $^1$H NMR (400 MHz, $(CD_3)_2SO$; assignment based on HSQC and HMBC spectra): $\delta$ = 3.35–3.49 (m, 2 H; $H_a$–C(2), $H_a$–C(5)), 3.71–3.98 (m, 2 H; $H_b$–C(2), $H_b$–C(5)), 3.90 (dd, $J$ = 17.8, 9.8 Hz, 1 H; H–C(4)), 4.60 (q, $J$ = 8.9 Hz, 1 H; H–C(3)), 7.56, 7.86 (AA'MM', $J$ = 8.4 Hz, 4 H; $C_6H_4I$), 7.59 (dd, $J$ = 8.4, 2.0 Hz, 1 H; H–C(6'')), 7.67 (d, $J$ = 1.6 Hz, 1 H; H–C(8'')), 8.07 (d, $J$ = 8.2 Hz, 1 H; H–C(5'')), 8.23 (s, 1 H; H–C(2'')), 9.58 and 9.58 (2 br. s, 2 H; $H_2N^+$), 12.1–12.9 ppm (br. s, 1 H; H–N(3'')); $^{13}$C NMR (100 MHz, $(CD_3)_2SO$, signal of C(2) not visible due to fast exchange, assignment based on HSQC and HMBC spectra): $\delta$ = 46.76 (C(4)), 47.82 (C(2 or 5)), 51.05 (C(2

or 5)), 51.35 (C(3)), 103.51 (C(4')), 122.03 (C(4a'')), 125.98 (C(8'')), 127.00 (C(5'')), 127.13 (C(6'')), 130.48 (C(2')), 135.32 (C(1')), 138.25 (C(3')), 145.43 (C(7'')), 146.80 (C(8a'')), 160.64 (C(4'')), 197.42 ppm (C=O); IR (ATR): $\tilde{n}$ = 3600–2200 (m, with 3359 (w), 3026 (m), 2855 (m), 2705 (m), 2640 (m), 2601 (m)), 1712 (s), 1652 (s), 1621 (m, sh), 1576 (m), 1498 (w), 1462 (w), 1393 (m), 1356 (m), 1245 (m), 1184 (m), 1057 (m), 1001 (m), 835 (m), 780 (m), 733 (w), 688 $cm^{-1}$ (m); HR-MS (ESI): *m/z* (%): 446.0356 (24, $[M + H]^+$, calcd for $C_{19}H_{17}IN_3O_2^+$: 446.0360).

**(3*R*,4*S*)-3-(4-Oxo-3,4-dihydroquinazolin-7-yl)-4-[4-(trifluoromethyl)benzoyl]-pyrrolidinium Chloride ((+)-1l).**

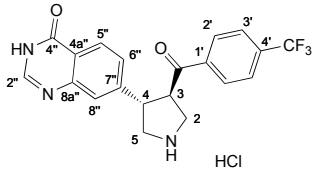


GP-D starting from pyrrolidine (+)-**13l** (15 mg, 0.03 mmol) gave pyrrolidinium salt (+)-**1l** (5 mg, 39%) as a white solid.

Prep. HPLC: $t_R$ = 19 min (amino phase: LiChrospher 100 $NH_2$ (5 □m); 17 mL $min^{-1}$, MeOH/$CHCl_3$ 10:90); m.p. 151 °C (decomp.); $[a]_D^{20}$ = +81.1 ($c$ = 0.1 in MeOH); $^1$H NMR (400 MHz, $(CD_3)_2SO$; assignment based on HSQC and HMBC spectra of (+)-**1l**): $\delta$ = 3.37–3.54 (m, 2 H; $H_a$–C(2), $H_a$–C(5)), 3.76–3.96 (m, 2 H; $H_b$–C(2), $H_b$–C(5)), 3.91 (dd, $J$ = 17.8, 9.8 Hz, 1 H; H–C(4)), 4.68 (q, $J$ = 8.9 Hz, 1 H; H–C(3)), 7.63 (dd, $J$ = 8.3, 1.7 Hz, 1 H; H–C(6'')), 7.66 (d, $J$ = 1.6 Hz, 1 H; H–C(8'')), 7.81, 7.97 (AA'MM', $J$ = 8.1 Hz, 4 H; $C_6H_4CF_3$), 8.06 (d, $J$ = 8.2 Hz, 1 H; H–C(5'')), 8.29 (s, 1 H; H–C(2'')), 9.70 and 9.95 (2 br. s, 2 H; $H_2N^+$), 12.1–13.0 ppm (br. s, 1 H; H–N(3'')); $^{13}$C NMR (150 MHz, $(CD_3)_2SO$; assignment based on HSQC and HMBC spectra of (+)-**1l**): $\delta$ = 46.22 (C(4)), 46.99 (C(2 or 5)), 50.55 (C(2 or 5)), 51.43 (C(3)), 121.50 (C(4a'')), 123.45 (q, $^1J$(C,F) = 271.1 Hz; $CF_3$), 125.60 (q, $^3J$(C,F) = 3.6 Hz;

C(3')), 125.75 (C(8'')), 126.35 (C(5'')), 126.43 (C(6'')), 129.09 (C(2')), 132.76 (q, $^2J$(C,F) = 31.8 Hz; C(4')), 138.78 (C(1')), 144.65 (C(7'')), 146.03 (C(8a'')), 147.93 (C(2'')), 160.10 (C(4'')), 196.97 ppm (C=O); $^{19}$F NMR (376 MHz, $(CD_3)_2SO$): $\delta$ = –61.74 ppm (s, 3 F; $CF_3$); IR (ATR): $\tilde{\eta}$ = 3600–2200 (m, with 3379 (w), 3034 (w), 2864 (m), 2705 (m), 2640 (m), 2601 (m)), 1713 (s), 1654 (s), 1571 (s), 1499 (m), 1463 (w), 1410 (m), 1323 (m), 1248 (m), 1166 (m), 1114 (s), 1065 (s), 1013 (m), 851 (m), 782 (m), 688 cm$^{-1}$ (m); HR-MS (ESI): *m/z* (%): 388.1262 (100, $[M + H]^+$, calcd for $C_{20}H_{17}F_3N_3O_2^+$: 388.1267).

**(3*S*,4*R*)-3-(4-Oxo-3,4-dihydroquinazolin-7-yl)-4-[4-(trifluoromethyl)benzoyl]-pyrrolidinium Chloride ((–)-1l).**

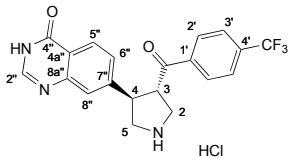


GP-D starting from pyrrolidine (–)-**13l** (17 mg, 0.03 mmol) gave pyrrolidinium salt (–)-**1l** (6 mg, 42%) as a white solid.

$[a]_D^{20}$ = –67.1 (*c* = 0.1 in MeOH); $^1$H NMR and HR-MS (ESI) data consistent with (+)-**1l**.

**(3*S*,4*R*)-3-[(4-Trifluoromethoxy)benzoyl]-4-(4-oxo-3,4-dihydroquinazolin-7-yl)pyrrolidinium Chloride ((–)1m).**

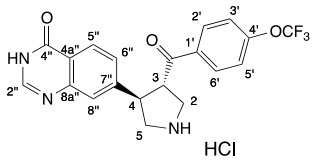


GP-D starting from pyrrolidine (–)-**13m** (11 mg, 0.021 mmol) gave pyrrolidinium salt (–)-**1m** (8 mg, 94%) as a yellow solid.

Prep. HPLC: $t_R$ = 22 min (amino phase: LiChrospher 100 $NH_2$ (5 □m); 15 mL min$^{-1}$,

MeOH/$CHCl_3$ 10:90); m.p. 174 °C (decomp.); $[a]^{D}_{20}$ = –61.7 (*c* = 0.05 in MeOH); $^{1}$H NMR (400 MHz, $(CD_3)_2SO$); assignment based on HSQC and HMBC spectra): $\delta$ = 3.39–3.51 (m, 2 H; $H_a$–C(2), $H_a$–C(5)), 3.78–3.91 (m, 3 H; $H_b$–C(2), $H_b$–C(5), H–C(4), overlay with the $(CD_3)_2SO$-signal), 4.43 (q, *J* = 8.9, 1 H; H–C(3)), 7.42 (d, *J* = 8.3 Hz, 2 H; H–C(3'), H–C(5')), 7.57 (dd, *J* = 8.3, 1.6 Hz, 1 H; H–C(6")), 7.65 (d, *J* = 1.5 Hz, 1 H; H–C(8")), 7.91 (d, *J* = 8.9 Hz, 2 H; H–C(2'), H–C(6')), 8.05 (d, *J* = 8.2 Hz, 1 H; H–C(5")), 8.17 (s, 1 H; H–C(2")), 9.55 and 9.79 (2 br. s, 2 H; $H_2N^+$), 12.24 ppm (br. s, 1 H; H–N(3'')); $^{13}$C NMR (150 MHz, $(CD_3)_2SO$); assignment based on HSQC and HMBC spectra): $\delta$ = 46.42 (C(4)), 47.22 (C(2)), 50.59 (C(5)), 51.18 (C(3)), 120.79 (C(3'), C(5')), 121.59 (C(4a")), 125.75 (C(8")), 126.45(C(5")), 126.56 (C(6")), 130.93 (C(2'), C(6')), 134.48 (C(1')), 144.77 (C(2")), 146.16 (C(7"), C(8a")), 151.85 (C(4')), 160.19 (C(4")), 196.23 ppm (C=O); $^{19}$F NMR (376 MHz, $(CD_3)_2SO$): $\delta$ = –56.68 ppm (s, 3 F; $CF_3$); IR (ATR): $\tilde{n}$ = 3374 (br.), 2920 (m), 2851 (m), 2741 (br.), 1715 (s), 1682 (s), 1656 (s), 1621 (m), 1602 (m), 1573 (m), 1504 (w), 1464 (w), 1415 (w), 1357 (w), 1302 (w), 1250 (s), 1206 (s), 1164 (s), 1058 (w), 1013 (w), 850 (m), 782 (m), 733 (w), 690 $cm^{-1}$ (m); HR-MS (MALDI): 404.1216 (100 $[M + H]^+$, calcd for $C_{20}H_{17}F_3N_3O_3^+$: 404.1217).

**(3*R*,4*S*)-3-[(4-Trifluormethoxy)benzoyl]-4-(4-oxo-3,4-dihydroquinazolin-7-yl)pyrrolidinium Chloride ((+)-1m).**

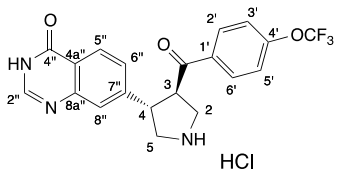


GP-D starting from pyrrolidine (+)-**13m** (11 mg, 0.021 mmol) gave pyrrolidinium salt (+)-**1m** (8 mg, 94%) as a yellow solid.

$[a]^{D20}$ = +62.7 (*c* = 0.05 in MeOH) $^{1}$H NMR and HR-MS (MALDI) data consistent with (–)-**1m**.

**(3*R*,4*S*)-3-(4-Oxo-3,4-dihydroquinolin-7-yl)-4-(thien-2-ylcarbonyl)pyrrolidinium Chloride ((+)-1n).**

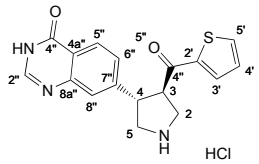


GP-D starting from pyrrolidine (+)-**13n** (24 mg, 0.06 mmol) gave pyrrolidinium salt (+)-**1n** (17 mg, 86%) as a white solid.

Prep. HPLC: $t_R$ = 16 min (amino phase: LiChrospher 100 $NH_2$ (5 □m); 15 mL $min^{-1}$, MeOH/$CHCl_3$ 10:90); m.p. 197 °C (decomp.); $[a]_D^{20}$ = +140.9 ($c$ = 0.1 in MeOH); $^1$H NMR (400 MHz, $(CD_3)_2SO$; assignment based on HSQC and HMBC spectra of (+)-**1n**): $\delta$ = 3.34–3.53 (m, 2 H; $H_a$–C(2), $H_a$–C(5)), 3.77–3.97 (m, 2 H; $H_b$–C(2), $H_b$–C(5)), 3.90 (dd, $J$ = 17.8, 10.2 Hz, 1 H; H–C(4)), 4.52 (q, $J$ = 9.0 Hz, 1 H; H–C(3)), 7.17 (dd, $J$ = 4.9, 3.9 Hz, 1 H; H–C(4')), 7.63 (dd, $J$ = 8.3, 1.7 Hz, 1 H; H–C(6'')), 7.72 (d, $J$ = 1.7 Hz, 1 H; H–C(8'')), 7.74 (dd, $J$ = 4.1, 1.1 Hz, 1 H; H–C(3')), 8.05 (dd, $J$ = 5.0, 1.0 Hz, 1 H; H–C(5')), 8.09 (d, $J$ = 8.2 Hz, 1 H; H–C(5'')), 8.28 (s, 1 H; H–C(2'')), 9.68 and 9.92 (2 br. s, 2 H; $H_2N^+$), 11.7–13.2 ppm (br. s, 1 H; H–N(3'')); $^{13}$C NMR (100 MHz, $(CD_3)_2SO$, signal of C(2) not visible due to fast exchange; assignment based on HSQC and HMBC spectra of (+)-**1n**): $\delta$ = 46.39 (C(4)), 48.23 (C(2 or 5)), 51.03 (C(2 or 5)), 52.28 (C(3)), 122.06 (C(4a'')), 125.71 (C(8'')), 127.08 (C(5'')), 127.20 (C(6'')), 129.48 (C(4')), 135.01 (C(3')), 137.28 (C(5')), 143.35 (C(2')), 145.25 (C(7'')), 144.98 (C(8a'')), 160.58 (C(4'')), 190.33 ppm (C=O); IR (ATR): $\tilde{n}$ = 3600–2200 (m, with 3379 (w), 3046 (w), 2855 (m), 2713 (m), 2640 (m), 2602 (m)), 1711 (s), 1651 (s), 1572 (m), 1411 (s), 1354 (m), 1298 (m), 1249 (m), 1194 (m), 1059 (m), 850 (m), 781 (m), 730 (m), 688 $cm^{-1}$ (m); HR-MS (ESI): *m/z* (%): 326.0961 (100, $[M + H]^+$, calcd for $C_{17}H_{16}N_3O_2S^+$: 326.0958).

**(3*S*,4*R*)-3-(4-Oxo-3,4-dihydroquinolin-7-yl)-4-(thien-2-ylcarbonyl)pyrrolidinium Chloride ((–)-1n).**

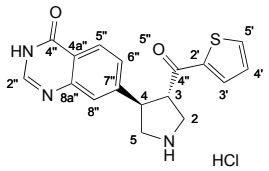


GP-D starting from pyrrolidine (–)-**1n** (25 mg, 0.06 mmol) gave pyrrolidinium salt (–)-**1n** (18 mg, 87%) as a white solid.

$[a]_D^{20} = -158.0$ ($c = 0.1$ in MeOH); $^1$H NMR and HR-MS (ESI) data consistent with (+)-**1n**.

**(3*R*,4*S*)-3-[(5-Chlorothien-2-yl)carbonyl]-4-(4-oxo-3,4-dihydroquinazolin-7-yl)pyrrolidinium Chloride ((+)-1o).**

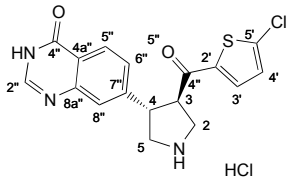


GP-D starting from pyrrolidine (+)-**13o** (25 mg, 0.05 mmol) gave pyrrolidinium salt (+)-**1o** (17 mg, 81%) as a yellow solid.

$[a]_D^{20} = +178.4$ ($c = 0.1$ in MeOH); $^1$H NMR and HR-MS (ESI) data consistent with (–)-**1o**.

**(3*S*,4*R*)-3-[(5-Chlorothien-2-yl)carbonyl]-4-(4-oxo-3,4-dihydroquinazolin-7-l)pyrrolidin-ium Chloride ((–)-1o).**

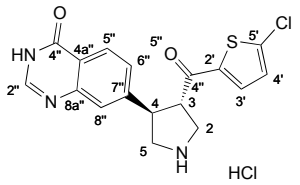


GP-D starting from pyrrolidine (–)-**13o** (24 mg, 0.05 mmol) gave pyrrolidinium salt (–)-**1o** (17 mg, 84%) as a yellow solid.

Prep. HPLC: $t_R$ = 20 min (amino phase: LiChrospher 100 $NH_2$ (5 □m); 15 mL $min^{-1}$, MeOH/$CHCl_3$ 10:90); m.p. 170 °C (decomp.); $[a]_D^{20}$ = –173.4 ($c$ = 0.1 in MeOH); $^1$H NMR (400 MHz, $(CD_3)_2SO$; assignment based on HSQC and HMBC spectra): $\delta$ = 3.34–3.52 (m, 2 H; $H_a$–C(2), $H_a$–C(5)), 3.76–3.92 (m, 2 H; $H_b$–C(2), $H_b$–C(5)), 3.88 (dd, $J$ = 17.6, 9.6 Hz, 1 H; H–C(4)), 4.50 (q, $J$ = 8.8 Hz, 1 H; H–C(3)), 7.24 (d, $J$ = 4.2 Hz, 1 H; H–C(4')), 7.61 (dd, $J$ = 8.4, 2.2 Hz, 1 H; H–C(6'')), 7.61 (d, $J$ = 4.0 Hz, 1 H; H–C(3')), 7.71 (d, $J$ = 1.7 Hz, 1 H; H–C(8'')), 8.09 (d, $J$ = 8.3 Hz, 1 H; H–C(5'')), 8.24 (s, 1 H; H–C(2'')), 9.63 and 9.89 (2 br. s, 2 H; $H_2N^+$), 12.0–12.9 ppm (br. s, 1 H; H–N(3'')); $^{13}$C NMR (100 MHz, $(CD_3)_2SO$; assignment based on HSQC and HMBC spectra): $\delta$ = 47.40 (C(4)), 48.05 (C(2 or 5)), 51.08 (C(2 or 5)), 51.49 (C(3)), 122.17 (C(4a'')), 125.96 (C(8'')), 127.08 (C(5'')), 127.11 (C(6'')), 129.74 (C(4')), 135.18 (C(3')), 139.80 (C(5')), 142.23 (C(2')), 144.96 (C(7'')), 146.16 (C(2'')), 146.87 (C(8a'')), 160.64 (C(4'')), 189.91 ppm (C=O); IR (ATR): $\tilde{n}$ = 3600–2200 (m, with 3375 (w), 3010 (m), 2855 (m), 2709 (m), 2636 (m), 2600 (m)), 1712 (s), 1651 (s), 1572 (m), 1499 (w), 1462 (w), 1413 (s), 1325 (m), 1299 (m), 1246 (m), 1058 (w), 1014 (m), 851 (m), 809 (m), 781 (m), 688 $cm^{-1}$ (m); HR-MS (ESI): *m/z* (%): 362.0541 (42, $[M + H]^+$, calcd for $C_{17}H_{15}{}^{37}ClN_3O_2S^+$: 362.0539), 360.0565 (100, $[M + H]^+$, calcd for $C_{17}H_{15}{}^{35}ClN_3O_2S^+$: 360.0568).

**(3*S*,4*R*)-3-(5-Bromothienyl)-4-(4-oxo-3,4-dihydroquinazolin-7-yl)pyrrolidinium Chloride ((–)-1p).**

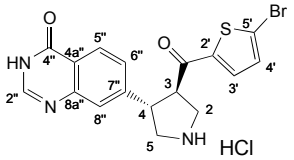


GP-D starting from pyrrolidine (–)-**13p** (8 mg, 0.015 mmol) gave pyrrolidinium salt (–)-**1p** (6 mg, 70%) as a yellow solid.

Prep. HPLC: $t_R$ = 21 min (amino phase: LiChrospher 100 $NH_2$ (5 □m); 15 mL $min^{-1}$, MeOH/$CHCl_3$ 10:90); m.p. 192 °C; $[a]^D_{20}$ = –137.5 ($c$ = 0.05 in MeOH); $^1$H NMR (600 MHz, $(CD_3)_2SO$); assignment based on HSQC and HMBC spectra): $\delta$ = 3.36–3.43 (m, 2 H; $H_a$–C(2), $H_a$–C(5)), 3.78–3.88 (m, 3 H; $H_b$–C(2), $H_b$–C(5), H–C(4)), 4.46 (q, $J$ = 9.0 Hz, 1 H; H–C(3)), 7.33 (d, $J$ = 4.1 Hz, 1 H; H–C(4')), 7.52 (d, $J$ = 4.2 Hz, 1 H; H–C(3')), 7.57 (dd, $J$ = 8.3, 1.8 Hz, 1 H; H–C(6")), 7.69 (d, $J$ = 1.7 Hz, 1 H; H–C(8")), 8.08 (d, $J$ = 8.2 Hz, 1 H; H–C(5")), 8.15 (s, 1 H; H–C(2")), 9.51 and 9.71 (2 br. s, 2 H; $H_2N^+$), 12.37 ppm (br. s, 1 H; H–N(3'')); $^{13}$C NMR (150 MHz, $(CD_3)_2SO$); assignment based on HSQC and HMBC spectra): $\delta$ = 46.96 (C(4)), 47.63 (C(2)), 50.72 (C(5)), 51.13 (C(3)), 121.80 (C(4a")), 123.82 (C(5')), 125.90 (C(8")), 126.51 (C(5")), 126.53 (C(6")), 132.64 (C(4')), 135.23 (C(3')), 144.36 (C(2")), 144.41 (C(2')), 146.15 (C(7")), 148.42 (C(8a")), 160.28 (C(4")), 189.26 ppm (C=O); IR (ATR): $\tilde{\eta}$ = 3379 (br.), 3034 (w), 2920 (w), 2855 (w), 2713 (br.), 1712 (s), 1651 (s), 1655 (s), 1573 (m), 1521 (w), 1463 (w), 1407 (s), 1299 (w), 1248 (m), 1149 (m), 1060 (w), 887 (m), 894 (m), 849 (w), 808 (w), 779 (m), 714 (w), 687 (s) , 664 (w), 631 $cm^{-1}$ (m); HR-MS (MALDI): 406.0043 (47, $[M + H]^+$, calcd for $C_{17}H_{15}{}^{81}BrNO_2S^+$: 406.0048), 404.0063 (49, $[M + H]^+$, calcd for $C_{17}H_{15}{}^{79}BrNO_2S^+$: 404.0063).

**(3*S*,4*R*)-3-(5-Bromothienyl)-4-(4-oxo-3,4-dihydroquinazolin-7-yl)pyrrolidinium Chloride ((+)-1p).**

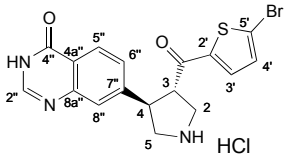


GP-D starting from pyrrolidine (+)-**13p** (8 mg, 0.015 mmol) gave pyrrolidinium (+)-**1p** (5 mg, 80%) as a yellow solid.

$[a]^{D}_{20}$ = +147.1 (*c* = 0.05 in MeOH); $^{1}$H NMR and HR-MS (MALDI) data consistent with (–)-**1p**.

**Diethyl (2-Oxo-2-phenylethyl)phosphonate (4a).**

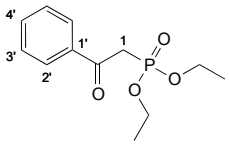


GP-A (10 mL THF) starting from ethyl benzoate (**2a**, 1 g, 6.7 mmol). FC ($SiO_2$; EtOAc) gave phosphonate **4a** (1.2 g, 70%) as a colorless oil.

$R_f$ = 0.45 (EtOAc); $^{1}$H NMR (400 MHz, $CDCl_3$): $\delta$ = 1.28 (td, *J* = 7.0 Hz, $^{4}J$(H,P) = 0.5 Hz, 6 H; 2 $CH_3$), 3.63 (d, $^{2}J$(H,P) = 22.7 Hz, 2 H; $H_2$–C(1)), 4.10–4.17 (m, 4 H; 2 $OCH_2$), 7.47 (br. t, *J* = 7.4 Hz, 1 H; H–C(3'), H–C(5')), 7.59 (tt, *J* = 7.4, 1.9 Hz, 1 H; H–C(4')), 8.01 ppm (br. d, *J* = 7.4 Hz, 2 H; H–C(2'), H–C(6')); $^{13}$C NMR (100 MHz, $CDCl_3$): $\delta$ = 16.38 (d, $^{3}J$(C,P) = 6.3 Hz; 2 $CH_3$), 38.67 (d, $^{1}J$(C,P) = 129.9 Hz; C(1)), 62.78 (d, $^{2}J$(C,P) = 6.5 Hz; 2 $OCH_2$), 128.74 (C(3'), C(5')), 129.20 (C(2')), 133.79 (C(4')), 136.71 (d, $^{3}J$(C,P) = 2.0 Hz; C(1')), 192.10 ppm (d, $^{3}J$(C,P) = 6.7 Hz; C=O); $^{31}$P NMR (162 MHz; $CDCl_3$): $\delta$ = 19.85 ppm (tquint., 1 P; $PO_3$); IR (ATR): $\tilde{\eta}$ = 2983 (w), 1736 (w), 1678 (s), 1598 (w), 1581 (w), 1478 (w), 1448 (w), 1392 (w), 1369 (w), 1249 (s), 1200 (w), 1162 (w), 1130 (w), 1097 (w), 1051 (m), 1020 (s), 1003 (s), 957 (s), 869 (w), 835 (w), 781 (s), 738 (m), 688 $cm^{-1}$ (m); HR-MS (ESI) *m/z* (%): 279.0756 (86, [*M*

+ Na]$^+$, calcd for $C_{12}H_{18}NaO_4P^+$: 279.0762), 257.0937 (100, [*M* + H]$^+$, calcd for $C_{12}H_{18}O_4P^+$: 257.0937), 229.0621 (60, [*M* – $C_2H_4$ + H]$^+$, calcd for $C_{10}H_{14}O_4P^+$: 229.0630), 201.0309 (90, [*M* – 2 $C_2H_4$ + H]$^+$, calcd for $C_8H_{10}O_4P^+$: 201.0317).

**Diethyl [2-(3-Fluorophenyl)-2-oxoethyl]phosphonate (4b).**

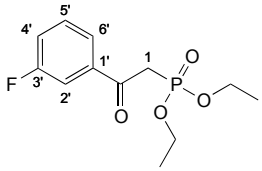


A solution of 3-fluorbenzoic acid (**1b**, 0.5g, 3.6 mmol) in EtOH (10 mL) was treated with 95% $H_2SO_4$ (19 µL, 0.36 mmol), heated to 80 °C for 22 H; cooled to 22 °C, and evaporated. The residue was treated with sat. aq. $NaHCO_3$ solution (50 mL). The aqueous phase was extracted with EtOAc (3 x 50 mL). The combined organic phases were dried over $MgSO_4$, filtered, and evaporated to afford ester **3b**.

GP-A (10 mL THF) starting from ester **3b**. FC ($SiO_2$; EtOAc) gave phosphonate **4b** (820 mg, 79%) as a colorless oil.

$R_f$ = 0.51 (EtOAc); $^1$H NMR (400 MHz, $CDCl_3$): $\delta$ = 1.28 (t, *J* = 7.0 Hz, 6 H; 2 $CH_3$), 3.60 (d, $^2J$(H,P) = 22.8 Hz, 2 H; $H_2$–C(1)), 4.06–4.20 (m, 4 H; 2 $OCH_2$), 7.27 (t, *J* = 8.5 Hz, 1 H; H–C(4')), 7.45 (td, *J* = 8.0 Hz, $^4J$(H,F) = 5.4 Hz, 1 H; H–C(5')), 7.68 (ddd, $^3J$(H,F) = 9.5 Hz, *J* = 2.7, 1.5 Hz, 1 H; H–C(2')), 7.80 ppm (ddd, *J* = 7.8, 2.4, 1.5 Hz, 1 H; H–C(6')); $^{13}$C NMR (100 MHz, $CDCl_3$): $\delta$ = 16.36 (q, $^3J$(C,P) = 6.3 Hz; $CH_3$), 38.90 (t, $^1J$(C,P) = 129.7 Hz; C(1)), 62.87 (t, $^2J$(C,P) = 6.5 Hz; 2 $OCH_2$), 115.76 (d, $^2J$(C,F) = 22.7 Hz; C(2')), 120.82 (d, $^2J$(C,F) = 21.5 Hz; C(4')), 125.09 (d, $^4J$(C,F) = 3.0 Hz; C(6')), 130.40 (d, $^3J$(C,F) = 7.6 Hz; C(5')), 138.70 (d, $^5J$(C,F) = 6.4 Hz, $^3J$(C,P) = 1.9 Hz; C(1')), 190.88 (d, $^2J$(C,P) = 6.8 Hz; C=O); $^{31}$P NMR (162 MHz; $CDCl_3$): $\delta$ = 18.95–19.44 ppm (m, 1 P; $PO_3$); $^{19}$F NMR (376 MHz; $CDCl_3$): $\delta$ = –111.72 ppm (td, *J* = 8.8, 5.4 Hz, 1 F); IR (ATR): $\tilde{\eta}$ = 2984 (w), 1682 (m), 1588 (m),1485 (w), 1443 (w), 1393

(w), 1369 (w), 1251 (s), 1199 (m), 1163 (w)1098 (w), 1052 (s), 1018 (s), 961 (s), 901 (m), 888 (m), 831 (w), 788 (s), 711 (w), 681 (w), 667 $cm^{-1}$ (m); HR-MS (ESI) *m/z* (%): 275.0840 (44, $[M]^+$, calcd for $C_{12}H_{17}FO_4P^+$: 275.0843), 297.0670 (100, $[M + Na]^+$, calcd for $C_{12}H_{17}FO_4PNa^+$: 297.0668), 268.9975 (35, calcd for $C_8H_{14}O_4FP^+$: 268.9979), 247.0523 (31, calcd for $C_{10}H_{13}FO_4P^+$: 298.9821).

**Diethyl [2-(3-Chlorophenyl)-2-oxoethyl]phosphonate (4c).**

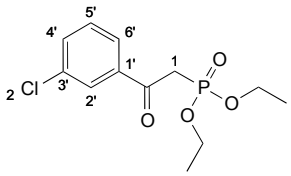


A solution of 3-chlorobenzoic acid (**3c**, 800 mg, 5.11 mmol) in EtOH (20 mL) was treated with 95% $H_2SO_4$ (27 µL, 0.51 mmol), heated to 80 °C for 6.5 h, cooled to 22 °C, and evaporated. The residue was treated with sat. aq. $NaHCO_3$ solution (100 mL). The aqueous phase was extracted with EtOAc (3 x 100 mL). The combined organic phases were dried over $MgSO_4$, filtered, and evaporated to afford ester **2c**.

GP-A (10 mL THF) starting from ester **2c**. FC ($SiO_2$; EtOAc/heptane 4:1) gave phosphonate **4c** (1075 mg, 72%) as a colorless oil.

$R_f$ = 0.40 ($SiO_2$; EtOAc); $^1$H NMR (300 MHz, $CDCl_3$): $\delta$ = 1.28 (br. t, $J$ = 7.1 Hz, 6 H; 2 $OCH_2CH_3$), 3.59 (dd, $^2J$(H,P) = 22.8 Hz, $J$ = 0.5 Hz, 2 H; H–C(1)), 4.06–4.20 (m, 4 H; 2 $OCH_2CH_3$), 7.41 (t, $J$ = 7.9 Hz, 1 H; H–C(5')), 7.54 (ddd, $J$ = 7.7, 1.9, 1.0 Hz, 1 H; H–C(4')), 7.89 (ddd, $J$ = 7.8, 1.5, 1.2 Hz, 1 H; H–C(6')), 7.97 ppm (t, $J$ = 2.0 Hz, 1 H; H–C(2')); $^{13}$C NMR (75 MHz, $CDCl_3$): $\delta$ = 16.11 (d, $^3J$(C,P) = 6.4 Hz; 2 $OCH_2CH_3$), 38.62 (d, $^1J$(C,P) = 128.8 Hz; C(1)), 62.63 (d, $^2J$(C,P) = 6.6 Hz; 2 $OCH_2CH_3$), 127.13 (C(6')), 128.92 (C('2)), 129.80 (C(5')), 133.41 (C(4')), 134.83 (C(3')), 137.89 (C(1')), 190.95 ppm (C=O); $^{31}$P NMR (121 MHz, $CDCl_3$): $\delta$ = 19.46 ppm (s, 1 P; $PO_3$); IR (ATR): $\tilde{\nu}$ = 2983 (w), 2932 (w), 2912 (w), 1683 (m),

1571 (m), 1475 (w), 1424 (w), 1392 (w), 1284 (m), 1248 (s), 1199 (w), 1163 (w), 1098 (w), 1052 (m, sh), 1016 (s), 959 (s), 871 (w), 786 (s), 675 (m), 660 $cm^{-1}$ (m); HR-MS (ESI): *m/z* (%): 293.0524 (29, $[M + H]^+$, calcd for $C_{12}H_{17}{}^{37}ClO_4P^+$: 293.0519), 291.0550 (85, $[M + H]^+$, calcd for $C_{12}H_{17}{}^{35}ClO_4P^+$: 291.05472), 265.0212 (25), 263.0238 (71, $[M - C_2H_4 + H]^+$), 236.9893 (36), 234.9923 (100).

**Diethyl (2-(3-Bromophenyl)-2-oxoethyl)phosphonate (4d).**

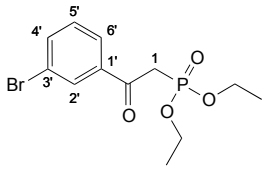


GP-A (10 mL THF) starting from ethyl-3-bromobenzoate (**2d**, 1.0 g, 4.3 mmol). FC $SiO_2$; EtOAc) gave phosphonate **4d** (213 mg, 88%) as a colorless oil.

$R_f$ = 0.52 (EtOAc); $^1$H NMR (400 MHz, $CDCl_3$): $\delta$ = 1.29 (td, $J$ = 7.1 Hz, $^4J$(H,P) = 0.6 Hz, 6 H; 2 $CH_3$), 3.59 (d, $^2J$(H,P) = 22.8 Hz, 2 H; $H_2$–C(1)), 4.10–4.18 (m, 4 H; $CH_2$), 7.23 (t, $J$ = 7.9 Hz, 1 H; H–C(5')), 7.71 (ddd, $J$ = 8.0, 2.0, 1.0 Hz, 1 H; H–C(4')), 7.95 (ddd, $J$ = 7.8, 1.7, 1.0 Hz, 1 H; H–C(6')), 8.14 ppm (t, $J$ = 1.8 Hz; H–C(2')); $^{13}$C NMR (100 MHz, $CDCl_3$): $\delta$ = 16.39 (d, $^3J$(C,P) = 6.4 Hz; $CH_3$), 38.87 (d, $^1J$(C,P) = 129.5 Hz; C(1)), 62.92 (d, $^2J$(C,P) = 6.5 Hz; 2 $OCH_2$), 123.07 (C(3')), 127.84 (C(6')), 130.31 (C(5')), 132.16 (C(2')), 136.61 (C(4')), 138.32 (d, $^3J$(C,P) = 1.7 Hz; C(1')), 190.79 ppm (d, $^2J$(C,P) = 6.8 Hz; C=O); $^{31}$P NMR (162 MHz; $CDCl_3$): $\delta$ = 18.90–19.29 ppm (m. 1 P; $PO_3$); IR (ATR): $\tilde{\eta}$ = 2982 (w), 1735 (w), 1682 (s), 1567 (m), 1475 (w), 1442 (w), 1369 (w), 1248 (s), 1198 (w), 1163 (w), 1134 (w), 1097 (w), 1052 (s), 1017 (s), 961 (s), 870 (w), 833 (w), 787 (s), 670 (m), 654 $cm^{-1}$ (m); HR-MS (EI) *m/z* (%): 337.0014 (98, $[M]^+$, calcd for $C_{12}H_{17}{}^{81}BrO_4P^+$: 337.0027), 335.0034 (100, $[M]^+$, calcd for $C_{12}H_{17}{}^{79}BrO_4P^+$: 335.0042), 306.9724 (36, $[M - C_2H_4]^+$, calcd for $C_{10}H_{13}{}^{79}BrO_4P^+$: 306.9735), 308.9703 (45, calcd for $C^{10}H_{13}{}^{81}BrO_4P^+$: 308.9703), 280.9390 (39, calcd for $C_8H_9{}^{81}BrO_4P^+$: 280.9401),

278.9410 (44, [$M$ – 2 x $C_2H_4$]$^+$, calcd for $C_8H_9{}^{79}BrO_4P^+$: 278.9422).

**Diethyl [2-(3-Iodophenyl)-2-oxoethyl]phosphonate (4e).**

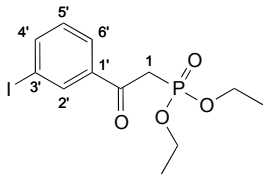


GP-A (10 mL THF) starting from ethyl-3-iodobenzoate (**2e,** 1.0 g, 3.6 mmol). FC $SiO_2$; EtOAc) gave phosphonate **4e** (213 mg, 15%) as a colorless oil.

$R_f$ = 0.14 (EtOAc/cHex, 1:1); $^1$H NMR (400 MHz, $CDCl_3$): $\delta$ = 1.29 (td, $J$ = 7.0, 0.5 Hz, 6 H, $CH_3$), 3.58 (d, $^2J$(H,P) = 22.8 Hz, 2 H; $H_2$–C(1)), 4.09–4.19 (m, 4 H; 2 $OCH_2$), 7.23 (t, $J$ = 7.8 Hz, 1 H; H–C(5')), 7.91 (ddd, $J$ = 7.8, 1.7, 1.0 Hz, 1 H; H–C(4')), 7.98 (ddd, $J$ = 7.8, 1.7, 1.0 Hz, 1 H; H–C(6')), 8.33 ppm (t, $J$ = 1.7 Hz, 1 H; H–C(2')); $^{13}$C NMR (100 MHz, $CDCl_3$): $\delta$ = 16.26 (d, $^3J$(C,P) = 6.4 Hz; $CH_3$), 38.63 (d, $^1J$(C,P) = 129.3 Hz; C(1)), 62.76 (d, $^2J$(C,P) = 6.5 Hz; 2 $OCH_2$), 94.27 (C(3')), 128.28 (C(6')), 130.28 (C(5')), 137.92 (C(2')), 142.35 (C(4')), 190.59 ppm (d, $^2J$ C,P) = 6.8 Hz; C=O); $^{31}$P NMR (162 MHz; $CDCl_3$): $\delta$ = 18.94–19.32 ppm (m. 1 P; $PO_3$); IR (ATR: $\tilde{\eta}$ = 2981 (w), 2931 (w), 1681 (m), 1562 (w), 1442 (w), 1418 (w), 1368 (w), 1248 (s), 1197 (w), 1162 (w), 1133 (w), 1097 (w), 1050 (m), 1015 (s), 960(s), 870 (w), 833 (w), 790 (m), 669 (m), 647 cm$^{-1}$ (m); HR-MS (ESI) *m/z* (%): 382.9906 (100, [$M$]$^+$, calcd for $C_{12}H_{17}IO_4P^+$: 382.9904).

**Diethyl {2-Oxo-2-[4-(trifluoromethyl)phenyl]ethyl}phosphonate (4f).**

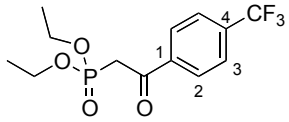


A solution of 4-(trifluoromethyl)benzoic acid (**1f**, 861 µL, 5.26 mmol) in EtOH (18.4 mL) was treated with 95% $H_2SO_4$ (28 µL, 0.53 mmol). The mixture was stirred at 80 °C for 4 h and evaporated. The residue was treated with 0.1 M aq. NaOH (50 mL). The aqueous phase was extracted with EtOAc (3 x 50 mL). The combined organic phases were washed with brine (50 mL), dried over $MgSO_4$, filtered, and evaporated to afford ester **3f** as a colorless oil.

GP-A (10 mL THF) starting from ester **2f**. FC ($SiO_2$; EtOAc/heptane 2:1 → 4:1) gave phosphonate **4f** (1314 mg, 77%) as a colorless oil.

$R_f$ = 0.58 ($SiO_2$; EtOAc); $^1$H NMR (400 MHz, $CDCl_3$): $\delta$ = 1.29 (td, $J$ = 7.0 Hz, $^4J$(H,P) = 1.4 Hz, 6 H; 2 $OCH_2CH_3$), 3.66 (d, $^2J$(H,P) = 22.9 Hz, 2 H; $CH_2$), 4.14 and 4.16 (2 qd, $J$ = 7.2 Hz, $^3J$(H,P) = 0.9 Hz, 4 H; 2 $OCH_2CH_3$), 7.75, 8.14 ppm (AA'MM', $J$ = 8.2 Hz, 4 H; $C_6H_4$); $^{13}$C NMR (100 MHz, $CDCl_3$): $\delta$ = 16.21 (d, $^3J$(C,P) = 6.2 Hz; 2 $OCH_2CH_3$), 38.96 (d, $^1J$(C,P) = 128.3 Hz; C–P), 62.81 (d, $^3J$(C,P) = 6.4 Hz; 2 $OCH_2CH_3$), 123.49 (q, $^1J$(C,F) = 271.1 Hz; $CF_3$), 125.65 (q, $^3J$(C,F) = 3.7 Hz; C(3)), 129.41 (C(2)), 134.82 (q, $^2J$(C,F) = 32.6 Hz; C(4)), 139.10 (C(1)), 191.09 ppm (d, $^2J$(C,P) = 6.6 Hz; C=O); $^{19}$F NMR (376 MHz, $CDCl_3$): $\delta$ = –63.25 ppm (s, 3 F; $CF_3$); $^{31}$P NMR (162 MHz, $CDCl_3$): $\delta$ = 18.52–19.26 ppm (m, 1 P; $PO_3$); IR (ATR): $\tilde{n}$ = 2986 (w), 1686 (m, C=O), 1582 (w), 1513 (w), 1445 (w), 1412 (w), 1326 (s), 1251 (s), 1166 (m), 1125 (m), 1064 (s), 1020 (s), 1002 (s), 959 (s), 858 (w), 818 (m), 719 $cm^{-1}$ (m); HR-MS (ESI): *m/z* (%): 325.0827 (100, $[M + H]^+$, calcd for $C_{13}H_{17}F_3O_4P^+$: 325.0811).

**Diethyl {2-Oxo-2-[3-(trifluoromethoxy)phenyl]ethyl}phosphonate (4g).**

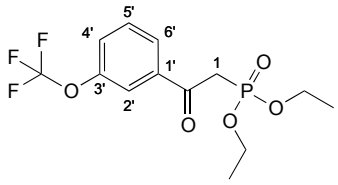


A solution of 3-trifluormethoxybenzoic acid (**3g**, 1.0 g, 4.7 mmol) in EtOH (10 mL) was treated with 95% $H_2SO_4$ (25 µL, 0.47 mmol), heated to 80 °C for 22 H; cooled to 22 °C, and evaporated. The residue was treated with sat. aq. $NaHCO_3$ solution (50 mL). The aqueous phase was extracted with EtOAc (3 x 50 mL). The combined organic phases were dried over $MgSO_4$, filtered, and evaporated to afford ester **2g**.

GP-A (10 mL THF) starting from ester **2g**. FC ($SiO_2$; EtOAc) gave phosphonate **4g** (1.1 g, 69%) as a colorless oil.

$R_f$ = 0.46 (EtOAc); $^1$H NMR (400 MHz, $CDCl_3$): $\delta$ = 1.28 (t, $J$ = 7.1 Hz, 6 H; 2 $CH_3$), 3.61 (d, $^2J$(H,P) = 22.9 Hz, 2 H; $H_2$–C(1)), 4.10–4.18 (m, 4 H; $CH_2$), 7.44 (br. d, $J$ = 8.2 Hz, 1 H; H–C(4')), 7.53 ppm (t, $J$ = 8.0 Hz, 1 H; H–C(5')), 7.85 (br. s, 1 H; H–C(2')), 7.96 ppm (dt, $J$ = 7.8, 1.3 Hz, 1 H; H–C(6')); $^{13}$C NMR (100 MHz, $CDCl_3$): $\delta$ = 16.35 (d, $^3J$(C,P) = 6.3 Hz; $CH_3$), 38.97 (d, $^1J$(C,P) = 129.3 Hz; C(1)), 62.93 (d, $^2J$(C,P) = 6.6 Hz; 2 $OCH_2$), 121.39 (q, $^1J$(C,F) = 259.2 Hz; $CF_3$), 120.40 (C(2')), 126.07 (C(4')), 127.64 (C(6')), 130.30 (C(5')), 138.45 (d, $^3J$(C,P) = 1.8 Hz; C(1')), 149.61 (q, $^3J$(C,F) = 2.0 Hz; C(3')), 190.69 ppm (d, $^2J$(C,P) = 6.8 Hz; C=O); $^{31}$P NMR (162 MHz; $CDCl_3$): $\delta$ = 19.00 ppm (tquint., 1 P; $PO_3$); $^{19}$F NMR (376 MHz, $CDCl_3$): $\delta$ = –57.89 ppm (s, 3 F; $CF_3$); IR (ATR): $\tilde{\eta}$ = 2994 (w), 2923 (w), 1679 (s), 1611 (w), 1584 (w), 1487 (w), 1454 (w), 1415 (w), 1397 (w), 1371 (w),1241 (s), 1209 (s), 1160 (s), 1124 (m), 1056 (m), 1016 (s), 967 (s), 943 (s), 900 (w), 878 (m), 833 (m), 788 (s), 749 (w), 733 (w), 694 (w), 679 (w), 666 (w), 634 cm$^{-1}$ (w); HR-MS (ESI) *m/z* (%): 341.0766 (100, $[M]^+$, calcd for $C_{13}H_{17}F_3O_5P^+$: 341.0760), 313.0452 (40, $[M - C_2H_4]^+$, calcd for $C_{11}H_{13}F_3O_5P^+$: 313.0453), 285.0139 (34, $[M - 2\ C_2H_4]^+$, calcd for $C_9H_9F_3O_5P^+$: 285.0140).

**Diethyl [2-(4-Fluorophenyl)-2-oxoethyl]phosphonate (4h).**

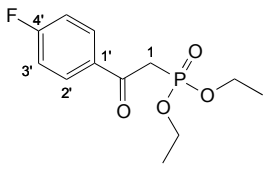


GP-A (10 mL THF) starting from ethyl 4-fluorobenzoate (**2h**, 351 µL, 2.38 mmol). FC ($SiO_2$; EtOAc/heptane 4:1) gave phosphonate **4h** (652 mg, quant.) as colorless oil.

$R_f$ = 0.20 ($SiO_2$; EtOAc/heptane 4:1); $^1$H NMR (400 MHz, $CDCl_3$): $\delta$ = 1.29 (td, $J$ = 7.2 Hz, $^4J$(H,P) = 0.4 Hz, 6 H; 2 $OCH_2CH_3$), 3.61 (d, $^2J$(H,P) = 22.8 Hz, 2 H; H–C(1)), 4.09–4.21 (m, 4 H; 2 $OCH_2CH_3$), 7.13–7.20 (m, 2 H; H–C(3')), 8.03–8.13 ppm (m, 2 H; H–C(2')); $^{13}$C NMR (100 MHz, $CDCl_3$): $\delta$ = 16.25 (d, $^3J$(C,P) = 6.3 Hz; 2 $OCH_2CH_3$), 38.66 (d, $^1J$(C,P) = 128.6 Hz; C(1)), 62.70 (d, $^2J$(C,P) = 6.5 Hz; 2 $OCH_2CH_3$), 115.75 (d, $^2J$(C,F) = 21.9 Hz; C(3')), 131.87 (d, $^3J$(C,F) = 9.5 Hz; C(2')), 132.98 (dd, $^4J$(C,F) = 2.8 Hz, $^3J$(C,P) = 1.8 Hz; C(1')), 166.10 (d, $^1J$(C,F) = 254.5 Hz; C(4')), 190.33 ppm (d, $^2J$(C,P) = 6.5 Hz; C=O); $^{19}$F NMR (376 MHz, $CDCl_3$): $\delta$ = (–104.17)–(–104.06) ppm (m, 1 F); $^{31}$P NMR (162 MHz, $CDCl_3$): $\delta$ = 19.55 ppm (tquint., $^2J$(P,H) = 24.0 Hz, $^3J$(P,H) = 8.1 Hz, 1 P; $PO_3$); IR (ATR): $\tilde{n}$ = 2984 (w), 2934 (w), 1678 (m), 1595 (m), 1508 (w), 1479 (w), 1444 (w), 1413 (w), 1393 (w), 1276 (m, sh), 1238 (s), 1159 (m), 1098 (w), 1052 (m, sh), 1020 (s), 1003 (s), 958 (s), 852 (w, sh), 806 (s), 719 (w), 643 $cm^{-1}$ (w); HR-MS (ESI): *m/z* (%): 275.0837 (95, $[M + H]^+$, calcd for $C_{12}H_{17}FO_4P^+$: 275.0843), 219.0210 (100)

**Diethyl [2-(4-Chlorophenyl)-2-oxoethyl]phosphonate (4i).**

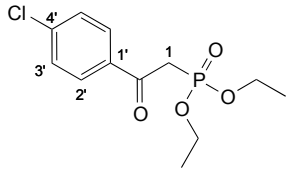


GP-A (20 mL THF) starting from ethyl-4-chlorobenzoate (**2i**, 649 µL, 4.08 mmol). FC ($SiO_2$; EtOAc/heptane 2:1 → 1:0) gave phosphonate **4i** (892 mg, 75%) as a colorless oil.

$R_f$ = 0.51 ($SiO_2$; EtOAc); $^1$H NMR (400 MHz, $CDCl_3$): $\delta$ = 1.31 (t, $J$ = 7.1 Hz, 6 H; 2 $OCH_2CH_3$), 3.62 (d, $^2J$(H,P) = 22.8 Hz, 2 H; H–C(1)), 4.10–4.20 (m, 4 H; $OCH_2CH_3$), 7.48, 7.99 ppm (AA'MM', $J$ = 8.8 Hz, 4H; $C_6H_4$); $^{13}$C NMR (100 MHz, $CDCl_3$): $\delta$ = 16.26 (d, $^3J$(C,P) = 6.3 Hz; 2 $OCH_2CH_3$), 38.69 (d, $^1J$(C,P) = 128.5 Hz; C(1)), 62.75 (d, $^3J$(C,P) = 6.5 Hz; $OCH_2CH_3$), 128.94 (C(3')), 130.52 (C(2')), 134.85 (C(1')), 140.28 (C(4')), 190.75 ppm (d, $^2J$(C,P) = 6.5 Hz; C=O); $^{31}$P NMR (161 MHz, $CDCl_3$): $\delta$ = 19.11–19.68 ppm (m, 1 P; $PO_3$); IR (ATR): $\tilde{n}$ = 2983 (w), 2932 (w), 1679 (m, C=O), 1588 (m), 1571 (w), 1489 (w), 1443 (w), 1397 (w), 1249 (s), 1091 (m), 1052 (m), 1020 (s), 1000 (s), 958 (s), 804 (m), 762 cm$^{-1}$ (m); HR-MS (ESI): *m/z* (%): 313.0383 (100, $[M + Na]^+$, calcd for $C_{12}H_{16}ClNaO_4P^+$: 313.0367), 291.0547 (63, $[M + H]^+$, calcd for $C_{12}H_{17}ClO_4P^+$: 291.0547).

**Diethyl [2-(4-Bromophenyl)-2-oxoethyl]phosphonate (4j).**

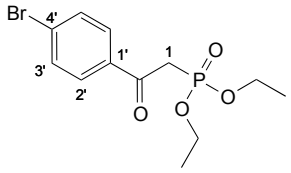


GP-A (10 mL THF) starting from ethyl 4-bromobenzoate (**2j**, 346 µL, 2.07 mmol). FC ($SiO_2$; EtOAc/heptane 4:1) gave phosphonate **4j** (614 mg, quant.) as a colorless oil.

$R_f$ = 0.26 ($SiO_2$; EtOAc/heptane 4:1); $^1$H NMR (400 MHz, $CDCl_3$): $\delta$ = 1.30 (td, $J$ = 7.1 Hz, $^4J$(H,P) = 2.1 Hz, 6 H; 2 $OCH_2CH_3$), 3.60 (d, $^2J$(H,P) = 22.8 Hz, 2 H; H–C(1)), 4.09–4.19 (m, 4 H; 2 $OCH_2CH_3$), 7.63, 7.90 ppm (AA'MM', $J$ = 9.1 Hz, 4 H; $C_6H_4$); $^{13}$C NMR (100 MHz, $CDCl_3$): $\delta$ = 16.26 (d, $^3J$(C,P) = 6.2 Hz; 2 $OCH_2CH_3$), 38.67 (d, $^1J$(C,P) = 128.4 Hz; C(1)), 62.74 (d, $^2J$(C,P) = 6.4 Hz; 2 $OCH_2CH_3$), 129.07 (C(4')), 130.51 (C(2')), 131.94 ((3')), 135.24 (d, $^3J$(C,P) = 1.7 Hz; C(1')), 190.95 ppm (d, $^2J$(C,P) = 6.5 Hz; C=O); $^{31}$P NMR (162 MHz, $CDCl_3$): $\delta$ = 19.33 ppm (tquint., $^2J$(P,H) = 24.1 Hz, $^3J$(P,H) = 8.1 Hz, 1 P; $PO_3$); IR (ATR): $\tilde{n}$ = 2982 (w), 2932 (w), 1679 (m), 1585 (m), 1568 (w, sh), 1484 (w), 1443 (w), 1395 (w), 1248 (s), 1200 (w), 1163 (w), 1098 (w), 1052 (s, sh), 1019 (s), 998 (s), 956 (s), 872 (w), 802 (s), 738 (m), 704 $cm^{-1}$ (w); HR-MS (ESI): *m/z* (%): 337.0027 (100, $[M + H]^+$, calcd for $C_{12}H_{17}{}^{81}BrO_4P^+$: 337.0022), 335.0044 (88, $[M + H]^+$, calcd for $C_{12}H_{17}{}^{79}BrO_4P^+$: 335.0042).

**Diethyl [2-(4-Iodophenyl)-2-oxoethyl]phosphonate (4k).**

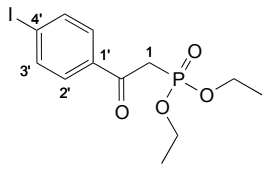


GP-A (10 mL THF) starting from ethyl 4-bromobenzoate (**2k,** 346 µL, 2.07 mmol). FC ($SiO_2$; EtOAc/heptane 4:1) gave phosphonate **4k** (789 mg, quant.) as a colorless oil.

$R_f$ = 0.28 ($SiO_2$; EtOAc/heptane 4:1); $^1$H NMR (400 MHz, $CDCl_3$): $\delta$ = 1.30 (td, $J$ = 7.1 Hz, $^4J$(H,P) = 0.4 Hz, 6 H; 2 $OCH_2CH_3$), 3.59 (d, $^2J$(H,P) = 22.8 Hz, 2 H; H–C(1)), 4.09–4.19 (m, 4 H; 2 $OCH_2CH_3$), 7.74, 7.86 ppm (AA'MM', $J$ = 8.8 Hz, 4 H; $C_6H_4$); $^{13}$C NMR (100 MHz, $CDCl_3$): $\delta$ = 16.27 (d, $^3J$(C,P) = 6.2 Hz; 2 $OCH_2CH_3$), 38.60 (d, $^1J$(C,P) = 128.4 Hz; C(1)), 62.74 (d, $^2J$(C,P) = 6.5 Hz; 2 $OCH_2CH_3$), 102.00 (C(4')), 130.42 (C(3')), 135.77 (d, $^3J$(C,F) = 1.7 Hz; C(1')), 137.95 (C(2')), 191.27 ppm (d, $^2J$(C,P) = 6.6 Hz; C=O); $^{31}$P NMR (162 MHz, $CDCl_3$): $\delta$ = 19.32 ppm (tquint., $^2J$(P,H) = 24.0 Hz, $^3J$(P,H) = 8.1 Hz, 1 P; $PO_3$); IR (ATR): $\tilde{n}$ = 2981 (w), 2931 (w), 1677 (m), 1580 (m), 1561 (w), 1480 (w), 1442 (w), 1391 (m), 1368 (w), 1247 (s), 1199 (w), 1162 (w), 1097 (w), 1053 (s), 1019 (s), 995 (s), 956 (s), 872 (w), 800 (s), 733 (m), 701 cm$^{-1}$ (w); HR-MS (ESI): *m/z* (%): 382.9898 (100, $[M + H]^+$, calcd for $C_{12}H_{17}IO_4P^+$: 382.9904).

**Diethyl {2-Oxo-2-[4-(trifluoromethyl)phenyl]ethyl}phosphonate (4l).**

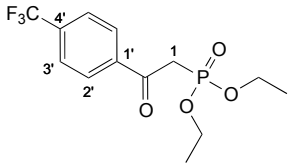


A solution of 4-(trifluoromethyl)benzoic acid (**3l**, 861 µL, 5.26 mmol) in EtOH (18.4 mL) was treated with 95% $H_2SO_4$ (28 µL, 0.53 mmol). The mixture was stirred at 80 °C for 4 h and evaporated. The residue was treated with 0.1 M aq. NaOH (50 mL). The aqueous phase was extracted with EtOAc (3 x 50 mL). The combined organic phases were washed with brine (50 mL), dried over $MgSO_4$, filtered, and evaporated to afford ester **2l** as a colorless oil.

GP-A (20 mL THF) starting from ester **2l**. FC ($SiO_2$; EtOAc/heptane 2:1 → 4:1) gave phosphonate **4l** (1314 mg, 77%) as a colorless oil.

$R_f$ = 0.58 ($SiO_2$; EtOAc); $^1$H NMR (400 MHz, $CDCl_3$): $\delta$ = 1.29 (td, $J$ = 7.0 Hz, $^4J$(H,P) = 1.4 Hz, 6 H; 2 $OCH_2CH_3$), 3.66 (d, $^2J$(H,P) = 22.9 Hz, 2 H; H–C(1)), 4.14 and 4.16 (2 qd, $J$ = 7.2 Hz, $^3J$(H,P) = 0.9 Hz, 4 H; 2 $OCH_2CH_3$), 7.75, 8.14 ppm (AA'MM', $J$ = 8.2 Hz, 4 H; $C_6H_4$); $^{13}$C NMR (100 MHz, $CDCl_3$): $\delta$ = 16.21 (d, $^3J$(C,P) = 6.2 Hz; 2 $OCH_2CH_3$), 38.96 (d, $^1J$(C,P) = 128.3 Hz; C(1)), 62.81 (d, $^3J$(C,P) = 6.4 Hz; 2 $OCH_2CH_3$), 123.49 (q, $^1J$(C,F) = 271.1 Hz; $CF_3$), 125.65 (q, $^3J$(C,F) = 3.7 Hz; C(3')), 129.41 (C(2')), 134.82 (q, $^2J$(C,F) = 32.6 Hz; C(4')), 139.10 (C(1')), 191.09 ppm (d, $^2J$(C,P) = 6.6 Hz; C=O); $^{19}$F NMR (376 MHz, $CDCl_3$): $\delta$ = –63.25 ppm (s, 3 F; $CF_3$); $^{31}$P NMR (162 MHz, $CDCl_3$): $\delta$ = 18.52–19.26 ppm (m, 1 P; $PO_3$); IR (ATR): $\tilde{n}$ = 2986 (w), 1686 (m, C=O), 1582 (very w), 1513 (w), 1445 (w), 1412 (w), 1326 (s), 1251 (s), 1166 (m), 1125 (m), 1064 (s), 1020 (s), 1002 (s), 959 (s), 858 (w), 818 (m), 719 $cm^{-1}$ (m); HR-MS (ESI): *m/z* (%): 325.0827 (100, $[M + H]^+$, calcd for $C_{13}H_{17}F_3O_4P^+$: 325.0811).

**Diethyl {2-Oxo-2-[4-(trifluoromethoxy)phenyl]ethyl}phosphonate (4m).**

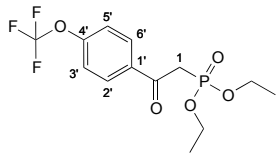

A solution of 4-trifluormethoxybenzoic acid (**3m**, 1.0 g, 4.7 mmol) in EtOH (10 mL) was treated with 95% $H_2SO_4$ (25 µL, 0.47 mmol), heated to 80 °C for 20 h, cooled to 22 °C, and evaporated. The residue was treated with sat. aq. $NaHCO_3$ solution (50 mL). The aqueous phase was extracted with EtOAc (3 x 50 mL). The combined organic phases were dried over $MgSO_4$, filtered, and evaporated to afford ester **2m**.

GP-A (10 mL THF) starting from ester **2m**. FC ($SiO_2$; EtOAc) gave phosphonate **4m** (1.1 g, 69%) as a colorless oil.

$R_f$ = 0.46 (EtOAc); $^1$H NMR (400 MHz, $CDCl_3$): $\delta$ = 1.28 (t, $J$ = 7.1 Hz, 6 H; 2 $CH_3$), 3.60 (d, $^2J$(H,P) = 22.9 Hz, 2 H; $H_2$–C(1)), 3.95–4.30 (m, 4 H; 2 $OCH_2$), 7.29 (br. d, $J$ = 8.2 Hz, 2 H; H–C(3'), H–C(5')), 8.08 ppm (br. d, $J$ = 8.8 Hz, 2 H; H–C(2'), H–C(6')); $^{13}$C NMR (100 MHz, $CDCl_3$): $\delta$ = 16.38 (d, $^3J$(C,P) = 6.3 Hz; $CH_3$), 38.93 (d, $^1J$(C,P) = 129.1 Hz; C(1)), 62.92 (d, $^2J$(C,P) = 6.5 Hz; 2 $OCH_2$), 120.39 (q, $^1J$(C,F) = 259.1 Hz; $CF_3$), 120.40 (C(3')), 131.34 (C(2')), 134.81 (d; $^3J$(C,P) = 1.7 Hz; C(1')), 153.17 (q, $^3J$(C,F) = 1.8 Hz; C(4')), 190.57 ppm (d, $^2J$(C,P) = 6.5 Hz; C=O); $^{31}$P NMR (162 MHz; $CDCl_3$): $\delta$ = 19.25 ppm (tquint., $J$ = 24.2, 8.2 Hz, 1 P; $PO_3$); $^{19}$F NMR (376 MHz; $CDCl_3$): $\delta$ = –57.61 ppm (s, 3 F; $CF_3$); IR (ATR): $\tilde{\eta}$ = 2986 (w), 1683 (s), 1602 (m), 1507 (w), 1445 (w), 1416 (w), 1247 (s), 1206 (s), 1162 (s), 1099 (m), 1053 (s), 1021 (s), 1003 (s), 959 (s), 804 (m), 730 (w), 659 $cm^{-1}$ (w); HR-MS (EI) *m/z* (%): 341.0756 (100, $[M]^+$, calcd for $C_{13}H_{17}F_3O_5P^+$: 341.0760), 313.0442 (46, $[M - C_2H_4]^+$, calcd for $C_{11}H_{13}F_3O_5P^+$: 313.0453), 285.0128 (38, $[M - 2\ C_2H_4]^+$, calcd for $C_9H_9F_3O_5P^+$: 285.0140).

**Diethyl [2-Oxo-2-(thien-2-yl)ethyl]phosphonate (4n).**

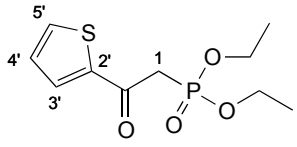


GP-A (10 mL THF) starting from ethyl thiophene-2-carboxylate (**2n**, 215 µL, 1.60 mmol). FC ($SiO_2$; EtOAc/heptane 2:1 → 1:0) gave phosphonate **4n** (261 mg, 62%) as an off-white oil.

$R_f$ = 0.43 ($SiO_2$; EtOAc); $^1$H NMR (400 MHz, $CDCl_3$): $\delta$ = 1.30 (t, $J$ = 7.1 Hz, 6 H; 2 $OCH_2CH_3$), 3.55 (d, $^2J$(H,P) = 22.5 Hz, 2 H; H–C(1)), 4.14 and 4.17 (2 qd, $^3J$(H,P) = 1.1 Hz, $J$ = 7.1 Hz, 4 H; 2 $OCH_2CH_3$), 7.16 (dd, $J$ = 4.9, 3.9 Hz, 1 H; H–C(4')), 7.70 (dd, $J$ = 4.9, 1.1 Hz, 1 H; H–C(5')), 7.83 ppm (dd, $J$ = 3.8, 1.1 Hz, 1 H; H–C(3')); $^{13}$C NMR (100 MHz, $CDCl_3$): $\delta$ = 16.25 (d, $^3J$(C,P) = 6.3 Hz; 2 $OCH_2CH_3$), 39.42 (d, $^1J$(C,P) = 129.2 Hz; C(1)), 62.77 (d, $^3J$(C,P) = 6.5 Hz; 2 $OCH_2CH_3$), 128.33 (C(5')), 134.17 (C(4')), 135.09 (C('3)), 143.93 (d, $^3J$(C,P) = 2.2 Hz; C(2')), 184.21 ppm (d, $^2J$(C,P) = 6.5 Hz; C=O); $^{31}$P NMR (161 MHz, $CDCl_3$): $\delta$ = 19.00–19.71 ppm (m, 1 P; $PO_3$); IR (ATR): $\tilde{\nu}$ = 2924 (w), 2852 (w), 1658 (w), 1557 (s; C=O), 1480 (s), 1440 (s), 1367 (m), 1302 (m), 1232 (s), 1163 (m), 1114 (m), 1037 (s), 989 (m), 966 (m), 934 (m), 857 (w), 799 $cm^{-1}$ (s); HR-MS (ESI): *m/z* (%): 285.0350 (100, $[M + Na]^+$, calcd for $C_{10}H_{15}NaO_4PS^+$: 285.0321).

**Diethyl [2-(5-Chloro-thien-2-yl)-2-oxoethyl]phosphonate (4o).**

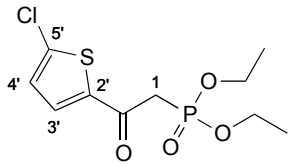


A solution of 5-chlorothiophene-2-carboxylic acid (**3o**, 321 µL, 2.29 mmol) in EtOH (8 mL) was treated with 95% $H_2SO_4$ (12 µL, 0.23 mmol), stirred at 80 °C for 30 h, and evaporated. The residue was treated with 1.0 M aq. NaOH (50 mL). The aqueous phase was extracted with EtOAc (3 x 50 mL). The combined organic phases were washed with brine (50 mL), dried over $MgSO_4$, filtered, and evaporated to afford ester **2o** as a yellow oil.

GP-A (10 mL THF) starting from ester **2o**. FC ($SiO_2$; EtOAc) afforded phosphonate **4o** (594 mg, 87%) as a slightly yellow oil.

$R_f$ = 0.27 ($SiO_2$; EtOAc); $^1$H NMR (400 MHz, $CDCl_3$): $\delta$ = 1.31 (t, $J$ = 7.2 Hz, 6 H; 2 $OCH_2CH_3$), 3.47 (d, $^2J$(H,P) = 22.6 Hz, 2 H; H–C(1)), 4.06–4.23 (m, 4 H; $OCH_2CH_3$), 6.98 (d, $J$ = 4.1 Hz, 1 H; H–C(4')), 7.63 ppm (d, $J$ = 4.1 Hz, 1 H; H–C(3')); $^{13}$C NMR (100 MHz, $CDCl_3$): $\delta$ = 16.26 (d, $^3J$(C,P) = 6.2 Hz; $OCH_2CH_3$), 38.96 (d, $^1J$(C,P) = 129.0 Hz; C(1)), 62.84 (d, $^3J$(C,P) = 6.5 Hz; $OCH_2CH_3$), 127.85 (C(4')), 133.84 (C(3')), 141.11 (C(1')), 142.32 (d, $^3J$(C,P) = 2.0 Hz; C(5')), 183.33 ppm (d, $^2J$(C,P) = 6.4 Hz; C=O); $^{31}$P NMR (162 MHz, $CDCl_3$): $\delta$ = 18.88 ppm (tquint., $^2J$(P,H) = 24.5 Hz, $^3J$(P,H) = 8.2 Hz, 1 P; $PO_3$); IR (ATR): $\tilde{n}$ = 2982 (w), 2931 (w), 1715 (w), 1655 (m), 1528 (w), 1418 (s), 1327 (w), 1283 (m), 1249 (s), 1202 (w), 1162 (w), 1049 (m, sh), 1012 (s), 943 (s), 869 (w), 796 (m), 738 (m), 682 cm$^{-1}$ (w); HR-MS (ESI): *m/z* (%): 299.0077 (34, $[M + H]^+$, calcd for $C_{10}H_{15}{}^{37}ClO_4PS^+$: 299.0082), 297.0102 (100, $[M + H]^+$, calcd for $C_{10}H_{15}{}^{35}ClO_4PS^+$: 297.0112).

**Diethyl [2-(5-Bromothien-2-yl)-2-oxoethyl]phosphonat (4p).**

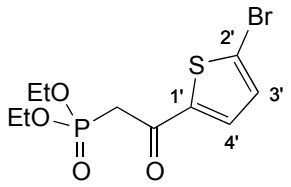


A solution of 5-bromothiophen-2-carbonic acid (**3p**, 1.0 g, 4.8 mmol) in EtOH (18~mL) was treated with 95% $H_2SO_4$ (28 µL, 0.53 mmol). The mixture was stirred at 80 °C for 4 h and evaporated. The residue was treated with 0.1 M aq. NaOH (50 mL). The aqueous phase was extracted with EtOAc (3 x 50 mL). The combined organic phases were washed with brine (50 mL), dried over $MgSO_4$, filtered, and evaporated to afford ester **2p** as a colorless oil.

GP-A (10 mL THF) starting from ester **2p**. FC ($SiO_2$; EtOAc) gave phosphonate **4p** (1.1 mg, 67%) as a yellow solid.

$R_f$ = 0.34 (EtOAc); m.p. 60–62 °C; $^1$H NMR (400 MHz, $CDCl_3$): $\delta$ = 1.30 (td, $^4J$(H,P) = 0.6 Hz, $J$ = 7.0 Hz, 6 H; 2 $CH_3$), 3.47 (d, $^2J$(H,P) = 22.6 Hz, 2 H; $H_2$–C(1)), 4.10–4.18 (m, 4 H; 2 $OCH_2$), 7.12 (d, $J$ = 4.1 Hz, 1 H; H–C(4')), 7.57 ppm (d, $J$ = 4.0 Hz; H–C(3')); $^{13}$C NMR (100 MHz, $CDCl_3$): $\delta$ = 16.41 (d, $^3J$(C,P) = 6.3 Hz; CH3), 39.09 (d, $^1J$(C,P) = 129.7 Hz; C(1)), 62.99 (d, $^2J$(C,P) = 6.5 Hz; $OCH_2$), 124.47 (C(5')), 130.28 (C(3')), 131.62 (C(4')), 145.35 (d, $^3J$(C,P) = 2.0 Hz; C(2')), 183.28 ppm (d, $^2J$(C,P) = 8.4 Hz; C(2)); $^{31}$P NMR (162 MHz, $CDCl_3$): $\delta$ = 18.88 ppm (tquint., J = 24.2, 8.2 Hz, 1 P; PO3); IR (ATR): $\tilde{n}$ = 3106 (w), 3080 (w), 2967 (w), 2915 (w), 1652 (s), 1522 (w), 1482 (w), 1441 (w), 1404 (s), 1369 (w), 1322 (w), 1208(s), 1237 (s), 1212 (s), 1165 (m), 1127 (m), 1098 (w), 1020 (s), 984 (s), 968 (s), 945 (s), 881 (m), 801 (s), 738 (m), 679 cm$^{-1}$ (m); HR-MS (ESI): *m/z* (%): 364.9408 (100, [$M$ + Na]+, calcd for $C_{10}H_{14}{}^{81}BrNaO_4PS^+$: 364.9406), 362.9427 (99, [$M$ + Na]$^+$, calcd for $C_{10}H_{14}{}^{79}BrNaO_4PS^+$: 362.9426), 342.9587 (66, [$M$ + H]$^+$, calcd for $C_{10}H_{15}{}^{81}BrO_4PS^+$: 342.9586), 340.9608 (59, [$M$ + H]$^+$, calcd for $C_{10}H_{15}{}^{79}BrO_4PS^+$: 340.9607).

**4-Methoxyquinazoline-7-carbaldehyde (5).**

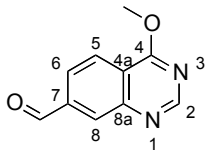


A suspension of alcohol **9** (317 mg, 1.45 mmol) in $CH_2Cl_2$ (10 mL) at 0 °C ander argon was treated with PCC (470 mg, 2.18 mmol) and stirred for 40 min at 0 °C and for 3 h 20 min at 22 °C. The mixture was filtered over Celite and washed with $CH_2Cl_2$. Evaporation and chromatography ($SiO_2$; MeOH/$CH_2Cl_2$ 2:98) gave aldehyde **5** (273 mg, 99%) as a white solid. $R_f$ = 0.37 ($SiO_2$; MeOH/$CH_2Cl_2$ 1:19); m.p. 156–157 °C; $^1$H NMR (400 MHz, $CDCl_3$): $\delta$ = 4.22 (s, 3 H; OMe), 8.05 (dd, $J$ = 8.5, 1.5 Hz, 1 H; H–C(6)), 8.29 (d, $J$ = 8.5 Hz, 1 H; H–C(5)), 8.39 (d, $J$ = 1.0 Hz, 1 H; H–C(8)), 8.91 (s, 1 H; H–C(2)), 10.23 ppm (s, 1 H; H–C=O); $^{13}$C NMR (100 MHz, $CDCl_3$): $\delta$ = 54.73 (OMe), 120.01 (C(4a)), 124.20, 124.82, 132.58 (C(8)), 139.93 (C(7)), 151.04 (C(8a)), 155.53 (C(2)), 167.16 (C(4)), 191.62 ppm (CHO); IR (ATR): $\tilde{n}$ = 2962 (w), 2923 (w), 2855 (w), 1942 (w), 1693 (s), 1569 (s), 1493 (s), 1450 (s), 1396 (w, sh), 1370 (s), 1351 (s), 1295 (m), 1256 (m), 1155 (s), 1091 (s), 1005 (w), 970 (s), 873 (s), 833 (m), 790 (s), 768 (s), 744 (w), 677 (s), 639 (m), 626 cm$^{-1}$ (m); HR-MS (ESI): *m/z* (%): 189.0659 (100, [$M$ + H]$^+$, calcd for $C_{10}H_9N_2O_2^+$: 189.0659).

**Methyl 4-Oxo-3,4-dihydroquinazoline-7-carboxylate (7).[23]**

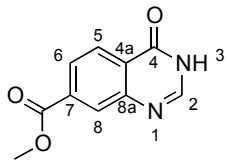


A solution of dimethyl-2-aminoterephthalate (5000 mg, 23.9 mmol) in formamide (30 mL) under argon was stirred for 3 h at 150 °C, for 14.5 h at 22 °C, for 5 h at 150 °C, and cooled to 0 °C. The brown suspension was treated with ice-cold $H_2O$ (100 mL), the solid was filtered off and washed with ice-cold $H_2O$ (25 mL). The filtrate was dried in the vacuum oven at 50 °C for several days to afford quinazolinone **7** (3057 mg, 63%) as an off-white solid.

$R_f$ = 0.12 ($SiO_2$; EtOAc/heptane 2:1); m.p. 250–254 °C (Ref:[23] 252–254 °C); $^1$H NMR (300 MHz, $CD_3OD$): $\delta$ = 3.97 (s, 3 H; OMe), 8.11 (dd, $J$ = 8.4, 1.6 Hz, 1 H; H–C(6)), 8.15 (s, 1 H; H–C(2)), 8.29–8.32 ppm (m, 2 H; H–C(5); H–C(8)). $^{13}$C NMR (100 MHz, $CDON(CD_3)_2$): $\delta$ = 52.50 (OMe), 126.48 (C(8)), 126.50 (C(4a)), 126.89 (C(6)), 128.85 (C(5)), 135.29 (C(7)), 146.81 (C(2)), 149.39 (C(8a)), 160.61 (C(4)), 165.91 ppm ($CO_2$Me); IR (ATR): $\tilde{n}$ = 3165 (w), 3016 (w), 2871 (w), 1732 (s, CO), 1661 (s, CO), 1607 (s), 1558 (m), 1434 (s), 1389 (m), 1266 (s), 1220 (s), 1155 (m), 1098 (m), 988 (s), 916 (s), 881 (m), 790 cm$^{-1}$ (m); HR-EI-MS: *m/z* (%): 204.0529 (88, $[M]^+$, calcd for $C_{10}H_8N_2O_3^+$: 204.0530); 173.0342 (100, $[M - OMe]^+$, calcd for $C_9H_5N_2O_2^+$: 173.0346.

**Methyl 4-Methoxyquinazoline-7-carboxylate (8).**

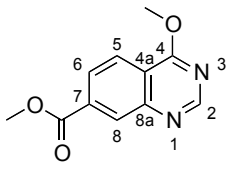


A solution of quinazolinone **7** (1000 mg, 4.90 mmol) in toluene (12 mL) was degassed with argon, heated to 80 °C, treated with $POCl_3$ (2242 µL, 24.49 mmol), stirred for 5 min, treated with DBU (732 µL, 4.90 mmol) at 90 °C, and stirred at 120 °C for 1 h. The mixture was cooled to 0 °C and carefully treated with 25% NaOMe in MeOH (10.6 g, 49 mmol) yielding a brown suspension, which was stirred at 22 °C for 30 min, and diluted with sat. aq. $NH_4Cl$ solution (100 mL) and brine (100 mL). The aqueous phase was extracted with EtOAc (5x100 mL). The combined organic phases were washed with brine (200 mL), dried over $MgSO_4$, filtered, and evaporated. Chromatography ($SiO_2$; EtOAc/heptane 1:1) gave ester **8** (862 mg, 81%) as a white solid.

$R_f$ = 0.44 ($SiO_2$; MeOH/$CH_2Cl_2$ 1:19); m.p. 154–155 °C; $^1$H NMR (400 MHz, $CDCl_3$): $\delta$ = 4.02 (s, 3 H; $CO_2Me$), 4.21 (s, 3 H; OMe), 8.16 (dd, $J$ = 8.5, 1.6 Hz, 1 H; H–C(6)), 8.22 (dd, $J$ = 8.5, 0.6 Hz, 1 H; H–C(5)), 8.62 (dd, $J$ = 0.8, 0.4 Hz, 1 H; H–C(8)), 8.88 ppm (s, 1 H; H–C(2)); $^{13}$C NMR (100 MHz, $CDCl_3$): $\delta$ = 52.67, 54.57, 119.05, 123.90, 126.73, 129.91, 134.67, 150.52, 155.14, 166.15, 167.04 ppm; IR (ATR): $\tilde{\eta}$ = 2959 (w), 1961 (w), 1721 (s), 1629 (w), 1574 (s), 1496 (s), 1454 (m), 1438 (m), 1392 (s), 1367 (m), 1312 (s), 1280 (s), 1235 (m), 1183 (m), 1166 (m), 1137 (m), 1091 (s), 961 (m), 907 (m), 872 (s), 847 (w), 791 (m), 758 (s), 677 (m), 648 $cm^{-1}$ (w); HR-MS (ESI): *m/z* (%): 219.0763 (100, $[M + H]^+$, calcd for $C_{11}H_{11}N_2O_3^+$: 219.0764); elemental analysis (%) calcd for $C_{11}H_{10}N_2O_3$ (218.2): C 60.55, H 4.62, N 12.84; found: C 60.51, H 4.73, N 12.64.

**(4-Methoxyquinazolin-7-yl)methanol (9).**

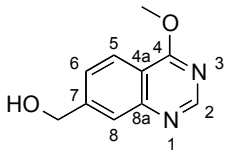


A suspension of ester **8** (862 mg, 3.95 mmol) in THF (20 mL) at 0 °C under argon was carefully treated with a 2 M $LiAlH_4$ solution in THF (1975 µL, 3.95 mmol). The resulting black mixture was stirred at 0 °C for 1 h 20 min and carefully diluted with sat. aq. $NH_4Cl$ solution (100 mL). The aqueous phase was extracted with $CH_2Cl_2$ (3 x 100 mL). The combined organic phases were dried over $MgSO_4$, filtered, and evaporated. Chromatography ($SiO_2$; MeOH/$CH_2Cl_2$ 1:99 → 3:97) gave alcohol **9** (636 mg, 85%) as a white solid.

$R_f$ = 0.29 ($SiO_2$; MeOH/$CH_2Cl_2$ 1:19); m.p. 119–121 °C; $^1$H NMR (400 MHz, $CDCl_3$): $\delta$ = 2.09–2.42 (br. s, 1 H; OH), 4.21 (s, 3 H; OMe), 4.94 (s, 2 H; $CH_2$), 7.59 (dd, $J$ = 8.5, 1.5 Hz, 1 H; H–C(6)), 7.96 (d, $J$ = 0.7 Hz, 1 H; H–C(8)), 8.16 (d, $J$ = 8.4 Hz, 1 H; H–C(5)), 8.82 ppm (s, 1 H; H–C(2)); $^{13}$C NMR (100 MHz, $CDCl_3$): $\delta$ = 54.38 (OMe), 64.64 ($CH_2OH$), 115.74 (C(4a)), 123.77 (C(5)), 124.42 (C(8)), 125.83 (C(6)), 147.28 (C(7)), 150.86 (C(8a)), 154.62 (C(2)), 167.10 ppm (C(4)); IR (ATR): $\tilde{\nu}$ = 3167 (br. m), 2850 (m), 1945 (w), 1629 (m), 1574 (s), 1494 (s), 1452 (s), 1392 (s), 1372 (s), 1344 (s), 1311 (m), 1195 (w), 1161 (m), 1118 (w), 1098 (s), 1062 (s), 976 (s), 883 (s), 834 (w), 785 (s), 737 (m), 683 (s), 638 (w), 624 $cm^{-1}$ (w); HR-MS (ESI): *m/z* (%): 191.0821 (100, $[M + H]^+$, calcd for $C_{10}H_{11}N_2O_2^+$: 191.0815).

**(2*E*)-3-(4-Methoxyquinazolin-7-yl)-1-phenylprop-2-en-1-one (10a).**

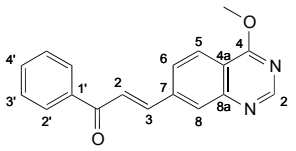

GP-B2 starting from phosphonate **4a** (136 mg, 531 μmol) (0.5 equiv. KO*t*Bu; 4 h at 22 °C). MPLC (40 g $SiO_2$; 40 mL $min^{-1}$, $MeOH/CH_2Cl_2$ 0:100 → 2:98) gave impure alkene **10a** (38 mg, 25%) as an off white solid, which was used for the next step without further purification.

HR-MS (MALDI) *m/z* (%): 291.1127 (100, $[M + H]^+$, calcd for $C_{18}H_{15}N_2O_2^+$: 291.1128).

**(2*E*)-1-(3-Fluorophenyl)-3-(4-methoxyquinazolin-7-yl)prop-2-en-1-one (10b).**

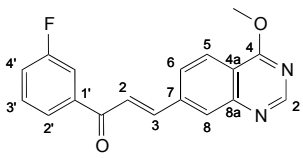

GP-B2 starting from phosphonate **4b** (146 mg, 542 μmol) (0.6 equiv. of KO*t*Bu; 5 h at 22 °C). MPLC (40 g $SiO_2$; 40 mL $min^{-1}$, $MeOH/CH_2Cl_2$ 0:100 → 2:98) gave impure alkene **10b** (173 mg, quant.) as a clear oil which was used for the next step without further purification.

HR-MS (MALDI) *m/z* (%): 309.1033 (100, $[M + H]^+$, calcd for $C_{18}H_{14}FN_2O_2^+$: 309.1034).

**(2*E*)-1-(3-Chlorophenyl)-3-(4-methoxyquinazolin-7-yl)prop-2-en-1-one (10c).**

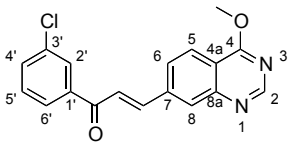


GP-B1 starting from phosphonate **4c** (200 mg, 0.69 mmol) in THF (4 mL) (2 h 45 min at 22 °C). FC ($SiO_2$; MeOH/$CH_2Cl_2$ 2:98 → 2.5:97.5) gave impure alkene **10c** (171 mg, 77%; (*E*/*Z*) 87:13) as an off-white solid, of which a small amount was purified by HPLC (Reprosil; 15 mL $min^{-1}$, hexane/*i*PrOH/$CHCl_3$ 75:3:22) to afford impure alkene **10c** (*E*/*Z*) 87:13) as an off-white solid. The compound appears to react upon concentration and was therefore used for the next step without further purification.

$R_f$ = 0.43 ($SiO_2$; MeOH/$CH_2Cl_2$ 1:19); $^1$H NMR (400 MHz, $CDCl_3$; contains approx. 15% of (*Z*)-isomer): signals of (*E*)-isomer: $\delta$ = 4.24 (s, 3 H; OMe), 7.51 (t, *J* = 7.8 Hz, 1 H; H–C(5')), 7.62 (ddd, *J* = 8.0, 2.1, 1.1 Hz, 1 H; H–C(4')), 7.69 (d, *J* = 15.7 Hz, 1 H; CH=C*H*–C=O), 7.86 (dd, *J* = 8.6, 1.5 Hz, 1 H; H–C(6)), 7.95 (dt, *J* = 7.6, 1.4 Hz, 1 H; H–C(6')), 7.98 (d, *J* = 15.2 Hz, 1 H; C*H*=CH–C=O), 8.05 (t, *J* = 1.8 Hz, 1 H; H–C(2')), 8.19 (d, *J* = 1.2 Hz, 1 H; H–C(8)), 8.23 (d, *J* = 8.4 Hz, 1 H; H–C(5)), 8.88 ppm (s, 1 H; H–C(2)); additional signals of (*Z*)-isomer: $\delta$ = 4.18 (s, 0.4 H; OMe), 6.83 ppm (d, *J* = 12.8 Hz, 0.2 H; C*H*=CH–C=O); HR-MS (ESI): *m/z* (%): 327.0706 (31, $[M + H]^+$, calcd for $C_{18}H_{14}{}^{37}ClN_2O_2^+$: 327.0710), 325.0726 (100, $[M + H]^+$, calcd for $C_{18}H_{14}{}^{35}ClN_2O_2^+$: 325.0738).

**(2*E*)-1-(3-Bromophenyl)-3-(4-methoxyquinazolin-7-yl)prop-2-en-1-one (10d).**

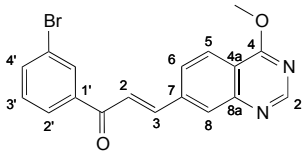


GP-B2 starting from phosphonate **4d** (178 mg, 531 μmol) (0.6 equiv. of KO*t*Bu; 4 h at 22 °C) gave impure alkene **10d** (50 mg, 34%) as an off white solid. The compound appears to react upon concentration and was therefore used for the next step without further purification.

**(2*E*)-1-(3-iodophenyl)-3-(4-methoxyquinazolin-7-yl)prop-2-en-1-one (10e).**

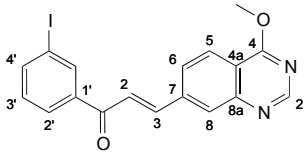


GP-B2 starting from phosphonate **4e** (203 mg, 531 μmol) (0.6 equiv. of KO*t*Bu; 5 h at 22 °C). MPLC (40 g $SiO_2$; 40 mL $min^{-1}$, MeOH/$CH_2Cl_2$ 0:100 → 2:98) gave impure alkene **10e** (116 mg, 53%) as a clear oil which was used for the next step without further purification.

HR-MS (MALDI) *m/z* (%): 417.0093 (100, $[M + H]^+$, calcd for $C_{18}H_{14}IN_2O_2^+$: 417.0094).

**(2*E*)-3-(4-Methoxyquinazolin-7-yl)-1-[3-(trifluoromethyl)phenyl]prop-2-en-1-on (10f).**

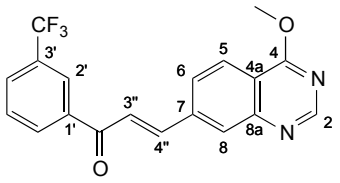


GP-B1 starting from phosponate **4f** (210 mg, 530 mmol) in THF (5 mL) (2 h at 22 °C). FC ($SiO_2$; MeOH/$CH_2Cl_2$ 0:100 → 98:2) gave impure alkene **10f** (150 mg, 78%) as an off-white solid. The compound appears to react upon concentration and was therefore used for the next step without further purification.

HR-MS (MALDI): 359.1001 (100, $[M + H]^+$, cald for $C_{19}H_{14}F_3N_2O_2^+$: 359.1002).

**(2*E*)-3-(4-Methoxyquinazolin-7-yl)-1-[3-(trifluoromethoxy)phenyl]prop-2-en-1-one (10g).**

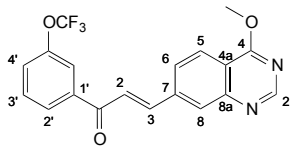


GP-B2 starting from phosphonate **4g** (181 mg, 772 μmol) (0.4 equiv. of KO*t*Bu; 5 h at 22 °C). MPLC (40 g $SiO_2$; 40 mL $min^{-1}$, MeOH/$CH_2Cl_2$ 0:100 → 2:98) gave impure alkene **10g** (156 mg, 79%) as a yellow solid which was used for the next step without further purification.

HR-MS (MALDI) *m/z* (%): 375.0949 (100, $[M + H]^+$, calcd for $C_{19}H_{14}F_3N_2O_2^+$: 375.0951).

**(2*E*)-1-(4-Fluorophenyl)-3-(4-methoxyquinazolin-7-yl)prop-2-en-1-one (10h).**

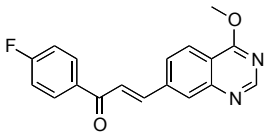

GP-B1 starting from the phosphonate **4h** (100 mg, 0.37 mmol). After addition of aldehyde **5** (69 mg, 0.37 mmol), stirring for 40 min at 0 °C and LC/MS control, aldehyde **5** (30 mg, 0.16 mol) was added. FC ($SiO_2$; MeOH/$CH_2Cl_2$ 1:99 → 1.5:98.5) and MPLC (80 g $SiO_2$; 120 mL $min^{-1}$, MeOH/$CH_2Cl_2$ 0:100 → 2:98), and MPLC (80 g $SiO_2$; 120 mL $min^{-1}$, MeOH/$CH_2Cl_2$ 0:100 → 1.5:98.5) gave impure alkene **10h** (56 mg, 50%) as an off-white solid, of which a small amount was purified by HPLC (Reprosil; 15 mL $min^{-1}$, hexane/*i*PrOH/$CHCl_3$ 75:3:22) to afford impure alkene **10h** as an off-white solid. The compound decomposed into several unidentified compounds upon concentration and was therefore used for the next step without further purification.

$R_f$ = 0.31 ($SiO_2$; MeOH/$CH_2Cl_2$ 1:19); HR-MS (ESI): *m/z* (%): 309.1029 (100, $[M + H]^+$, calcd for $C_{18}H_{14}FN_2O_2^+$: 309.1034).

**(2*E*)-1-(4-Chlorophenyl)-3-(4-methoxyquinazolin-7-yl)prop-2-en-1-one (10i).**

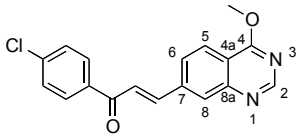

GP-B1 starting with phosphonate **4i** (150 mg, 0.52 mmol), 15 h at 22 °C). FC ($SiO_2$; MeOH/$CH_2Cl_2$ 1:99 → 2:98) gave impure alkene **10i** (140 mg, 84%; (*E*/*Z*) 95:5) as an off-white solid, of which a small amount was purified by HPLC (Reprosil; 12 mL $min^{-1}$, hexane/$CHCl_3$ 45:55 → 40:60) to afford impure alkene **10i** ((*E*/*Z*) 95:5) as an off-white solid. The compound appears to react upon concentration and was therefore used for the next step without further purification.

$R_f$ = 0.42 ($SiO_2$; MeOH/$CH_2Cl_2$ 1:19); $^1$H NMR (400 MHz, $CDCl_3$; (*E*/*Z*) 95:5): signals of the (*E*)-isomer: $\delta$ = 4.22 (s, 3 H; OMe), 7.52, 8.02 (AA'MM', *J* = 8.8 Hz, 4 H; $C_6H_4Cl$), 7.69 (d, *J* = 15.7 Hz, 1 H; CH=C*H*–C=O), 7.83 (dd, *J* = 8.5, 1.6 Hz, 1 H; H–C(6)), 7.95 (d, *J* = 16.0 Hz, 1 H; C*H*=CH–C=O), 8.16 (d, *J* = 1.2 Hz, 1 H; H–C(8)), 8.20 (d, *J* = 8.4 Hz, 1 H; H–C(5)), 8.86 ppm (s, 1 H; H–C(2)); additional signals of the (*Z*)-isomer: $\delta$ = 4.16 (s, 0.1 H; OMe), 6.79 ppm (d, *J* = 12.8 Hz, 0.1 H; CH=C*H*–C=O); $^{13}$C NMR (100 MHz, $CDCl_3$): signals of the (*E*)-isomer: $\delta$ = 54.52, 117.45, 124.33, 124.38, 125.71, 128.34, 129.11 (2 C), 129.99 (2 C), 136.08, 139.64, 139.69, 143.50, 151.20, 155.28, 166.96, 188.59 ppm; IR (ATR): $\tilde{n}$ = 2937 (w), 2864 (w), 1658 (m), 1620 (w), 1590 (s), 1574 (s), 1495 (m), 1455 (m), 1399 (m), 1380 (s), 1362 (s), 1323 (m), 1275 (s), 1209 (m), 1168 (m), 1092 (s), 1025 (m), 1009 (m), 993 (s), 978 (s), 906 (w), 875 (m), 863 (m), 815 (s), 784 (s), 746 (m), 674 (s), 629 cm$^{-1}$ (m); HR-MS (ESI): *m/z* (%): 327.0717 (33, [*M* + H]$^+$, calcd for $C_{18}H_{14}{}^{37}ClN_2O_2^+$: 327.0738), 325.0739 (100, [*M* + H]$^+$, calcd for $C_{18}H_{14}{}^{35}ClN_2O_2^+$: 325.0738).

**(2*E*)-1-(4-Bromophenyl)-3-(4-methoxyquinazolin-7-yl)prop-2-en-1-one (10j).**

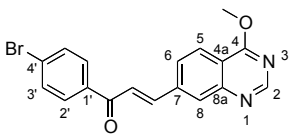


GP-B1 starting from phosphonate **4j** (110 mg, 0.33 mmol), 20 h at 22 °C. MPLC (80 g $SiO_2$; 120 mL min$^{-1}$, MeOH/$CH_2Cl_2$ 0:100 → 2:98) gave impure alkene **10j** (77 mg, 64%; (*E*/*Z*) 99:1) as an off-white solid, of which a small amount was purified by HPLC (Reprosil; 15 mL min$^{-1}$, hexane/*i*PrOH/$CHCl_3$ 72:3:25) to afford impure alkene **10d** as an off-white solid. The compound appears to react upon concentration and was therefore used for the next step without further purification.

$R_f$ = 0.38 ($SiO_2$; MeOH/$CH_2Cl_2$ 1:19); m.p. 203–206 °C; $^1$H NMR (400 MHz, $CDCl_3$): $\delta$ = 4.23 (s, 3 H; OMe), 7.69 (d, *J* = 15.8 Hz, 1 H; CH=C*H*–C=O), 7.70, 7.95 (AA'MM', *J* = 8.4 Hz, 4 H;

$C_6H_4Br$), 7.84 (dd, $J$ = 8.5, 1.6 Hz, 1 H; H–C(6)), 7.97 (d, $J$ = 15.6 Hz, 1 H; C*H*=CH–C=O), 8.17 (d, $J$ = 1.2 Hz, 1 H; H–C(8)), 8.22 (d, $J$ = 8.8 Hz, 1 H; H–C(5)), 8.87 ppm (s, 1 H; H–C(2)); $^{13}$C NMR (100 MHz, $CDCl_3$): $\delta$ = 54.52 (OMe), 117.48 (C(4a)), 124.35, 124.38, 125.73 (C(5)), 128.36 (CH=*C*H–C=O), 128.41 (C(4')), 130.10 (C(2')), 132.11 (C(3')), 136.52 (C(1')), 139.64 (C(7)), 143.58 (*C*H=CH–C=O), 151.22 (C(8a)), 155.30 (C(2)), 166.98 (C(4)), 188.84 ppm (C=O); IR (ATR): $\tilde{n}$ = 2923 (w), 2853 (w), 1658 (m), 1619 (w), 1586 (m), 1574 (s), 1495 (m), 1455 (m), 1397 (w), 1380 (s), 1361 (s), 1322 (m), 1276 (m), 1209 (m), 1168 (m), 1096 (m), 1071 (m), 1025 (m), 993 (s), 977 (m), 906 (w), 875 (m), 862 (m), 813 (s), 784 (s), 764 (w), 745 (m), 732 (m), 682 (m), 673 (m), 629 cm$^{-1}$ (m); HR-MS (ESI): *m/z* (%): 371.0211 (63, $[M + H]^+$, calcd for $C_{18}H_{14}{}^{81}BrN_2O_2^+$: 371.0213), 369.0230 (67, $[M + H]^+$, calcd for $C_{18}H_{14}{}^{79}BrN_2O_2^+$: 369.0233), 177.1271 (96), 150.0367 (100).

**(2*E*)-1-(4-Iodophenyl)-3-(4-methoxyquinazolin-7-yl)prop-2-en-1-one (10k).**

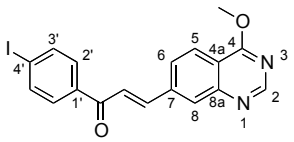


GP-B2 starting from phosphonate **4k** (120 mg, 0.31 mmol) (5 h at 22 °C). The crude product was purified by MPLC (80 g $SiO_2$; 120 mL min$^{-1}$, MeOH/$CH_2Cl_2$ 0:100 → 2:98) to afford impure alkene **10k** (116 mg, 89%; (*E*/*Z*) 92:8) as an off-white solid, of which a small amount was purified by HPLC (Reprosil; 15 mL min$^{-1}$, hexane/*i*PrOH/$CHCl_3$ 73:3:25) to afford impure alkene **10k** as an off-white solid. The compound appears to react upon concentration and was therefore used for the next step without further purification.

$R_f$ = 0.29 ($SiO_2$; MeOH/$CH_2Cl_2$ 1:19); m.p. 218–220 °C; $^1$H NMR (400 MHz, $CDCl_3$; contains 9% of (*Z*)-isomer): $\delta$ = 4.23 (s, 3 H; OMe), 7.68 (d, $J$ = 15.7 Hz, 1 H; CH=C*H*–C=O), 7.79, 7.93 (AA'MM', $J$ = 8.4, 2.0 Hz, 4 H; $C_6H_4I$), 7.84 (dd, $J$ = 8.4, 1.6 Hz, 1 H; H–C(6)), 7.97 (d, $J$ = 16.0 Hz, 1 H; C*H*=CH–C=O), 8.17 (d, $J$ = 1.4 Hz, 1 H; H–C(8)), 8.22 (d, $J$ = 8.5 Hz, 1 H; H–

C(5)), 8.87 ppm (s, 1 H; H–C(2)); $^{13}$C NMR (100 MHz, $CDCl_3$): $\delta$ = 54.53 (OMe), 101.17 (C(4')), 117.48 (C(4a)), 124.34 (C(6), C(8)), 125.74 (C(5)), 128.35 (CH=*C*H–C=O), 129.96 (C(2')), 137.06 (C(1')), 138.11 (C(3')), 139.65 (C(7)), 143.58 (*C*H=CH–C=O), 151.21 (C(8a)), 155.30 (C(2)), 166.98 (C(4)), 189.14 ppm (C=O); IR (ATR): $\tilde{\nu}$ = 3049 (w), 2924 (w), 1915 (w), 1660 (m), 1621 (m), 1603 (m), 1576 (s), 1558 (s), 1494 (m), 1456 (m), 1441 (s), 1378 (s), 1358 (s), 1305 (m), 1288 (s), 1247 (m), 1221 (m), 1190 (m), 1178 (m), 1159 (m), 1124 (m), 1103 (m), 1094 (m), 1062 (m), 1024 (m), 1007 (s), 970 (s), 847 (m), 832 (m), 810 (s), 789 (s), 738 (m), 671 (s), 630 cm$^{-1}$ (s); HR-MS (ESI): *m/z* (%): 417.0084 (100, $[M + H]^+$, calcd for $C_{18}H_{14}IN_2O_2^+$: 417.0094).

**(2*E*)-3-(4-Methoxyquinazolin-7-yl)-1-[4-(trifluoromethyl)phenyl]prop-2-en-1-one (10l).**

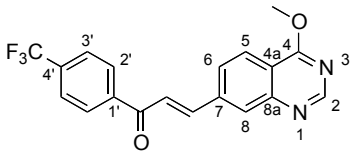


GP-B2 starting from phosphonate **4l** (110 mg, 0.34 mmol) (3 h at 22 °C). MPLC (80 g $SiO_2$; 120 mL min$^{-1}$, MeOH/$CH_2Cl_2$ 0:100 → 2:98) gave impure alkene **10l** (105 mg, 86%; (*E*/*Z*) 96:4) as an off-white solid, of which a small amount was purified by HPLC (Reprosil; 15 mL min$^{-1}$, hexane/*i*PrOH/$CHCl_3$ 75:3:22) to afford impure alkene **10l** as an off-white solid. The compound appears to react upon concentration and was therefore used for the next step without further purification.

$R_f$ = 0.36 ($SiO_2$; MeOH/$CH_2Cl_2$ 1:19); $^1$H NMR (400 MHz, $CDCl_3$): $\delta$ = 4.24 (s, 3 H; OMe), 7.71 (d, *J* = 15.7 Hz, 1 H; CH=C*H*–C=O), 7.83, 8.18 (AA'MM', *J* = 8.0 Hz, 4 H; $C_6H_4CF_3$), 7.82 (dd, *J* = 8.4, 1.6 Hz, 1 H; H–C(6)), 7.99 (d, *J* = 15.7 Hz, 1 H; C*H*=CH–C=O), 8.16 (d, *J* = 1.6 Hz, 1 H; H–C(8)), 8.24 (d, *J* = 8.5 Hz, 1 H; H–C(5)), 8.88 ppm (s, 1 H; H–C(2)); $^{13}$C NMR (100 MHz, $CDCl_3$): $\delta$ = 54.55 (OMe), 117.60 (C(4a)), 123.61 (q, $^1J$(C,F) = 271.1 Hz; $CF_3$), 124.39 (CH=*C*H–C=O), 124.42 (C(5)), 125.71 (C(8)), 125.84 (q, $^3J$(C,F) = 3.7 Hz; C(3')),

128.54 (C(6)), 128.88 (C(2')), 134.43 (q, $^2J$(C,F) = 32.7 Hz; C(4')), 139.42 (C(7)), 140.60 (C(1')), 144.26 (*C*H=CH–C=O), 151.22 (C(8a)), 155.36 (C(2)), 166.98 (C(4)), 189.09 ppm (C=O); $^{19}$F NMR (376 MHz, $CDCl_3$): $\delta$ = –63.07 ppm (s, 3 F; $CF_3$); IR (ATR): $\tilde{n}$ = 2964 (w), 1933 (w), 1660 (m), 1605 (s), 1575 (s), 1563 (s), 1496 (s), 1454 (m), 1384 (s), 1360 (m), 1320 (s), 1283 (m), 1213 (m), 1165 (s), 1124 (s), 1109 (s), 1097 (s), 1066 (s), 1032 (m), 1012 (m), 985 (s), 978 (s), 883 (m), 874 (m), 831 (s), 796 (s), 748 (m), 728 (m), 699 (m), 680 cm$^{-1}$ (s); HR-MS (ESI): *m/z* (%): 359.1001 (100, $[M + H]^+$, calcd for $C_{19}H_{14}F_3N_2O_2^+$: 359.1002).

**(2*E*)-3-(4-Methoxyquinazolin-7-yl)-1-(4-(trifluoromethoxy)phenyl)prop-2-en-1-one (10m).**

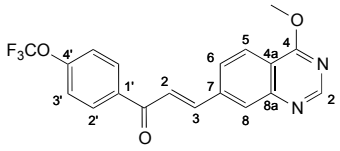


GP-B2 starting from phosphonate **4m** (181 mg, 772 µmol) (0.4 equiv. of Ko*t*Bu; 5 h at 22 °C). MPLC (40 g $SiO_2$; 40 mL min$^{-1}$, MeOH/$CH_2Cl_2$ 0:100 → 2:98) gave impure alkene **10m** (156 mg, 79%) as a yellow solid which was used for the next step without further purification. HR-MS (MALDI) *m/z* (%): 375.0950 (100, $[M + H]^+$, calcd for $C_{19}H_{14}F_3N_2O_2^+$: 375.0951).

**(2*E*)-3-(4-Methoxyquinazolin-7-yl)-1-(thien-2-yl)prop-2-en-1-one (10n).**

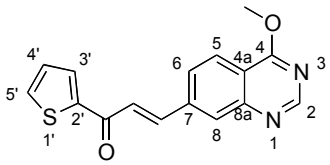


GP-B1 starting from phosphonate **4n** (130 mg, 0.50 mmol) (1 h at 22 °C. FC ($SiO_2$; MeOH/$CH_2Cl_2$ 1:99 → 3:97) gave impure alkene **10n** (147 mg, quant.; (*E*/*Z*) 92:8) as an off-white solid, of which a small amount was purified by HPLC (Reprosil; 15 mL min$^{-1}$, hexane/$CHCl_3$ 50:50 → 35:65) to afford impure alkene **10n** as an off-white solid. The

compound appears to react upon concentration and was therefore used for the next step without further purification.

$R_f$ = 0.18 ($SiO_2$; MeOH/$CH_2Cl_2$ 2:98); m.p. 191 °C (decomp.); $^1$H NMR (400 MHz, $CDCl_3$; contains 9% of the (*Z*)-isomer): $\delta$ = 4.23 (s, 3 H; OMe), 7.25 (dd, *J* = 4.9, 3.8 Hz, 1 H; H–C(4')), 7.64 (d, *J* = 15.6 Hz, 1 H; CH=C*H*–C=O), 7.76 (dd, *J* = 4.9, 1.1 Hz, 1 H; H–C(5')), 7.85 (dd, *J* = 8.6, 1.5 Hz, 1 H; H–C(6)), 7.94 (dd, *J* = 3.8, 1.1 Hz, 1 H; H–C(3')), 8.00 (d, *J* = 15.6 Hz, 1 H; C*H*=CH–C=O), 8.23 (d, *J* = 8.4 Hz, 1 H; H–C(5)), 8.23 (d, *J* = 0.8 Hz, 1 H; H–C(8)), 8.88 ppm (s, 1 H; H–C(2)); $^{13}$C NMR (100 MHz, $CDCl_3$): $\delta$ = 54.66 (OMe), 117.30 (C(4a)), 124.35 (C(4')), 124.87 (C(6)), 126.20 (C(8)), 127.65 (C(5)), 128.44 (CH=*C*H–C=O), 132.30 (C(5')), 134.53 (C(3')), 139.94 (C(7)), 142.18 (*C*H=CH–C=O), 145.17 (C(2')), 150.70 (C(8a)), 155.07 (C(2)), 167.16 (C(4)), 181.51 ppm (C=O); IR (ATR): $\tilde{n}$ = 3061 (w), 2922 (w), 2852 (w), 1647 (s), 1618 (m), 1591 (s), 1575 (s), 1563 (s), 1496 (s), 1455 (s), 1414 (s), 1382 (s), 1365 (s), 1326 (m), 1282 (s), 1235 (m), 1211 (m), 1167 (m), 1095 (s), 1061 (m), 1046 (m), 975 (s), 877 (s), 827 (s), 790 (s), 747 (s), 738 (s), 712 (s), 678 (s), 632 cm$^{-1}$ (m); HR-MS (ESI): *m/z* (%): 297.0682 (100, $[M + H]^+$, calcd for $C_{16}H_{13}N_2O_2S^+$: 297.0692).

**(2*E*)-1-(5-Chlorothien-2-yl)-3-(4-methoxyquinazolin-7-yl)prop-2-en-1-one (10o).**

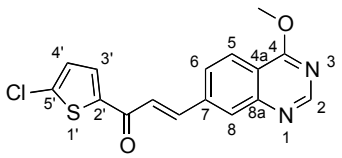


GP-B1 starting from phosphonate **4o** (100 mg, 0.34 mmol) (20.5 h at 22 °C. FC ($SiO_2$; MeOH/$CH_2Cl_2$ 1:99 → 1.5:98.5) and MPLC (80 g $SiO_2$; 120 mL min$^{-1}$, MeOH/$CH_2Cl_2$ 0:100 → 3:97) gave impure alkene **10o** (105 mg, 94%; (*E*/*Z*) 93:7) as an off-white solid, of which a small amount was purified by HPLC (Reprosil; 15 mL min$^{-1}$, hexane/$CHCl_3$ 55:45 → 43:57) to afford impure alkene **10o** as an off-white solid. The compound appears to react upon concentration and was therefore used for the next step without further purification.

$R_f$ = 0.49 ($SiO_2$; MeOH/$CH_2Cl_2$ 1:19); $^1$H NMR (400 MHz, $CDCl_3$; contains traces of the (*Z*)-isomer): $\delta$ = 4.23 (s, 3 H; OMe), 7.07 (d, *J* = 4.1 Hz, 1 H; H–C(4')), 7.53 (d, *J* = 15.6 Hz, 1 H; CH=C*H*–C=O)), 7.71 (d, *J* = 4.1 Hz, 1 H; H–C(3')), 7.82 (dd, *J* = 8.5, 1.6 Hz, 1 H; H–C(6)), 7.98 (d, *J* = 15.6 Hz, 1 H; C*H*=CH–C=O), 8.18 (d, *J* = 1.4 Hz, 1 H; H–C(8)), 8.22 (d, *J* = 8.5 Hz, 1 H; H–C(5)), 8.87 ppm (s, 1 H; H–C(2)); $^{13}$C NMR (100 MHz, $CDCl_3$; contains traces of the (*Z*)-isomer): $\delta$ = 54.53 (OMe), 117.51 (C(4a)), 123.38 (C(6)), 124.36 (C(8)), 125.87 (C(5)), 127.88 (C(4')), 128.23 (CH=*C*H–C=O), 131.64 (C(3')), 139.47 (2'), 140.51 (C(5')), 142.77 (*C*H=CH–C=O), 143.91 (C(7)), 151.20 (C(8a)), 155.31 (C(2)), 166.98 (C(4)), 180.57 ppm (C=O); IR (ATR): $\tilde{n}$ = 2922 (w), 1646 (m), 1616 (m), 1592 (s), 1573 (s), 1526 (m), 1495 (m), 1455 (m), 1443 (w), 1422 (s), 1383 (s), 1363 (s), 1325 (s), 1283 (s), 1214 (m), 1167 (m), 1095 (s), 1075 (m), 1017 (s), 989 (m), 973 (m), 875 (s), 851 (m), 828 (m), 798 (m), 786 (s), 747 (m), 710 (m), 677 (s), 632 cm$^{-1}$ (m); HR-MS (ESI): *m/z* (%): 333.0273 (38, [*M* + H]$^+$, calcd for $C_{16}H_{12}{}^{37}ClN_2O_2S^+$: 333.0274), 331.0295 (100, [*M* + H]$^+$, calcd for $C_{16}H_{12}{}^{35}ClN_2O_2S^+$: 331.0303).

**(2*E*)-1-(5-Bromothien-2-yl)-3-(4-methoxyquinazolin-7-yl)prop-2-en-1-one (10p).**

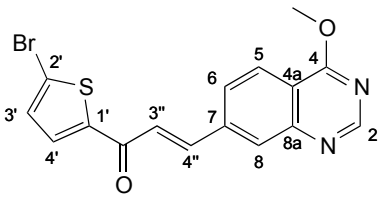


GP-B2 starting from phosphonate **4p** (180 mg, 530 **m**mol) (0.4 equiv. of KO*t*Bu; 6 h at 22 °C). MPLC (40 g $SiO_2$; 40 mL min$^{-1}$, MeOH/$CH_2Cl_2$ 100:0 → 98:2) gave impure **10p** (130 mg, 65%) as a white solid which was used for the next step without further purification.

HR-MS (MALDI): 374.9797 (100, [*M* + H]$^+$, calcd for $C_{16}H_{12}BrN_2O_2S^+$: 374.9797).

**(3*R*,4*S*)- and (4*R*,3*S*)-*tert*-Butyl 3-Benzoyl-4-(4-methoxyquinazolin-7-yl)pyrrolidine-1-carboxylate ((+)-13a and (–)-13a).**

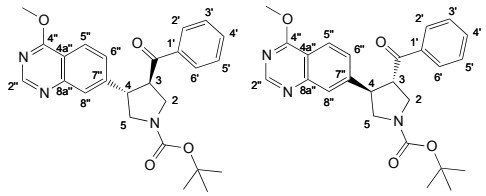

GP-C starting from alkene **10a** (100 mg, 0.34 mmol). FC ($SiO_2$; MeOH/$CH_2Cl_2$ 1:99) and chiral HPLC (Reprosil; 15 mL $min^{-1}$, hexane/*i*PrOH/$CHCl_3$ 75:3:22) gave pyrrolidines (+)-**13a** (12 mg, 7%) and (–)-**13a** (12 mg, 7%) as colorless oils.

Data of (+)-**13a**: $R_f$ = 0.28 ($CH_2Cl_2$/MeOH 98:2); prep. HPLC: $t_R$ = 67 min (Reprosil, 15 mL $min^{-1}$; Hex/*i*PrOH/$CHCl_3$ 75:3:22); $[a]_D^{20}$ = +35.2 (*c* = 0.05 in $CHCl_3$); $^1$H NMR (400 MHz, $CDCl_3$): $\delta$ = 1.49 (s, 9 H; $C(CH_3)_3$), 3.57–3.68 (m, 2 H; $H_a$–C(2), $H_a$–C(5)), 3.96–4.30 (m, 4 H; $H_b$–C(2), Hb–C(5), H–C(3), H–C(4)), 4.16 (s, 3 H; $OCH_3$), 7.42 (t, *J* = 7.8 Hz, 2 H; H–C(3')), 7.49 (dd, *J* = 8.5 Hz, 1 H; H–C(6")), 7.54 (br. t, *J* = 7.4 Hz; H–C(4')), 7.82 (br. s, 1 H; H–C(8")), 7.88 (d, *J* = 7.4 Hz, 2 H; H–C(2')), 8.09 (d, *J* = 8.5 Hz, H–C(5)), 8.77 ppm (br. s, 1 H; H–C(2)); $^{13}$C NMR (100 MHz, $CDCl_3$): $\delta$ = 28.64 ($C(CH_3)_3$), 46.40 and 46.71 (C(4)), 49.63 (C(2)), 52.11 and 52.38 (C(3)), 52.75 (C(5)), 54.47 ($OCH_3$), 80.16 ($C(CH_3)_3$), 115.79 (C(4a")), 124.30 (C(5")), 125.70 (C(8")), 127.39 (C(6")), 128.59 (C(3')), 128.98 (C(2')), 133.90 (C(4')), 151.29 (C(8a")), 154.95 (C(2")), 167.09 (C(4")), 197.97 ppm (s; C=O) (two signals of N–C=O and C(1') in noise); IR (ATR): $\tilde{\nu}$ = 2975 (w), 2933 (w), 2880 (w), 1681 (s), 1624 (m), 1596 (w), 1568 (s), 1496 (m), 1454 (m), 1377 (s), 1364 (s), 1256 (w), 1168 (m), 1122 (m), 1099 (m), 1013 (w), 976 (w), 910 (w), 877 (m), 825 (w), 796 (w), 770 (w), 749 (m), 730 (s), 687 (m), 659 $cm^{-1}$ (w); HR-MS (ESI) *m/z* (%): 456.1890 (75, $[M + Na]^+$, calcd for $C_{25}H_{27}NaN_3O_4^+$: 456.1894), 434.2074 (24, $[M + H]^+$, calcd for $C_{25}H_{28}N_3O_4^+$: 434.2080), 378.1448 (100, $[M – C_4H_8 + H]^+$,calcd for $C_{21}H_{20}N_3O_4^+$: 378.1448).

Data of (–)-**13a**: $t_R$ = 97 min; $[a]_D^{20}$ = –41.7 ($c$ = 0.1 in $CHCl_3$); $^1$H NMR and HR-MS (ESI) data consistent with (+)-**13a**.

**(3*R*,4*S*)- and (4*R*,3*S*)-*tert*-Butyl 3-(3-Fluorobenzoyl)-4-(4-methoxyquinazolin-7-yl)-pyrrolidine-1-carboxylate ((+)-13b and (–)-13b).**

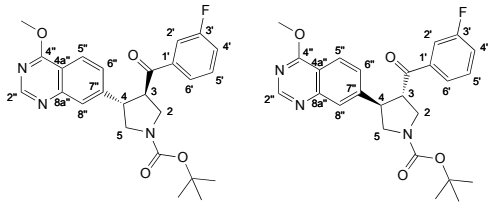

GP-C1 starting from alkene **10b** (100 µg, 324 µmol) in toluene (20 mL). FC ($SiO_2$; MeOH/$CH_2Cl_2$ 1:99) and chiral HPLC (Reprosil; 15 mL min$^{-1}$, hexane/*i*PrOH/$CHCl_3$ 75:3:22) gave pyrrolidines (+)-**13b** (14 mg, 10%) and (–)-**13b** (14 mg, 10%) as yellow oils.

Data for (+)-**13b**: $R_f$ = 0.27 ($CH_2Cl_2$/MeOH 1:20); prep. HPLC: $t_R$ = 42 min (Reprosil, 15 mL min$^{-1}$; Hex/*i*PrOH/$CHCl_3$ 75:3:22); $[a]_D^{20}$ = +33.9 ($c$ = 0.05 in $CHCl_3$); $^1$H NMR (400 MHz, $CDCl_3$): $\delta$ = 1.49 (s, 9 H; $C(CH_3)_3$), 3.56–3.65 (m, 2 H; $H_a$–C(2), $H_a$–C(5)), 3.96–4.20 (m, 4 H; $H_b$–C(2), $H_b$–C(5), H–C(3), H–C(4)), 4.16 (s, 3 H; $OCH_3$),7.24 (tdd, $^3J$(H,F) = 8.2 Hz, $J$ = 8.2, 2.6, 1.0 Hz, 1 H; H–C(4')), 7.40 (td, $^4J$(H,F) = 5.5 Hz, $J$ = 8.0 Hz, 1 H; H–C(5')) 7.49 (dd, $J$ = 8.5, 1.5 Hz, 1 H; H–C(6")), 7.56 (br. d, $^2J$(H,F) = 9.5 Hz, 1 H; H–C(2')), 7.64 (br. d, $J$ = 7.8 Hz, 1 H; H–C(6')), 7.81 (br. s, 1 H; H–C(8")), 8.10 (d, $J$ = 8.4 Hz, 1 H; H–C(5")), 8.77 ppm (s, 1 H; H–C(2)). $^{13}$C NMR (100 MHz, $CDCl_3$): $\delta$ = 28.63 ($C(CH_3)_3$), 46.49 and 46.75 (C(4)), 49.54 (C(2)), 52.07 and 52.35 (C(3) and C(5)), 54.50 ($OCH_3$), 80.27 ($C(CH_3)_3$), 115.32 (d, $^2J$(C,F) = 22.5 Hz; C(4')), 115.86 (C(4a")), 120.98 (d, $^2J$(C,F) = 22.5 Hz; C(2')), 124.28, 124.30, 124.40 (C(5")), 125.73 (C(8")), 127.25, 130.63, 130.71, 151.30 (C(8a")), 155.02 (C(2")), 163.06 (d, $^1J$(C,F) = 248.9 Hz, C(3')), 167.10 (C(4")), 196.83 ppm (C=O) (N–C=O and C(7) signals not visible); $^{19}$F NMR (376 MHz; $CDCl_3$): $\delta$ = –111.11 ppm (d, $J$ = 30.5 Hz, 1 F); IR (ATR): $\tilde{n}$ = 2969 (w), 2923 (w), 2855 (w), 1685 (s), 1624 (m), 1569 (s), 1497 (m), 1455 (m), 1379 (s),

1251 (w), 1164 (m), 1122 (m), 976 (w), 878 (m), 797 (w), 688 $cm^{-1}$ (s); HR-MS (ESI) *m/z* (%): 474.1805 (27, $[M + Na]^+$, calcd for $C_{25}H_{26}FN_3NaO_4^+$: 474.1800), 452.1986 (38, $[M + H]^+$, calcd for $C_{25}H_{27}FN_3O_4^+$: 452.1980), 396.1366 (100, $[M - C_4H_8 + H]^+$, calcd for $C_{21}H_{19}FN_3O_4^+$: 396.1354).

Data for (–)-**13b**: $t_R$ (prep. HPLC) = 62 min; $[\alpha]_D^{20}$ = –25.1 ($c$ = 0.1 in $CHCl_3$); $^1H$ NMR and HR-MS (ESI) data consistent with (+)-**13b**.

**(3*R*,4*S*)- and (4*R*,3*S*)-*tert*-Butyl 3-(3-Chlorobenzoyl)-4-(4-methoxyquinazolin-7-yl)pyrolidine-1-carboxylate ((+)-13c and (–)-13c).**

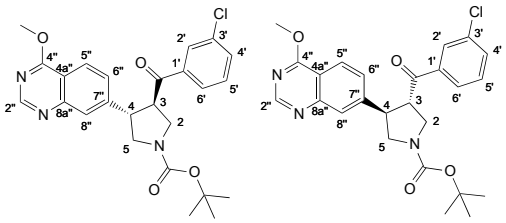

GP-C starting from alkene **10c** (100 mg, 0.30 mmol). FC ($SiO_2$; MeOH/$CH_2Cl_2$ 1:99) and chiral HPLC (Reprosil; 15 mL $min^{-1}$, hexane/*i*PrOH/$CHCl_3$ 75:3:22) gave pyrrolidines (+)-**13c** (12 mg, 8%) and (–)-**13c** (12 mg, 8%) as colorless waxes.

Data of (+)-**13c**: $R_f$ = 0.23 ($CH_2Cl_2$/MeOH 98:2); prep. HPLC: $t_R$ = 49 min (Reprosil, 15 mL $min^{-1}$; Hex/*i*PrOH/$CHCl_3$ 75:3:22); $[\alpha]_D^{20}$ = +37.6 ($c$ = 0.05 in $CHCl_3$); $^1H$ NMR (400 MHz, $CDCl_3$): $\delta$ = 1.48 (s, 9 H; $C(CH_3)_3$), 3.56–3.67 (m, 2 H; $H_a$–C(2), $H_a$–C(5)), 3.94–4.21 (m, 4 H; $H_b$–C(2), $H_b$–C(5), H–C(3), H–C(4)), 4.16 (s, 3 H; $OCH_3$), 7.35 (t, $J$ = 7.9 Hz, 1 H; H–C(5'), 7.48 (br. d, $J$ = 8.4, 1.6 Hz, 1 H; H–C(6")), 7.50 (ddd, $J$ = 8.0, 2.1, 1.0 Hz; H–C(4')), 7.72 (br. d, $J$ = 7.8 Hz, 1 H; H–C(6')), 7.81 (br. s, 2 H; H–C(2'), H–C(8")), 8.09 (d, $J$ = 8.4 Hz, 1 H; H–C(5")), 8.77 ppm (br. s, 1 H; H–C(2)); $^{13}C$ NMR (100 MHz, $CDCl_3$): $\delta$ = 28.62 ($C(CH_3)_3$), 46.54 and 46.75 (C(4)), 49.48 (C(2)), 52.03 and 52.94 (C(3)), 52.32 (C(5), 54.51 ($OCH_3$), 80.29 ($C(CH_3)_3$), 115.86 (C(4a")), 124.41 (C(5")), 125.72 (C(8")), 126.59 (C(6")), 127.25 (C(1')), 127.26 (C(3')), 128.66, 130.27, 133.80, 135.40, 146.41 (C(7")), 151.24 (C(8a")), 154.20 (N–

C=O), 155.01 (C(2")), 167.09 (C(4")), 196.82 ppm (C=O); IR (ATR): $\tilde{\eta}$ = 2973 (w), 2930 (w), 2880 (w), 1683 (m), 1624 (m), 1568 (s), 1497 (m), 1477 (w), 1454 (m), 1377 (s), 1364 (s), 1254 (w), 1163 (m), 1123 (m), 1098 (m), 977 (w), 907 (w), 876 (m), 837 (w), 796 (m), 770 (w), 730 (s), 688 (m), 672 $cm^{-1}$ (w); HR-MS (ESI) *m/z* (%): 470.1662 (20, $[M + H]^+$, calcd for $C_{25}H_{27}{}^{37}ClN_3O_4^+$: 470.1657), 468.1677 (47,$[M + H]^+$, calcd for $C_{25}H_{27}{}^{35}ClN_3O_4^+$: 468.1685), 414.1030 (37; $[M - C_4H_8 + H]^+$, calcd for $C_{21}H_{19}{}^{37}ClN_3O_4^+$: 414.1029), 412.1052 (47; $[M - C_4H_8 + H]^+$, calcd for $C_{21}H_{19}{}^{35}ClN_3O_4^+$: 412.1059).

Data of (–)-**13c**: $t_R$ = 67 min; $[a]_D^{20}$ = –30.8 (*c* = 0.1 in $CHCl_3$); $^1$H NMR and HR-MS (ESI) data consistent with (+)-**13c**.

**(3*R*,4*S*)- and (4*R*,3*S*)-*tert*-Butyl 3-(3-Bromobenzoyl)-4-(4-methoxyquinazolin-7-yl)pyrrolidine-1-carboxylate ((+)-13d and (–)-13d).**

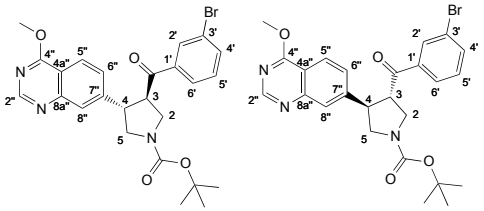


GP-C starting from alkene **10d** (100 µg, 271 µmol). FC ($SiO_2$; MeOH/$CH_2Cl_2$ 1:99) and chiral HPLC (Reprosil; 15 mL $min^{-1}$, hexane/*i*PrOH/$CHCl_3$ 75:3:22) gave pyrrolidines (+)-**13d** (10 mg, 7%) and (–)-**13d** (10 mg, 7%) as yellow oils.

Data of (+)-**13d** $R_f$ = 0.27 ($CH_2Cl_2$/MeOH 96:4); prep. HPLC: $t_R$ = 45 min (Reprosil, 15 mL $min^{-1}$; Hex/*i*PrOH/$CHCl_3$ 75:3:22); $[a]_D^{20}$ = +34.8 (*c* = 0.05 in $CHCl_3$); $^1$H NMR (400 MHz, $CDCl_3$): $\delta$ = 1.49 (s, 9 H; $C(CH_3)_3$), 3.57–3.68 (m, 2 H; $H_a$–C(2), $H_a$–C(5)), 3.94–4.23 (m, 4 H; $H_b$–C(2), $H_b$–C(5), H–C(3), H–C(4)), 4.16 (s, 3 H; $OCH_3$), 7.29 (t, *J* = 7.9 Hz, 1 H; H–C(5')), 7.48 (dd, *J* = 8.4, 1.8 Hz, 1 H; H–C(6")), 7.65 (ddd, *J* = 8.0, 2.0, 1.0 Hz; H–C(4')), 7.73–7.52 (m, 2 H; H–C(6'), H–C(8")), 7.95 (br. s, 1 H; H–C(2')), 8.10 (dd, *J* = 8.5, 0.5 Hz, 1 H; H–C(5")), 8.77 ppm (s, 1 H; H–C(2")); $^{13}$C NMR (100 MHz, $CDCl_3$): $\delta$ = 28.63 ($C(CH_3)_3$), 46.59 and 46.80

(C(4)), 49.46 (C(2)), 52.31 and 52.32 (C(3)), 52.32 (C(5)), 54.51 ($OCH_3$), 80.30 ($C(CH_3)_3$), 115.87 (C(4a")), 123.37 (C(3")) 124.42 (C(2")), 125.75 (C(8")), 127.03 (C(6")), 127.26 (C(5")), 129.94 (C(6')), 130.51 (C(2')), 131.16 (C(4')), 136.72 (C(1')), 146.38 (C(7")), 151.27 (C(8a")), 154.12 (N–C=O), 155.02 (C(2")), 167.10(C(4")), 196.76 ppm (C=O); IR (ATR): $\tilde{n}$ = 2965 (w), 2923 (w), 2852 (w), 1683 (s), 1624 (m), 1568 (s), 1497 (m), 1454 (m), 1378 (s), 1257 (w), 1163 (m), 1122 (m), 1100 (s), 977 (w), 876 (m), 796 (w), 770 (w), 749 (w), 730 (s), 688 (s), 671 (w), 646 $cm^{-1}$ (w); HR-MS (ESI) *m/z* (%): 514.1162 (36, $[M + H]^+$, calcd for $C_{26}H_{26}{}^{81}BrN_3O_5^+$: 514.1164), 512.1180 (36, $[M + H]^+$, calcd for $C_{25}H_{27}{}^{79}BrN_3O_4^+$: 512.1179), 456.0554 (100, $[M – C_4H_8 + H]^+$, calcd for $C_{21}H_{19}{}^{79}BrN_3O_4^+$: 456.0553), 458.0534 (96, $[M–C_4H_8 + H]^+$, calcd for $C_{21}H_{19}{}^{81}BrN_3O_4^+$: 458.0533).

Data of (–)-**13d**: $t_R$ = 41 min; $[a]_D^{20}$ = –39.5 (*c* = 0.1 in $CHCl_3$); $^1$H NMR and HR-MS (ESI) data consistent with (+)-**13d**.

**(3S,4R)- and (3R,4S)-*tert*-Butyl 3-(3-Iodobenzoyl)-4-(4-methoxyquinazolin-7-yl)pyrrolidine-1-carboxylate ((+)-13e und (–)-13e).**

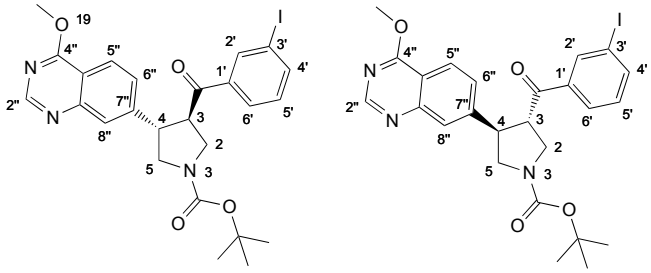

GP-C1 starting from alkene **10e** (100 µg, 240 mmol) (20~mL toluene; 10~equiv. *para*-formaldehyde). FC ($SiO_2$; MeOH/$CH_2Cl_2$ 1:99) and chiral HPLC (Reprosil; 15 mL $min^{-1}$, hexane/*i*PrOH/$CHCl_3$ 75:3:22) gave pyrrolidines (+)-**13e** (15 mg, 11%) and (–)-**13e** (10 mg, 7%) as yellow oils. This compound is instable and contains impurities in the spectra.

Data for (+)-**13e**: $R_f$ = 0.27 ($CH_2Cl_2$/MeOH 1:19); $t_R$ (prep. HPLC) = 61 min (Reprosil, 15 mL $min^{-1}$; Hex/*i*PrOH/$CHCl_3$ 75:3:22); $[a]_D^{20}$ = +27.0 (c = 0.05 in $CHCl_3$); $^1$H NMR (400 MHz,

$CDCl_3$): $\delta$ = 1.49 (s, 9 H; $C(CH_3)_3$), 3.57–3.67 (m, 2 H; H–C(2), H–C(5)), 3.92–4.21 (m, 4 H; H–C(2), H–C(5), H–C(3), H–C(4)), 4.16 (s, 3 H; $OCH_3$), 7.14 (t, $J$ = 7.8 Hz, 1 H; H–C(5')), 7.40–7.56 (m, 2 H; H–C(6), H–C(4') or H–C(6')), 7.78–7.89 (m, 3 H; H–C(6') or H–C(4'), H–C(8), H–C(2')), 8.08–8.13 (m, 1 H; H–C(5")), 8.77 ppm (s, 1 H; H–C(2")); $^{13}$C NMR (150 MHz, $CDCl_3$): $\delta$ = 28.63 ($C(CH_3)_3$), 46.72 und 46.88 (C(4)), 49.44 (C(2)), 52.11 und 52.29 (C(3)), 54.48 ($OCH_3$), 80.16 ($C(CH_3)3$), 124.30 (C(5)), 125.68 (C(8)), 127.40 (C(6)), 128.59, 128.98, 130.59, 133.90, 137.52, 142.58, 151.27 (C(8a")), 154.95 (N–C=O), 155.01 (C(2")), 167.10 (C(4")), 196.97 ppm (C=O) (signals of (4a") und C(7") not visible); IR (ATR): $\tilde{n}$ = 2969 (w), 2927 (w), 2860 (w), 1682 (s), 1624 (m), 1568 (s), 1496 (m), 1454 (m), 1378 (s), 1255 (w), 1167 (m), 1122 (m), 1100 (s), 976 (w), 877 (m), 796 (w), 770 (w), 749 (w), 730 (s), 688 (s), 645 $cm^{-1}$ (w); HR-MS (ESI) *m/z* (%): 622.0288 (74), 560.1041 (27, $[M + H]^+$, calcd for $C_{25}H_{27}IN_3O_4^+$: 560.1041), 378.1447 (78), 177.1274 (40), 150.0372 (100).

Data for (–)-**13e**: $t_R$ (prep. HPLC) = 85 min; $[a]_D^{20}$ = –32.3 ($c$ = 0.1 in $CHCl_3$); $^1$H NMR and HR-MS (ESI) data consistent with (+)-**13e**.

**(4*R*,3*S*)- and (3*R*,4*S*)-*tert*-Butyl 3-(4-Methoxyquinazolin-7-yl)-4-(3-(trifluoro-methyl)-benzoyl)pyrrolidine-1-carboxylate ((+)-13f and (–)-13f).**

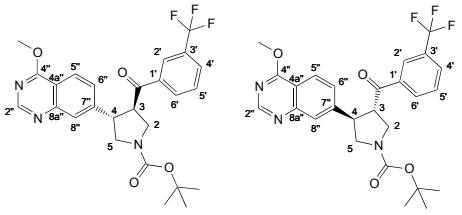

GP-C1 starting from alkene **10f** (100 µg, 279 µmol). FC ($SiO_2$; MeOH/$CH_2Cl_2$ 1:99) and chiral HPLC (Reprosil; 15 mL $min^{-1}$, hexane/*i*PrOH/$CHCl_3$ 75:3:22) gave pyrrolidines (+)-**13f** (10 mg, 7%) and (–)-**13f** (10 mg, 7%) as yellow oils.

Data for (+)-**13f**: prep. HPLC: $t_R$ = 34 min (Reprosil, 15 mL $min^{-1}$; Hex/*i*PrOH/$CHCl_3$ 75:3:22); $[a]_D^{20}$ = +57.7 ($c$ = 0.05 in $CHCl_3$); $^1$H NMR (400 MHz, $CDCl_3$): $\delta$ = 1.49 (s, 9 H; $C(CH_3)_3$),

3.60–3.70 (m, 2 H; $H_a$–C(2), $H_a$–C(5)), 3.96–4.25 (m, 4 H; $H_b$–C(2), $H_b$–C(5), H–C(3), H–C(4)), 4.16 (s, 3 H; $OCH_3$), 7.49 (br. d, $J$ = 8.0 Hz, 1 H; H–C(6''), 7.56 (t, $J$ = 7.7 Hz, 1 H; H–C(5')), 7.77–7.81 (m, 2 H; H–C(4'), H–C(8'')), 8.03 (br. s, 1 H; H–C(2')), 8.05 (d, $J$ = 8.3 Hz, 1 H; H–C(4')), 8.10 (d, $J$ = 8.5 Hz, 1 H; H–C(5'')), 8.77 ppm (s, 1 H; H–C(2'')); $^{13}$C NMR (150 MHz, $CDCl_3$): $\delta$ = 28.63 ($C(CH_3)_3$), 46.83 and 46.98 (C(4)), 49.37 (C(2)), 52.07 and 52.37 (C(3)), 53.05 (C(5)), 54.52 ($OCH_3$), 80.34 ($C(CH_3)_3$), 115.90 (C(4a'')), 123.56 (q, $^1J$(C,F) = 272.7 Hz; $CF_3$), 124.49 (C(5'')), 125.37 (q, $^3J$(C,F) = 3.6 Hz; C(2')), 125.38 (C(8'')), 125.78 (C(8')), 127.08 and 127.19 (C(6'')), 129.68 (C(5')), 130.24 (q, $^3J$(C,F) = 3.2 Hz; C(4')), 131.64 (q, $^2J$(C,F) = 33.0 Hz; C(3')), 131.64 (C(6')), 136.60 and 136.71 (C(1')), 151.25 (C(8a'')), 154.09 and 154.19 (N–C=O), 155.05 (C(2'')), 167.10 (C(4'')), 196.81 ppm (C=O); $^{19}$F NMR (376 MHz, $CDCl_3$): $\delta$ = –62.93 (s; $CF_3$); IR (ATR): $\tilde{n}$ = 2965 (w), 2924 (m), 2853 (w), 1686 (s), 1624 (m), 1568 (m), 1497 (m), 1455 (m), 1378 (s), 1329 (s), 1256 (w), 1165 (s), 1124 (s), 1256 (w), 1165 (s), 1124 (s), 1097 (s), 1072 (s), 976 (w), 876 (s), 838 (w), 796 (m), 838 (w), 796 (m), 769 (m), 749 (m), 733 (m), 689 (s), 648 $cm^{-1}$ (w); HR-MS (ESI) *m/z* (%): 524.1765 (38, $[M + Na]^+$, calcd for $C_{26}H_{26}F_3N_3NaO_4^+$: 524.1768), 502.1945 (38, $[M + H]^+$, calcd for $C_{26}H_{27}F_3N_3O_4^+$: 502.1948), 446.1318 (100, $[M – C_4H_8 + H]^+$, calcd for $C_{22}H_{19}F_3N_3O_4^+$: 446.1322).

Data for (–)-**13f**: $t_R$ (prep. HPLC) = 43 min; $[a]_D^{20}$ = –59.6 ($c$ = 0.1 in $CHCl_3$); $^1$H NMR and HR-MS (ESI) data consistent with (+)-**13f**.

**(3*R*,4*S*)- and (4*R*,3*S*)-*tert*-Butyl 3-(4-Methoxyquinazolin-7-yl)-4-(3-(trifluoro-methoxy)-benzoyl)pyrrolidine-1-carboxylate ((+)-13g and (–)-13g).**

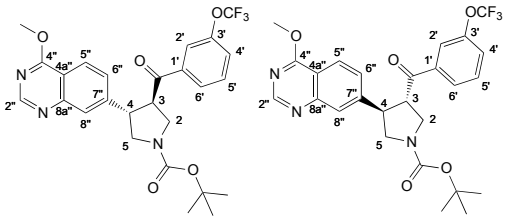

GP-C2 starting from alkene **10g** (100 µg, 267 µmol). FC ($SiO_2$; MeOH/$CH_2Cl_2$ 1:99) and chiral HPLC (Reprosil; 15 mL $min^{-1}$, hexane/*i*PrOH/$CHCl_3$ 75:3:22) gave pyrrolidines (+)-**13g** (10 mg, 7%) and (–)-**13g** (10 mg, 7%) as clear oils.

Data of (+)-**13g**: prep. HPLC: $t_R$ = 33 min (Reprosil, 15 mL $min^{-1}$; Hex/*i*PrOH/$CHCl_3$ 75:3:22); $[a]_D^{20}$ = +57.7 (*c* = 0.05 in $CHCl_3$); $^1$H NMR (400 MHz, $CDCl_3$): $\delta$ = 1.49 (s, 9 H; $C(CH_3)_3$), 3.58{3.66 (m, 2 H; $H_a$–C(2), $H_a$–C(5)), 3.96–4.22 (m, 4 H; $H_b$–C(2), $H_b$–C(5), H–C(3), H–C(4)), 4.16 (s, 3 H; OCH3), 7.39 (dm, *J* = 8.2 Hz, 1 H; H–C(4'), 7.45 (t, *J* = 7.9 Hz, 1 H; H–C(5')), 7.49 (dd, *J* = 7.1, 1.1 Hz, 1 H; H–C(6")), 7.69 (br. s, 1 H; H–C(2')), 7.78 (d, *J* = 8.0 Hz, 1 H; H–C(6')), 7.81 (br. s, 1 H; H–C(8")), 8.10 (d, *J* = 8.5, 1 H; H–C(5")), 8.77 ppm (s, 1 H; H–C(2")); $^{13}$C NMR (100 MHz, $CDCl_3$): $\delta$ = 28.62 ($C(CH_3)_3$), 46.59 and 46.84 (C(4)), 49.43 and 49.50 (C(2)), 52.33 (C(3)), 54.50 ($OCH_3$), 80.31 ($C(CH_3)_3$), 115.88 (C(4a")), 120.44 (q, $^1J$ C,F) = 258.0 Hz; $CF_3$), 120.85, 124.45 (C(5")), 125.75 (C(8")), 126.13, 126.79, 127.23 (arom. C and C(6")), 130.55, 149.79 (C(3')), 151.29 (C(8a")), 153.14 (N–C=O), 155.04 (C(2")), 167.09 (C(4")), 196.63 ppm (C=O) (2 signals missing); $^{19}$F NMR (376 MHz; CDCl3): $\delta$ = –57.90 ppm (s, 3 F; $OCF_3$); IR (ATR): $\tilde{n}$ = 2977 (w), 2933 (w), 2888 (w), 1683 (s), 1624 (m), 1568 (s), 1497 (m), 1455 (m), 1378 (s), 1252 (s), 1211 (s), 1155 (s), 1122 (m), 1099 (s), 1001 (w), 976 (w), 876 (m), 845 (w), 796 (w), 770 (w), 749 (w), 732 (m), 688 (m), 658 (w), 633 $cm^{-1}$ (w); HR-MS (ESI) *m/z* (%): 541.1759 (15), 540.1752 (50, $[M + Na]^+$, calcd for $C_{26}H_{26}F_3NaN_3O_5^+$: 540.1717), 518.1907 (35, $[M + H]^+$, calcd for $C_{26}H_{27}F_3N_3O_5^+$: 518.1897), 462.1276 (100, $[M – C_4H_8 + H]^+$, calcd for $C_{22}H_{19}F_3N_3O_4^+$: 462.1271).

Data of (–)-**13g**: $t_R$ = 41 min; $[a]_D^{20}$ = –59.6 ($c$ = 0.1 in $CHCl_3$); $^1$H NMR and HR-MS (ESI) data consistent with (+)-**13g**.

**(3*R*,4*S*)- and (4*R*,3*S*)-*tert*-Butyl 3-(4-Fluorobenzoyl)-4-(4-methoxyquinazolin-7-yl)pyrrolidine-1-carboxylate ((+)-13h and (–)-13h).**

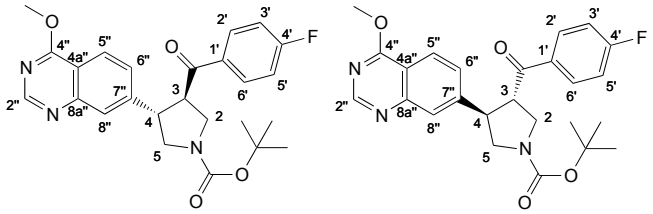

**GP-C** starting from alkene **10h** (83 mg, 0.27 mmol) (after addition of $Boc_2O$ stirred at 22 °C for 2 h 15 min and evaporated). FC ($SiO_2$; MeOH/$CH_2Cl_2$ 1:99 → 2.5:97.5) and chiral HPLC (Reprosil; 15 mL min$^{-1}$, hexane/*i*PrOH/$CHCl_3$ 75:3:22) gave pyrrolidines (+)-**13h** (30 mg, 25%) and (–)-**13h** (24 mg, 20%) as colorless waxes.

Data of (+)-**13h**: $R_f$ = 0.35 ($SiO_2$; MeOH/$CH_2Cl_2$ 1:19); $t_R$ (prep. HPLC) = 34 min; $[a]_D^{20}$ = +41.6 ($c$ = 0.1 in $CHCl_3$); $^1$H NMR (400 MHz, $CDCl_3$; approx. 1:1 mixture of diastereoisomers, assignment based on HSQC and HMBC spectra of (+)-**13h**): $\delta$ = 1.50 (s, 9 H; $C(CH_3)_3$, 3.56–3.70 (m, 2 H; $H_a$–C(2), $H_a$–C(5)), 3.96–4.27 (m, 4 H; $H_b$–C(2), H–C(3), H–C(4), $H_b$–C(5)), 4.18 (s, 3 H; $OCH_3$), 7.05–7.15 (m, 2 H; H–C(3')), 7.50 (dd, $J$ = 8.5, 1.4 Hz, 1 H; H–C(6'')), 7.82 (br. s, 1 H; H–C(8'')), 7.87–7.97 (m, 2 H; H–C(2')), 8.11 (d, $J$ = 8.5 Hz, 1 H; H–C(5'')), 8.79 ppm (s, 1 H; H–C(2'')); $^{13}$C NMR (100 MHz, $CDCl_3$; approx. 1:1 mixture of diastereoisomers): $\delta$ = 28.48, 46.43 and 46.68, 49.47, 51.92, 52.22 and 52.53, 54.34, 80.07, 115.68, 116.01 (d, $^2J$(C,F) = 21.9 Hz; C(3')), 124.21, 125.55, 127.18, 131.12 (d, $^3J$(C,F) = 9.4 Hz; C(4')), 132.48 (d, $^4J$(C,F) = 5.8 Hz; C(1')), 146.17 and 146.43, 151.13, 153.99 and 154.08, 154.86, 166.08 (d, $^1J$(C,F) =

254.8 Hz; C(4')), 166.94, 196.25 ppm (C=O); $^{19}$F NMR (376 MHz, $CDCl_3$): $\delta$ = (–103.75)–(–103.61) ppm (m, 1 F); IR (ATR): $\tilde{\eta}$ = 2965 (w), 2932 (w), 2872 (w), 1681 (s), 1624 (m), 1597 (m), 1568 (s), 1497 (m), 1454 (m), 1405 (s, sh), 1377 (s), 1364 (s, sh), 1296 (w), 1227 (m), 1156 (s), 1121 (s), 1099 (s), 976 (w), 877 (m), 847 (m), 796 (m), 769 (m), 749 (m), 687 cm$^{-1}$ (m); HR-MS (ESI): *m/z* (%): 452.1987 (52, $[M + H]^+$, calcd for $C_{25}H_{27}FN_3O_4^+$: 452.1980), 396.1359 (100).

Data of (–)-**13h**: $[a]_D^{20}$ = –39.8 (*c* = 0.1 in $CHCl_3$); $t_R$ (prep. HPLC) = 50 min; $^1$H NMR and HR-MS (ESI) data consistent with (+)-**13h**

**(3*R*,4*S*)- and (4*R*,3*S*)-*tert*-Butyl 3-(4-Chlorobenzoyl)-4-(4-methoxyquinazolin-7-yl)pyrrolidine-1-carboxylate ((+)-13i and (–)-13i).**

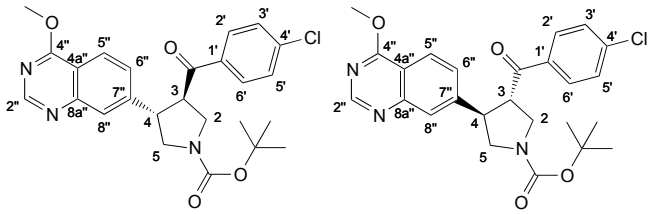

**GP-C** starting from alkene **10i** (66 mg, 0.20 mmol) (after addition of $Boc_2O$ stirred at 22 °C for 1 h 40 min and evaporated). FC ($SiO_2$; MeOH/$CH_2Cl_2$ 1:99 → 2.5:97.5) and chiral HPLC (Reprosil; 15 mL min$^{-1}$, hexane/*i*PrOH/$CHCl_3$ 75:3:22 → 66:4:30) gave pyrrolidines (+)-**13i** (20 mg, 21%) and (–)-**13i** (20 mg, 21%) as colorless waxes.

Data of (+)-**13i**: $R_f$ = 0.35 ($SiO_2$; MeOH/$CH_2Cl_2$ 1:19); $t_R$ (prep. HPLC) = 32 min; $[a]_D^{20}$ = +26.1 (*c* = 0.1 in $CHCl_3$); $^1$H NMR (400 MHz, $CDCl_3$; approx. 1:1 mixture of diastereoisomers, assignment based on HSQC and HMBC spectra of (+)-**13i**): $\delta$ = 1.50 (s, 9 H; $C(CH_3)_3$), 3.56–3.70 (m, 2 H; $H_a$–C(2), $H_a$–C(5)), 3.94–4.27 (m, 4 H; $H_b$–C(2), H–C(3), H–C(4), $H_b$–C(5)), 4.18 (s, 3 H; $OCH_3$), 7.40, 7.82 (AA'MM', *J* = 8.5 Hz, 4 H; H–C(3'), H–C(2')), 7.50 (dd, *J* = 8.5, 1.7 Hz, 1 H; H–C(6'')), 7.83 (br. s, 1 H; H–C(8'')), 8.11 (d, *J* = 8.4 Hz, 1 H; H–C(5'')), 8.79 ppm (s, 1 H; H–C(2'')); $^{13}$C NMR (100 MHz, $CDCl_3$; approx. 1:1 mixture of

diastereoisomers): $\delta$ = 28.48, 46.42 and 46.72, 49.42, 51.97, 52.21 and 52.59, 54.36, 80.10, 115.69, 124.25, 125.55, 127.13, 129.17, 129.80, 134.29 and 134.36, 140.36, 146.14 and 146.37, 151.11, 153.95 and 154.06, 154.87, 166.95, 197.70 ppm; IR (ATR): $\tilde{\nu}$ = 2974 (w), 2937 (w), 2884 (w), 1682 (s), 1624 (m), 1568 (s), 1496 (m), 1454 (m), 1377 (s), 1166 (s), 1092 (s), 1010 (m), 976 (m), 876 (m), 842 (m), 796 (m), 769 (m), 749 (m), 688 $cm^{-1}$ (m); HR-MS (ESI): *m/z* (%): 470.1682 (5, $[M + H]^+$, calcd for $C_{25}H_{27}{}^{37}ClN_3O_4^+$: 470.1657), 468.1694 (13, $[M + H]^+$, calcd for $C_{25}H_{27}{}^{35}ClN_3O_4^+$: 468.1685), 414.1046 (28), 412.1066 (85), 149.0236 (100).

Data of (–)-**13i**: $t_R$ (prep. HPLC) = 54 min; $[a]_D^{20}$ = –29.4 ($c$ = 0.1 in $CHCl_3$); $^1$H NMR and HR-MS (ESI) data consistent with (+)–**13i**.

**(3*R*,4*S*)- and (4*R*,3*S*)-*tert*-Butyl 3-(4-Bromobenzoyl)-4-(4-methoxyquinazolin-7-yl)pyrrolidine-1-carboxylate ((+)-13j and (–)-13j).**

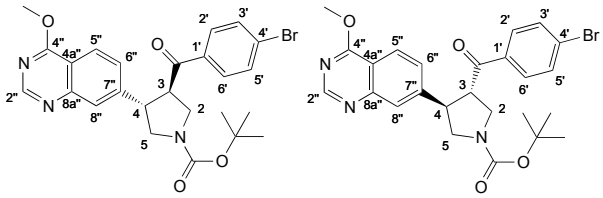

**GP-C** starting from alkene **10j** (67 mg, 0.18 mmol) (after addition of $Boc_2O$ stirred at 22 °C for 2 h 45 min and evaporated). FC ($SiO_2$; MeOH/$CH_2Cl_2$ 1:99 → 2.5:97.5) and chiral HPLC (Reprosil; 15 mL $min^{-1}$, hexane/*i*PrOH/$CHCl_3$ 75:3:22) gave pyrrolidines (+)-**13j** (18 mg, 19%) and (–)-**13j** (19 mg, 20%) as colorless waxes.

Data of (+)-**13j**: $R_f$ = 0.33 ($SiO_2$; MeOH/$CH_2Cl_2$ 1:19); $t_R$ (prep. HPLC) = 40 min; $[a]_D^{20}$ = +23.2 ($c$ = 0.1 in $CHCl_3$); $^1$H NMR (400 MHz, $CDCl_3$; approx. 1:1 mixture of diastereoisomers, assignment based on HSQC and HMBC spectra of (+)-**13j**): $\delta$ = 1.51 (s, 9 H; $C(CH_3)_3$), 3.60 (dd, $J$ = 10.5, 7.9 Hz, 1 H; $H_a$–C(2 or 5)), 3.64–3.71 (m, 1 H; $H_a$–C(2 or 5)), 3.96–4.26 (m, 4 H; $H_b$–C(2), H–C(3), H–C(4), $H_b$–C(5)), 4.18 (s, 3 H; $CH_3$), 7.49 (dd, $J$ = 8.5, 1.4 Hz, 1 H; H–C(6'')), 7.57, 7.74 (AA'MM', $J$ = 8.6 Hz, 4 H; H–C(2'), H–C(3')), 7.82 (br. s, 1 H; H–C(8'')), 8.11 (d, $J$ = 8.5 Hz, 1 H; H–C(5'')), 8.80 ppm (s, 1 H; H–C(2'')); $^{13}$C NMR (100 MHz, $CDCl_3$; approx. 1:1

mixture of diastereoisomers): $\delta$ = 28.48, 46.43 and 46.74, 49.39, 51.91 and 51.97, 52.20 and 52.60, 54.36, 80.11, 115.72, 124.26, 125.57, 127.10, 129.13, 129.87, 132.17, 134.70, 146.16 and 146.34, 151.13, 153.97 and 154.03, 154.88, 166.95, 196.93 ppm; IR (ATR): $\tilde{n}$ = 2974 (w), 2937 (w), 2876 (w), 1682 (s), 1624 (m), 1581 (m), 1567 (m), 1496 (m), 1454 (m), 1377 (s), 1256 (w), 1167 (m), 1121 (m), 1098 (m), 1070 (m), 1007 (m), 976 (w), 877 (m), 839 (m), 796 (m), 769 (m), 749 (m), 688 $cm^{-1}$ (m); HR-MS (ESI): *m/z* (%): 514.1168 (69, $[M + H]^+$, calcd for $C_{25}H_{27}{}^{81}BrN_3O_4^+$: 514.1160), 512.1183 (73, $[M + H]^+$, calcd for $C_{25}H_{27}{}^{79}BrN_3O_4^+$: 512.1179), 458.0540 (99), 456.0556 (100).

Data of (–)-**13j**: $t_R$ (prep. HPLC) = 58 min; $[a]_D^{20}$ = –23.1 ($c$ = 0.1 in $CHCl_3$); $^1$H NMR and HR-MS (ESI) data consistent with (+)-**13j**

**(3*R*,4*S*)- and (4*R*,3*S*)-*tert*-Butyl 3-(4-Iodobenzoyl)-4-(4-methoxyquinazolin-7-yl)pyrrolidine-1-carboxylate ((+)-13k and (–)-13k).**

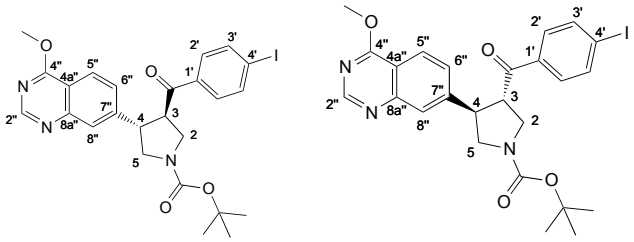

**GP-C** starting from alkene **10k** (170 mg, 0.33 mmol) (in 8 mL tolulene; second addition of glycine and *para*-formaldehyde at 120 °C; after addition of $Boc_2O$ stirred at 22 °C for 2.5 h). FC ($SiO_2$; MeOH/$CH_2Cl_2$ 1:99 → 2.5:97.5) and chiral HPLC (Reprosil; 15 mL $min^{-1}$, hexane/*i*PrOH/$CHCl_3$ 75:3:22) gave pyrrolidines (+)-**13k** (42 mg, 23%) and (–)-**13k** (42 mg, 23%) as colorless waxes.

Data for (+)-**13k:** $R_f$ = 0.29 ($SiO_2$; MeOH/$CH_2Cl_2$ 1:19); $t_R$ (prep. HPLC) = 41 min; $[a]_D^{20}$ = +18.4 ($c$ = 0.1 in $CHCl_3$); $^1$H NMR (400 MHz, $CDCl_3$; approx. 1:1 mixture of diastereoisomers, assignment based on HSQC and HMBC spectra of (+)-**13k**): $\delta$ = 1.51 (s, 9 H; C(C$H_3$)$_3$), 3.55–3.72 (m, 2 H; $H_a$–C(2), $H_a$–C(5)), 3.93–4.27 (m, 4 H; $H_b$–C(2), H–C(3), H–C(4), $H_b$–C(5)), 4.19

(s, 3 H; $OCH_3$), 7.49 (dd, $J$ = 8.5, 1.6 Hz, 1 H; H–C(6'')), 7.58, 8.02 (AA'MM', $J$ = 8.3 Hz, 4 H; $C_6H_4I$), 7.82 (br. s, 1 H; H–C(8'')), 8.11 (d, $J$ = 8.5 Hz, 1 H; H–C(5'')), 8.80 ppm (s, 1 H; H–C(2'')); $^{13}C$ NMR (100 MHz, $CDCl_3$; approx. 1:1 mixture of diastereoisomers, assignment based on HSQC and HMBC spectra of (+)-**13k**): $\delta$ = 28.48 (C($CH_3$)$_3$), 46.39 and 46.75 (C(3 or 4)), 49.37 (C(2 or 5)), 51.91 (C(2 or 5)), 52.20 and 52.54 (C(3 or 4)), 54.37 ($OCH_3$), 80.10 ($C$($CH_3$)$_3$), 102.00 (C(4')), 115.70 (C(4a'')), 124.26 (C(5'')), 125.56 (C(8'')), 127.11 (C(6'')), 129.69 (C(3')), 135.25 (C(1')), 138.18 (C(2')), 146.35 (C(7'')), 151.10 (C(8a'')), 154.04 ($CO_2$), 154.88 (C(2'')), 166.96 (C(4'')), 197.26 ppm (C=O); IR (ATR): $\tilde{n}$ = 2973 (w), 2937 (w), 2872 (w), 1682 (s), 1623 (w), 1579 (m), 1567 (m), 1496 (m), 1454 (m), 1378 (s), 1167 (m), 1121 (m), 1098 (m), 1058 (m), 1003 (m), 877 (m), 836 (w), 796 (m), 769 (m), 749 (m), 688 $cm^{-1}$ (m); HR-MS (ESI): *m/z* (%): 560.1039 (44, $[M + H]^+$, calcd for $C_{25}H_{27}IN_3O_4^+$: 560.1041), 504.0407 (100), 150.0367 (47).

Data for (–)-**13k**: $t_R$ (prep. HPLC) = 60 min; $[a]_D^{20}$ = –18.9 ($c$ = 0.1 in $CHCl_3$); $^1H$ NMR and HR-MS (ESI) data consistent with (+)-**13k**

**(3*R*,4*S*)- and (4*R*,3*S*)-*tert*-Butyl 3-(4-Methoxyquinazolin-7-yl)-4-[4-(trifluoromethyl)-benzoyl]pyrrolidine-1-carboxylate ((+)-13l and (–)-13l).**

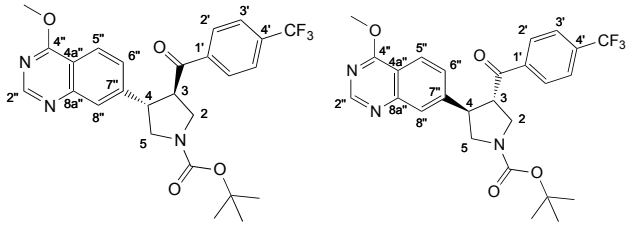

**GP-C** starting from alkene **10l** (220 mg, 0.14 mmol) (addition of 15 equiv. of *para*-formaldehyde; second addition of glycine and *para*-formaldehyde at 120 °C). FC ($SiO_2$; MeOH/$CH_2Cl_2$ 1:99 → 2.5:97.5) and chiral HPLC (Reprosil; 15 mL $min^{-1}$, hexane/*i*PrOH/$CHCl_3$ 75:3:22) gave pyrrolidines (+)-**13l** (15 mg, 8%) and (–)-**13l** (17 mg, 9%) as colorless waxes.

Data of (+)-**13l**: $R_f$ = 0.35 ($SiO_2$; MeOH/$CH_2Cl_2$ 1:19); $t_R$ (prep. HPLC) = 28 min; $[a]_D^{20}$ = +38.5 ($c$ = 0.1 in $CHCl_3$); $^1$H NMR (400 MHz, $CDCl_3$; approx. 1:1 mixture of diastereoisomers, assignment based on HSQC and HMBC spectra of (+)-**13l**): $\delta$ = 1.51 (s, 9 H; $C(CH_3)_3$), 3.63 (dd, $J$ = 10.8, 8.0 Hz, 1 H; H–C(2 or 5)), 3.66–3.74 (m, 1 H; H–C(2 or 5)), 3.96–4.24 (m, 4 H; H–C(2), H–C(3), H–C(4), H–C(5)), 4.18 (s, 3 H; $OCH_3$), 7.50 (dd, $J$ = 8.5, 1.7 Hz, 1 H; H–C(6'')), 7.69, 7.98 (AA'BB', $J$ = 8.2 Hz, 4 H; $C_6H_4CF_3$), 7.83 (br. s, 1 H; H–C(8'')), 8.12 (d, $J$ = 8.5 Hz, 1 H; H–C(5'')), 8.80 ppm (s, 1 H; H–C(2'')); $^{13}$C NMR (100 MHz, $CDCl_3$; approx. 1:1 mixture of diastereoisomers, assignment based on HSQC and HMBC spectra of (+)-**13l**): $\delta$ = 28.47 ($C(CH_3)_3$), 46.46 and 46.78 (C(3 or 4)), 49.24 (C(2 or 5)), 51.89 and 52.16 (C(2 or 5)), 52.36 and 53.01 (C(3 or 4)), 54.37 ($OCH_3$), 80.19 ($C(CH_3)_3$), 115.74 (C(4a'')), 123.36 (q, $^1J$(C,F) = 271.3 Hz; $CF_3$), 124.33 (C(5'')), 125.62 (C(8'')), 125.89 (q, $^3J$(C,F) = 3.7 Hz; C(3')), 127.00 (C(6'')), 128.74 (C(2')), 134.95 (q, $^2J$(C,F) = 32.7 Hz; C(4')), 138.62 and 138.65 (C(1')), 145.95 and 146.16 (C(7'')), 151.13 (C(8a'')), 153.95 and 154.05 ($CO_2$), 154.93 (C(2'')), 166.95 (C(4'')), 197.12 ppm (C=O); $^{19}$F NMR (376 MHz, $CDCl_3$): $\delta$ = –63.28 ppm (s, 3 F; $CF_3$); IR (ATR): $\tilde{\eta}$ = 2977 (w), 2941 (w), 2884 (w), 1687 (m), 1624 (w), 1568 (m), 1497 (w), 1455 (m), 1409 (m, sh), 1379 (s), 1323 (s), 1167 (s), 1127 (s), 1066 (s), 1013 (m), 877 (m), 769 (m), 749 (m), 688 $cm^{-1}$ (m); HR-MS (ESI): *m/z* (%): 502.1950 (48, $[M + H]^+$, calcd for $C_{26}H_{27}F_3N_3O_4^+$: 502.1948), 446.1327 (100).

Data of (–)-**13l**: $t_R$ (prep. HPLC) = 34 min; $[a]_D^{20}$ = –37.2 ($c$ = 0.1 in $CHCl_3$); $^1$H NMR and HR-MS (ESI) data consistent with (+)-**13l**

**(3*R*,4*S*)- and (4*R*,3*S*)-t*ert*-Butyl 3-(4-Methoxyquinazolin-7-yl)-4-(4-(trifluoromethoxy)-benzoyl)pyrrolidine-1-carboxylate ((+)-13m and (–)-13m).**

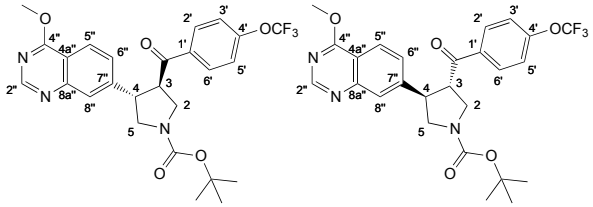

GP-C1 starting from alkene **10m** (100 µg, 267 µmol). FC ($SiO_2$; MeOH/$CH_2Cl_2$ 1:99) and chiral HPLC (Reprosil; 15 mL $min^{-1}$, hexane/*i*PrOH/$CHCl_3$ 75:3:22) gave pyrrolidines (+)-**13m** (12 mg, 9%) and (–)-**13m** (12 mg, 9%) as clear oils.

Data of (+)-**13m**: prep. HPLC: $t_R$ = 34 min (Reprosil, 15 mL $min^{-1}$; Hex/*i*PrOH/$CHCl_3$ 75:3:22); $[a]_D^{20}$ = +57.6 (*c* = 0.05 in $CHCl_3$); $^1$H NMR (400 MHz, $CDCl_3$): $\delta$ = 1.49 (s, 9 H; $C(CH_3)_3$), 3.57{3.66 (m, 2 H; $H_a$–C(2), $H_a$–C(5)), 3.95–4.24 (m, 4 H; $H_b$–C(2), $H_b$–C(5), H–C(3), H–C(4)), 4.16 (s, 3 H; $OCH_3$), 7.22 (dd, *J* = 8.8 Hz, $^5J$(C,F) = 0.8 Hz, 1 H; H–C(3')), 7.47 (dd, *J* = 8.5, 1.8 Hz, 1 H; H–C(6")), 7.80 (br. s, 1 H; H–C(8")), 7.91 (d, *J* = 8.5 Hz, 2 H; H–C(2')), 8.09 (dd, *J* = 8.4, 0.5 Hz, 1 H; H–C(5")), 8.77 ppm (s, 1 H; H–C(2")); $^{13}$C NMR (100 MHz, $CDCl_3$): $\delta$ = 28.63 ($C(CH_3)_3$), 46.83 and 46.87 (C(4)), 49.51 (C(2)), 52.02 and 52.35 (C(3)), 52.24 (C(5)), 54.50 ($OCH_3$), 80.28 ($C(CH_3)_3$), 115.84 (C(4a")), 120.33 (q, $^1J$(C,F) = 260.2 Hz; $CF_3$), 120.65 (q, $^4J$(C,F) = 0.8 Hz; C(3'), C(5')), 124.41 (C(5")), 125.72 (C(8")), 127.24 (C(6")), 130.62 (C(2'), C(6')), 134.29 (C(1')), 146.44 (C(7")), 151.27 (C(8a")), 153.18 (N–C=O), 155.04 (C(2")), 167.09 (C(4")), 196.52 ppm (C=O); $^{19}$F NMR (376 MHz; $CDCl_3$): $\delta$ = –57.32 ppm (t, *J* = 1.0 Hz, 3 F; $OCF_3$); IR (ATR): $\tilde{n}$ = 2972 (w), 2937 (w), 2884 (w), 1683 (s), 1624 (m), 1602 (w), 1568 (m), 1497 (m), 1455 (m), 1378 (s), 1252 (s), 1208 (s), 1162 (s), 1122 (s), 1099 (s), 1013 (w), 977 (w), 920 (w), 877 (m), 796 (w), 770 (w), 749 (w), 731 (m), 688 (m), 656 (w), 612 $cm^{-1}$ (w); HR-MS (ESI) *m/z* (%): 541.1743 (29), 540.1760 (100, $[M + Na]^+$, calcd for $C_{26}H_{26}F_3NaN_3O_5^+$: 540.1717), 518.1888 (34, $[M + H]^+$, calcd for $C_{26}H_{27}F_3N_3O_5^+$: 518.1897), 462.1258 (86, $[M – C_4H_8 + H]^+$, calcd for $C_{22}H_{19}F_3N_3O_4^+$: 462.1271), 304.2670 (50).

Data of (–)-**13m**: $t_R$ = 42 min; $[a]_D^{20}$ = –58.1 ($c$ = 0.1 in $CHCl_3$); $^1$H NMR and HR-MS (ESI) data consistent with (+)-**13m**.

**(3*R*,4*S*)- and (4*R*,3*S*)-*tert*-Butyl 3-(4-Methoxyquinazolin-7-yl)-4-(thien-2-ylcarbonyl)-pyrrolidine-1-carboxylate ((+)-13n and (–)-13n).**

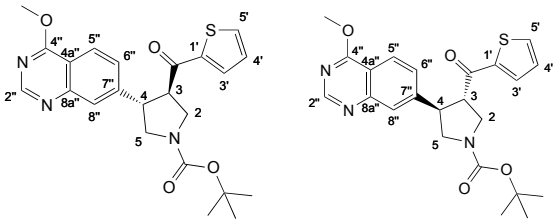

**GP-C** starting from alkene **10n** (105 mg, 0.35 mmol) (in 10~mL toluene; addition of 9~equiv. of *para*-formaldehyde; second addition of glycine and *para*-formaldehyde at 120 °C; after addition of $Boc_2O$ stirred for 1 h). FC ($SiO_2$; MeOH/$CH_2Cl_2$ 1:99 → 2.5:97.5) and chiral HPLC (Reprosil; 15 mL min$^{-1}$, hexane/*i*PrOH/$CHCl_3$ 75:3:22 → 65:5:30) gave pyrrolidines (+)-**13n** (15 mg, 10%) and (–)-**13n** (16 mg, 10%) as colorless waxes.

Data of (+)-**13n**: $R_f$ = 0.40 ($SiO_2$; MeOH/$CH_2Cl_2$ 1:19); $[a]_D^{20}$ = +62.3 ($c$ = 0.1 in $CHCl_3$); $^1$H NMR (400 MHz, $CDCl_3$; approx. 1:1 mixture of diastereoisomers, assignment based on HSQC and HMBC spectra of (+)-**13n**): $\delta$ = 1.50 (s, 9 H; C(C$H_3$)$_3$), 3.60–3.74 (m, 2 H; $H_a$–C(2), $H_a$–C(5)), 3.94–4.23 (m, 4 H; $H_b$–C(2), H–C(3), H–C(4), $H_b$–C(5)), 4.17 (s, 3 H; $OCH_3$), 7.07 (dd, $J$ = 4.8, 3.9 Hz, 1 H; H–C(4')), 7.50 (d, $J$ = 8.4 Hz, 1 H; H–C(6'')), 7.60–7.68 (m, 2 H; H–C(3'), H–C(5')), 7.84 (s, 1 H; H–C(8'')), 8.10 (d, $J$ = 8.5 Hz, 1 H; H–C(5'')), 8.79 ppm (s, 1 H; H–C(2'')); $^{13}$C NMR (100 MHz, $CDCl_3$; approx. 1:1 mixture of diastereoisomers, assignment based on HSQC and HMBC spectra of (+)-**13n**): $\delta$ = 28.49 (3 C; C($C$H$_3$)$_3$), 46.76 and 47.04 (C(3 or 4)), 49.70 and 49.81 (C(2 or 5)), 52.00 and 52.27 (C(2 or 5)), 53.25 and 54.00 (C(3 or 4)), 54.34 ($OCH_3$), 80.02 ($C$(CH$_3$)$_3$), 115.72 (C(4a'')), 124.19 (C(5'')), 125.57 (C(8'')), 127.20 (C(6'')), 128.39 (C(4')), 132.59 (C(3')), 134.93 (C(5')), 143.53 and 143.67 (C(2')), 146.00 and 146.25 (C(7'')), 151.13 (C(8a'')), 154.03 ($CO_2$), 154.81 (C(2'')), 166.94 (C(4'')), 190.54 ppm

(C=O); IR (ATR): $\tilde{\nu}$ = 2965 (w), 2926 (w), 2862 (w), 1686 (s), 1656 (m), 1624 (m), 1577 (m, sh), 1567 (s), 1495 (m), 1452 (m), 1404 (s), 1391 (s), 1378 (s), 1365 (s), 1345 (s), 1284 (m), 1260 (m), 1235 (m), 1201 (m), 1164 (m), 1126 (m), 1099 (m), 1054 (m), 980 (w), 970 (w), 880 (m), 845 (m), 800 (m), 770 (m), 738 (s), 688 $cm^{-1}$ (s); HR-MS (ESI): *m/z* (%): 440.1626 (26, [*M* + H]$^+$, calcd for $C_{23}H_{26}N_3O_4S^+$: 440.1639), 384.1000 (100).

Data of (–)-**13n** $[a]_D^{20}$ = –70.5 (*c* = 0.1 in $CHCl_3$); $^1$H NMR and HR-MS (ESI) data consistent with (+)-**13n**.

**(3*R*,4*S*)- and (4*R*,3*S*)-*tert*-Butyl 3-[(5-Chlorothien-2-yl)carbonyl]-4-(4-methoxy-quinazolin-7-yl)pyrrolidine-1-carboxylate ((+)-13o and (–)-13o).**

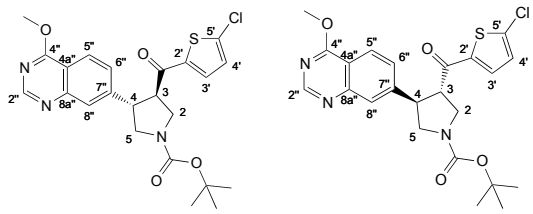

**GP-C** starting from alkene **10o** (100 mg, 0.30 mmol) (in 14~mL toluene; addition of 3 an 6~equiv. of *para*-formaldehyde; second addition of glycine and *para*-formaldehyde at 120 °C). FC ($SiO_2$; MeOH/$CH_2Cl_2$ 1:99 → 2.5:97.5) and chiral HPLC (Reprosil; 15 mL min$^{-1}$, hexane/*i*PrOH/$CHCl_3$ 75:3:22 → 66:4:30) gave pyrrolidines (+)-**13o** (25 mg, 17%) and (–)-**13o** (24 mg, 17%) as colorless waxes.

Data of (+)-**13o**: $R_f$ = 0.24 ($SiO_2$; MeOH/$CH_2Cl_2$ 1:19); $t_R$ = 36 min; $[a]_D^{20}$ = +84.0 (*c* = 0.1 in $CHCl_3$); $^1$H NMR (400 MHz, $CDCl_3$; approx. 1:1 mixture of diastereoisomers, assignment based on HSQC and HMBC spectra of (+)-**13o**): $\delta$ = 1.50 (s, 9 H; C(C*H*$_3$)$_3$), 3.60–3.72 (m, 2 H; H$_a$–C(2), H$_a$–C(5)), 3.93–4.13 (m, 4 H; H$_b$–C(2), H–C(3), H–C(4), H$_b$–C(5)), 4.18 (s, 3 H; $OCH_3$), 6.88 (d, *J* = 4.1 Hz, 1 H; H–C(4')), 7.38 (br. s, 1 H; H–C(5')), 7.48 (dd, *J* = 8.4, 1.7 Hz, 1 H; H–C(6)), 7.82 (br. s, 1 H; H–C(8'')), 8.11 (d, *J* = 8.4 Hz, 1 H; H–C(5'')), 8.80 ppm (s, 1 H; H–C(2'')); $^{13}$C NMR (100 MHz, $CDCl_3$; approx. 1:1 mixture of diastereoisomers, assignment based

on HSQC and HMBC spectra of (+)-**13o**): $\delta$ = 28.48 (C($CH_3$)$_3$), 46.89 and 47.17 (C(3 or 4)), 49.62 and 49.71 (C(2 or 5)), 52.00 and 52.25 (C(2 or 5)), 52.48 and 53.22 (C(3 or 4)), 54.37 ($OCH_3$), 80.11 ($C$($CH_3$)$_3$), 115.77 (C(4a'')), 124.30 (C(5'')), 125.53 (C(8'')), 127.09 (C(6'')), 127.85 (C(4')), 132.09 (C(3')), 141.20 (C(5')), 142.14 and 142.22 (C(2')), 145.71 and 145.95 (C(7'')), 151.11 (C(8a'')), 153.97 and 154.01 ($CO_2$), 154.89 (C(2'')), 166.96 (C(4'')), 189.74 ppm (C=O); IR (ATR): $\tilde{\eta}$ = 2975 (w), 2937 (w), 2884 (w), 1690 (m), 1656 (m), 1624 (m), 1567 (m), 1496 (m), 1454 (m), 1407 (s), 1376 (s), 1325 (m), 1163 (m), 1120 (m), 1098 (m), 1016 (m), 975 (w), 878 (m), 796 (m), 769 (m), 749 (w), 687 cm$^{-1}$ (m); HR-MS (ESI): *m/z* (%): 476.1234 (18, [$M$ + H]$^+$, calcd for $C_{23}H_{25}{}^{37}ClN_3O_4S^+$: 476.1221), 474.1255 (42, [$M$ + H]$^+$, calcd for $C_{23}H_{25}{}^{35}ClN_3O_4S^+$: 476.1249), 420.0605 (41), 418.0631 (100).

Data of (–)-**13o**: $t_R$ = 50 min; $[a]_D^{20}$ = –91.0 ($c$ = 0.1 in $CHCl_3$); $^1$H NMR and HR-MS (ESI) data consistent with (+)-**13o**.

**(3*R*,4*S*)- and (4*R*,3*S*)-t*ert*-Butyl 3-(5-Bromothioene-2-carbonyl)-4-(4-methoxy-quinazolin-7-yl)pyrrolidine-1-carboxylate ((+)-13p and (–)-13p).**

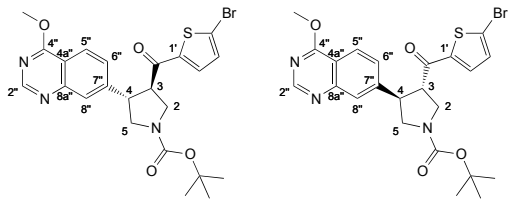

GP-C1 starting from alkene **10p** (100 µg, 266 µmol) in toluene (20 mL). FC ($SiO_2$; MeOH/$CH_2Cl_2$ 1:99) and chiral HPLC (Reprosil; 15 mL min$^{-1}$, hexane/*i*PrOH/$CHCl_3$ 75:3:22) gave pyrrolidines (+)-**13p** (10 mg, 7%) and (–)-**13p** (10 mg, 7%) as yellow oils.

Data of (+)-**13p**: prep. HPLC: $t_R$: 48 (Reprosil, 15 mL min$^{-1}$; Hex/*i*PrOH/$CHCl_3$ 75:3:22); $[a]_D^{20}$ = +72.4 ($c$ = 0.1 in $CHCl_3$); $^1$H NMR (600 MHz, $CDCl_3$): $\delta$ = 1.49 (s, 9 H; C($CH_3$)$_3$), 3.57–3.71 (m, 2 H; $H_a$–C(2), $H_a$–C(5)), 3.92–4.11 (m, 4 H; $H_b$–C(2), $H_b$–C(5), H–C(3), H–C(4)), 4.19 (s, 3 H; $OCH_3$), 7.03 (d, $J$ = 3.9 Hz, 1 H; H–C(4')), 7.35 (d, $J$ = 3.9 Hz, 1 H; H–C(3')), 7.50 (br. d, $J$ =

8.4 Hz; H–C(6")), 7.90 (br. s, 1 H; H–C(8")), 8.12 (d, $J$ = 8.1 Hz, 1 H; H–C(5")), 8.81 ppm (br. s, 1 H; H–C(2)); $^{13}$C NMR (150 MHz, $CDCl_3$): $\delta$ = 28.63 ($C(CH_3)_3$), 47.00 and 47.32 (C(4)), 49.79 and 49.92 (C(2)), 52.41 (C(3)), 52.81 (C(5)), 54.90 ($OCH_3$), 80.31 ($C(CH_3)_3$), 115.76 (C(4a")), 124.56 (C(5"), 131.65, 131.72, 132.97, 145.09, 146.56, 154.13, 154.60 (d; C(2)), 167.52 (q; C(4")), 189.62 ppm (s; C=O); IR (ATR): $\tilde{n}$ = 2953 (w), 2922 (m), 2851 (w), 1688 (m), 1657 (m), 1624 (w), 1568 (w), 1523 (w), 1497 (m), 1455 (m), 1405 (s), 1377 (s), 1320 (w), 1258 (w), 1163 (m), 1121 (s), 1098 (s), 975 (w), 878 (m), 796 (m), 770 (w), 749 (m), 730 (s), 688 $cm^{-1}$(w); HR-MS (ESI) *m/z* (%): 520.0724 (45, $[M + H]^+$, calcd for $C_{23}H_{25}{}^{81}BrN_3O_4S^+$: 520.0729), 518.0741 (45, $[M + H]^+$, calcd for $C_{23}H_{25}{}^{79}BrN_3O_4S^+$: 518.0744), 464.0093 (98, $[M - C_4H_8 + H]^+$, calcd for $C_{19}H_{17}{}^{81}BrN_3O_4S^+$: 464.0097), 462.0113 (100, $[M - C_4H_8 + H]^+$, calcd for $C_{19}H_{17}{}^{79}BrN_3O_4S^+$: 462.0118).

Data of (–)-**13p**: $t_R$ = 78 min; $[a]_D^{20}$ = –68.0 ($c$ = 0.1 in $CHCl_3$); $^1$H NMR and HR-MS (ESI) data consistent with (+)-**13p**.

# S6. $^{1}$H and $^{13}$C NMR spectra

As an example, the HSQC and COSY NMR spectra of (+)-**1i** are included.

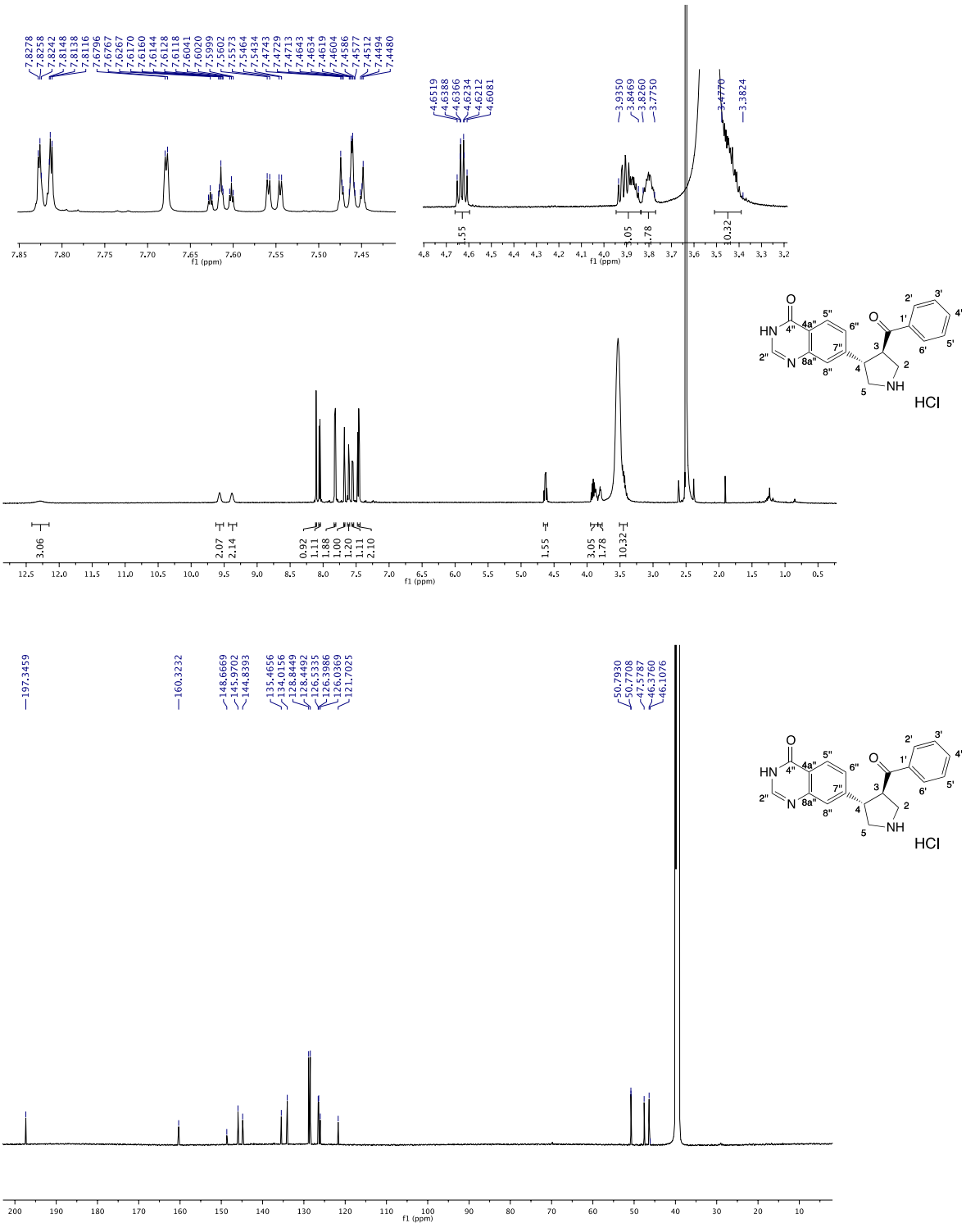


**Figure S7**. $^{1}$H NMR spectrum of (+)-**1a** in $(CD_3)_2SO$, 600 MHz, 298 K and $^{13}$C NMR spectrum of (+)-**1a** 3 in $(CD_3)_2SO$, 150 MHz, 298 K.

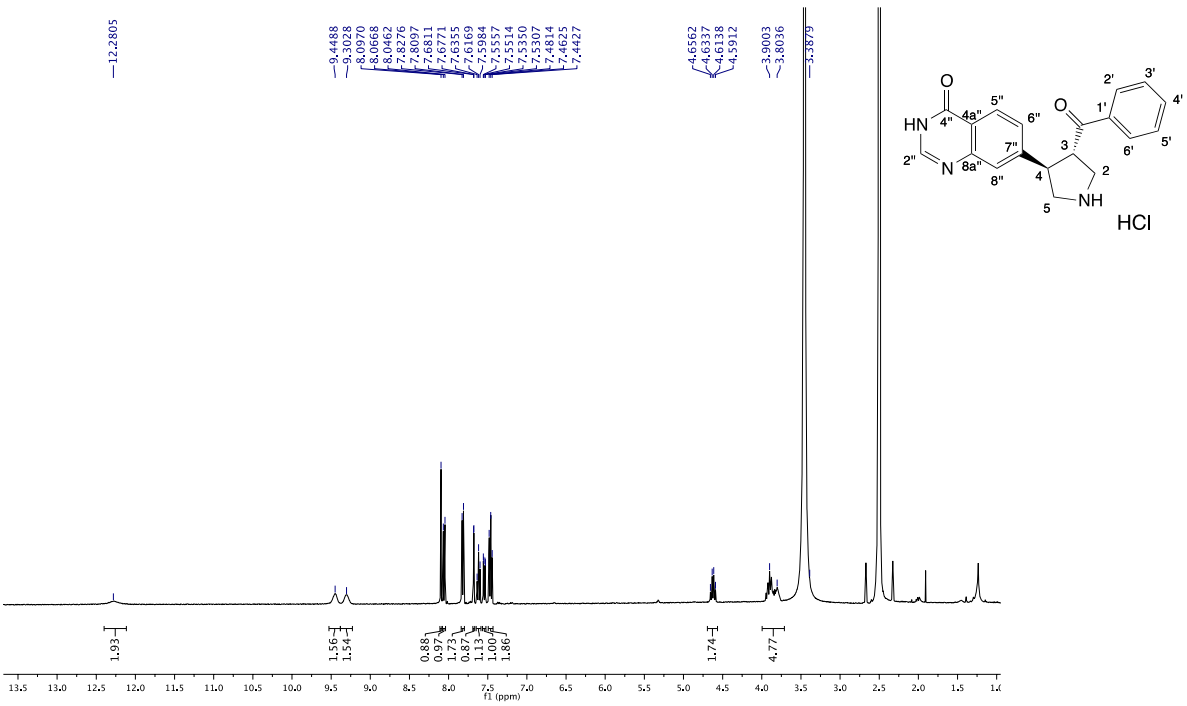

**Figure S8**. $^{1}$H NMR spectrum of (–)-**1a** in $(CD_3)_2SO$, 600 MHz, 298 K.

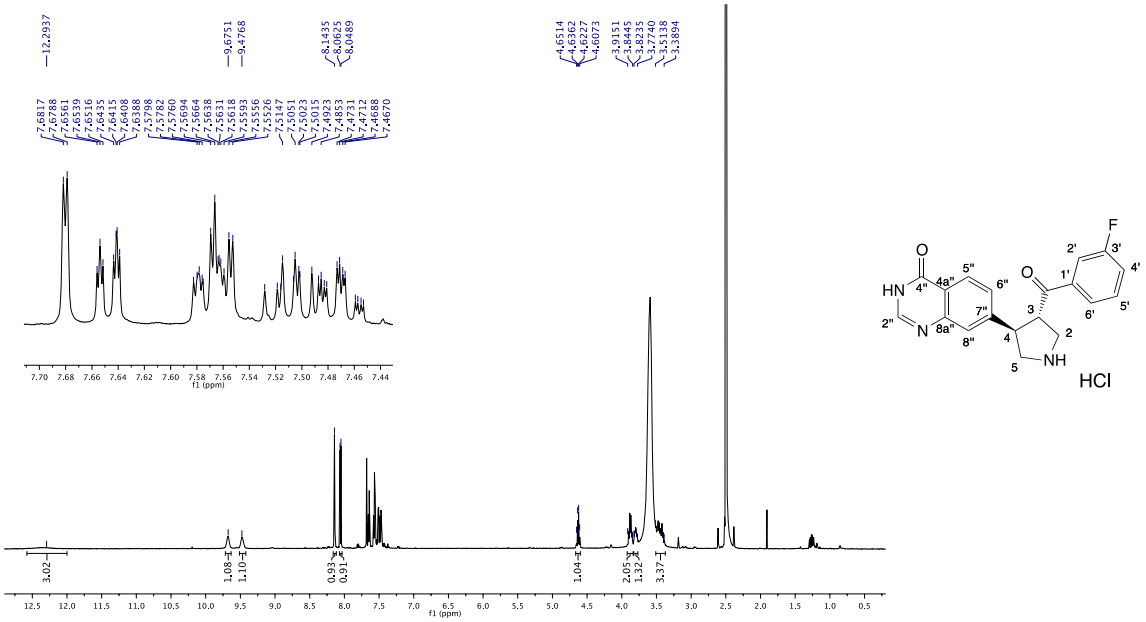

**Figure S9**. $^{1}$H NMR spectrum of (–)-**1b** in $(CD_3)_2SO$, 600 MHz, 298 K.

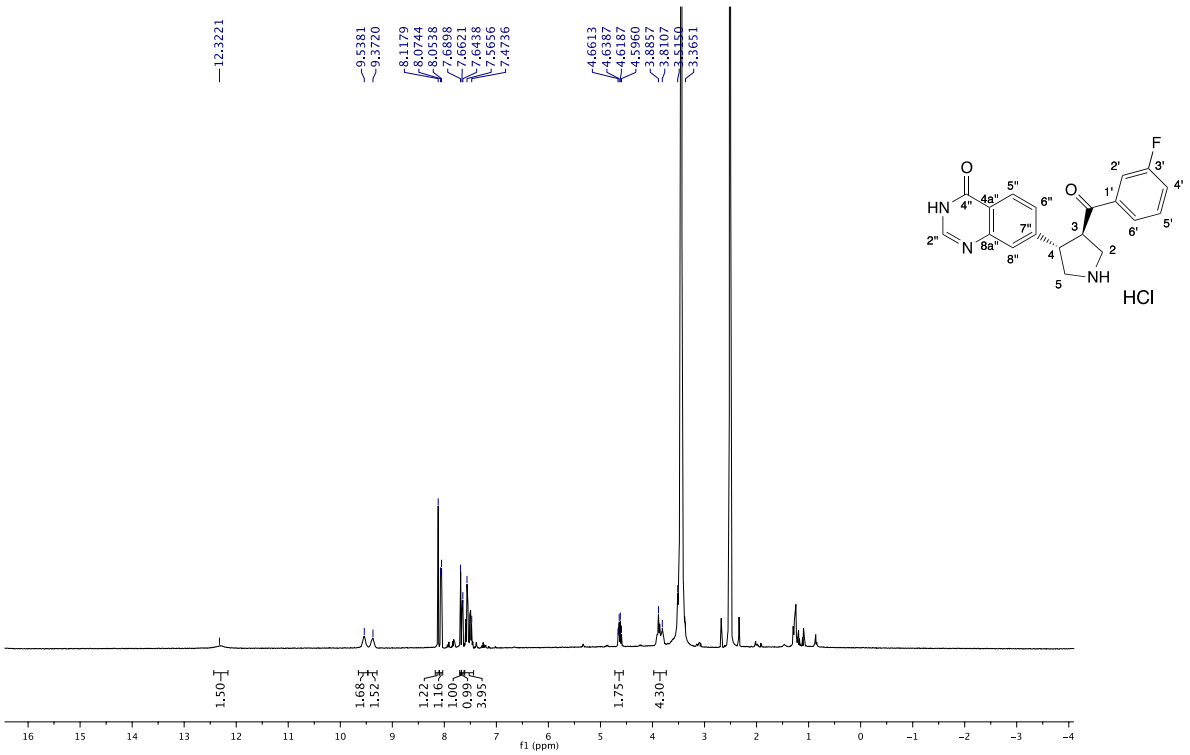


**Figure S10**. $^{1}$H NMR spectrum of (+)-**1b** in $(CD_3)_2SO$, 600 MHz, 298 K.

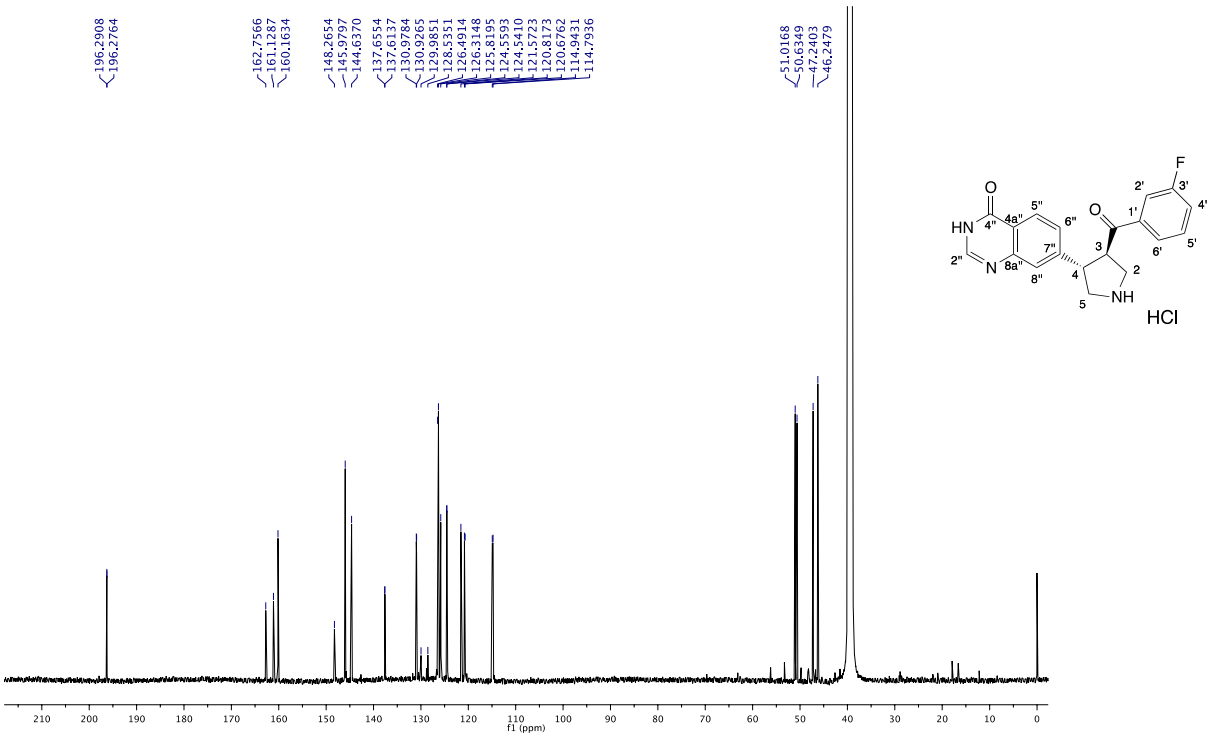


**Figure S11**. $^{13}$C NMR spectrum of (+)-**1b** in $(CD_3)_2SO$, 150 MHz, 298 K.

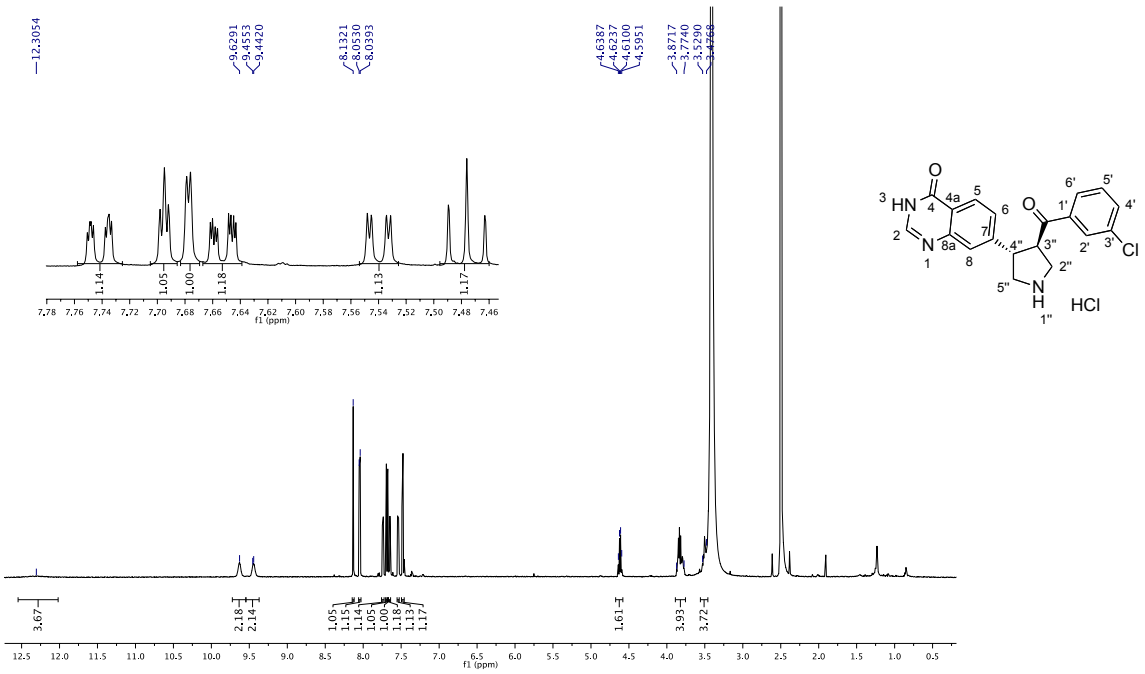


**Figure S12**. $^{1}$H NMR spectrum of (+)-**1c** in $(CD_3)_2SO$, 600 MHz, 298 K.

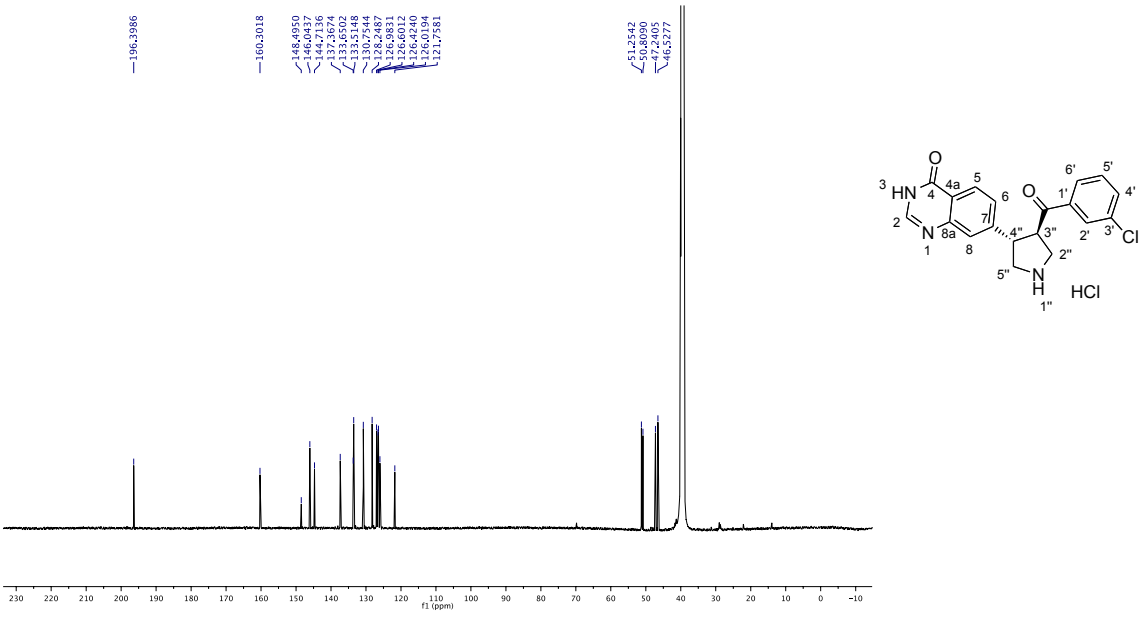


**Figure S13**. $^{13}$C NMR spectrum of (+)-**1c** in $(CD_3)_2SO$, 150 MHz, 298 K.

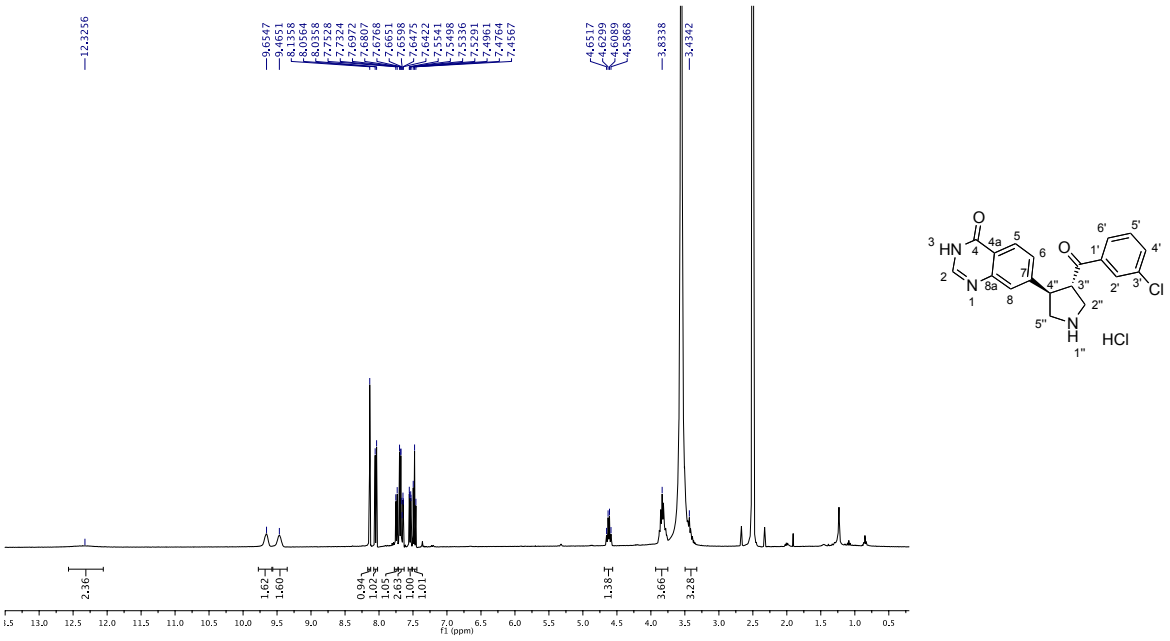

**Figure S14**. $^{1}$H NMR spectrum of (–)-**1c** in $(CD_3)_2SO$, 600 MHz, 298 K.

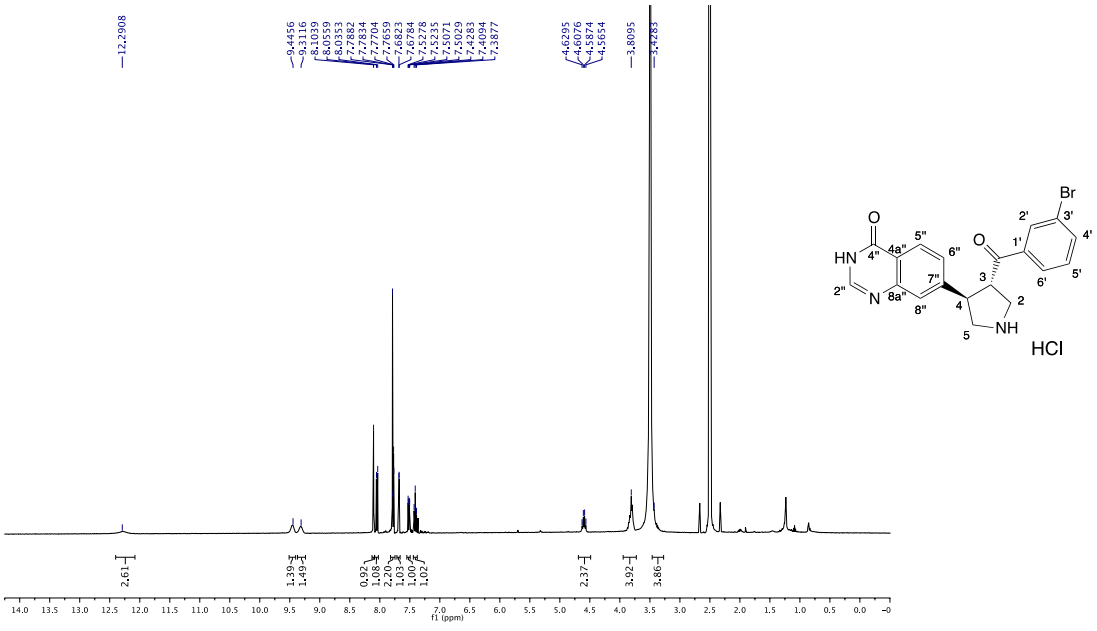

**Figure S15**. $^{1}$H NMR spectrum of (–)-**1d** in $(CD_3)_2SO$, 600 MHz, 298 K.

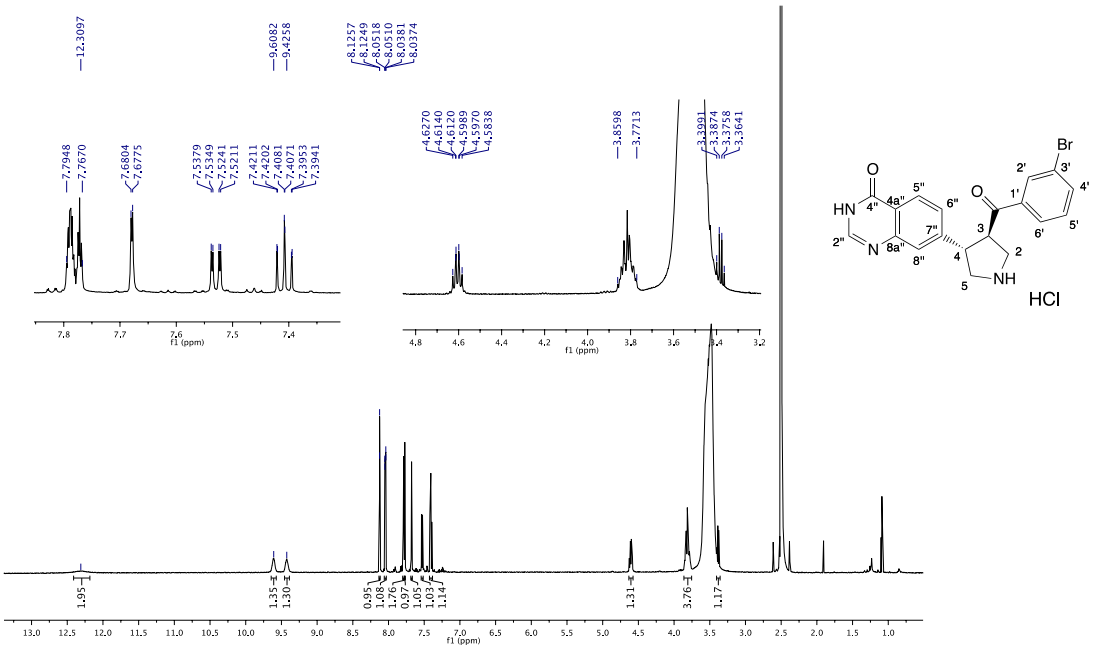


**Figure S16**. $^{1}$H NMR spectrum of (+)-**1d** in $(CD_3)_2SO$, 600 MHz, 298 K.

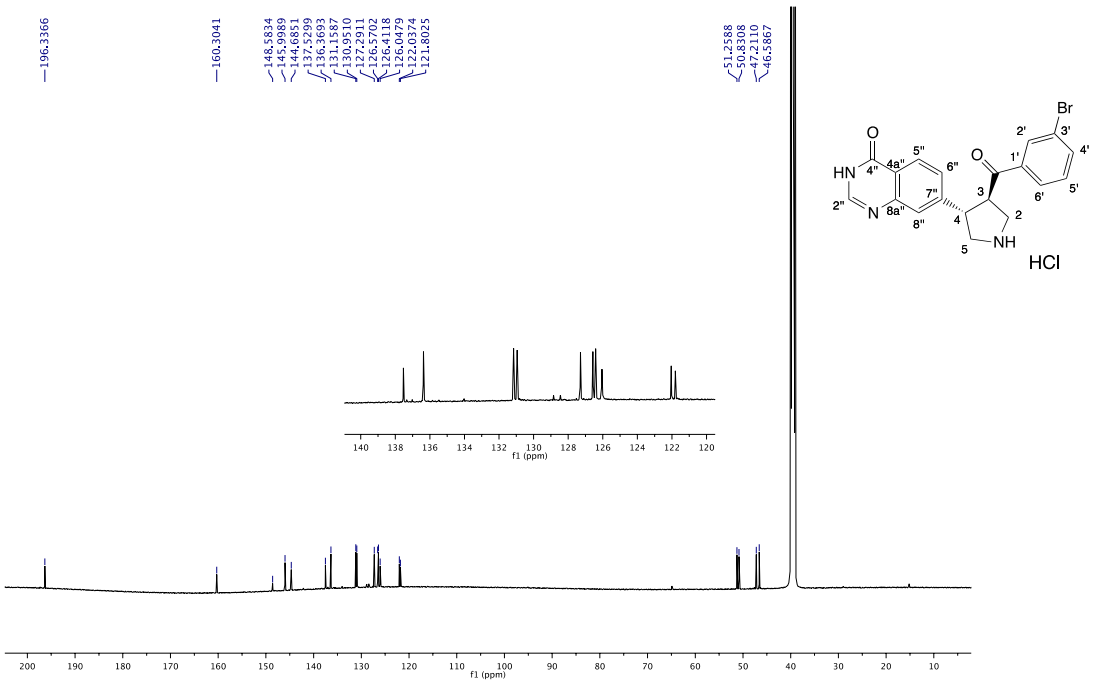


**Figure S17**. $^{13}$C NMR spectrum of (+)-**1d** in $(CD_3)_2SO$, 150 MHz, 298 K.

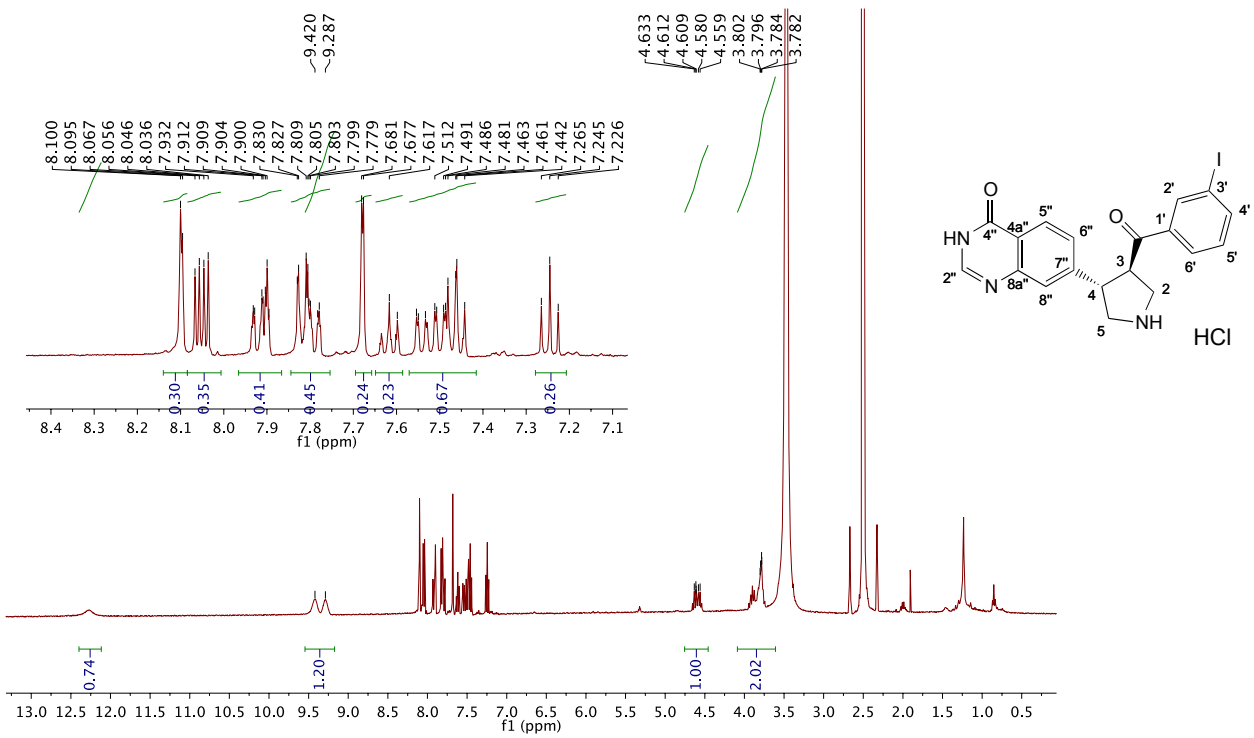

**Figure S18**. $^{1}$H NMR spectrum of unstable (–)-**1e** in $(CD_3)_2SO$, 600 MHz, 298 K.

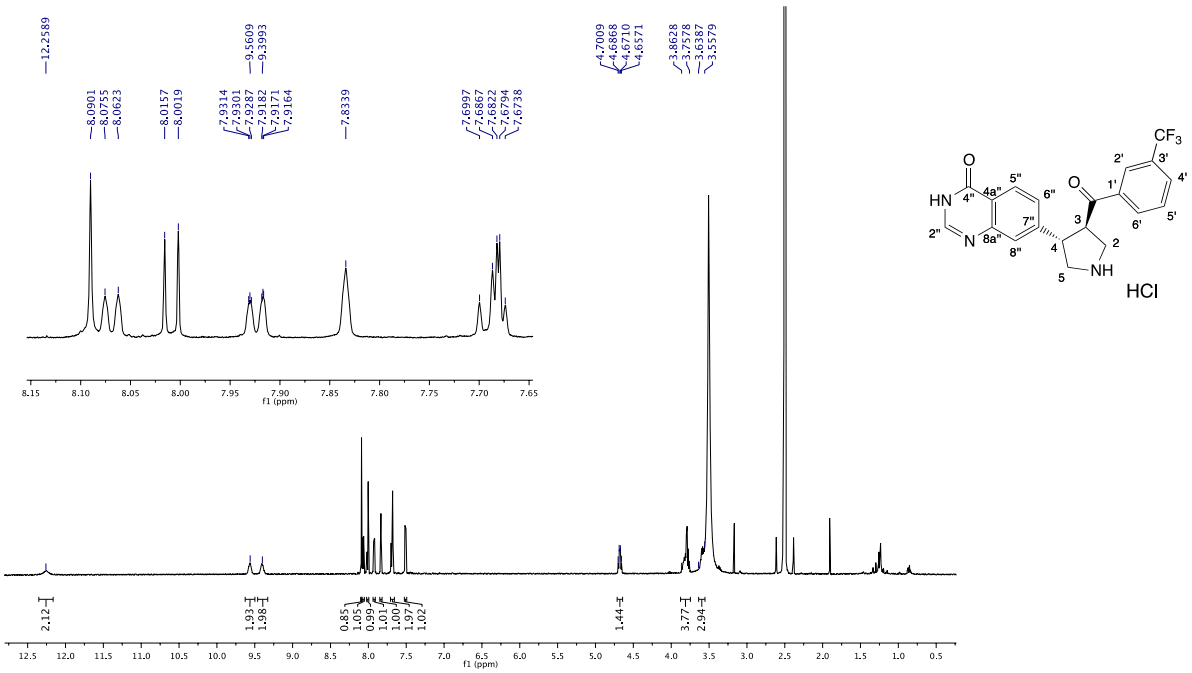

**Figure S19**. $^{1}$H NMR spectrum of (–)-**1f** in $(CD_3)_2SO$, 600 MHz, 298 K.

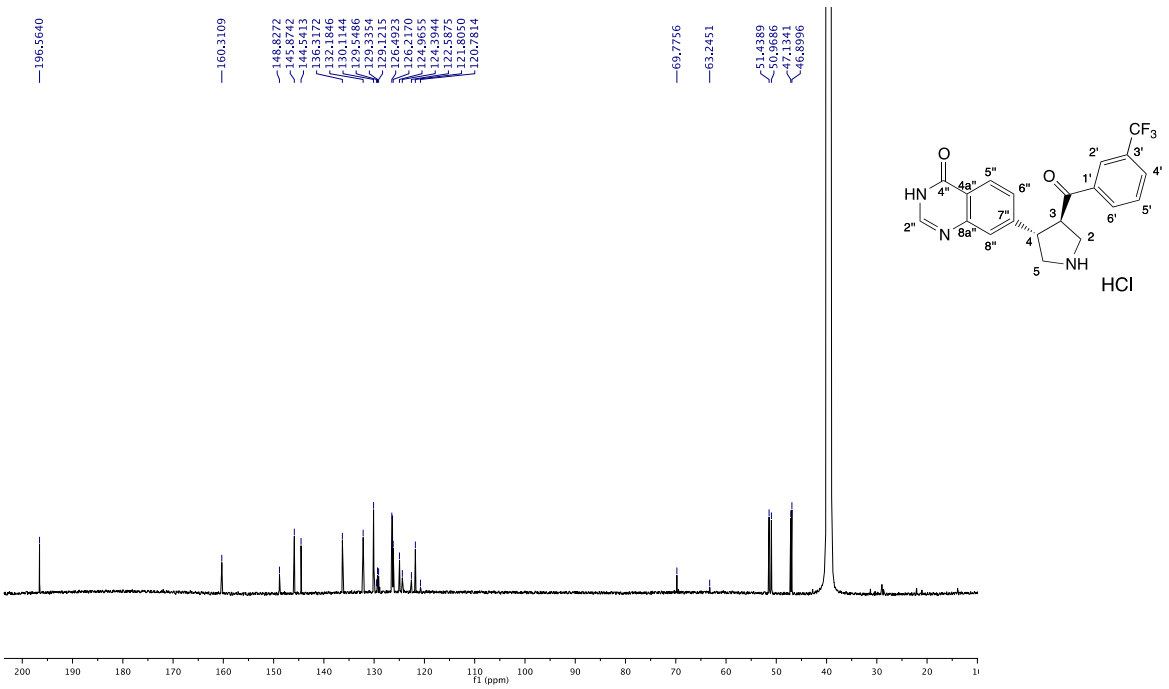


**Figure S20**. $^{13}$C NMR spectrum of (+)-**1f** in $(CD_3)_2SO$, 600 MHz, 298 K.

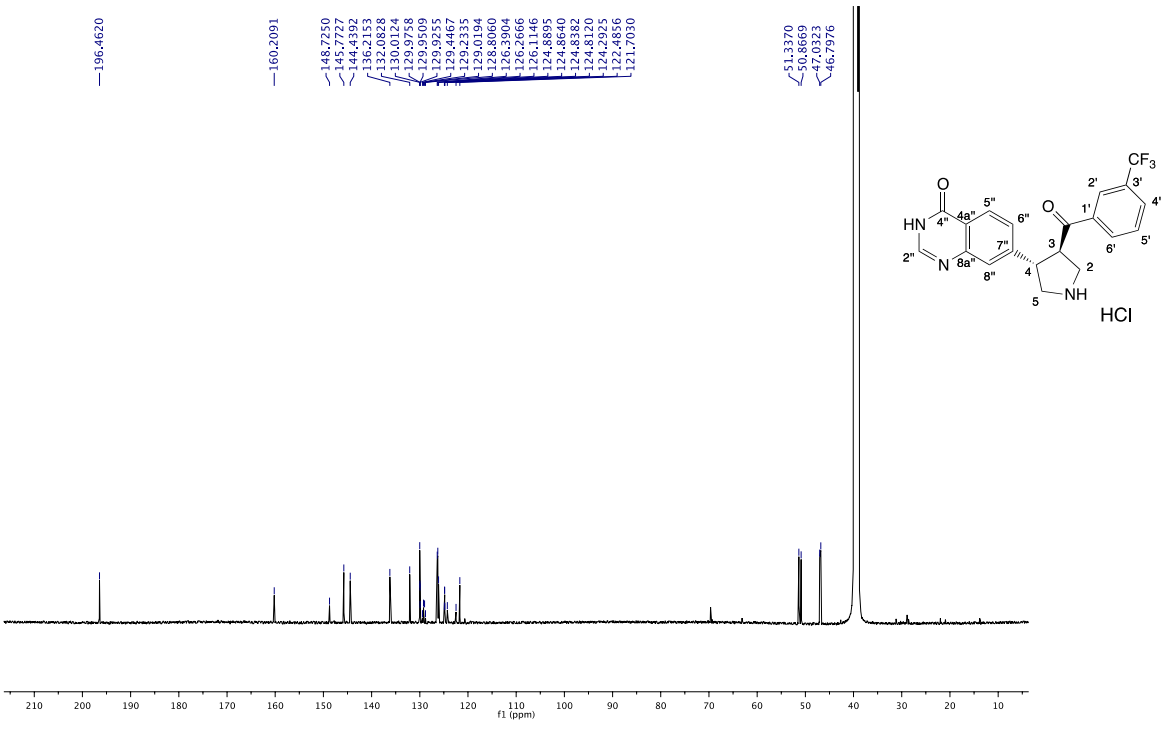


**Figure S21**. $^{13}$C NMR spectrum of (+)-**1f** in $(CD_3)_2SO$, 150 MHz, 298 K.

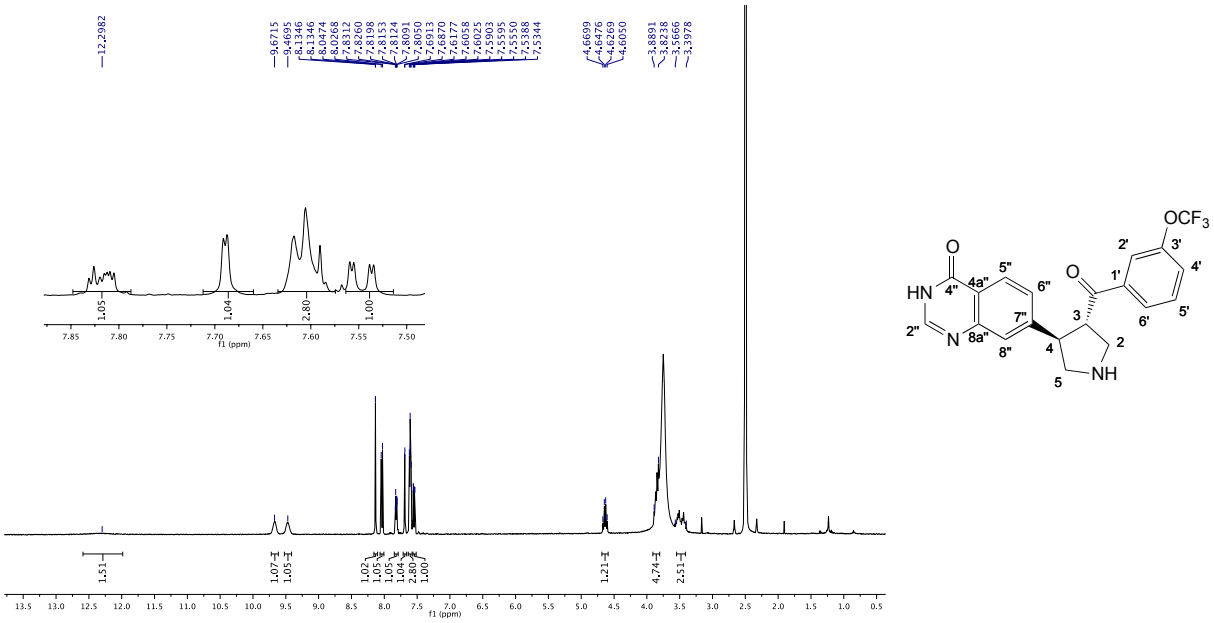

**Figure S22**. $^{1}$H NMR spectrum of (–)-**1g** in $(CD_3)_2SO$, 400 MHz, 298 K.

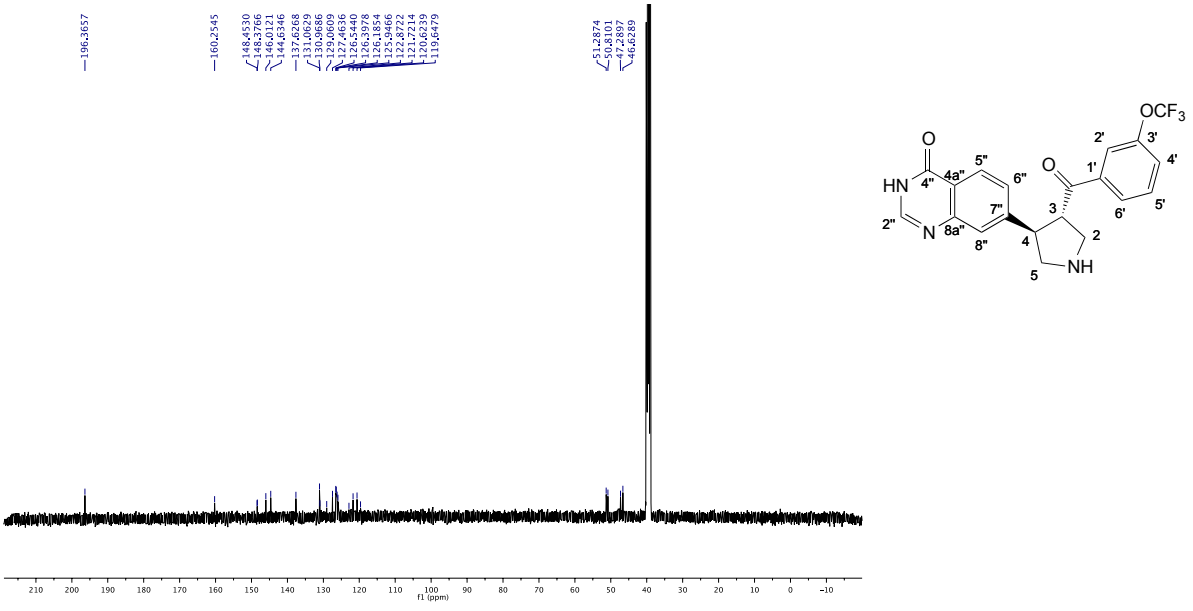

**Figure S23**. $^{13}$C NMR spectrum of (–)-**1g** in $(CD_3)_2SO$, 100 MHz, 298 K.

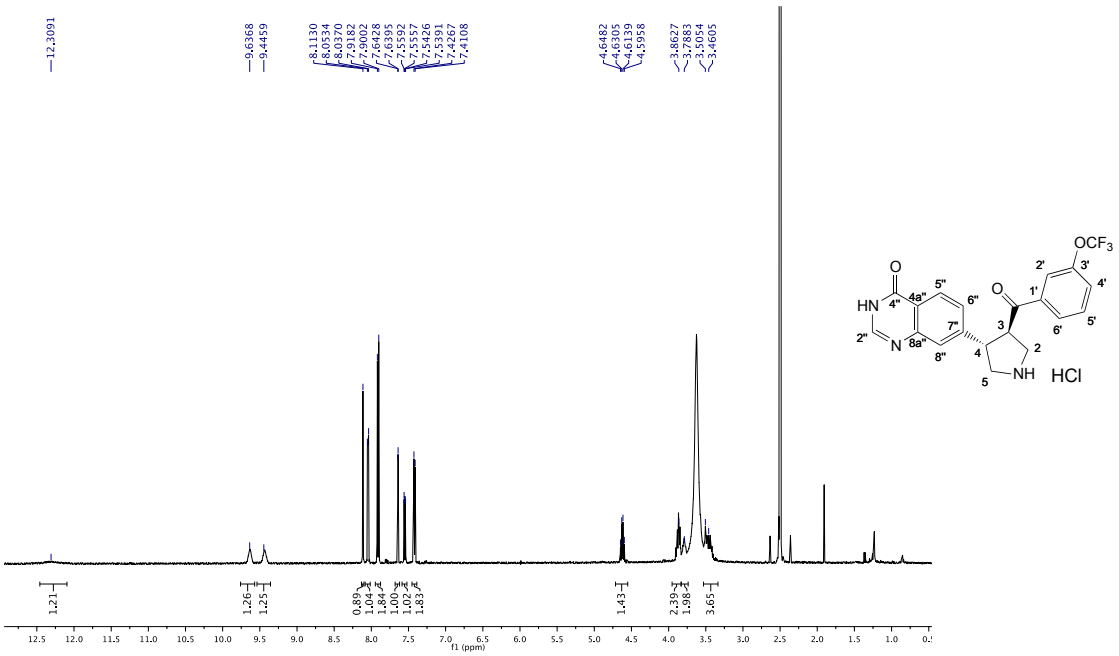


**Figure S24**. $^{1}$H NMR spectrum of (+)-**1g** in $(CD_3)_2SO$, 400 MHz, 298 K.

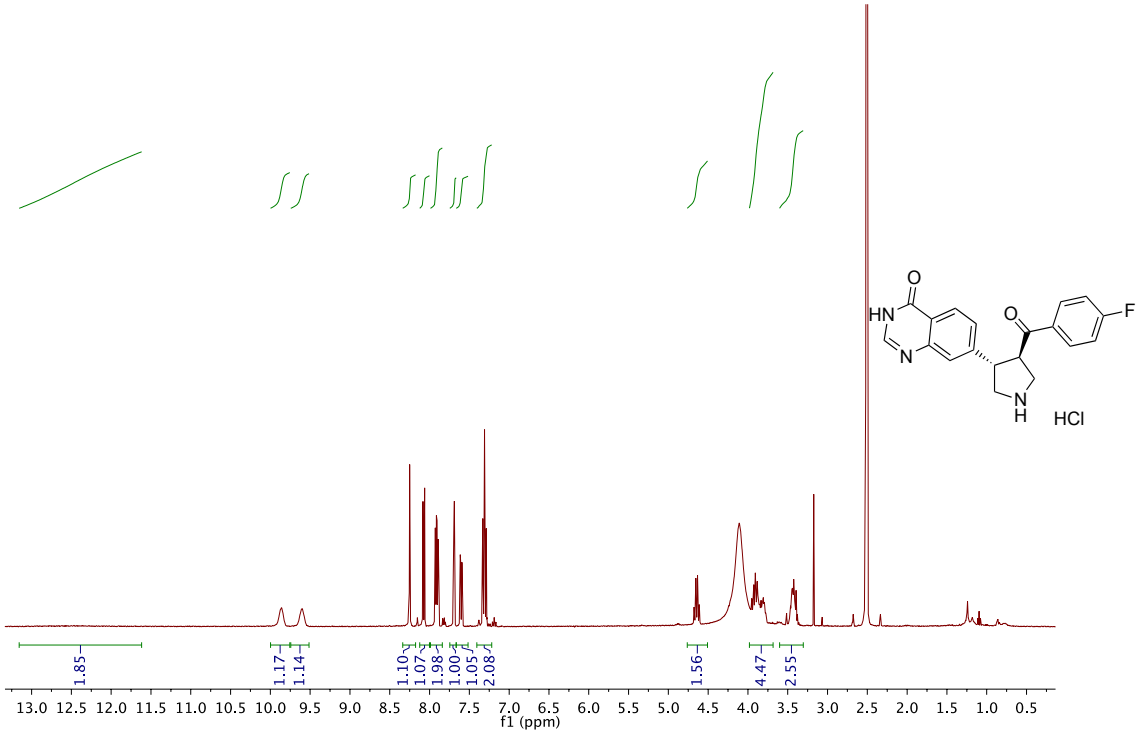


**Figure S25**. $^{1}$H NMR spectrum of (–)-**1h** in $(CD_3)_2SO$, 100 MHz, 298 K.

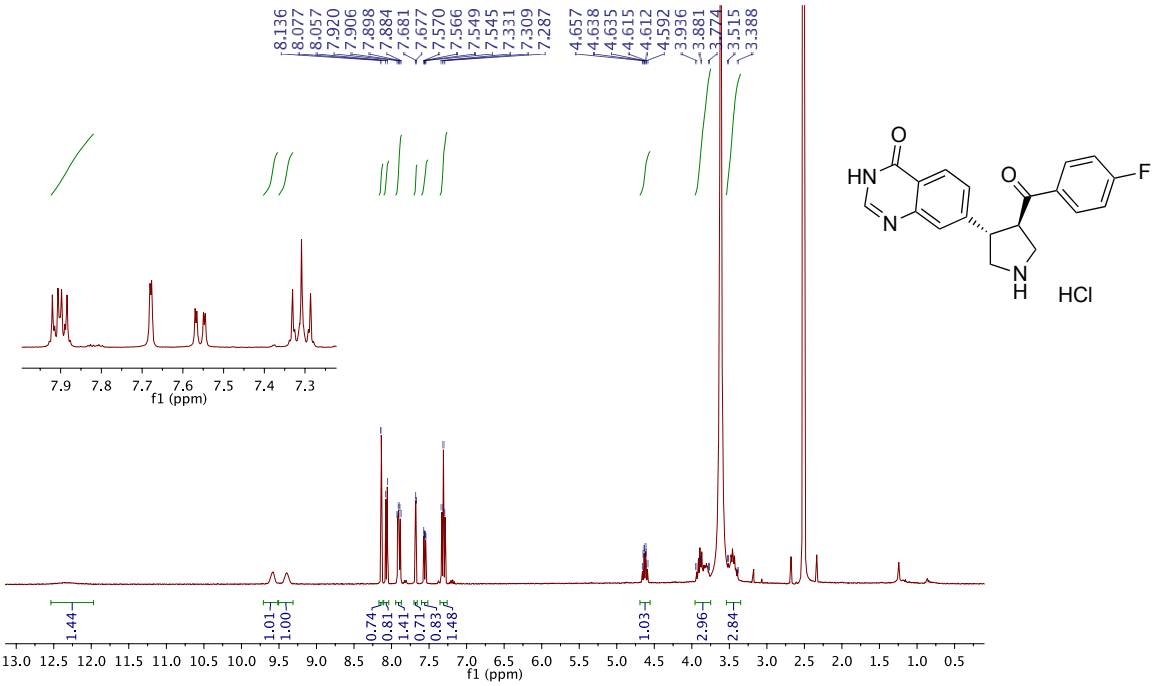


**Figure S26**. $^{1}$H NMR spectrum of (+)-**1h** in $(CD_3)_2SO$, 400 MHz, 298 K.

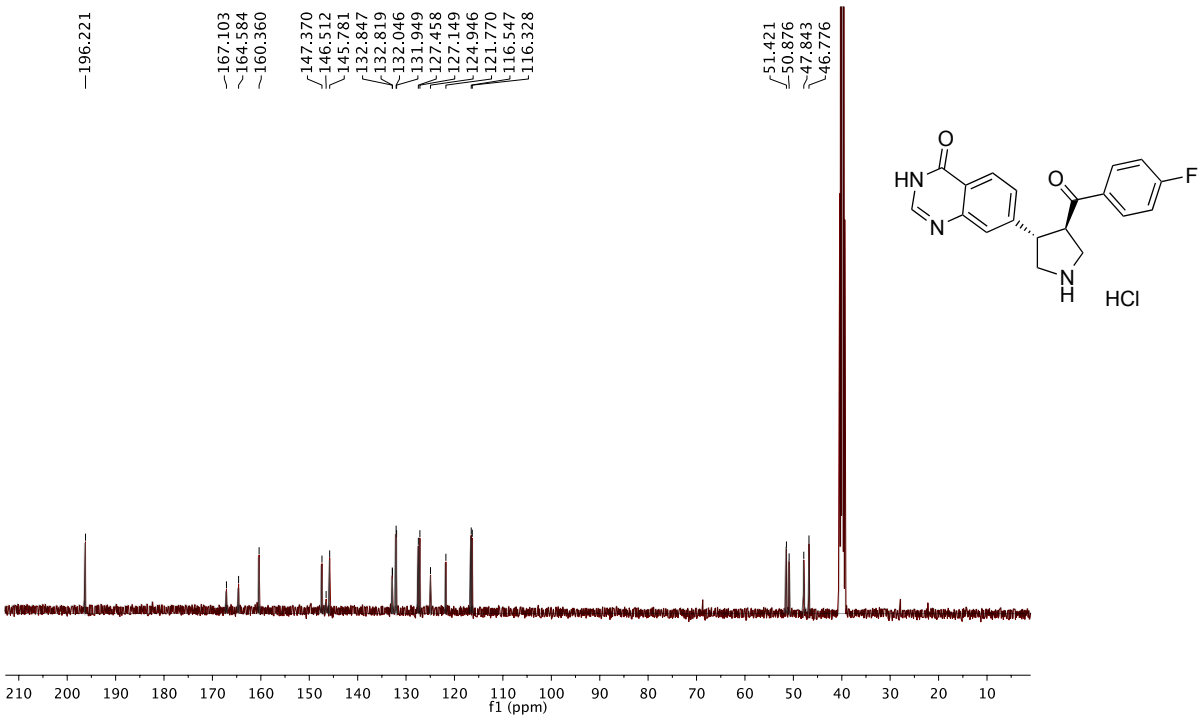


**Figure S27**. $^{13}$C NMR spectrum of (+)-**1h** in $(CD_3)_2SO$, 100 MHz, 298 K.

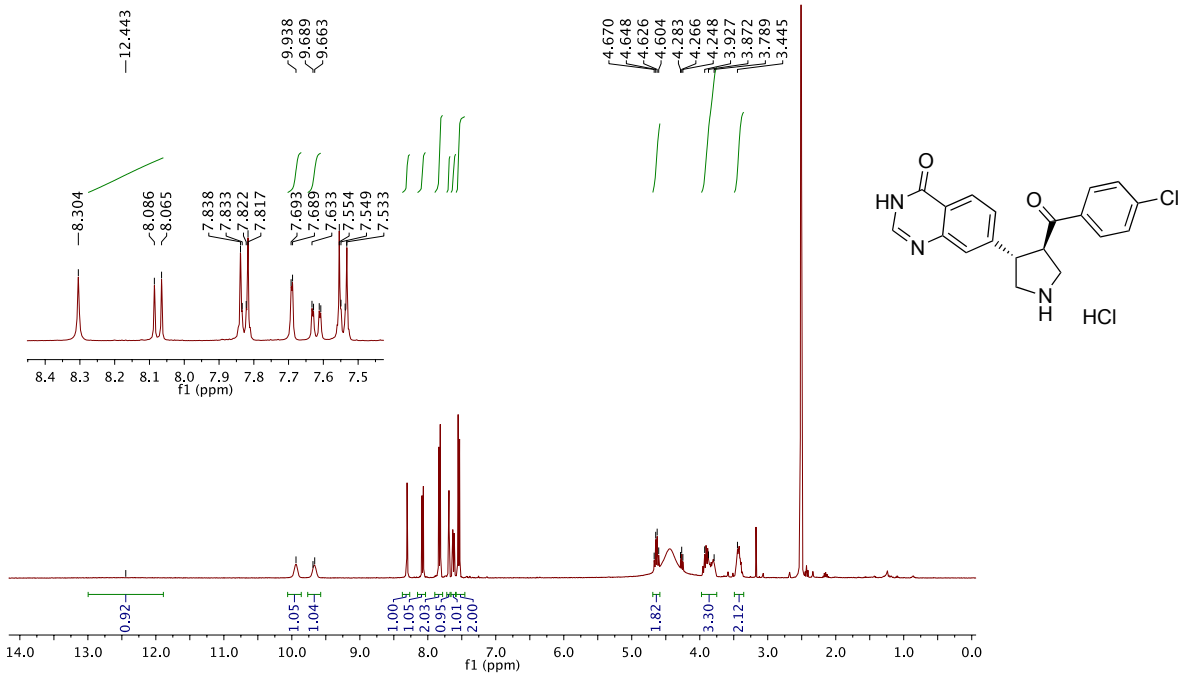


**Figure S28**. $^{1}$H NMR spectrum of (+)-**1i** in $(CD_3)_2SO$, 400 MHz, 298 K.

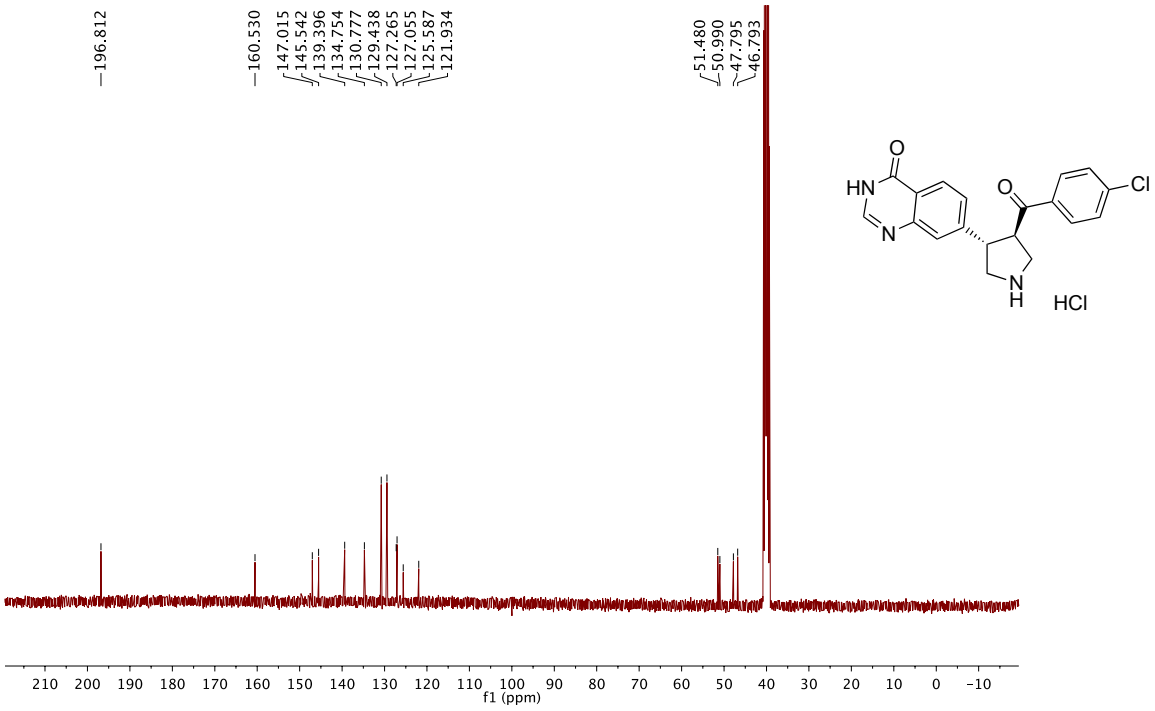


**Figure S29**. $^{13}$C NMR spectrum of (+)-**1i** in $(CD_3)_2SO$, 100 MHz, 298 K.

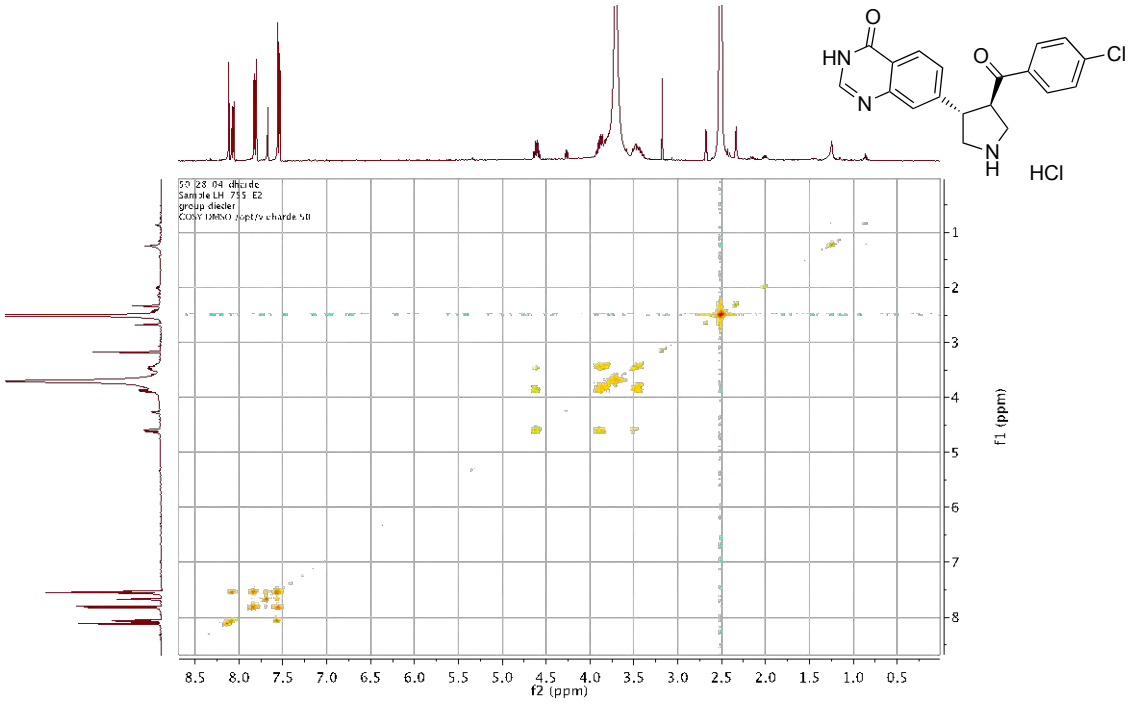


**Figure S30**. COSY spectrum of (+)-**1i** in $(CD_3)_2SO$, 400 MHz, 298 K.

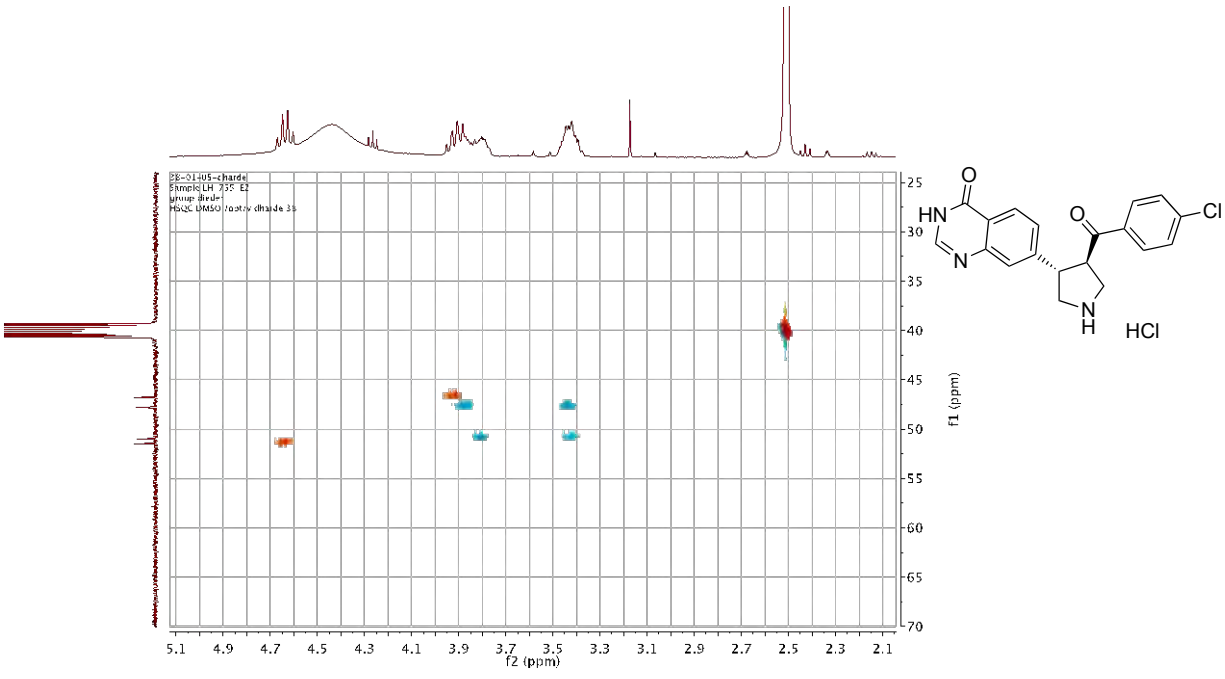


**Figure S31**. HSQC spectrum of (+)-**1i** in $(CD_3)_2SO$, 400 MHz, 298 K, part I

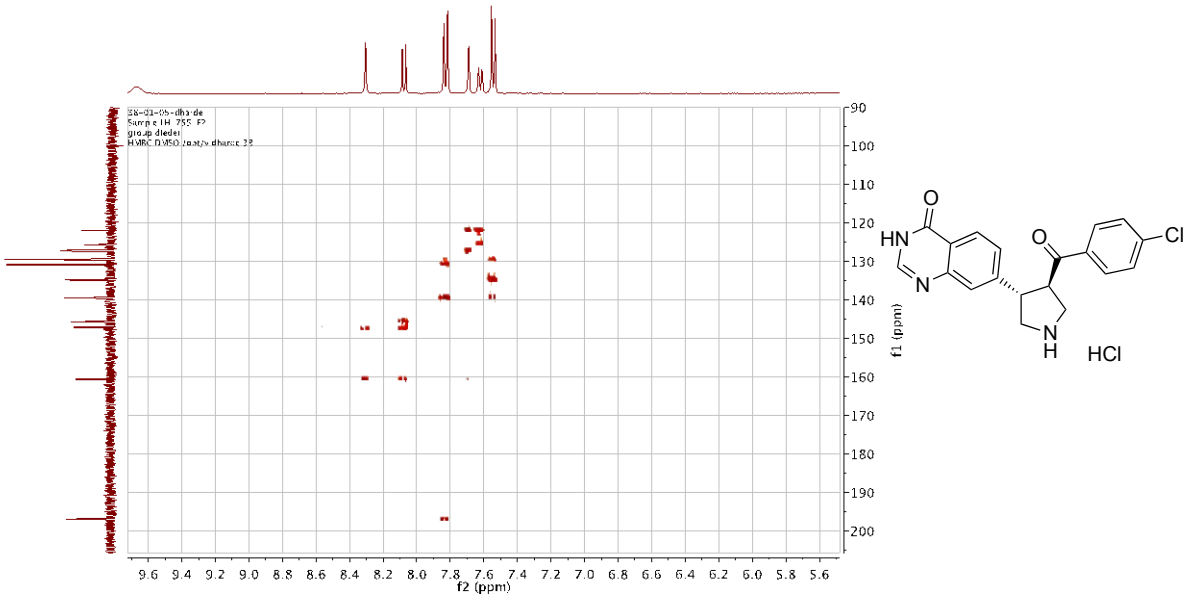


**Figure S32**. HSQC spectrum of (+)-**1i** in $(CD_3)_2SO$, 400 MHz, 298 K, part II

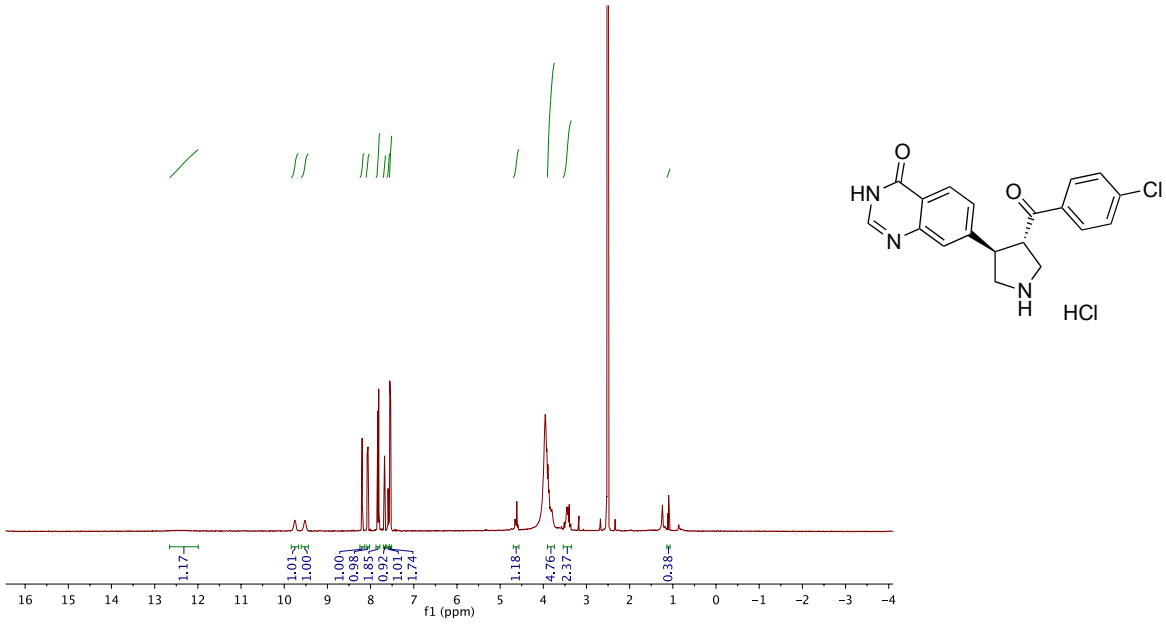


**Figure S33**. $^1$H NMR spectrum of (–)-**1i** in $(CD_3)_2SO$, 400 MHz, 298 K.

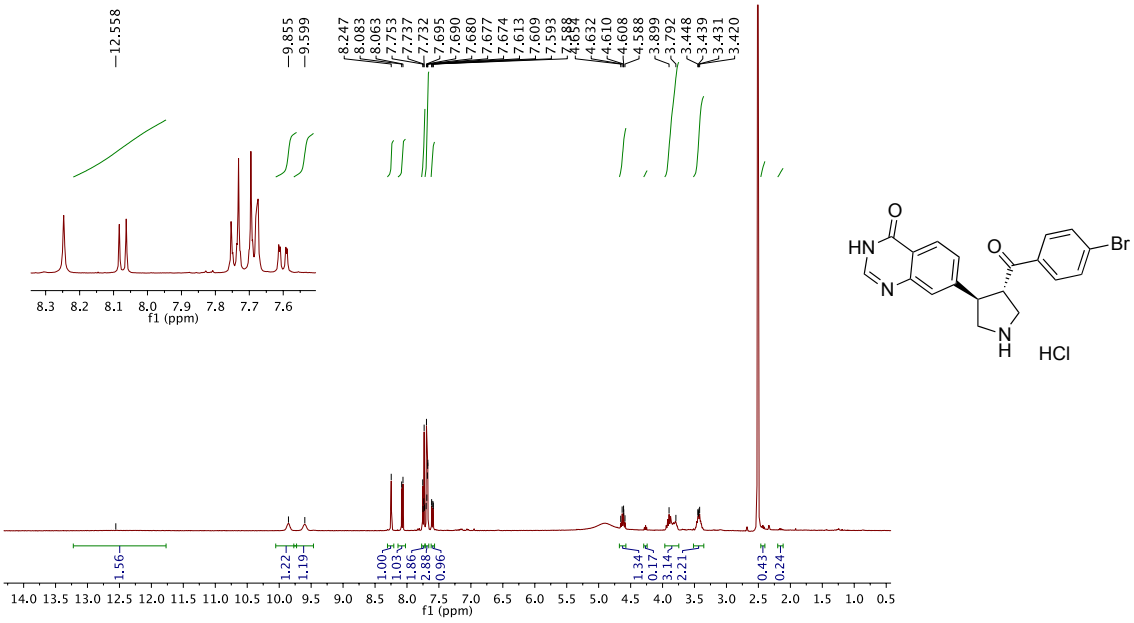


**Figure S34**. $^{1}$H NMR spectrum of (–)-**1j** in $(CD_3)_2SO$, 400 MHz, 298 K.

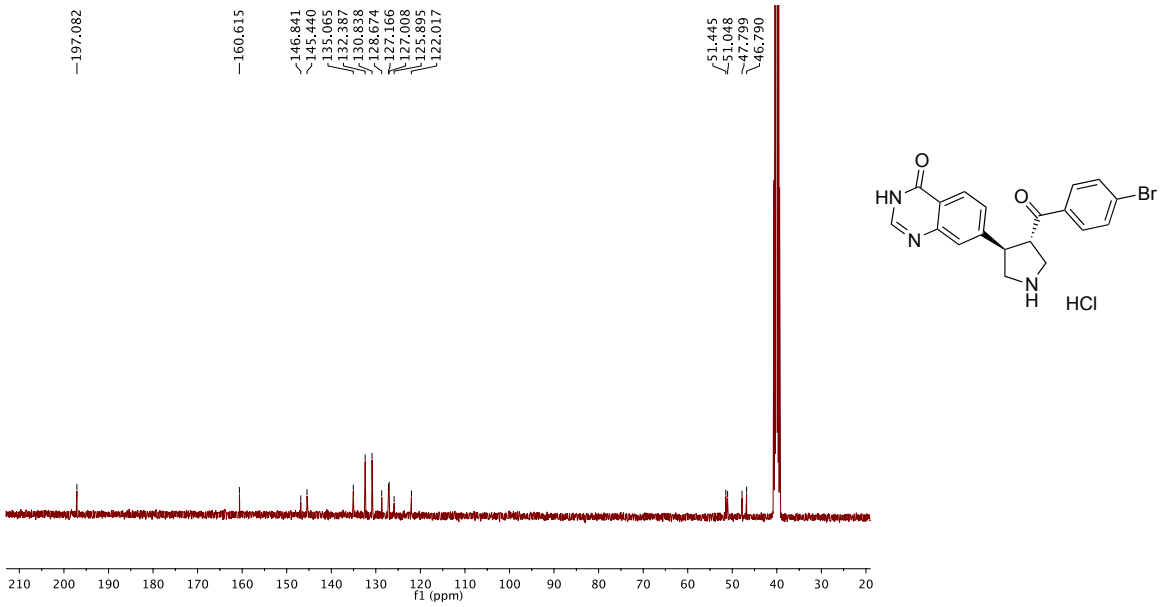


**Figure S35**. $^{13}$C NMR spectrum of (–)-**1j** in $(CD_3)_2SO$, 100 MHz, 298 K.

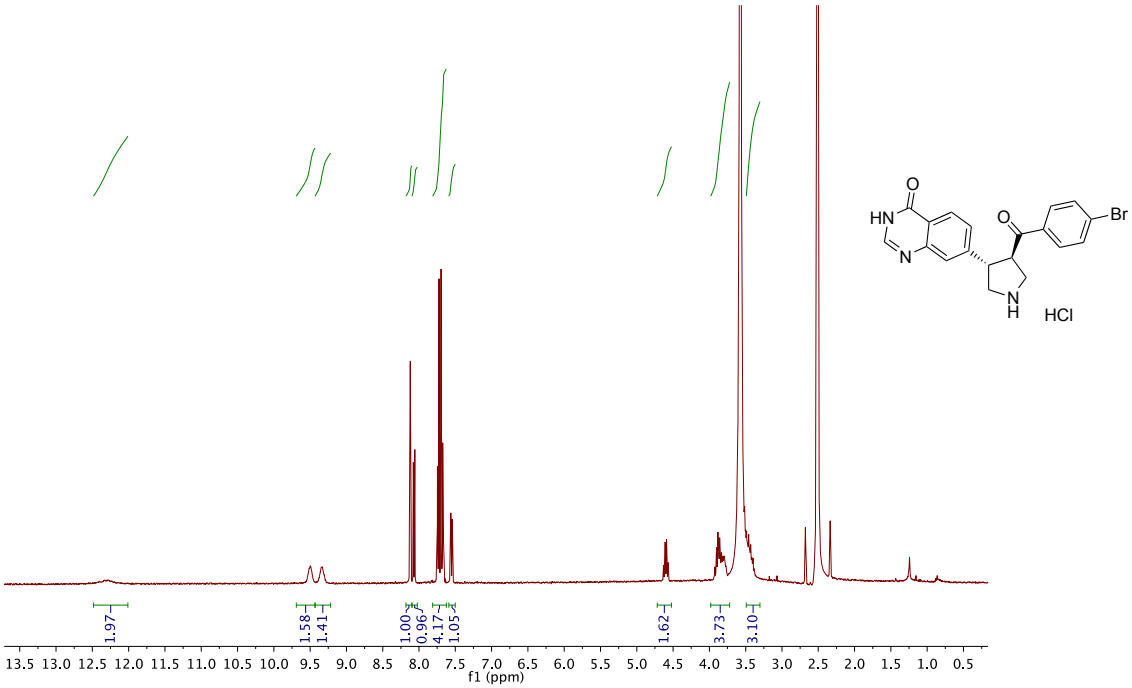


**Figure S36**. $^{1}$H NMR spectrum of (+)-**1j** in $(CD_3)_2SO$, 400 MHz, 298 K.

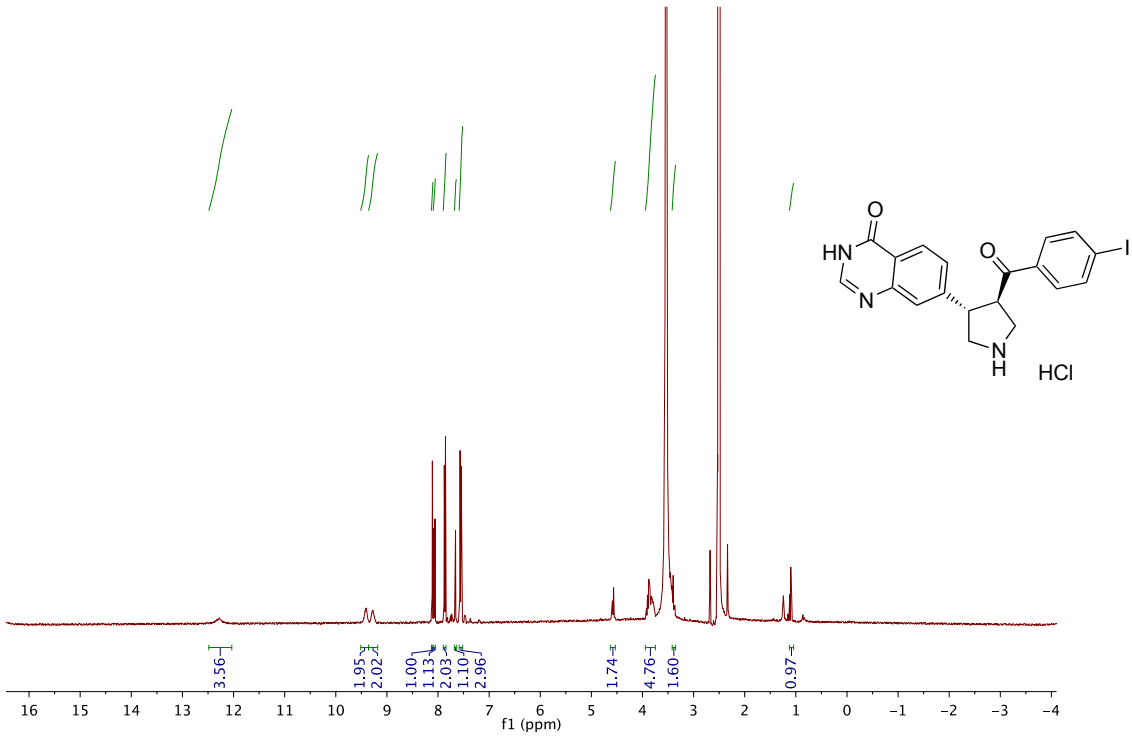


**Figure S37**. $^{1}$H NMR spectrum of (+)-**1k** in $(CD_3)_2SO$, 600 MHz, 298 K.

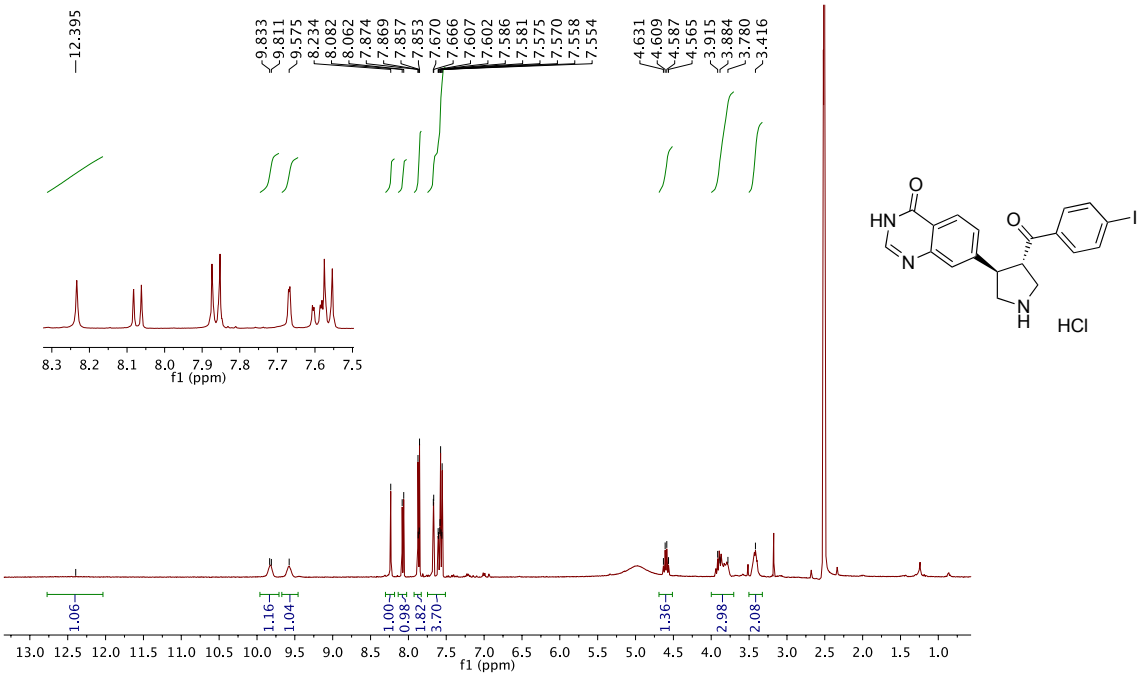


**Figure S38**. $^{1}$H NMR spectrum of (–)-**1k** in $(CD_3)_2SO$, 600 MHz, 298 K.

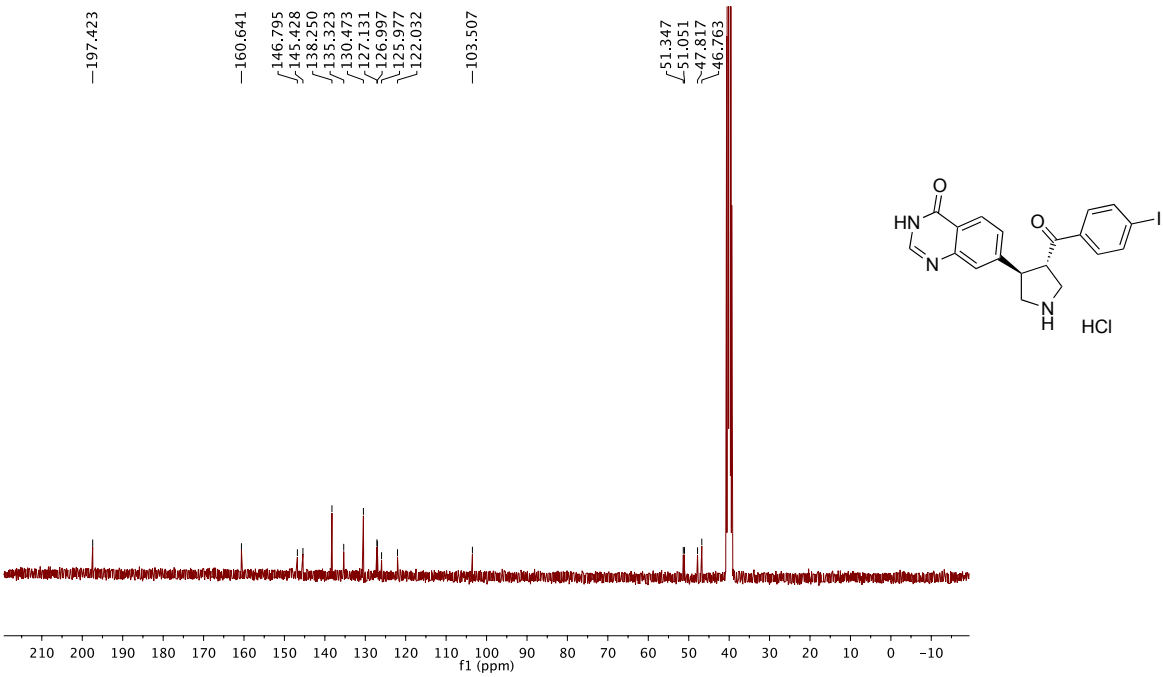


**Figure S39**. $^{13}$C NMR spectrum of (–)-**1k** in $(CD_3)_2SO$, 150 MHz, 298 K.

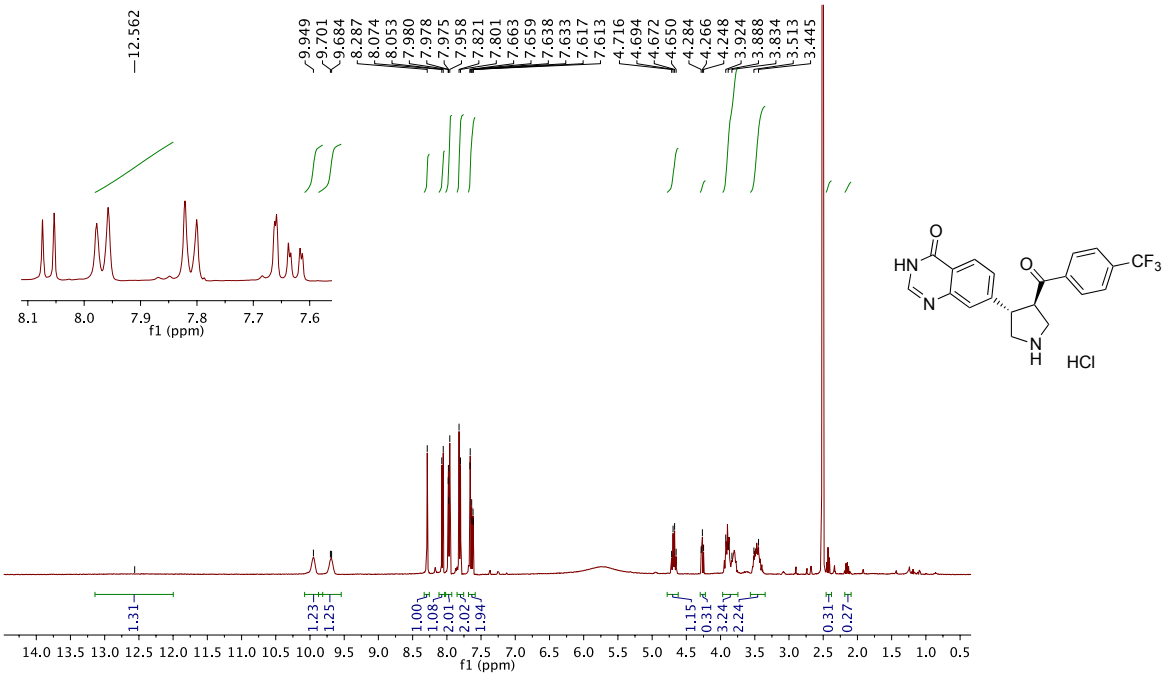


**Figure S40**. $^{1}$H NMR spectrum of (+)-**1l** in $(CD_3)_2SO$, 400 MHz, 298 K.

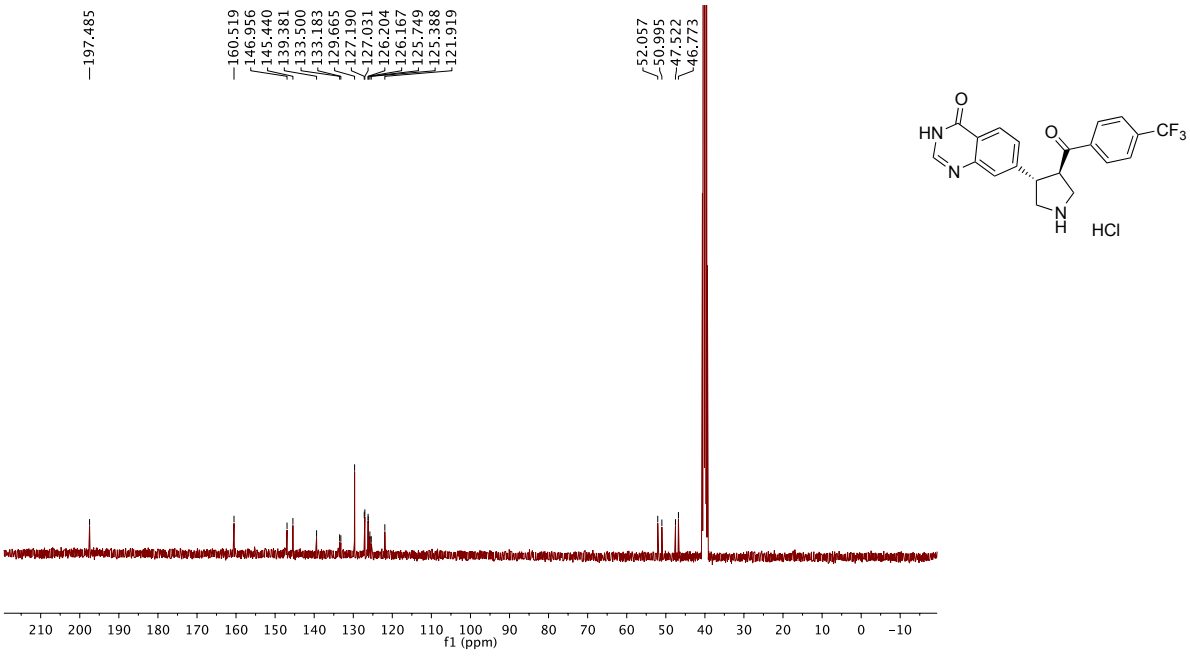


**Figure S41**. $^{13}$C NMR spectrum of (+)-**1l** in $(CD_3)_2SO$, 150 MHz, 298 K.

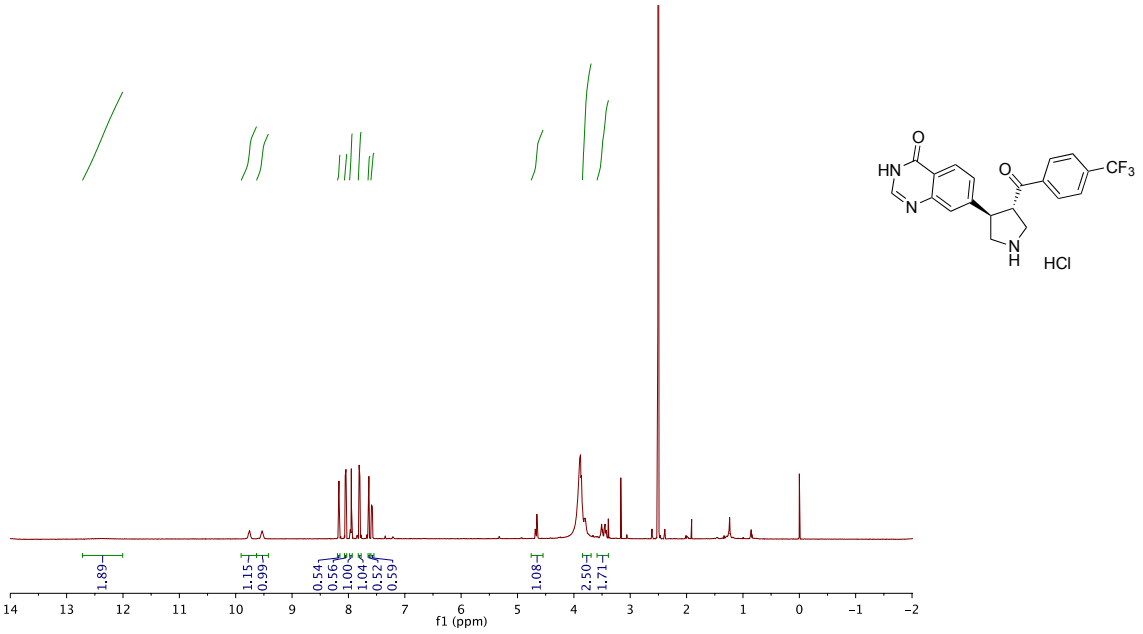


**Figure S42**. $^{1}$H NMR spectrum of (–)-**1l** in $(CD_3)_2SO$, 400 MHz, 298 K.

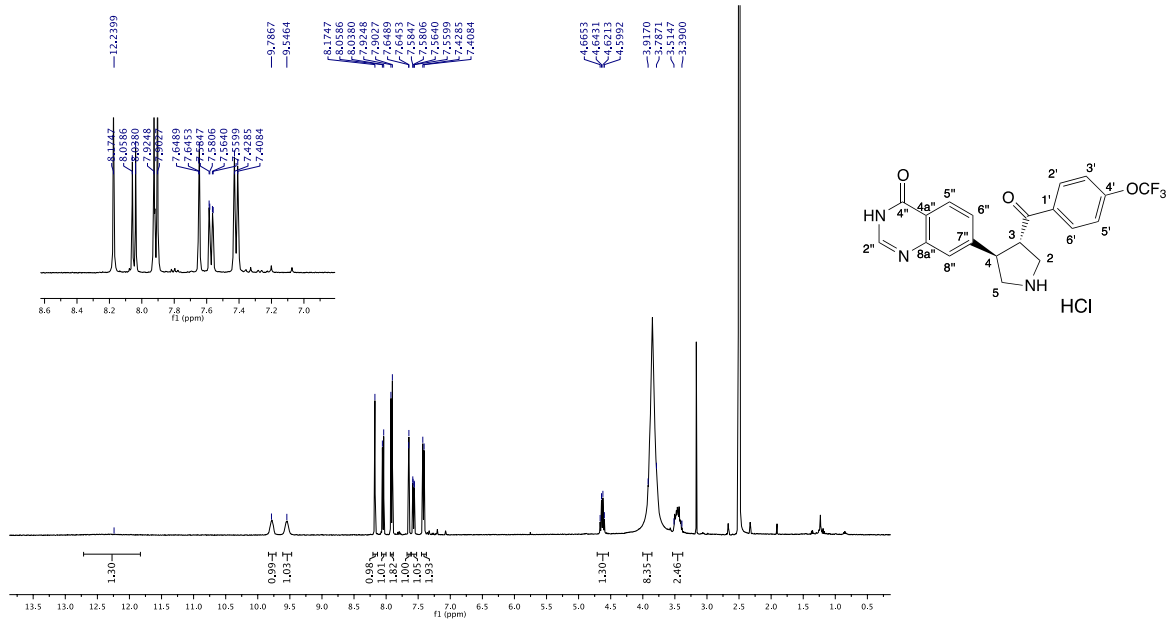


**Figure S43**. $^{1}$H NMR spectrum of (–)-**1m** in $(CD_3)_2SO$, 600 MHz, 298 K.

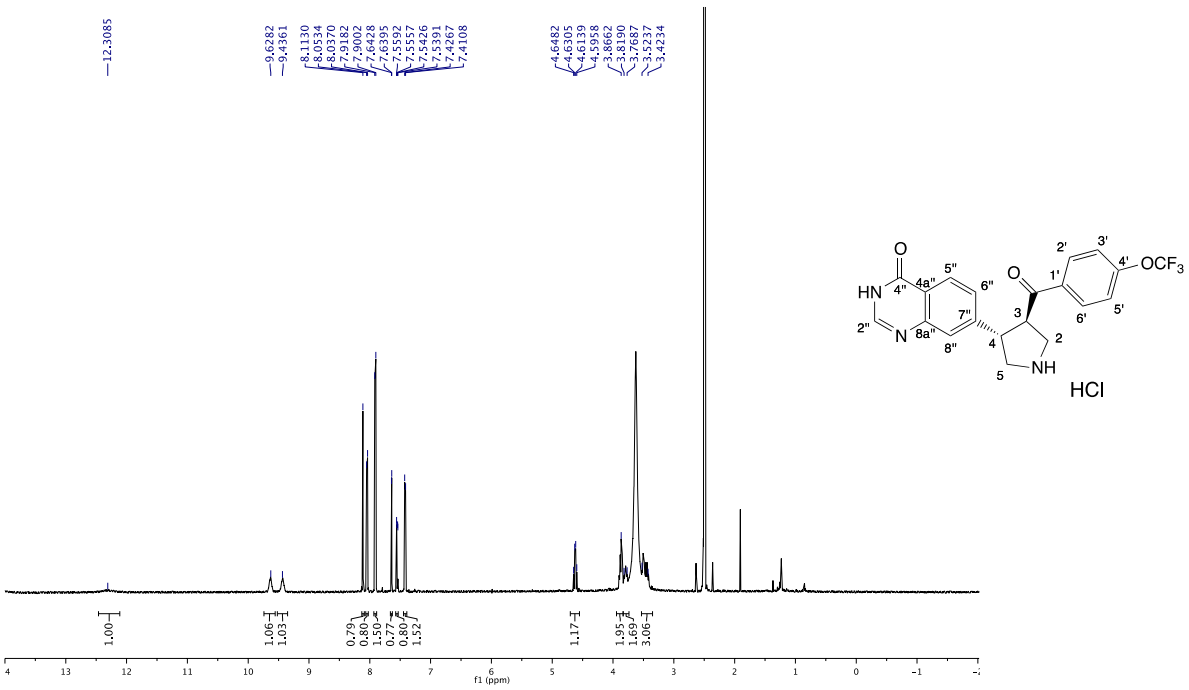


**Figure S44**. $^{1}$H NMR spectrum of (+)-**1m** in $(CD_3)_2SO$, 600 MHz, 298 K.

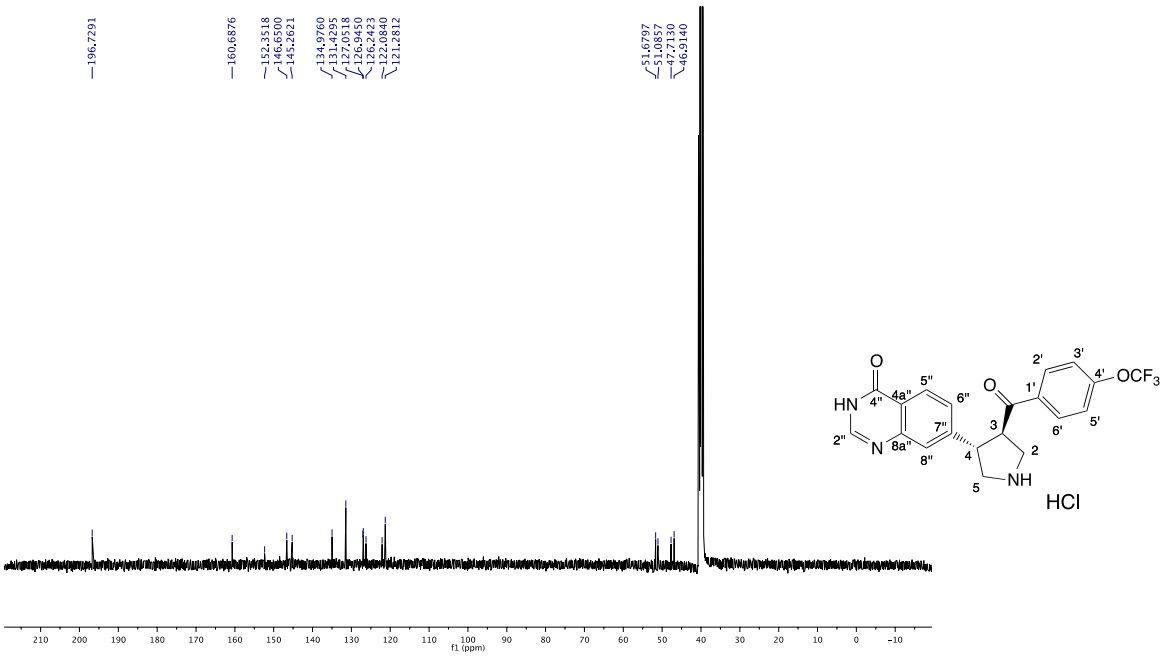


**Figure S45**. $^{1}$H NMR spectrum of (+)-**1m** in $(CD_3)_2SO$, 150 MHz, 298 K.

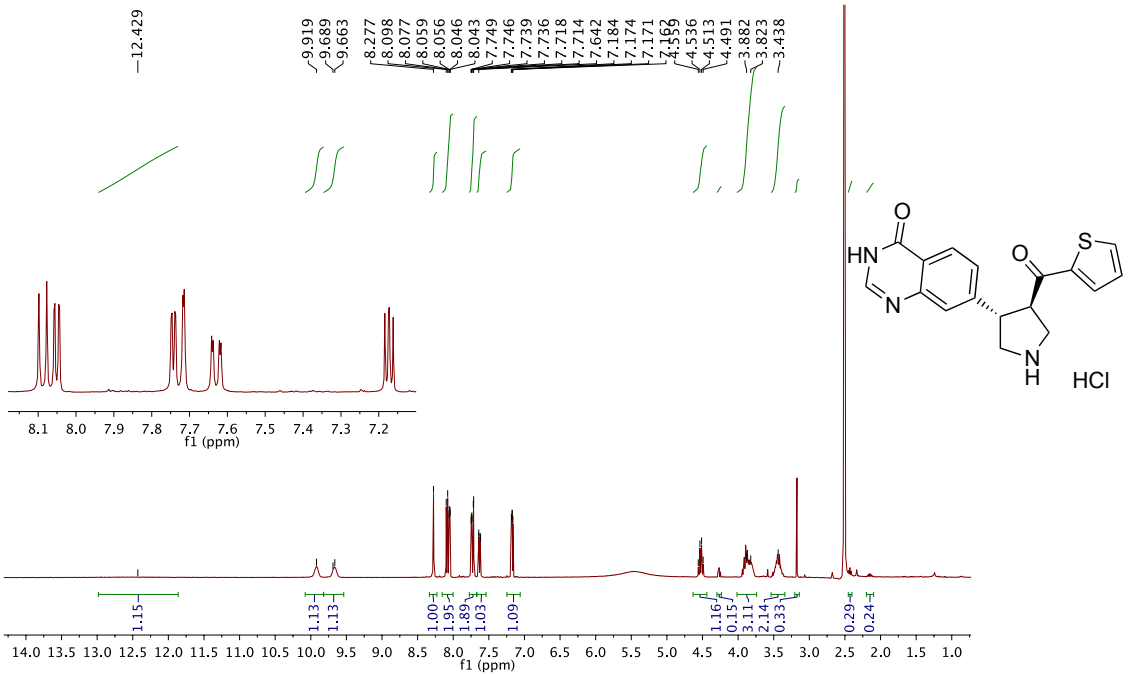


**Figure S46**. $^{1}$H NMR spectrum of (+)-**1n** in $(CD_3)_2SO$, 400 MHz, 298 K.

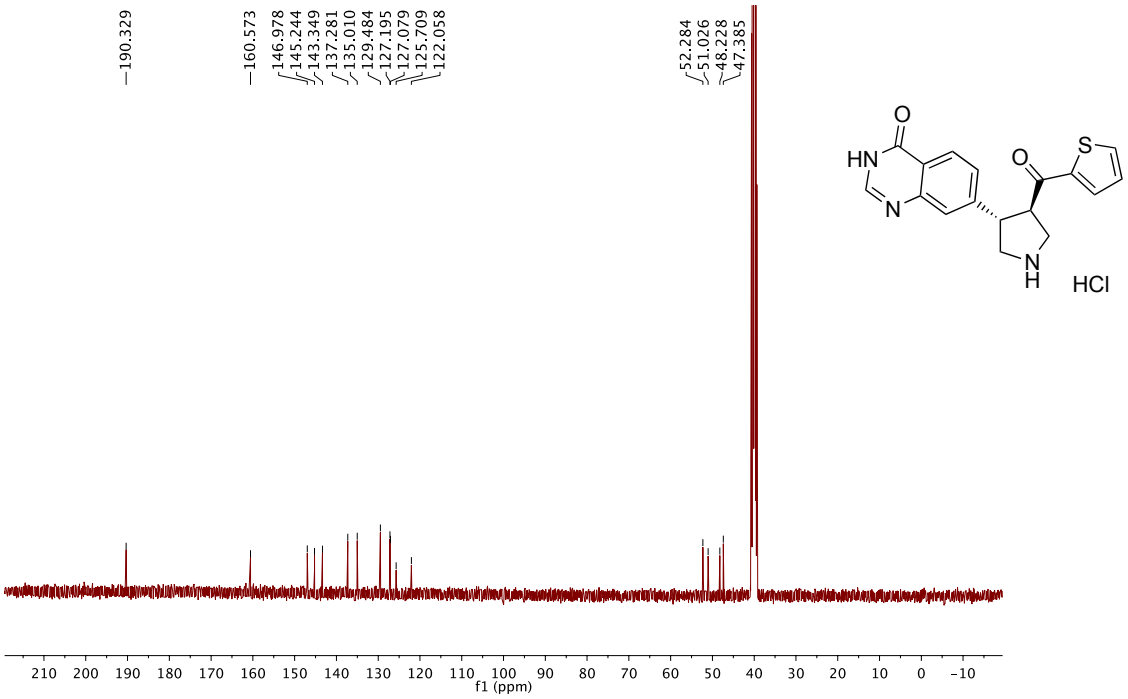


**Figure S47**. $^{13}$C NMR spectrum of (+)-**1n** in $(CD_3)_2SO$, 100 MHz, 298 K.

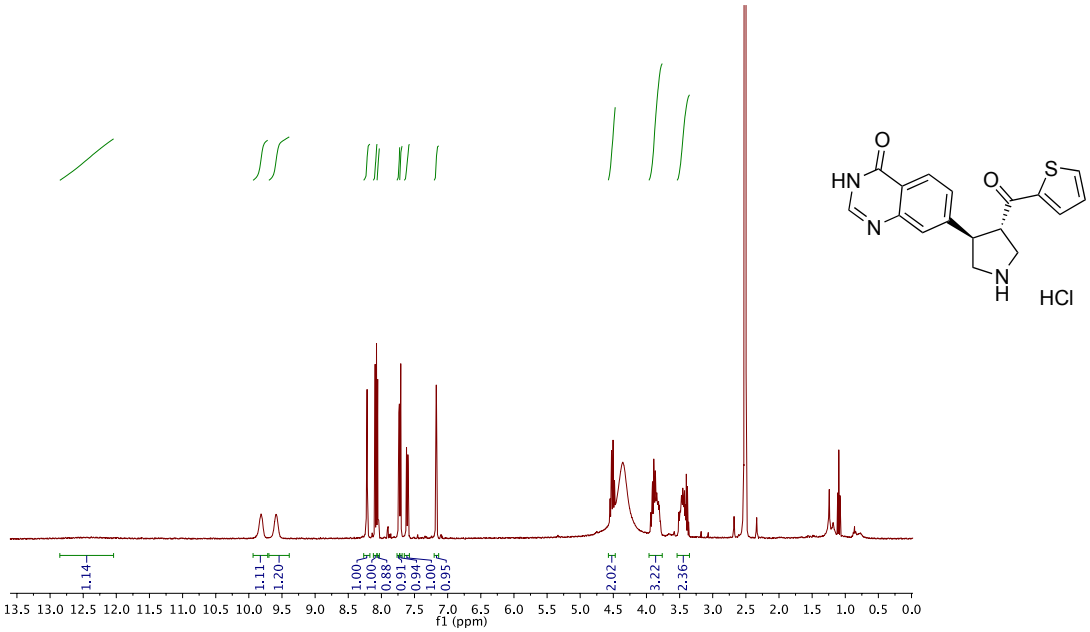


**Figure S48**. $^{1}$H NMR spectrum of (–)-**1n** in $(CD_3)_2SO$, 400 MHz, 298 K.

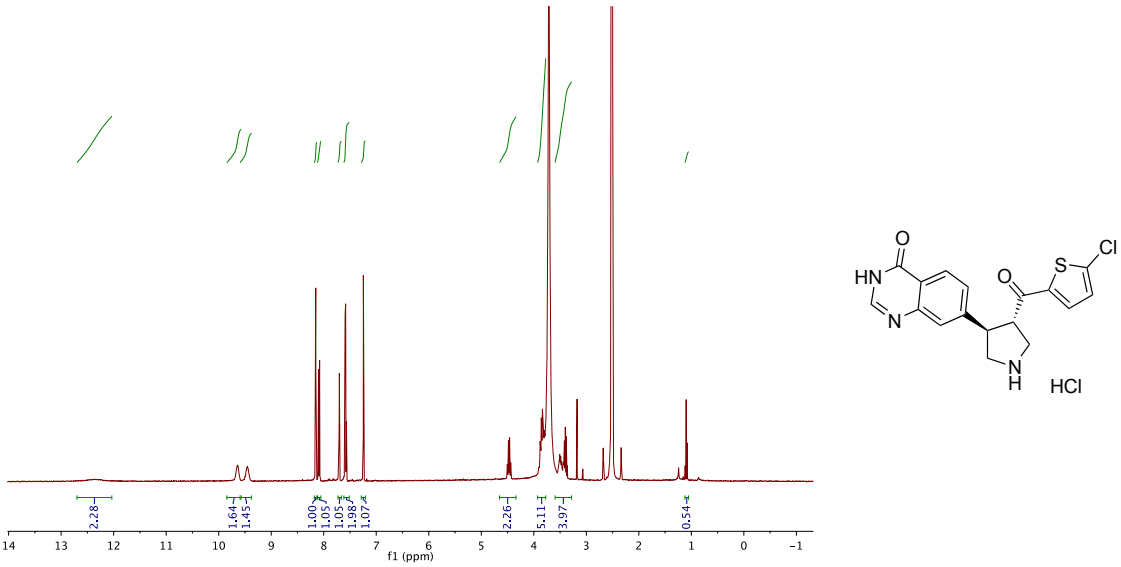


**Figure S49**. $^{1}$H NMR spectrum of (+)-**1o** in $(CD_3)_2SO$, 400 MHz, 298 K.

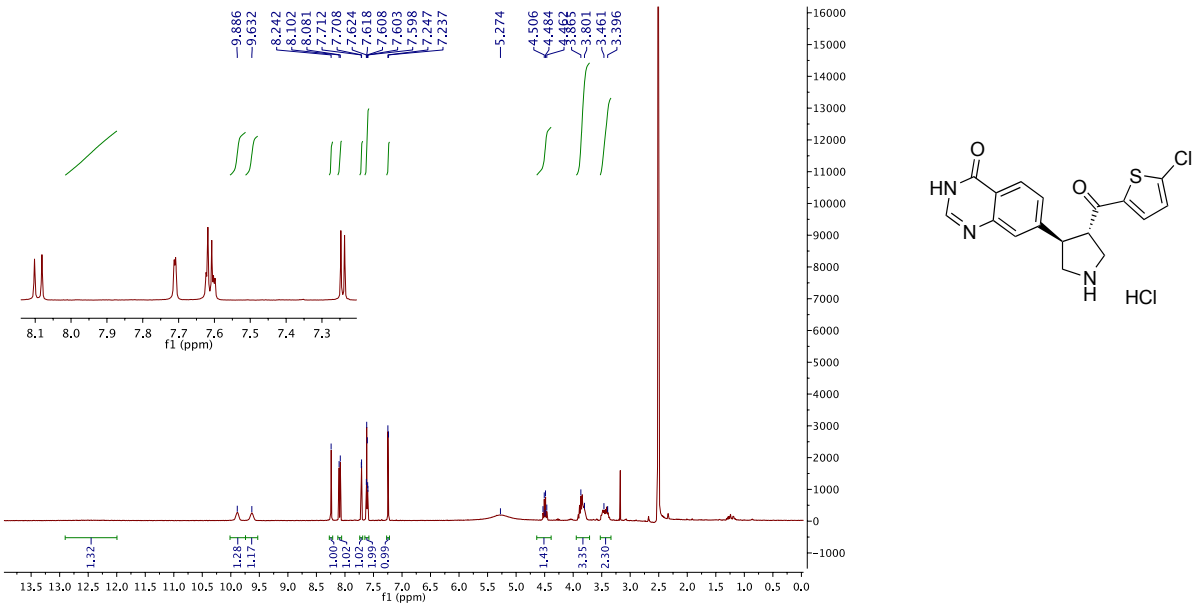


**Figure S50**. $^{1}$H NMR spectrum of (–)-**1o** in $(CD_3)_2SO$, 400 MHz, 298 K.

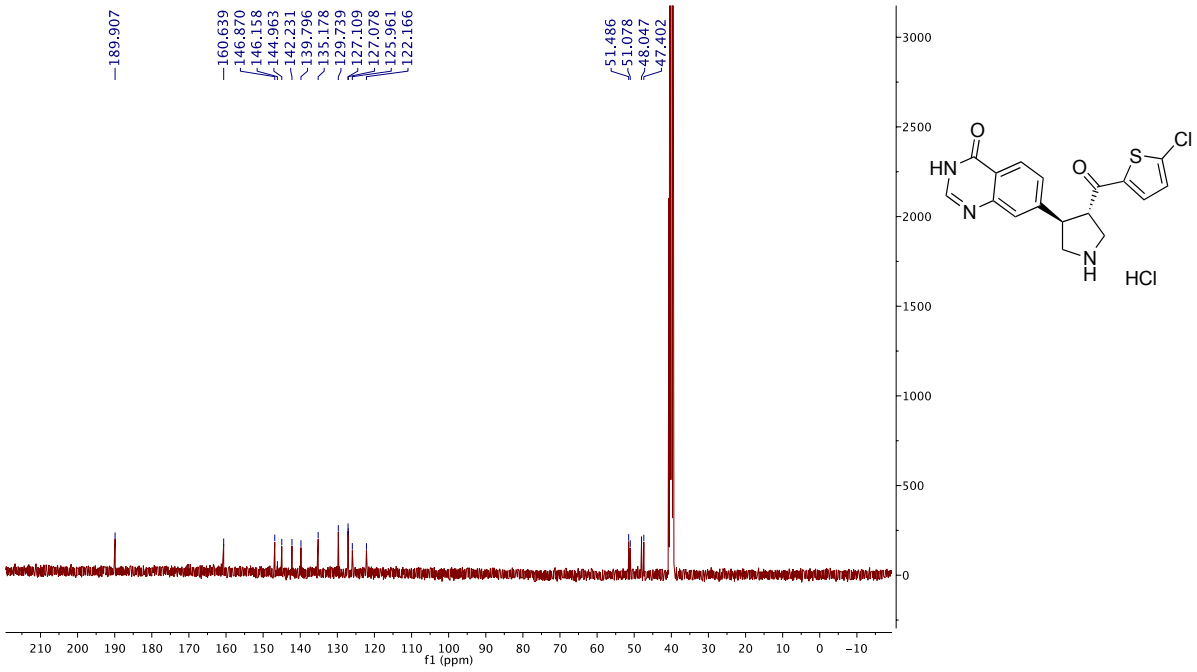


**Figure S51**. $^{13}$C NMR spectrum of (–)-**1o** in $(CD_3)_2SO$, 100 MHz, 298 K.

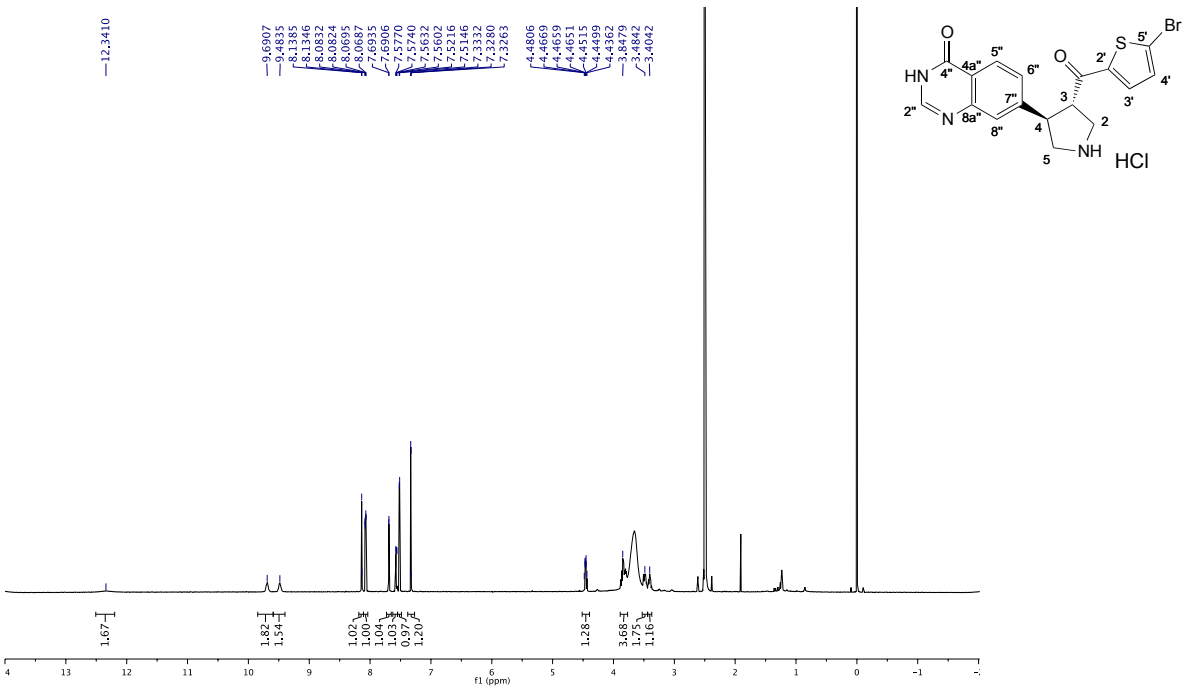


**Figure S52**. $^{1}$H NMR spectrum of (+)-**1p** in $(CD_3)_2SO$, 600 MHz, 298 K.

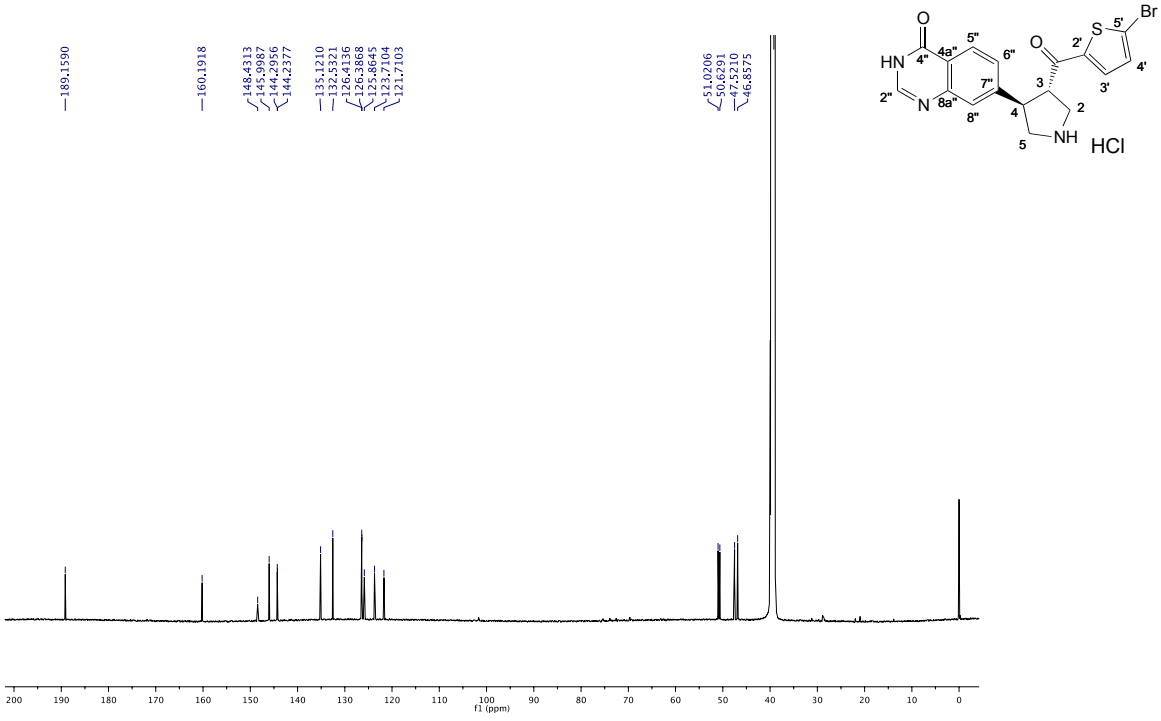


**Figure S53**. $^{13}$C NMR spectrum of (+)-**1p** in $(CD_3)_2SO$, 150 MHz, 298 K.

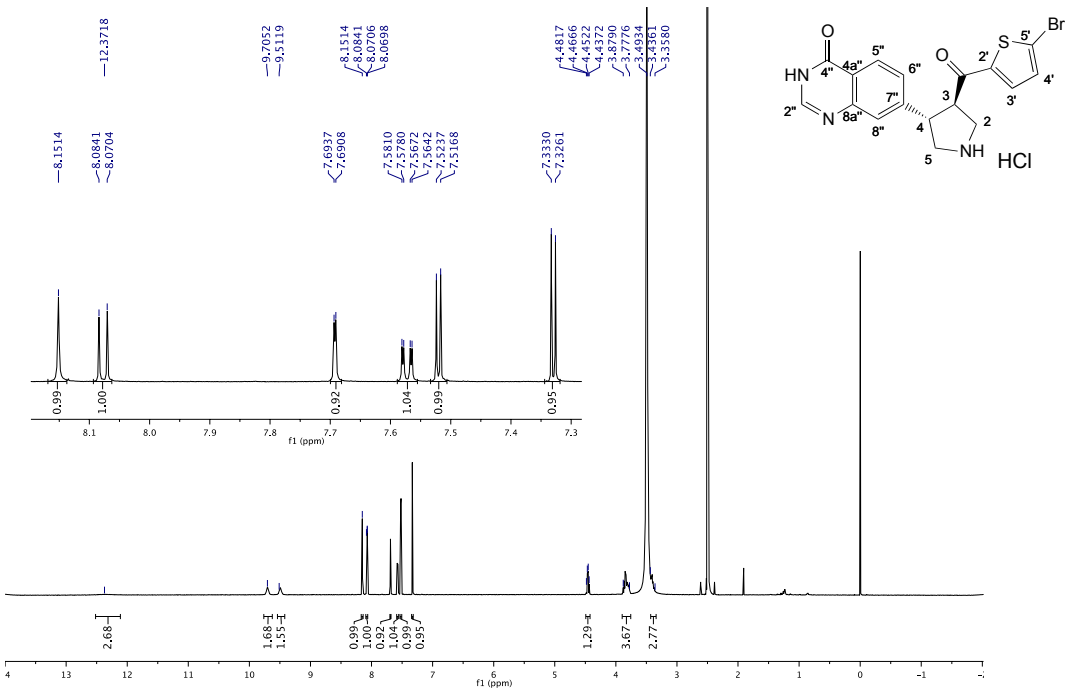


**Figure S54**. $^{1}$H NMR spectrum of (–)-**1p** in $(CD_3)_2SO$, 600 MHz, 298 K.

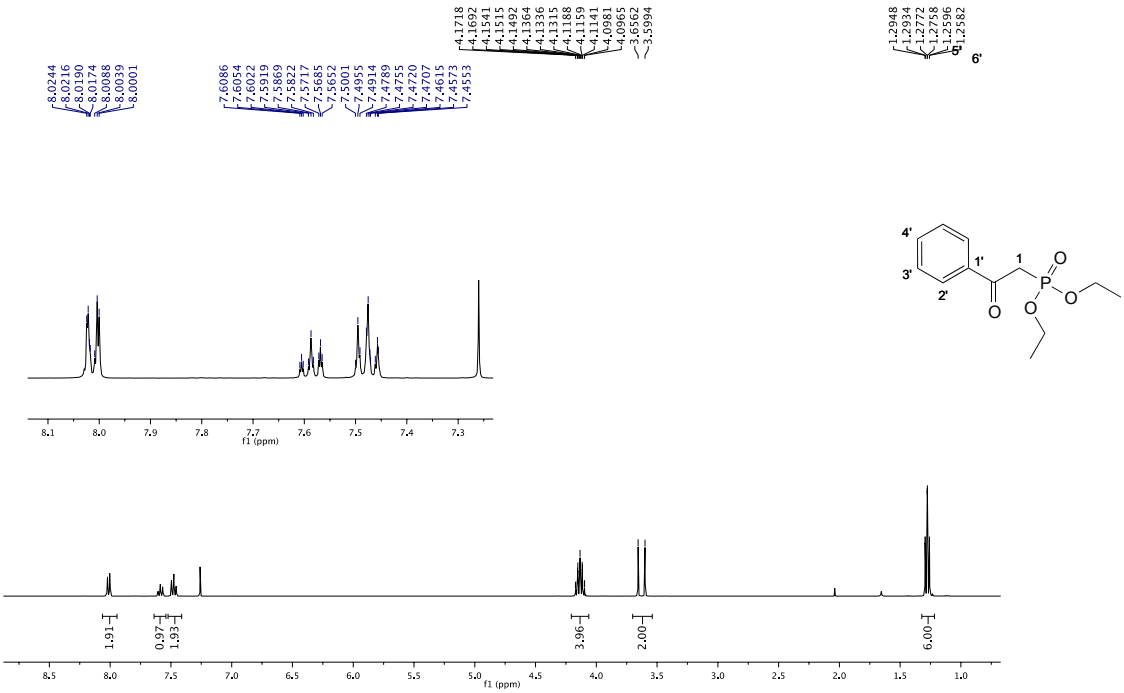

**Figure S55**. $^{1}H$ NMR spectrum of **4a** in $CDCl_3$, 400 MHz, 298 K.

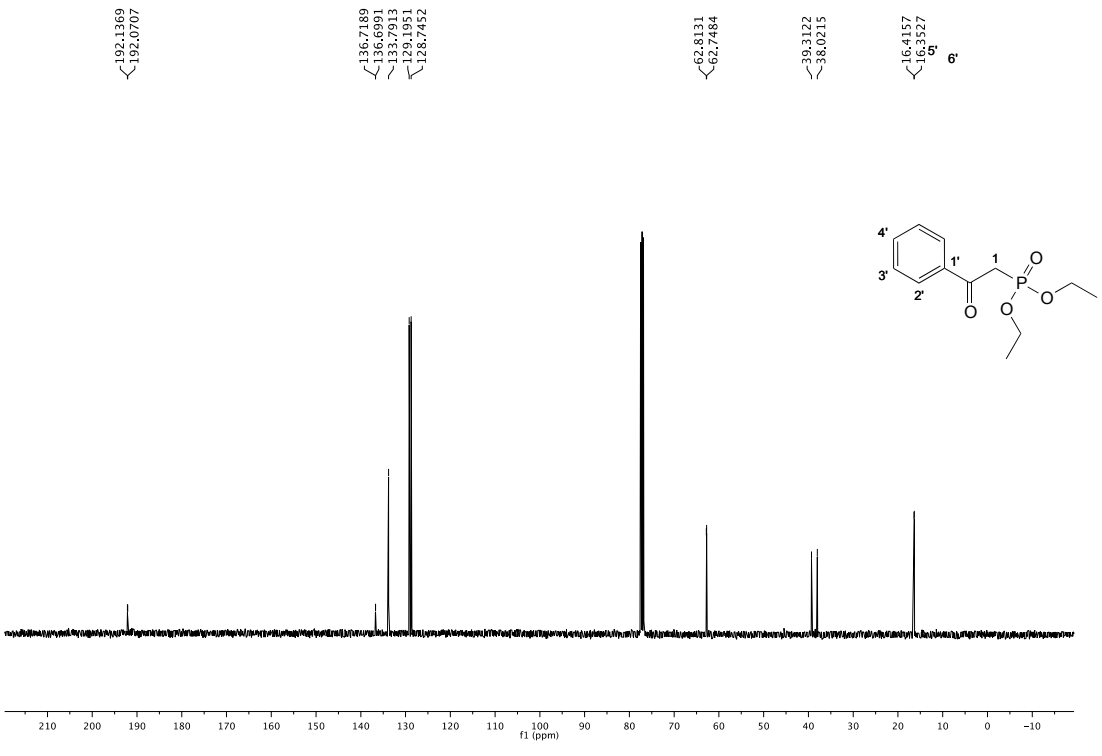

**Figure S56**. $^{13}C$ NMR spectrum of **4a** in $CDCl_3$, 100 MHz, 298 K.

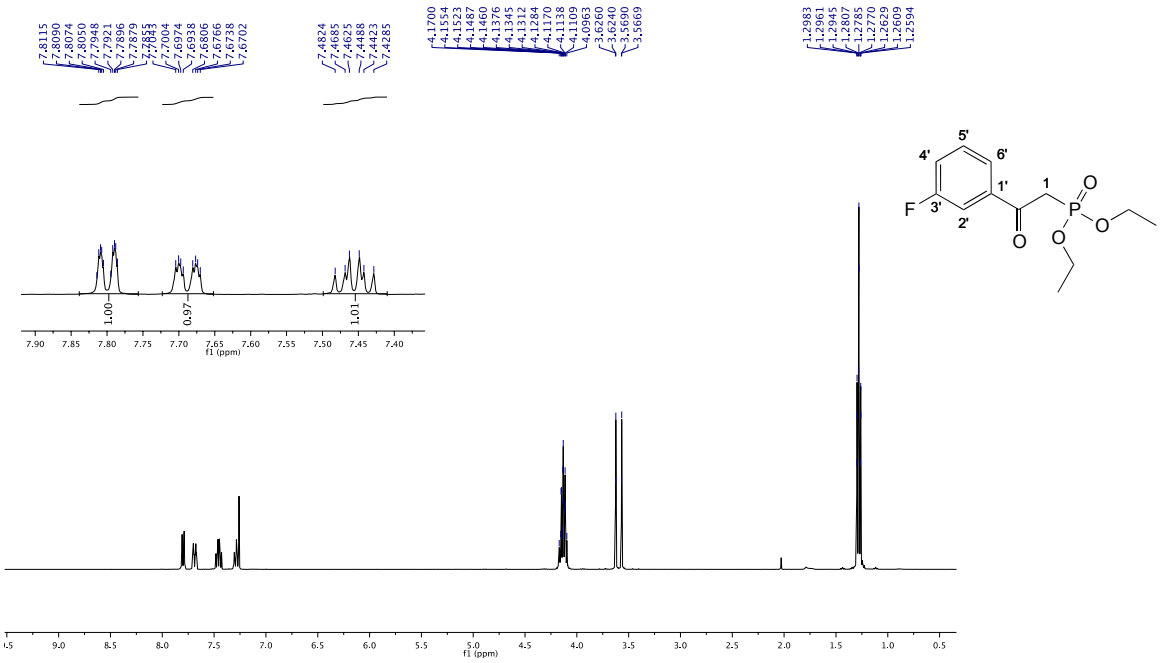

**Figure S57**. $^{1}$H NMR spectrum of **4b** in $CDCl_3$, 400 MHz, 298 K.

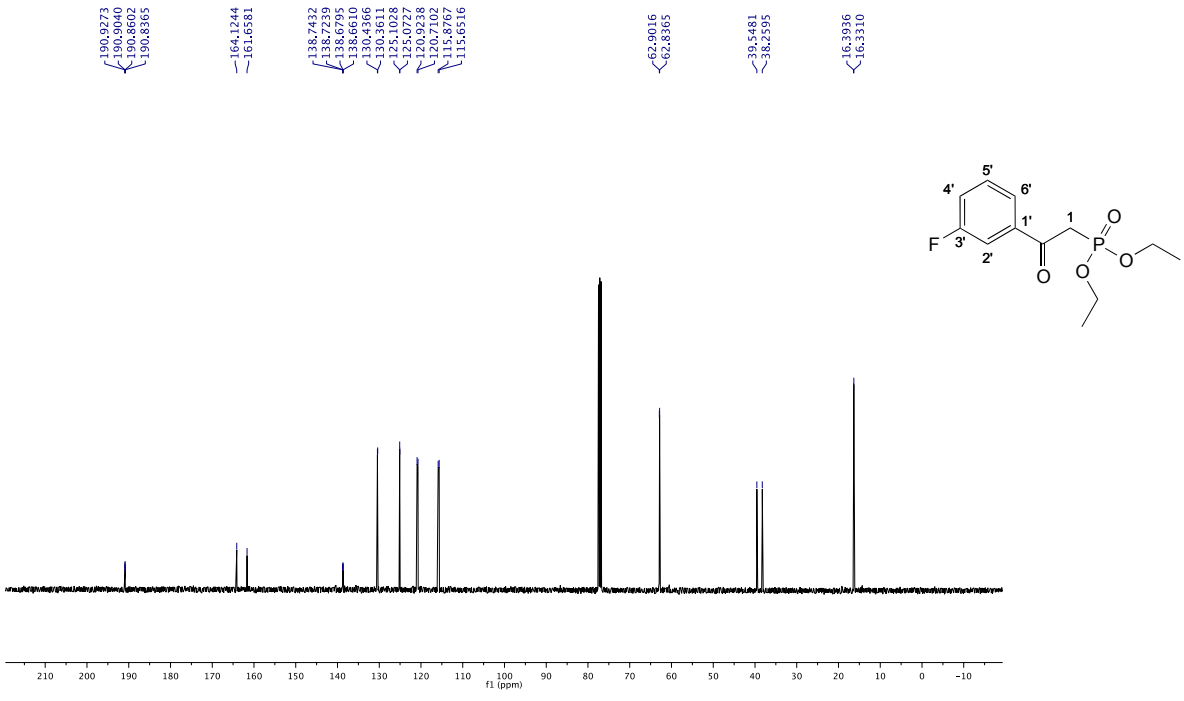

**Figure S58**. $^{13}$C NMR spectrum of **4b** in $CDCl_3$, 100 MHz, 298 K.

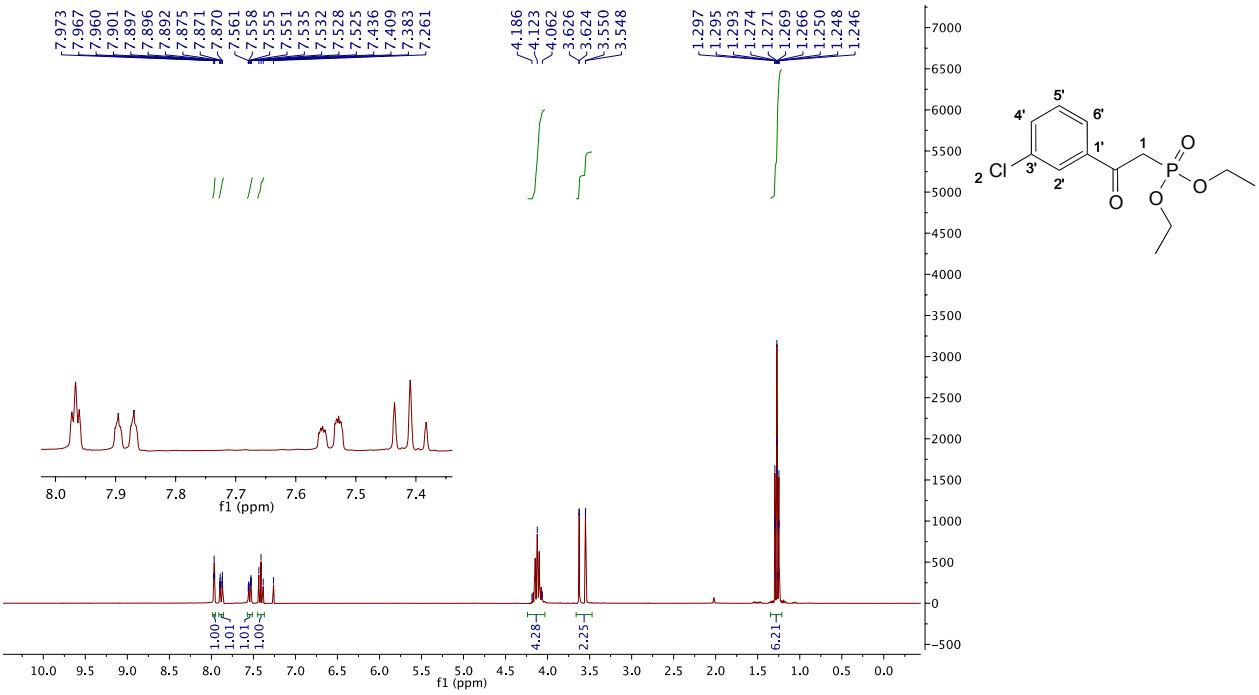

**Figure S59**. $^{1}$H NMR spectrum of **4c** in $CDCl_3$, 300 MHz, 298 K.

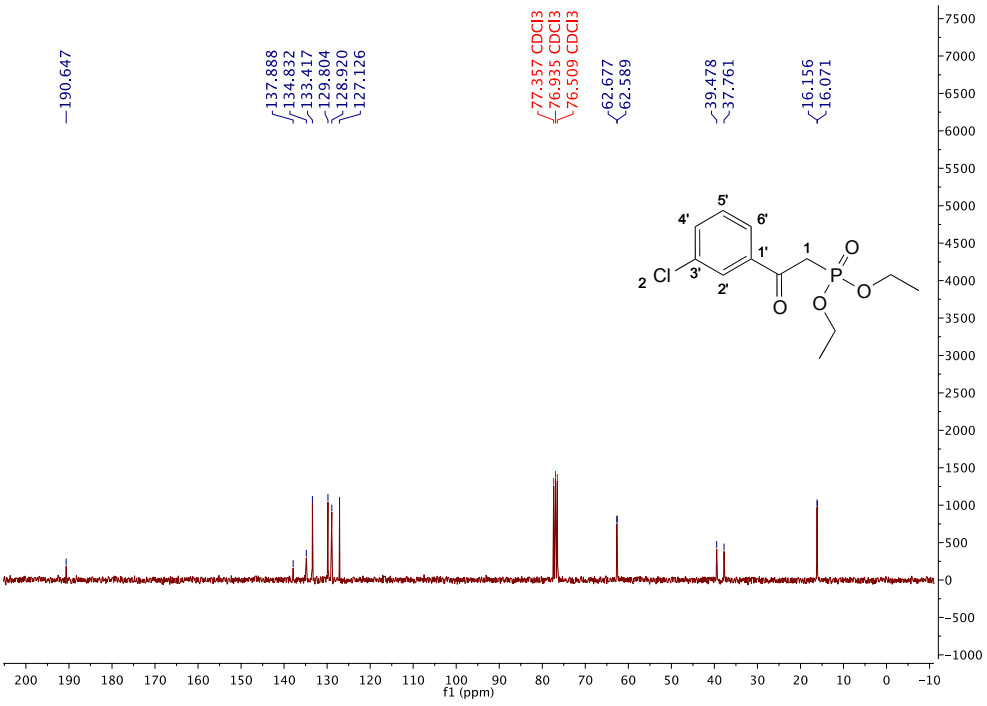

**Figure S60**. $^{13}$C NMR spectrum of **4c** in $CDCl_3$, 75 MHz, 298 K.

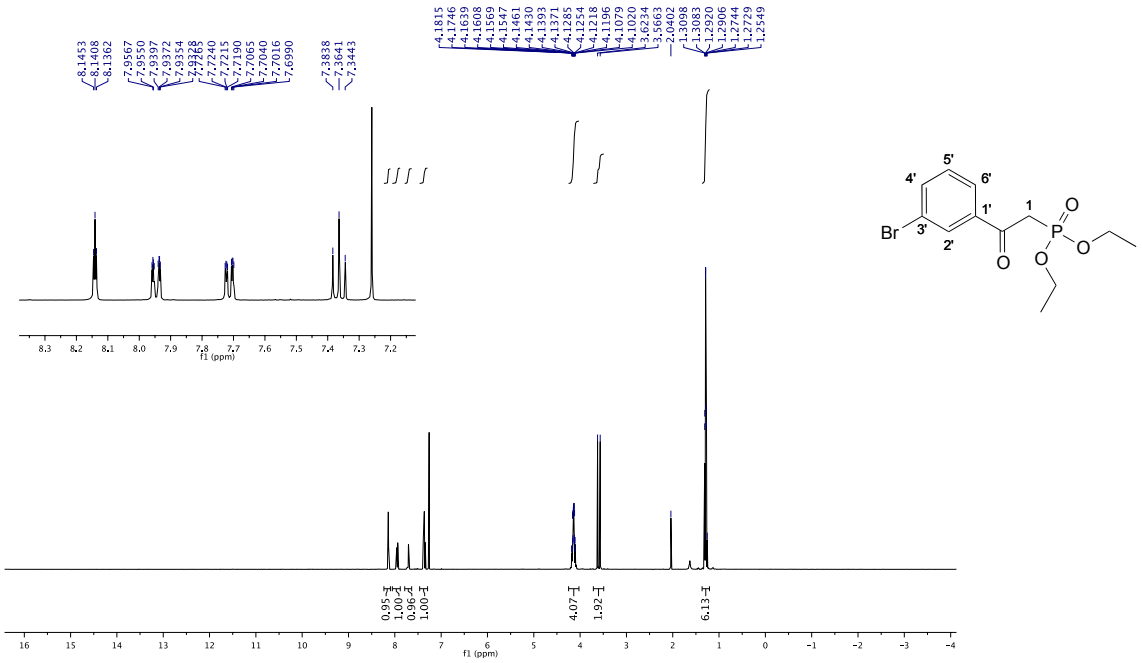

**Figure S61**. $^{1}$H NMR spectrum of **4d** in $CDCl_3$, 400 MHz, 298 K.

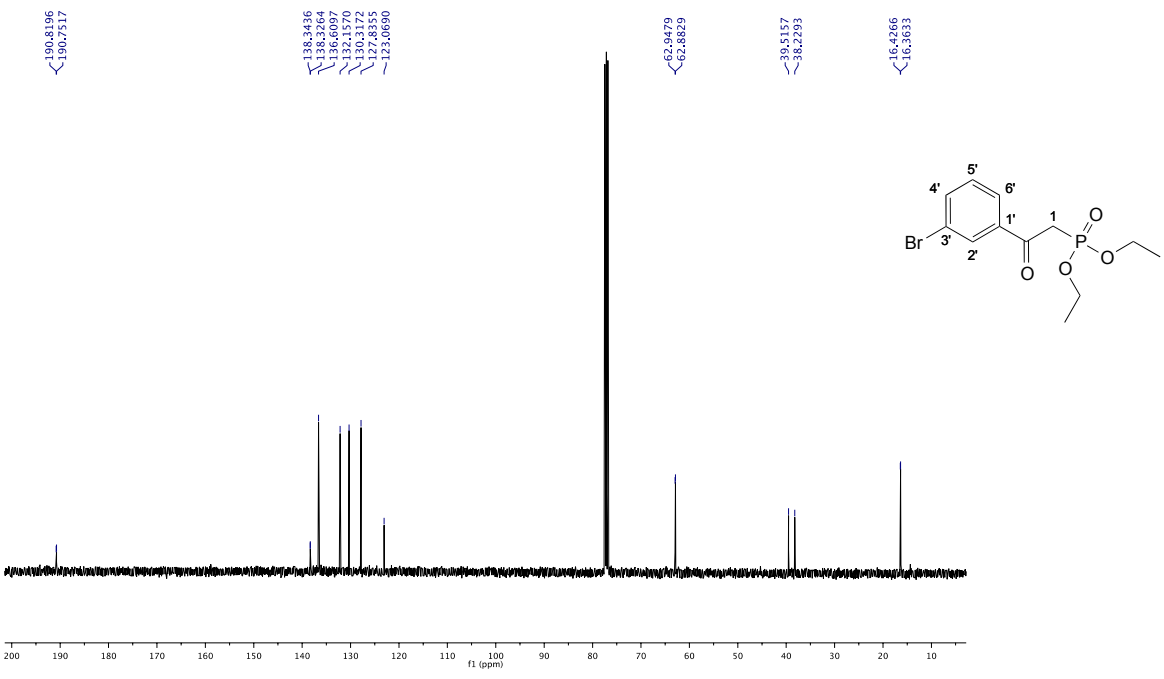

**Figure S62**. $^{13}$C NMR spectrum of **4d** in $CDCl_3$, 100 MHz, 298 K

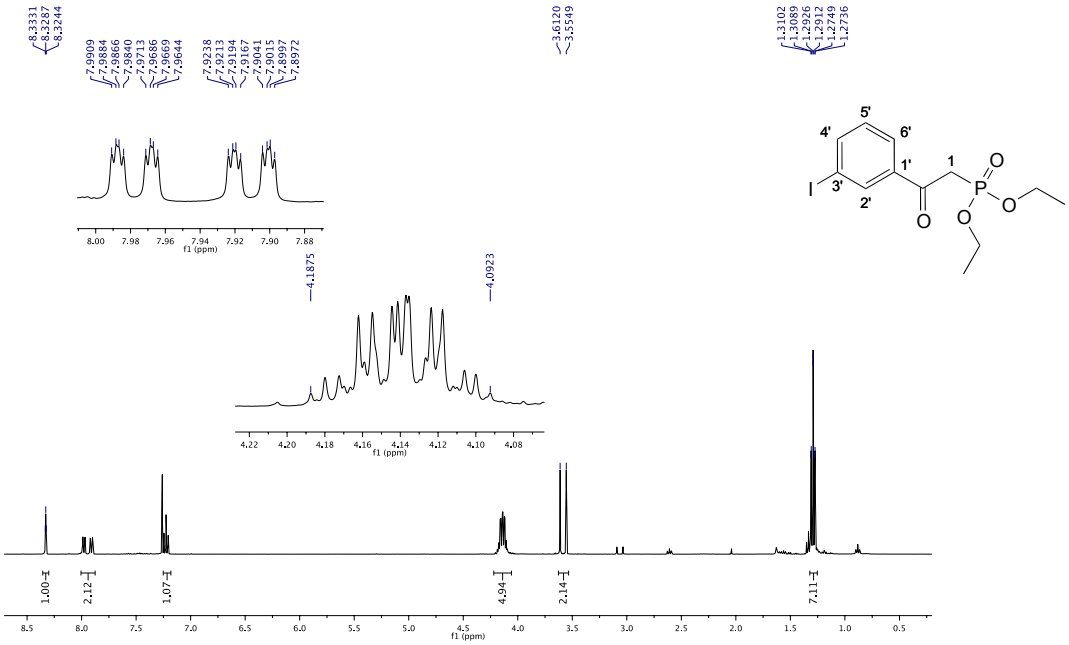

**Figure S63**. $^{1}$H NMR spectrum of **4e** in $CDCl_3$, 400 MHz, 298 K.

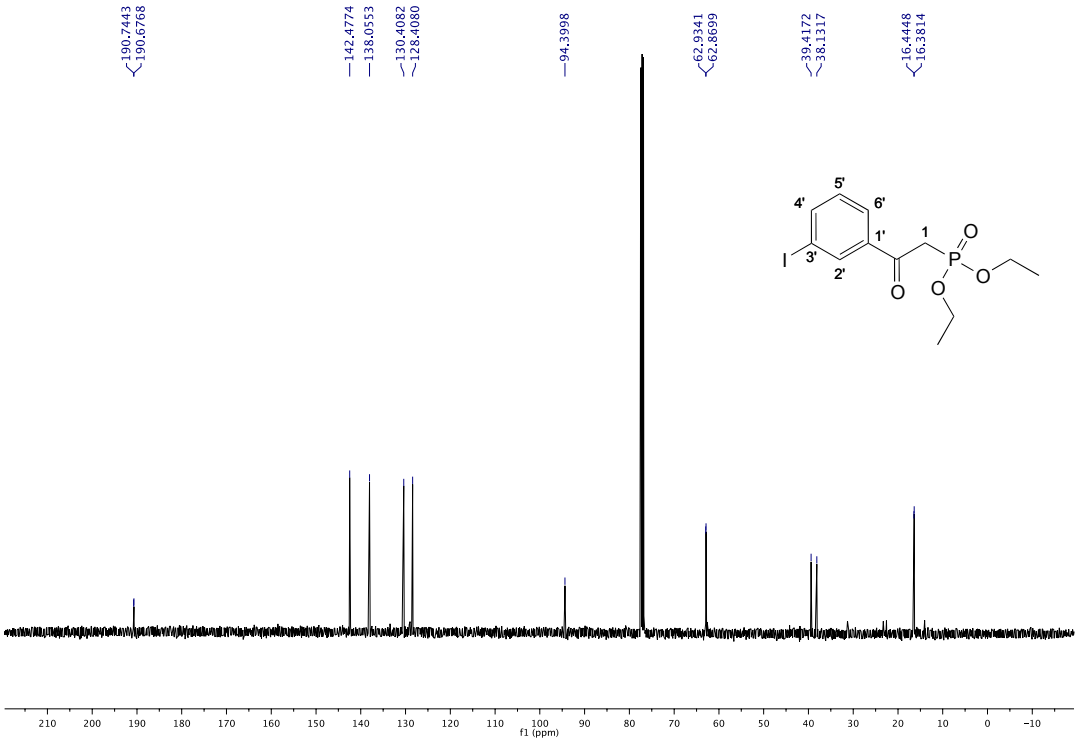

**Figure S64**. $^{13}$C NMR spectrum of **4e** in $CDCl_3$, 100 MHz, 298 K.

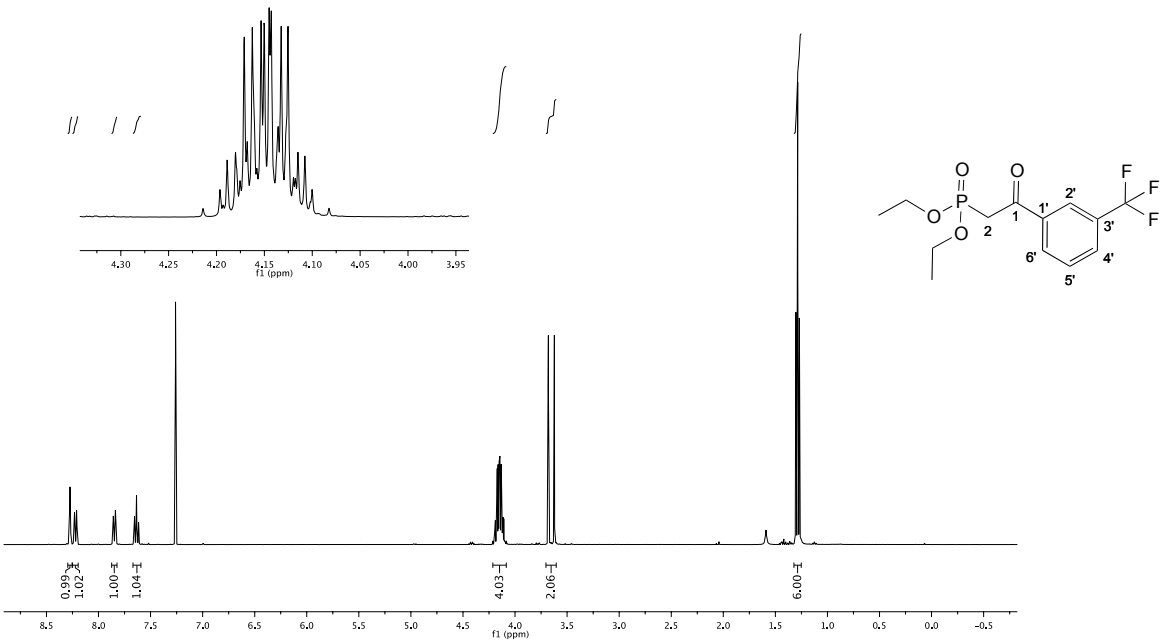


**Figure S65**. $^{1}H$ NMR spectrum of **4f** in $CDCl_3$, 400 MHz, 298 K.

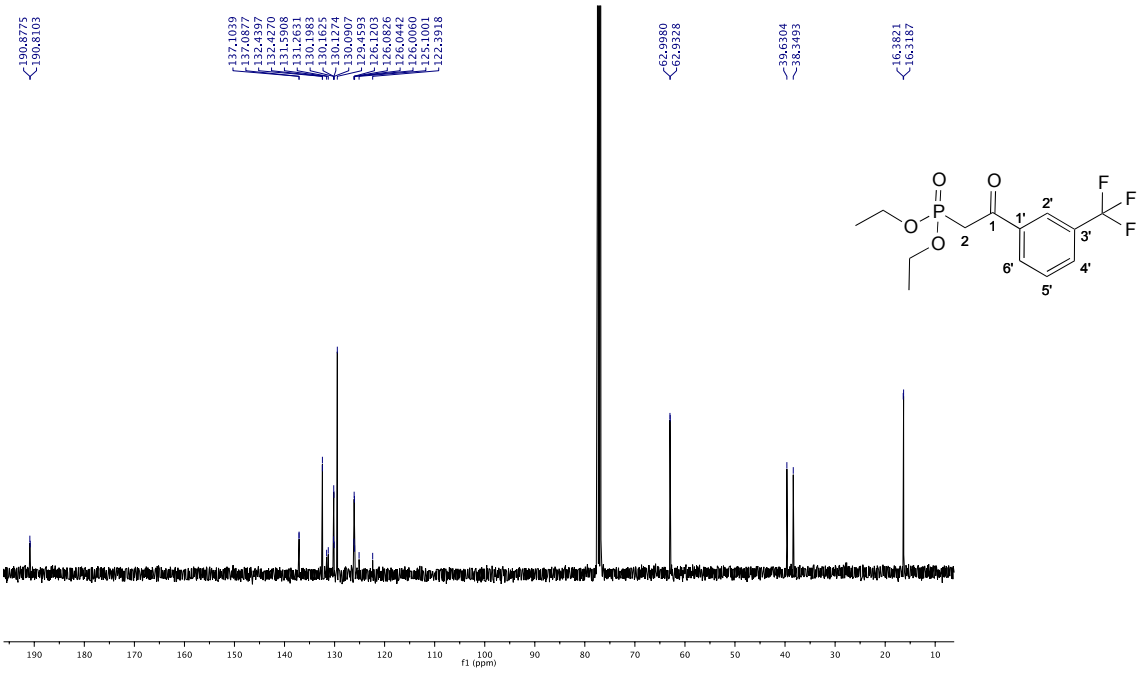


**Figure S66**. $^{13}C$ NMR spectrum of **4f** in $CDCl_3$, 100 MHz, 298 K.

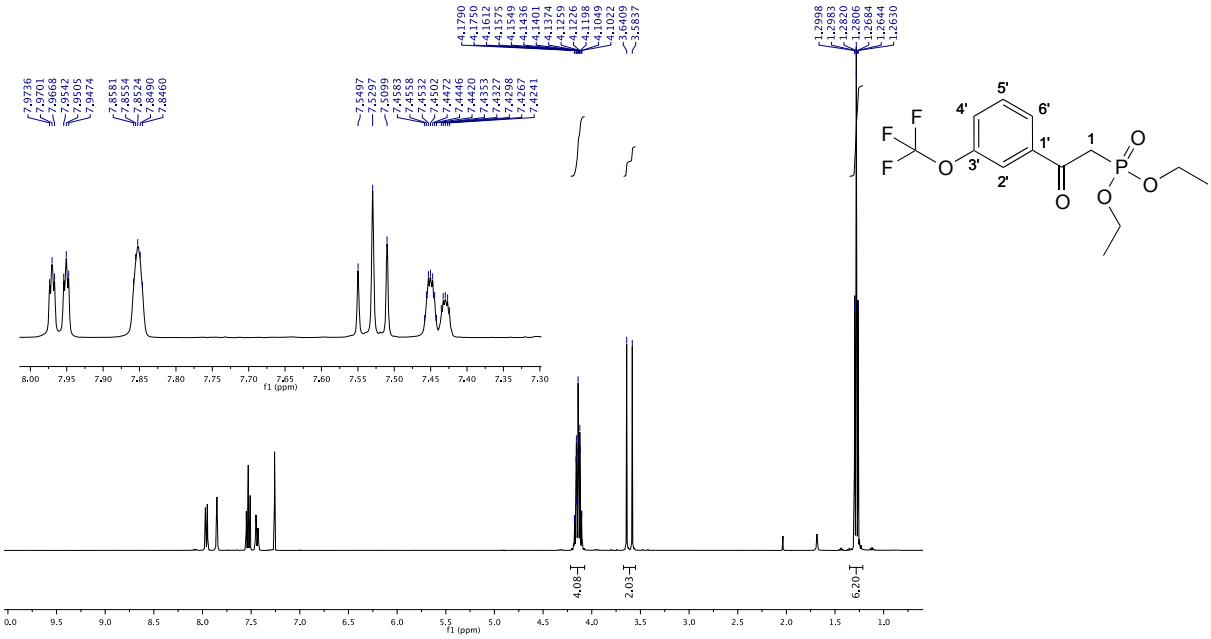

**Figure S67**. $^{1}$H NMR spectrum of **4g** in $CDCl_3$, 400 MHz, 298 K.

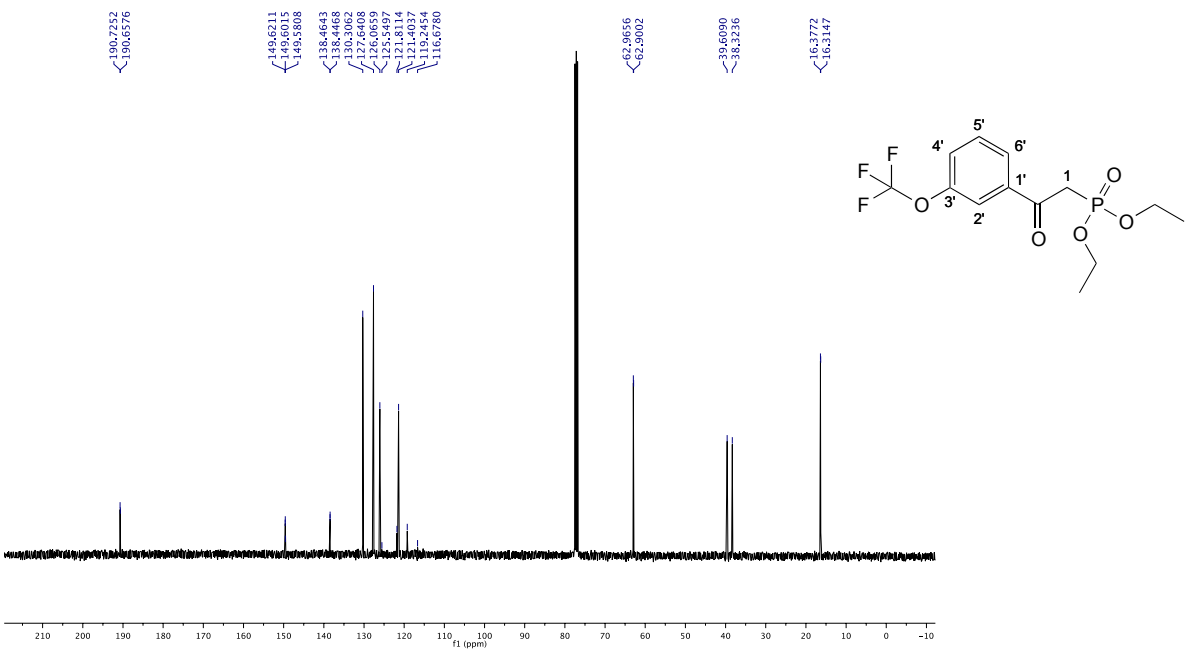

**Figure S68**. $^{13}$C NMR spectrum of **4g** in $CDCl_3$, 100 MHz, 298 K.

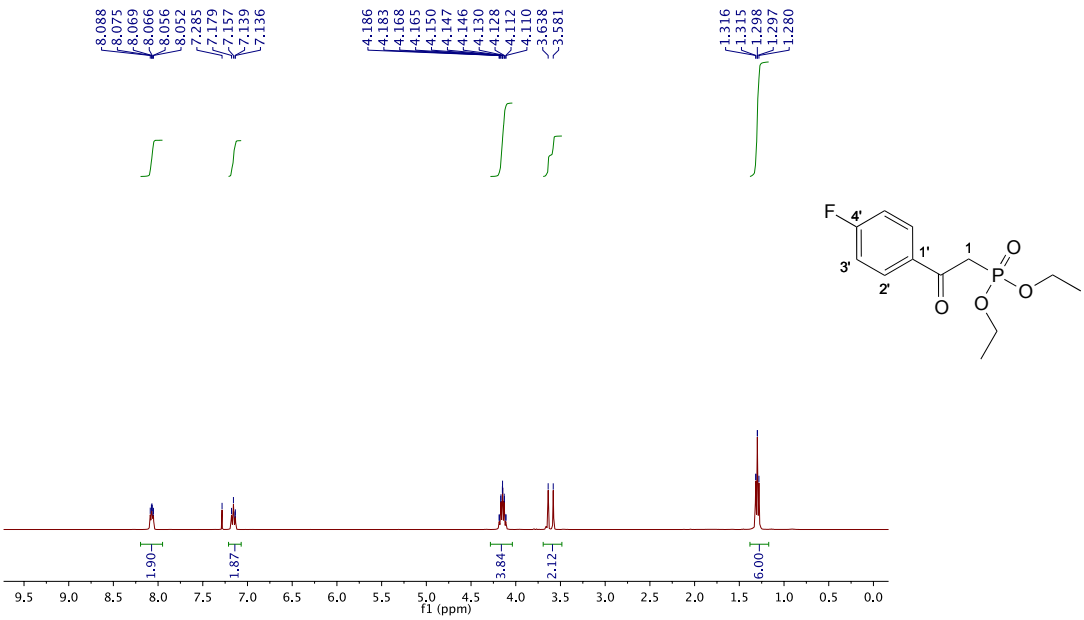


**Figure S69**. $^{1}$H NMR spectrum of **4h** in $CDCl_3$, 400 MHz, 298 K.

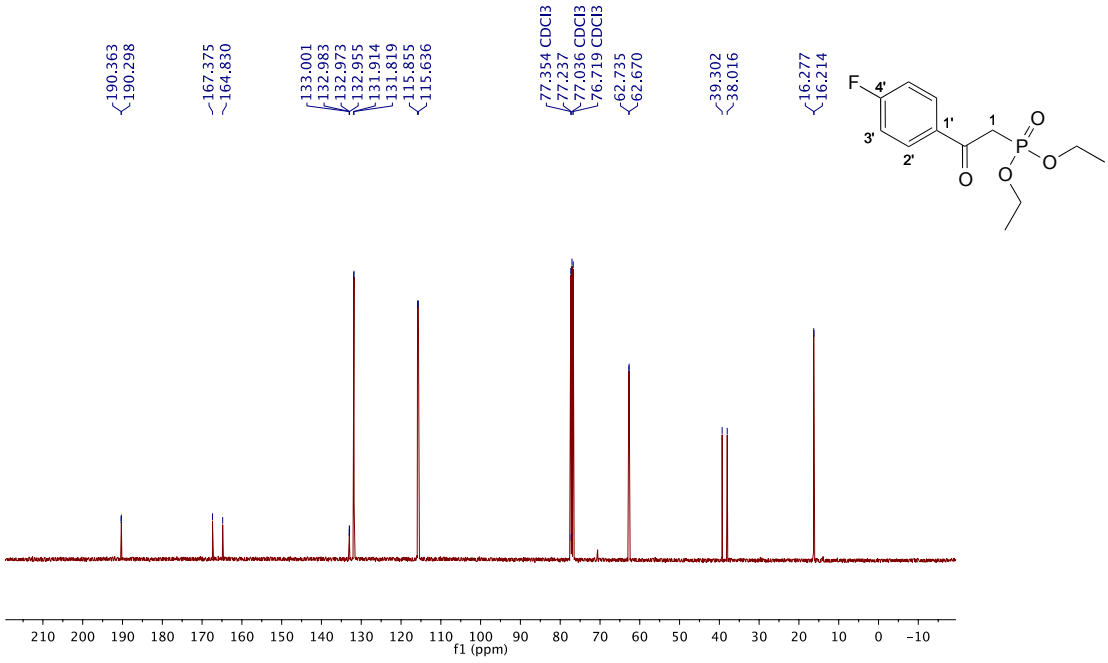


**Figure S70**. $^{13}$C NMR spectrum of **4h** in $CDCl_3$, 100 MHz, 298 K.

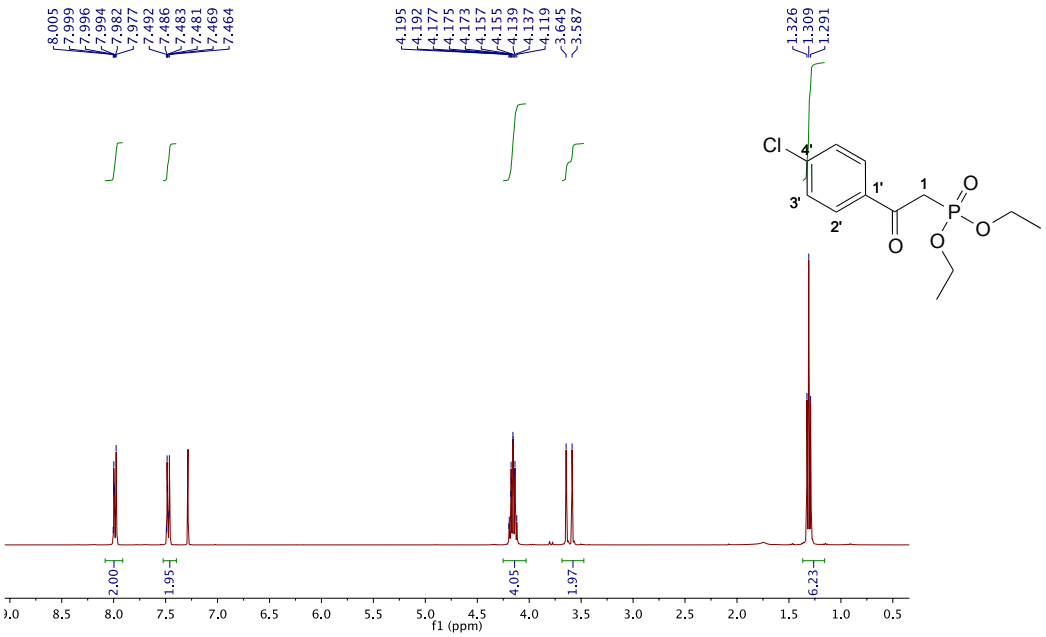


**Figure S71**. $^{1}$H NMR spectrum of **4i** in $CDCl_3$, 400 MHz, 298 K.

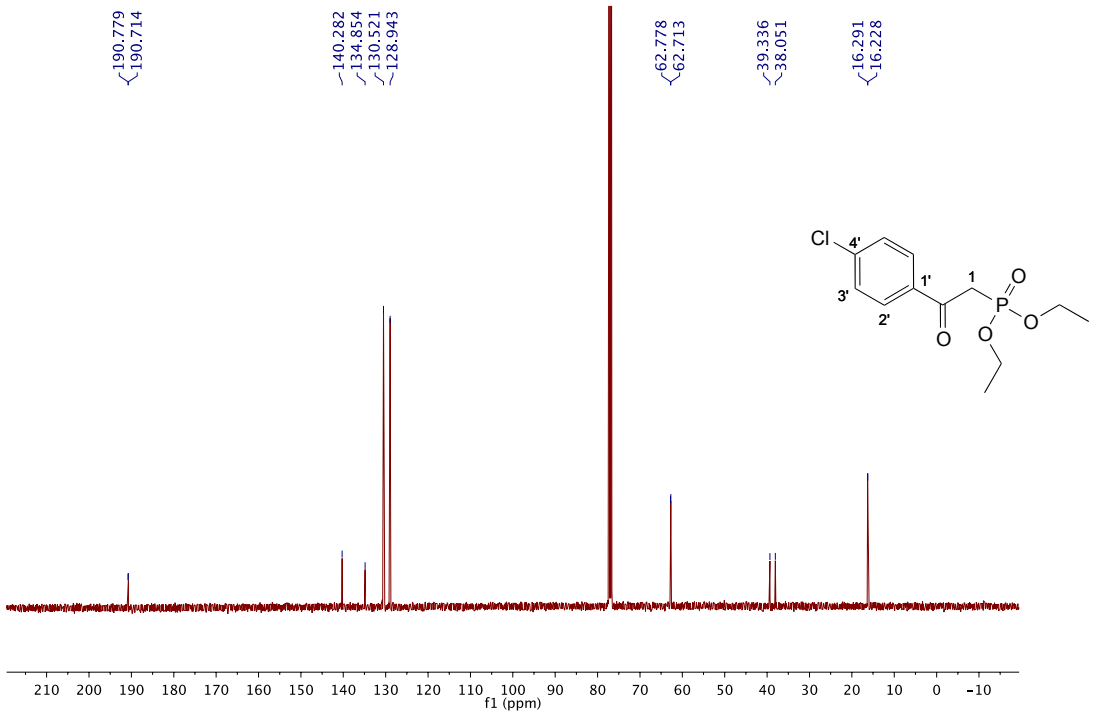


**Figure S72**. $^{13}$C NMR spectrum of **4i** in $CDCl_3$, 100 MHz, 298 K.

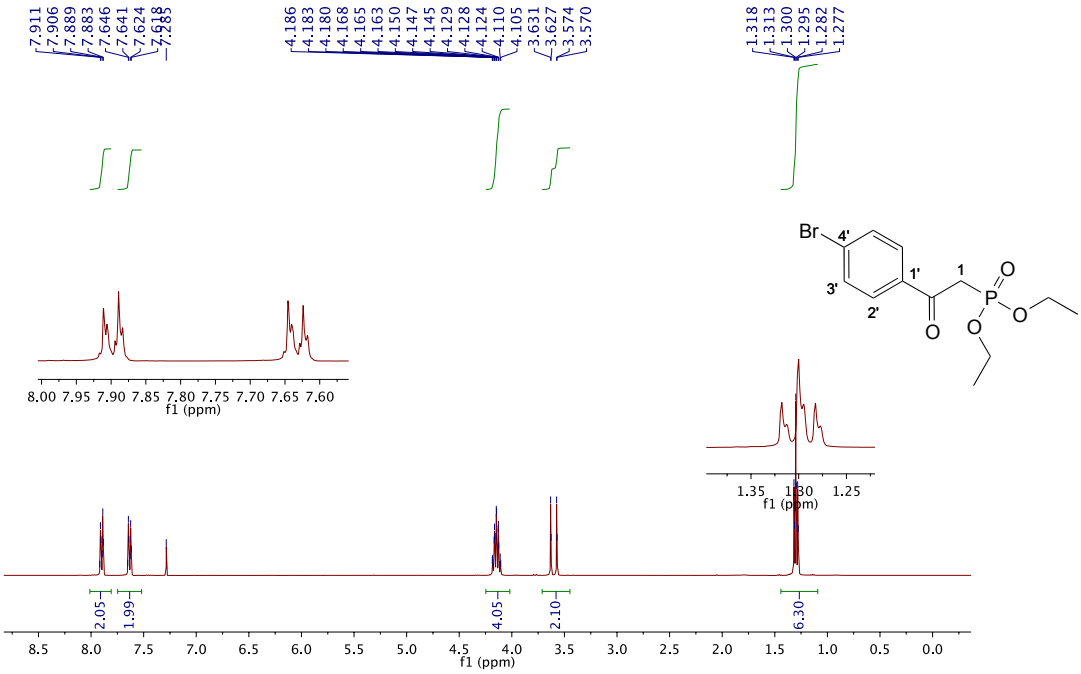


**Figure S73**. $^{1}$H NMR spectrum of **4j** in $CDCl_3$, 400 MHz, 298 K.

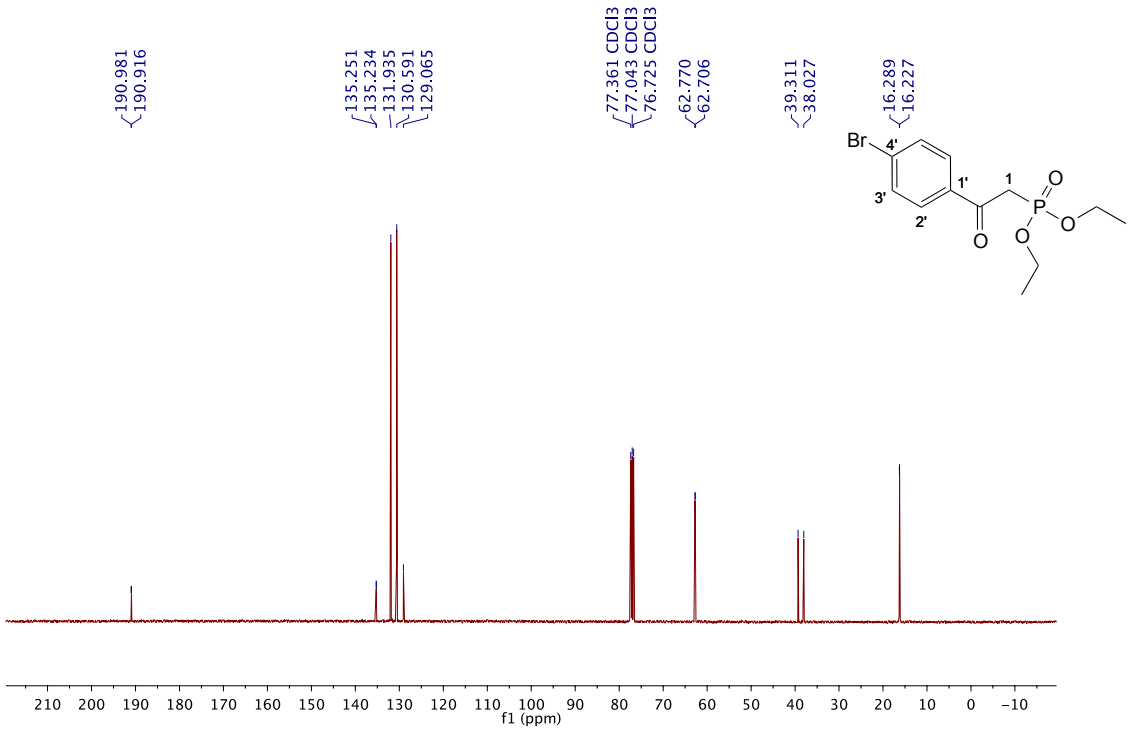


**Figure S74**. $^{13}$C NMR spectrum of **4j** in $CDCl_3$, 100 MHz, 298 K.

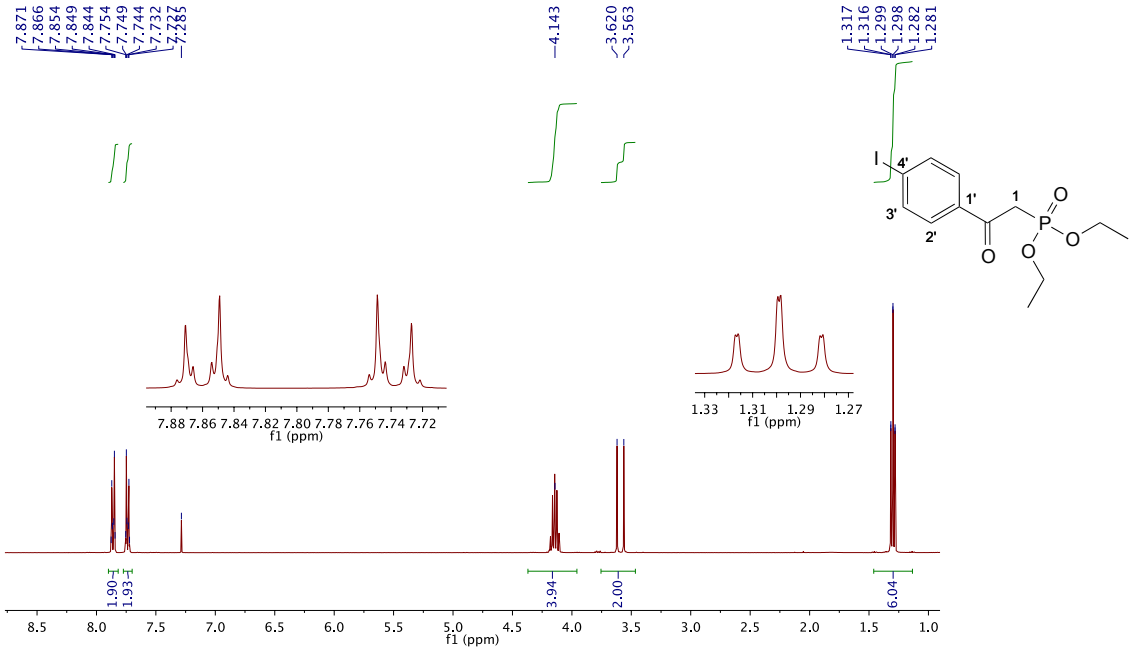

**Figure S75**. $^{1}$H NMR spectrum of **4k** in $CDCl_3$, 400 MHz, 298 K.

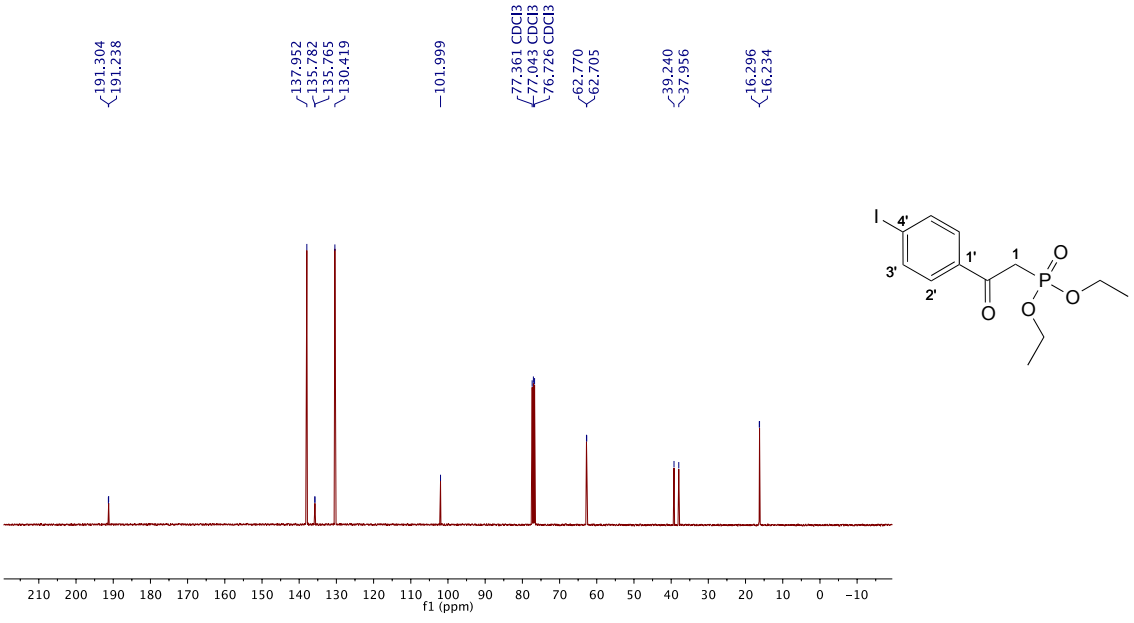

**Figure S76**. $^{13}$C NMR spectrum of **4k** in $CDCl_3$, 100 MHz, 298 K.

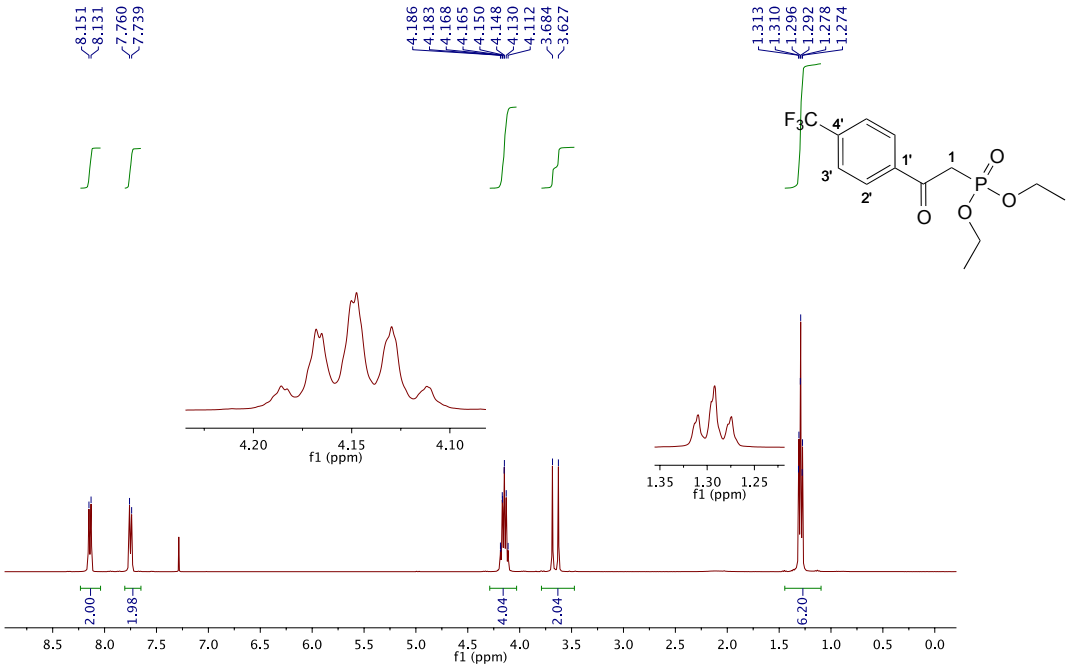


**Figure S77**. $^{1}$H NMR spectrum of **4l** in $CDCl_3$, 400 MHz, 298 K.

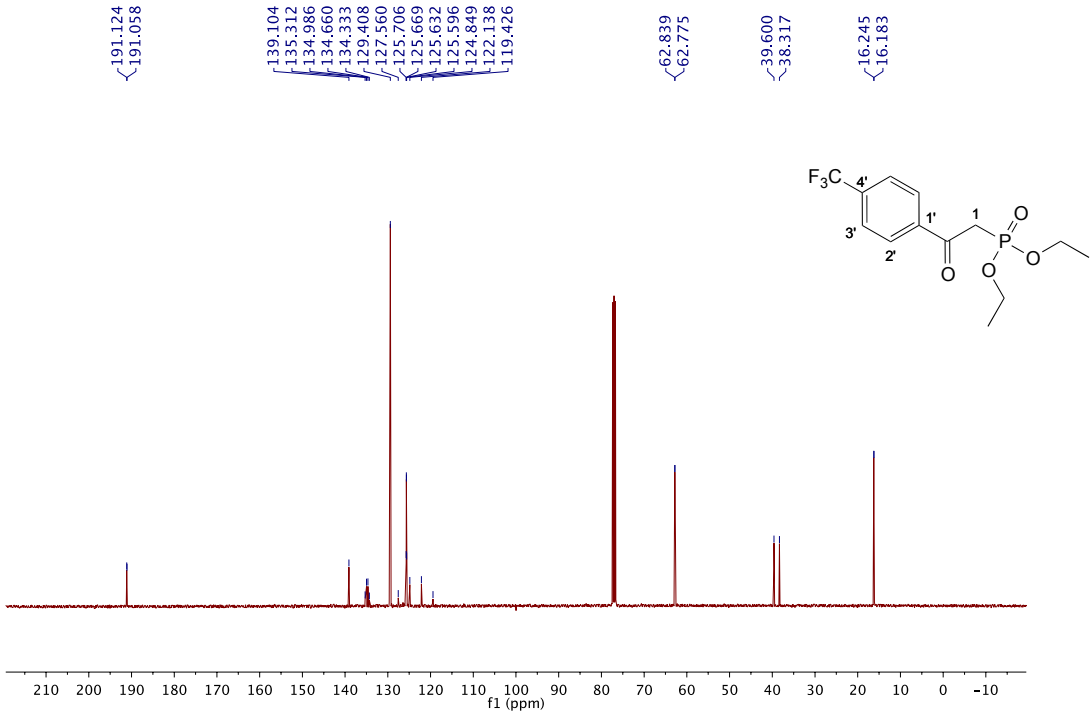


**Figure S78**. $^{13}$C NMR spectrum of **4l** in $CDCl_3$, 100 MHz, 298 K.

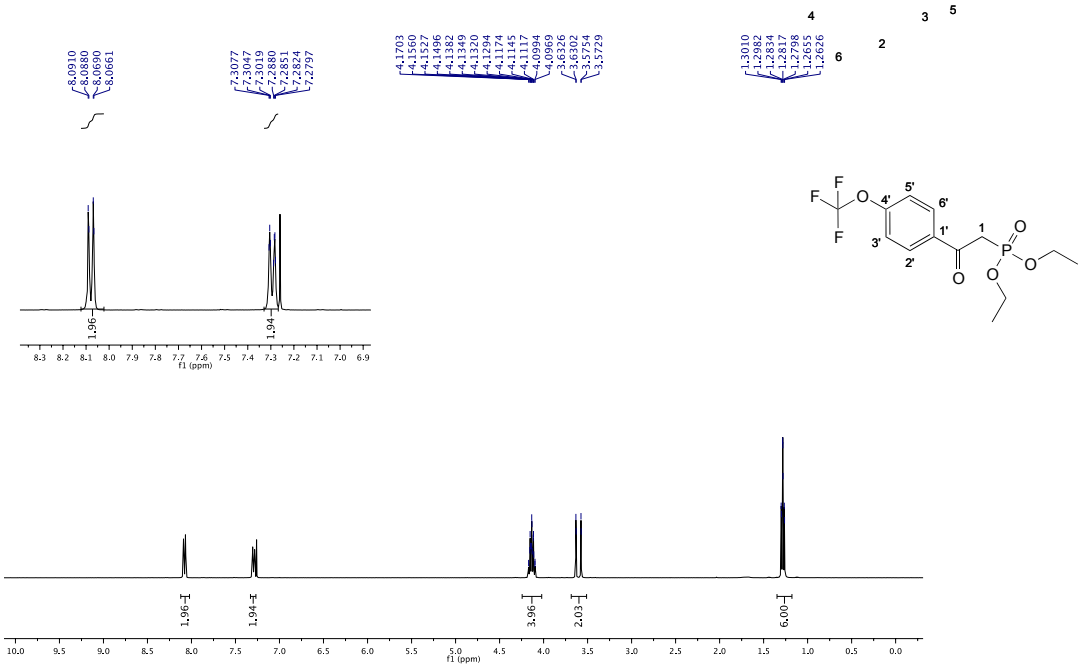

**Figure S79**. $^{1}H$ NMR spectrum of **4m** in $CDCl_3$, 400 MHz, 298 K.

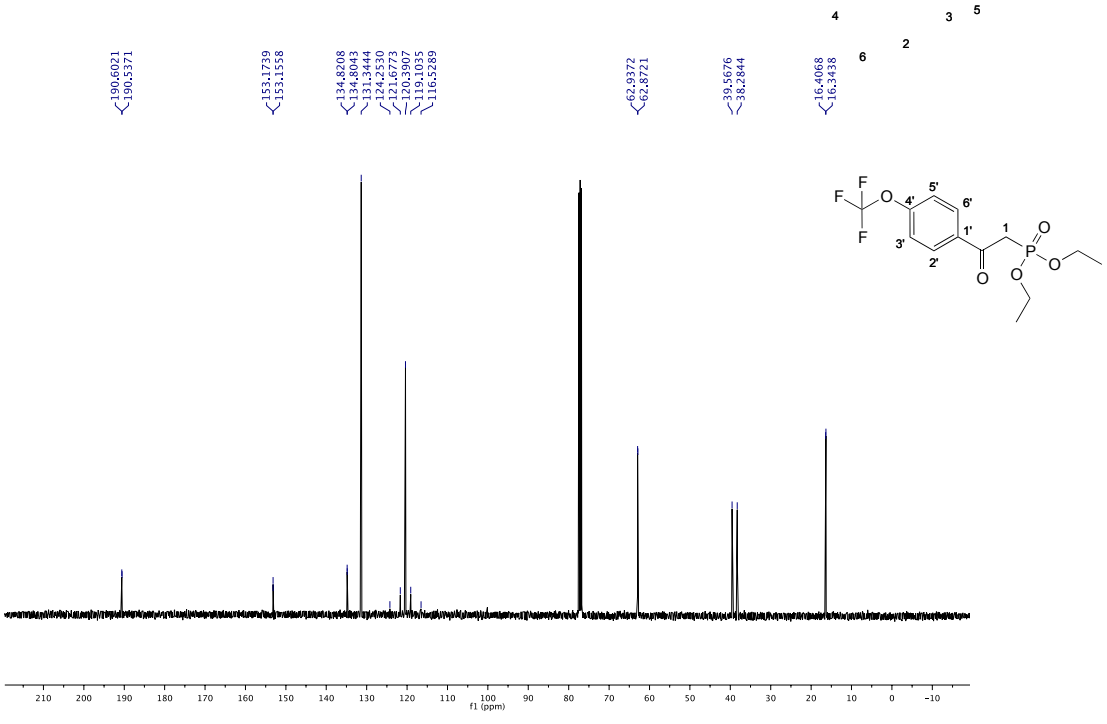

**Figure S80**. $^{13}C$ NMR spectrum of **4m** in $CDCl_3$, 100 MHz, 298 K.

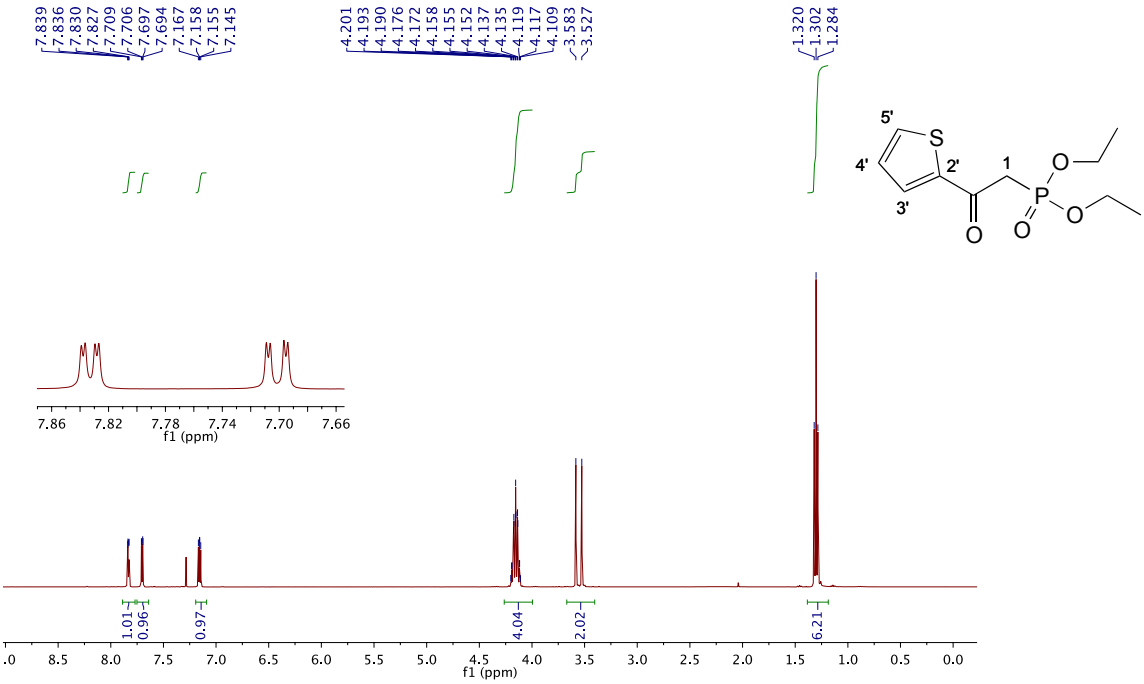


**Figure S81**. $^{1}$H NMR spectrum of **4n** in $CDCl_3$, 400 MHz, 298 K.

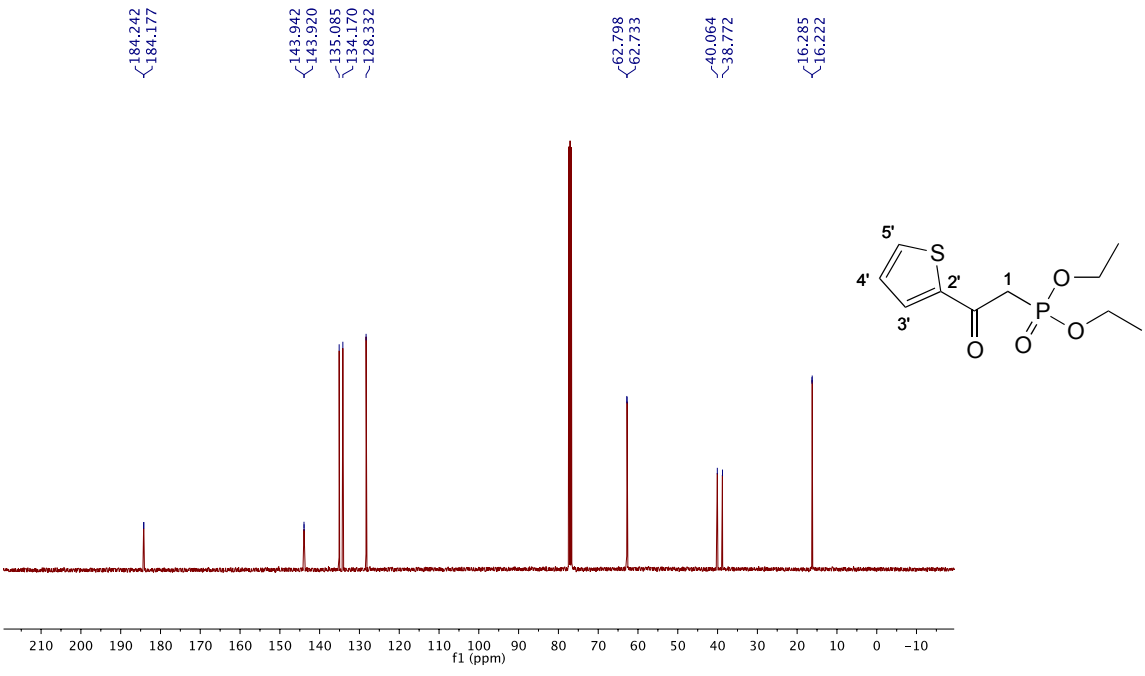


**Figure S82**. $^{13}$C NMR spectrum of **4n** in $CDCl_3$, 100 MHz, 298 K.

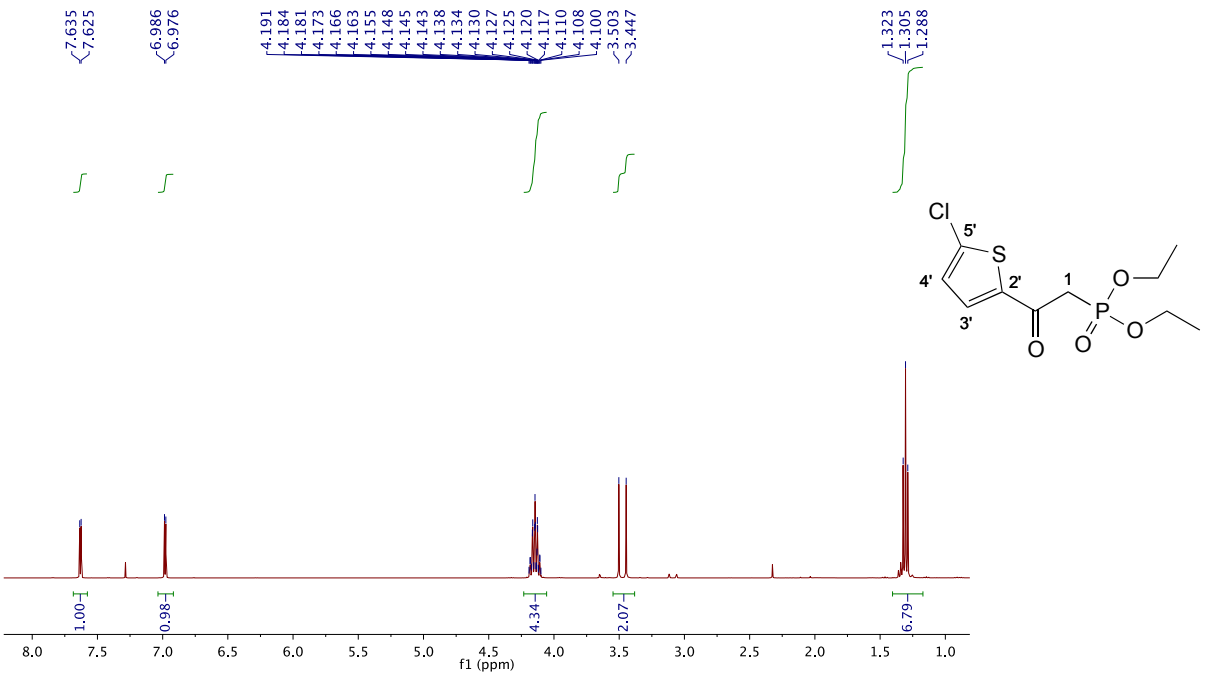


**Figure S83**. $^{1}$H NMR spectrum of **4o** in $CDCl_3$, 400 MHz, 298 K.

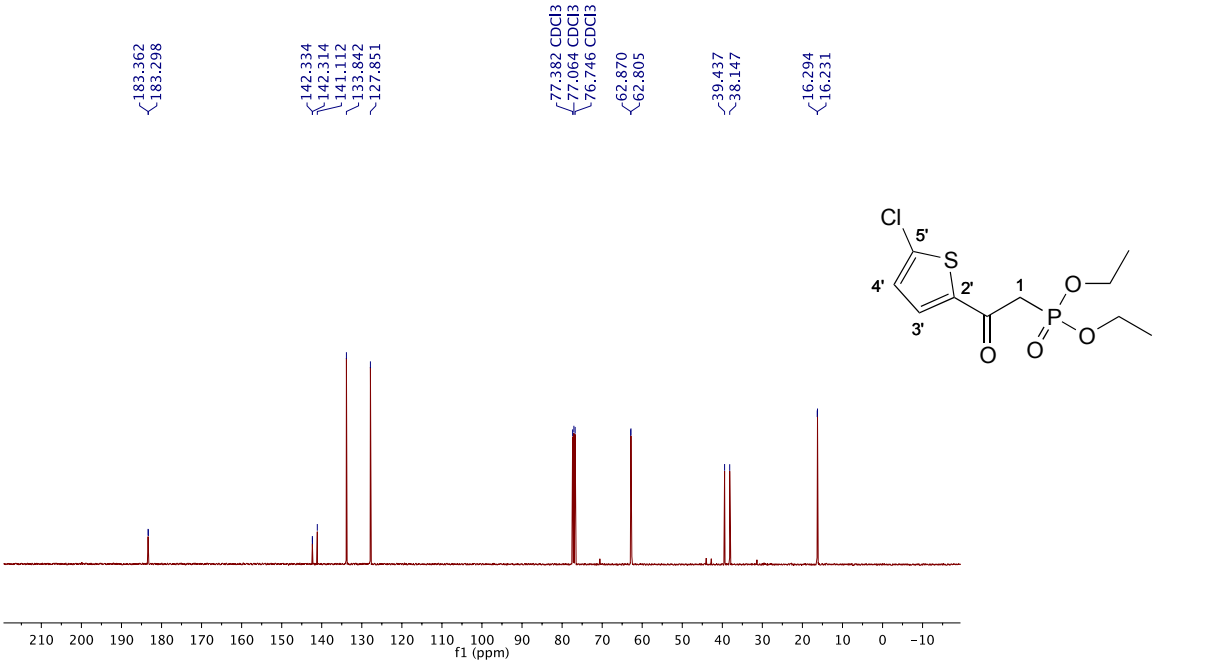


**Figure S84**. $^{13}$C NMR spectrum of **4o** in $CDCl_3$, 100 MHz, 298 K.

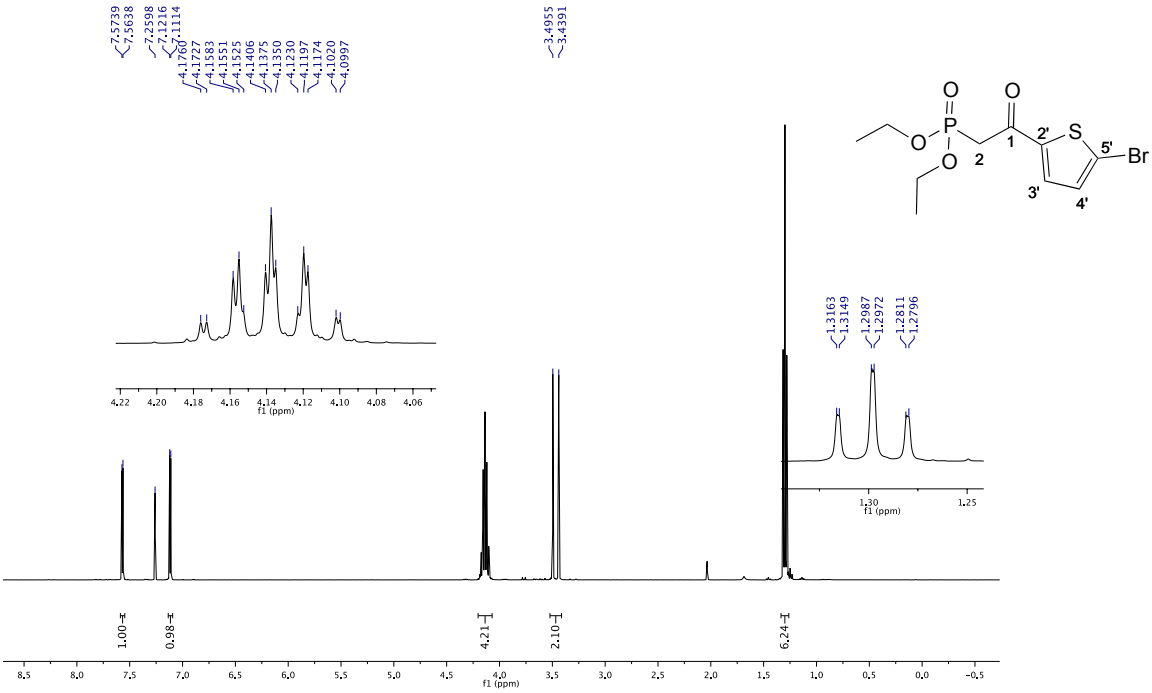

**Figure S85** $^{1}$H NMR spectrum of **4p** in $CDCl_3$, 400 MHz, 298 K.

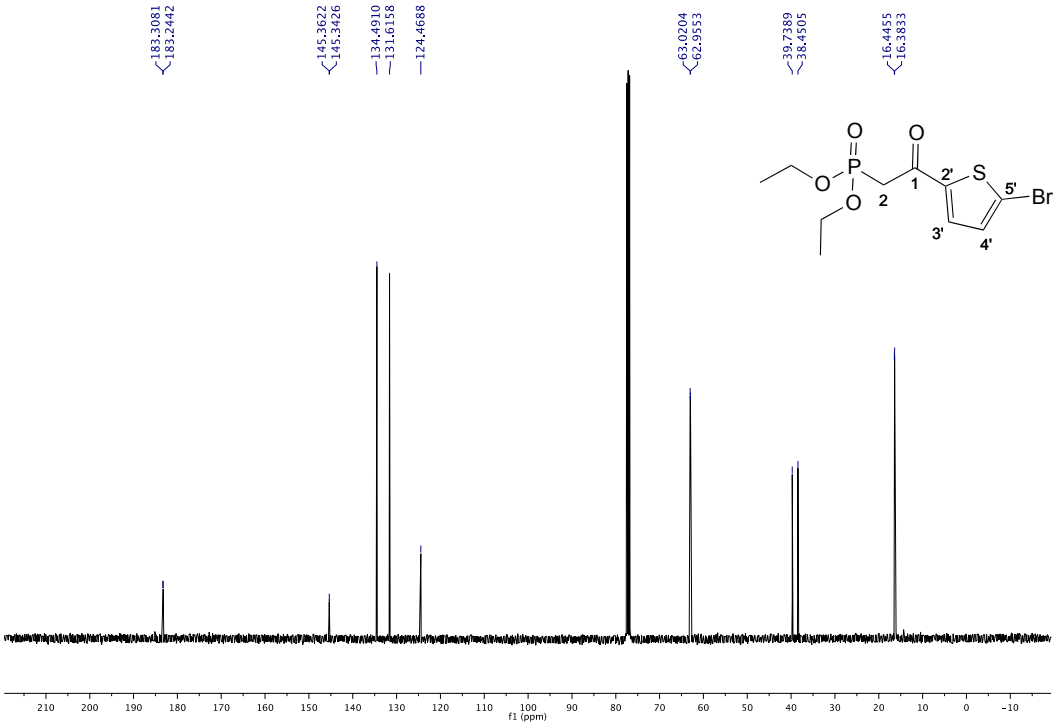

**Figure S86**. $^{13}$C NMR spectrum of **4p** in $CDCl_3$, 100 MHz, 298 K.

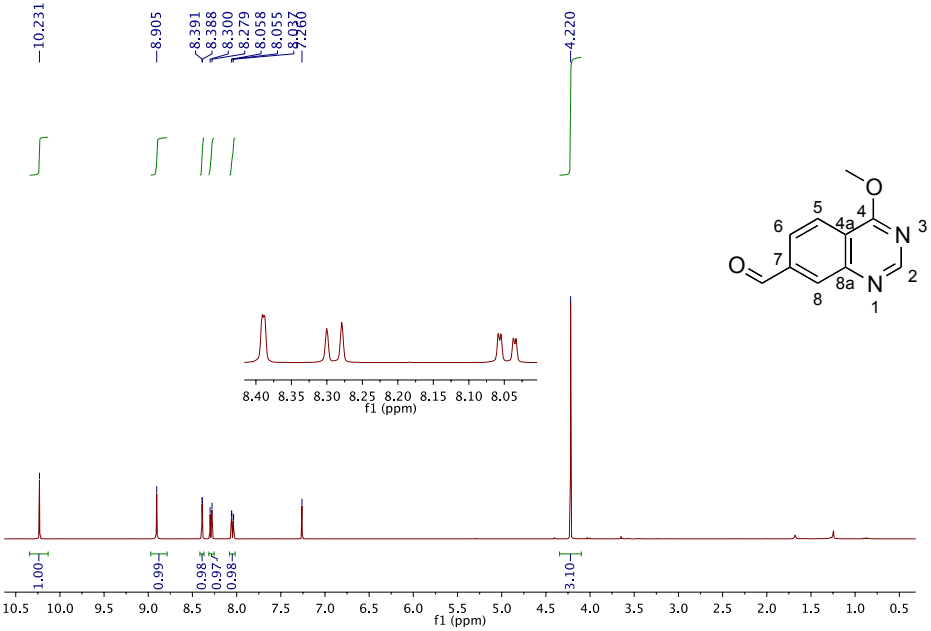


**Figure S87**. $^{1}$H NMR spectrum of **5** in $CDCl_3$, 400 MHz, 298 K.

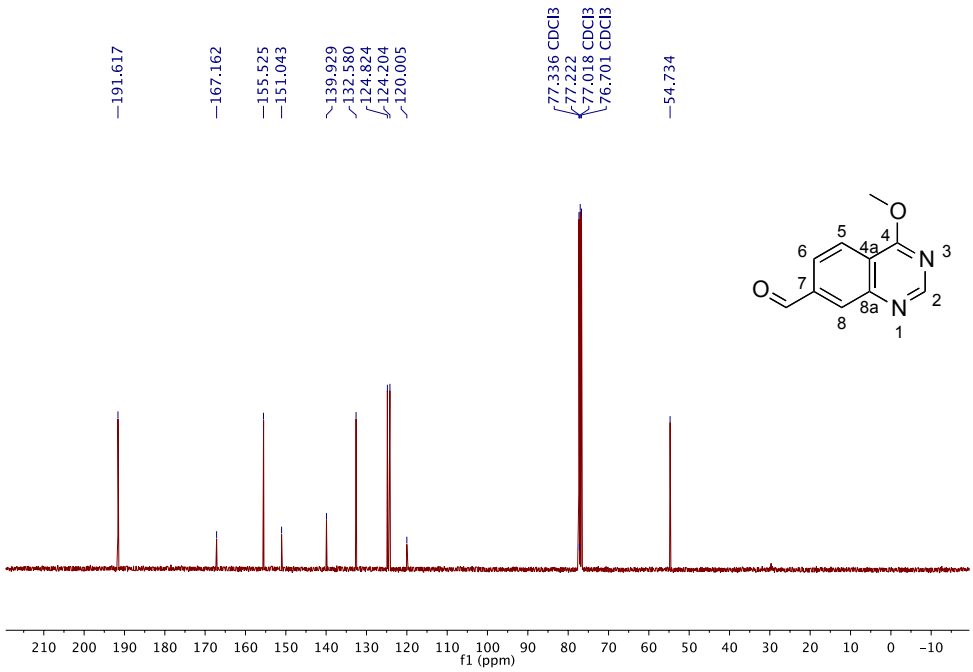


**Figure S88**. $^{13}$C NMR spectrum of **5** in $CDCl_3$, 100 MHz, 298 K.

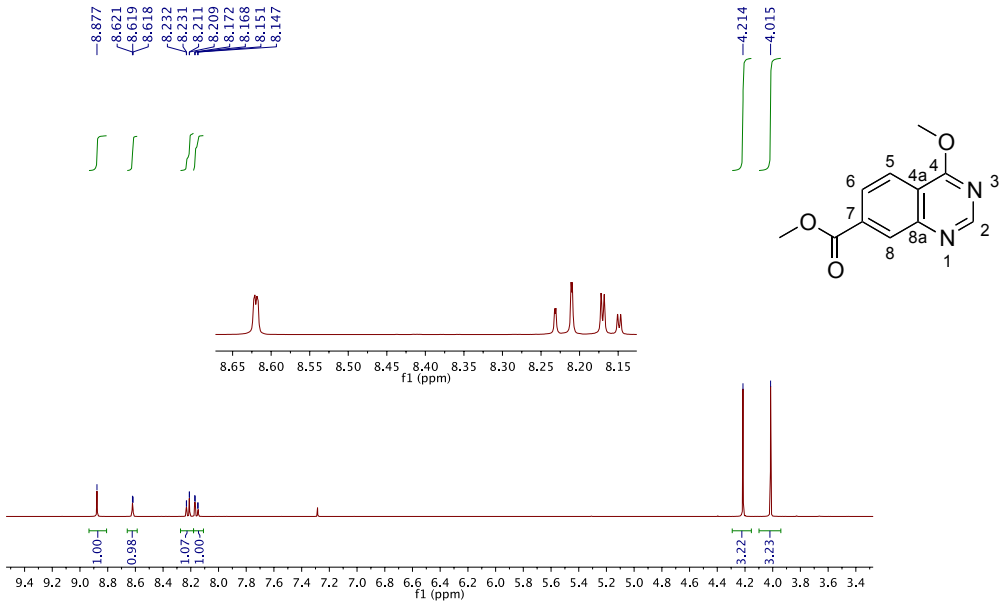


**Figure S89**. $^{1}$H NMR spectrum of **8** in $CDCl_3$, 400 MHz, 298 K.

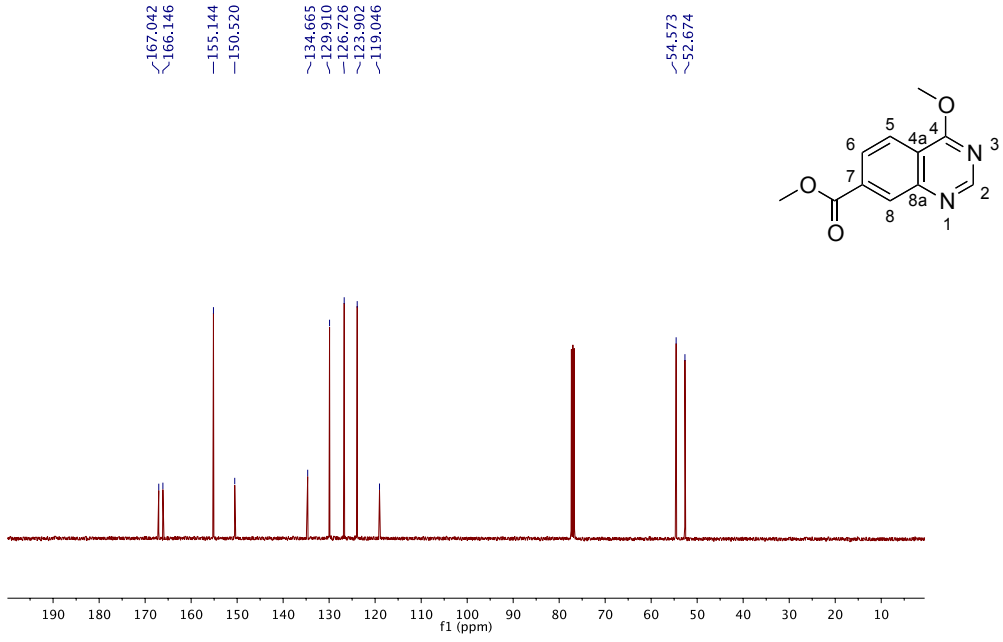


**Figure S90** $^{13}$C NMR spectrum of **8** in $CDCl_3$, 100 MHz, 298 K.

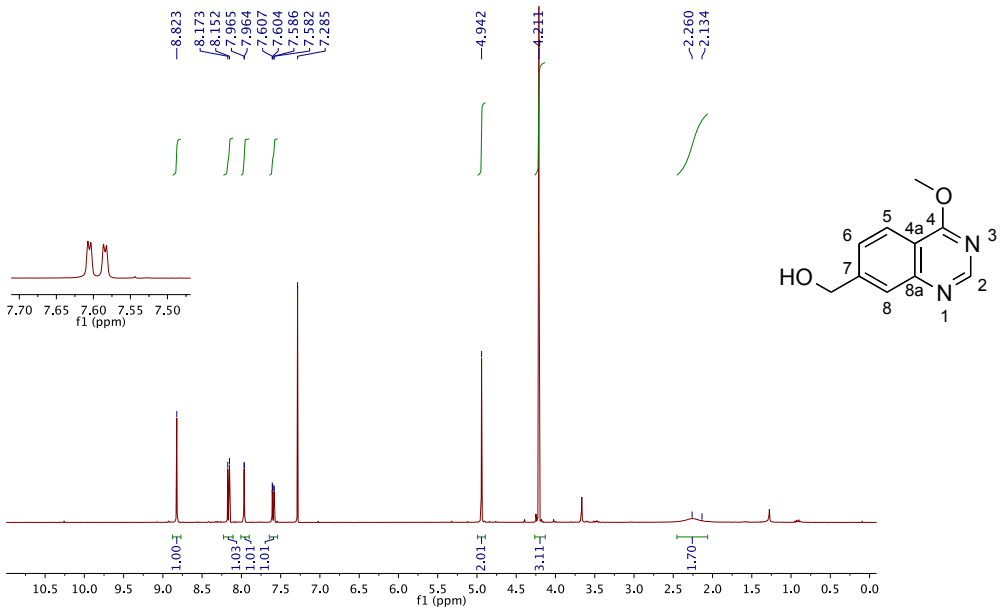


**Figure S91**. $^{1}$H NMR spectrum of **9** in $CDCl_3$, 400 MHz, 298 K.

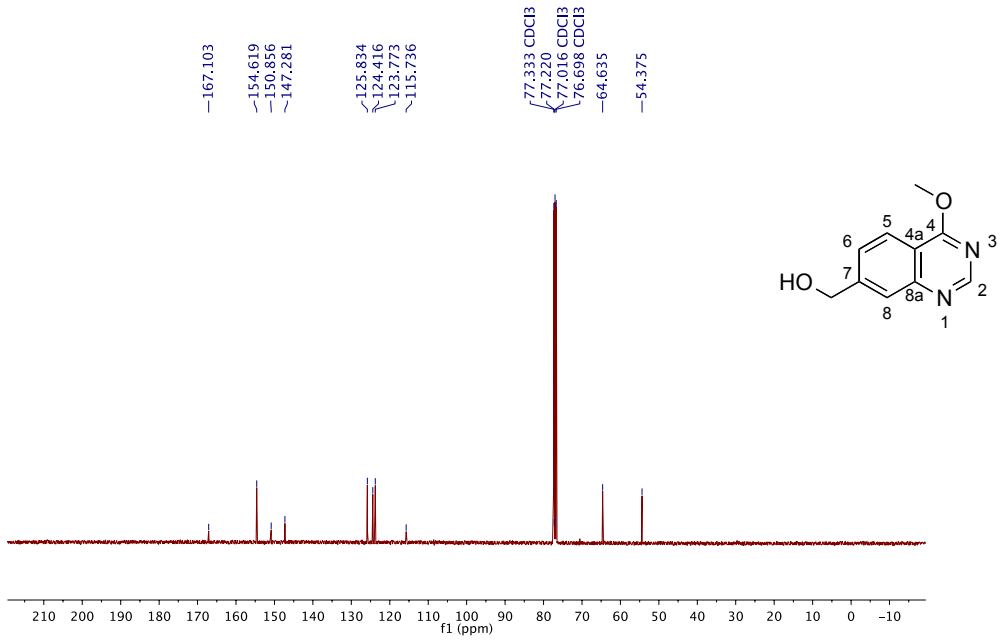


**Figure S92**. $^{13}$C NMR spectrum of **9** in $CDCl_3$, 100 MHz, 298 K.

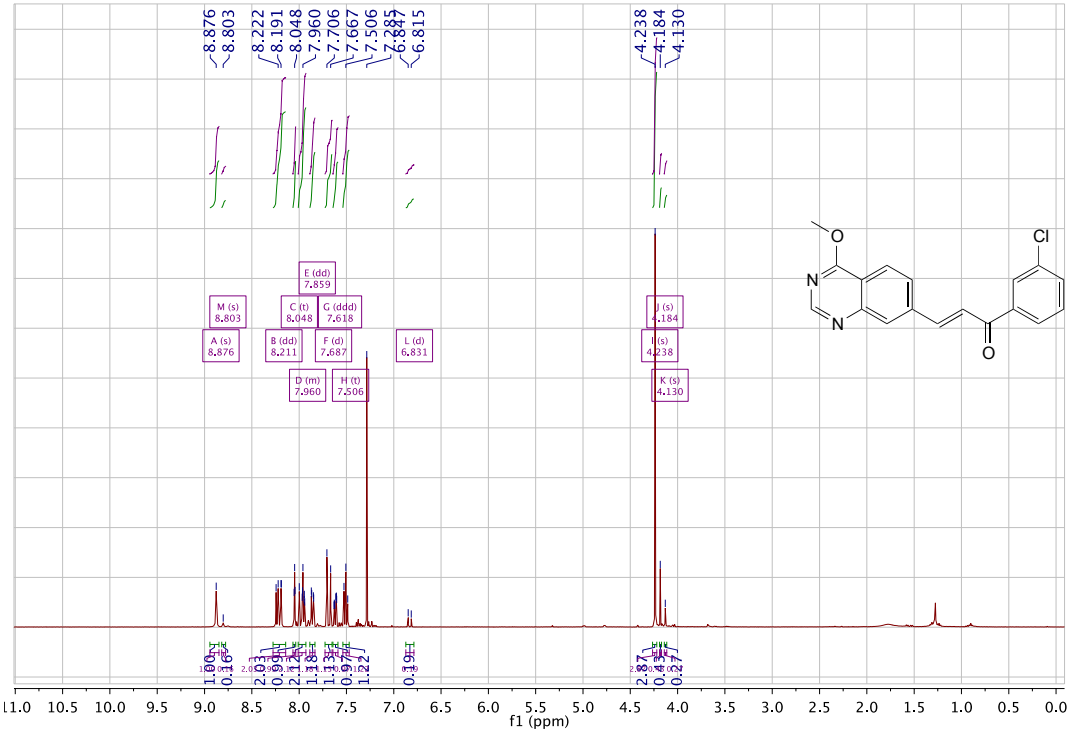


**Figure S93**. $^{1}$H NMR spectrum of **10c** in $CDCl_3$, 400 MHz, 298 K.

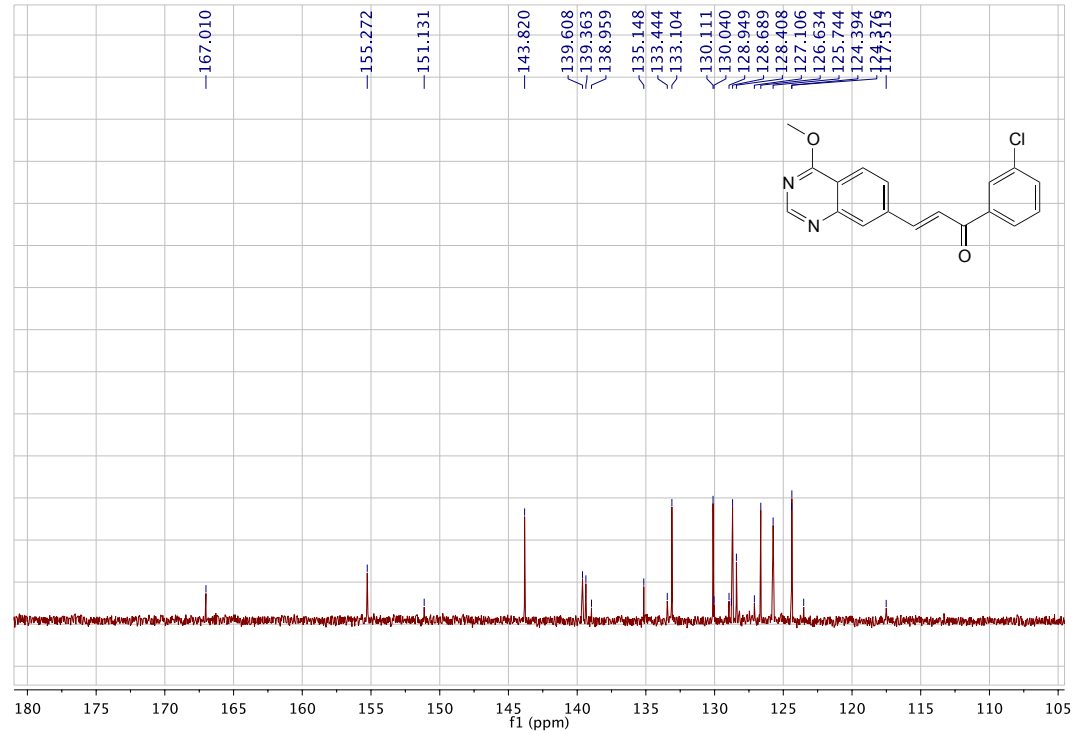


**Figure S94**. $^{13}$C NMR spectrum of **10c** in $CDCl_3$, 100 MHz, 298 K.

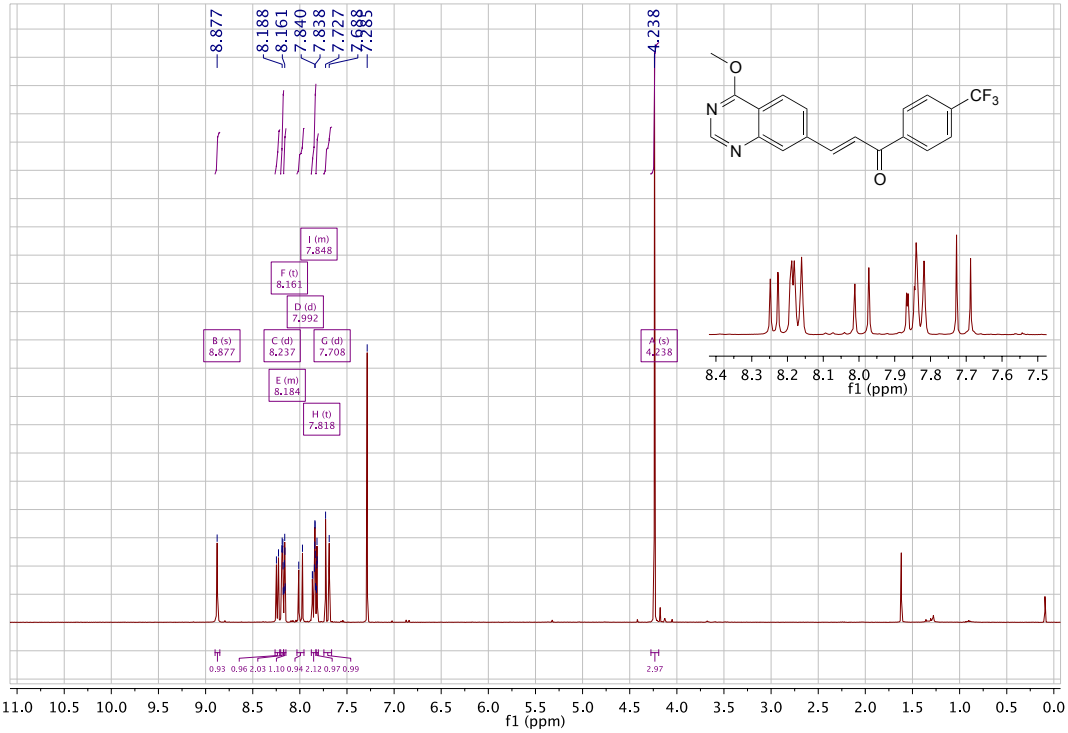


**Figure S95**. $^{1}$H NMR spectrum of **10h** in $CDCl_3$, 400 MHz, 298 K.

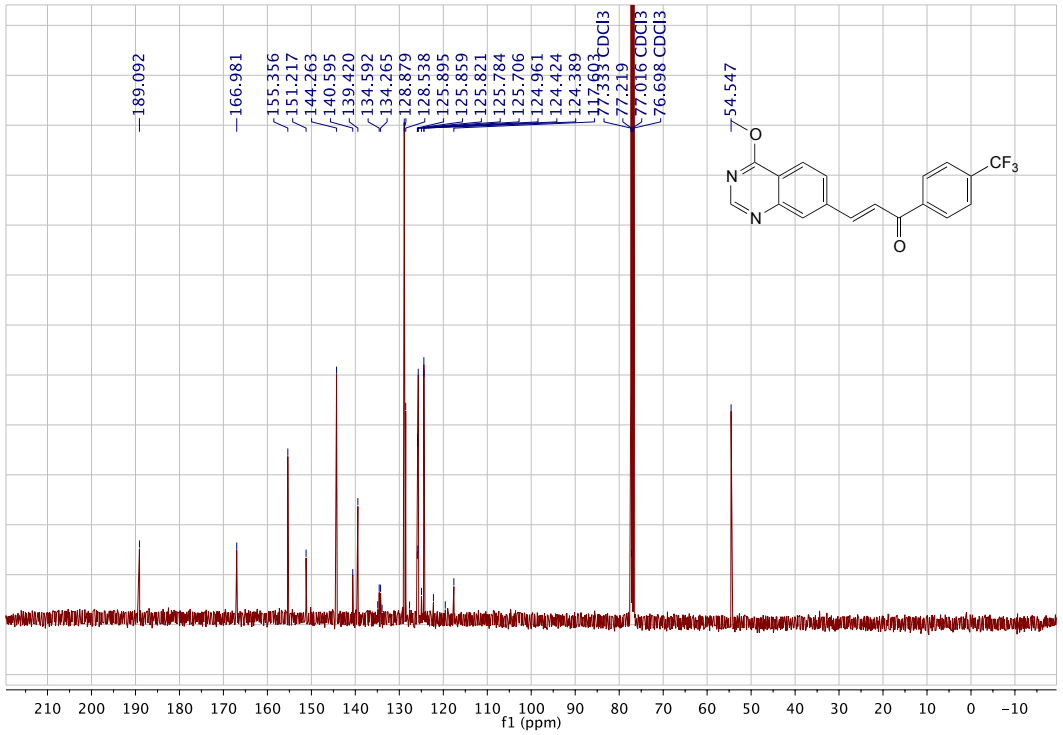


**Figure S96**. $^{13}$C NMR spectrum of **10h** in $CDCl_3$, 100 MHz, 298 K.

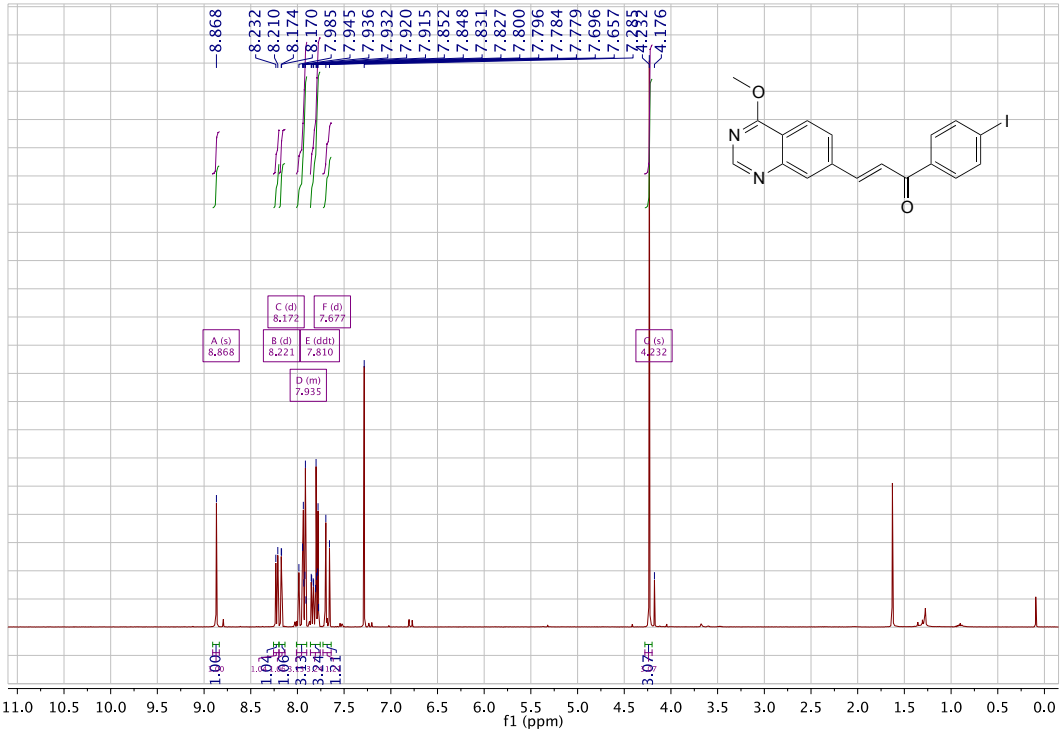


**Figure S97**. $^{1}$H NMR spectrum of **10i** in $CDCl_3$, 400 MHz, 298 K.

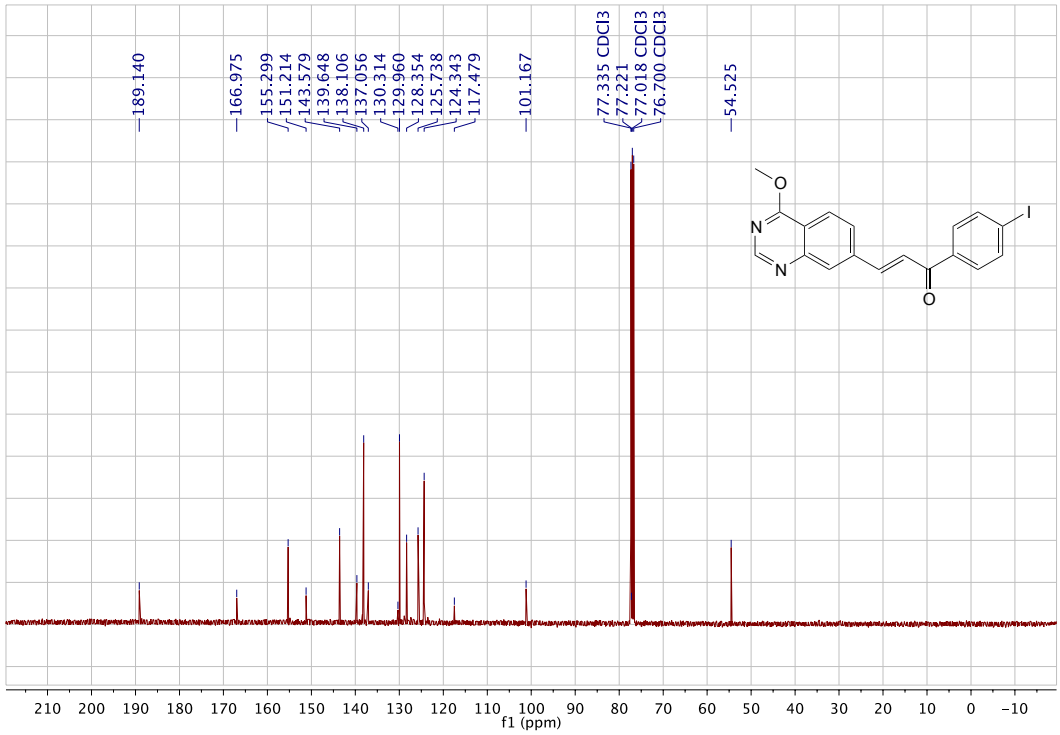


**Figure S98**. $^{13}$C NMR spectrum of **10i** in $CDCl_3$, 100 MHz, 298 K.

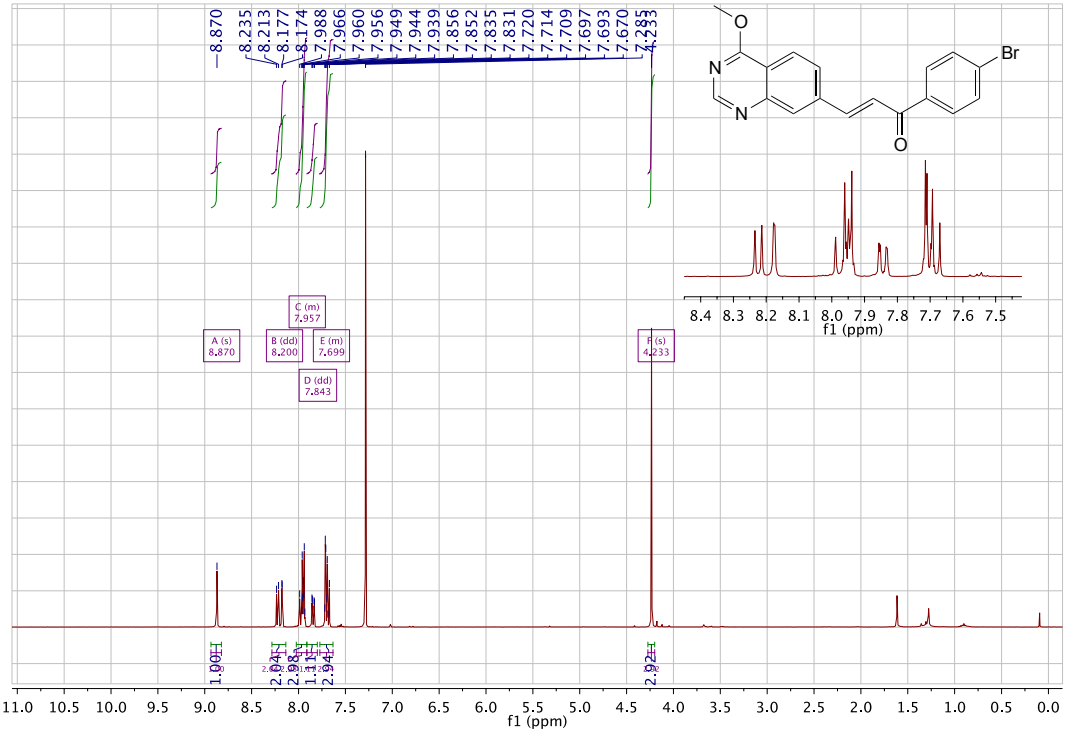


**Figure S99**. $^{1}$H NMR spectrum of **10j** in $CDCl_3$, 400 MHz, 298 K.

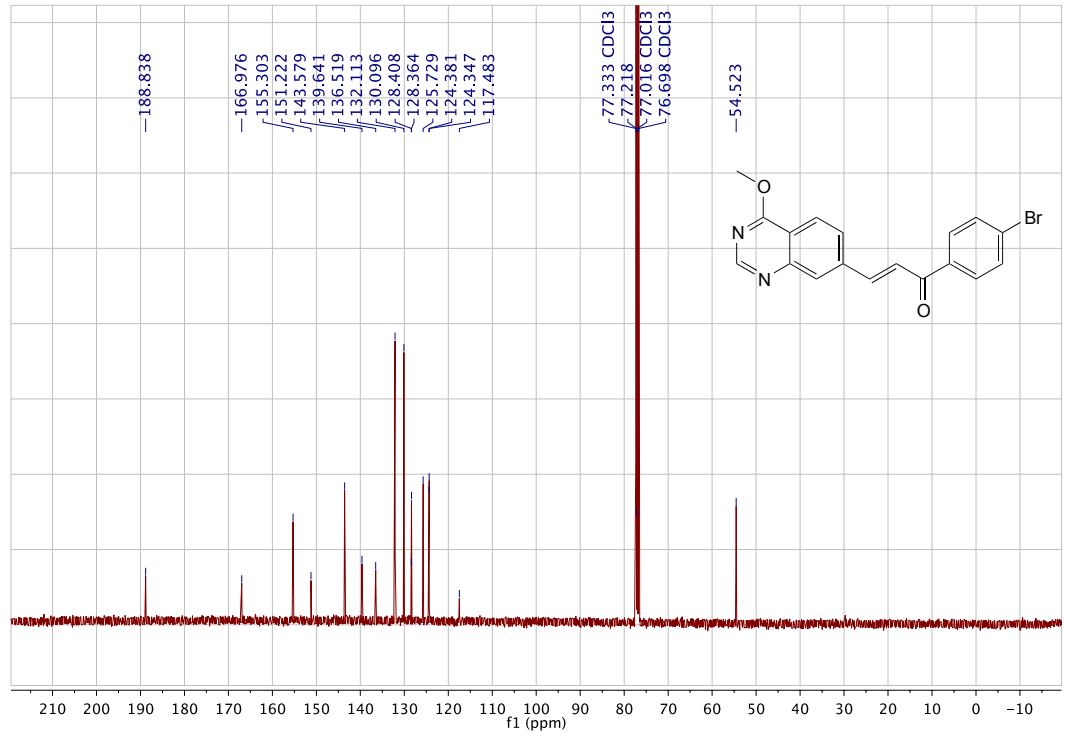


**Figure S100**. $^{13}$C NMR spectrum of **10j** in $CDCl_3$, 100 MHz, 298 K.

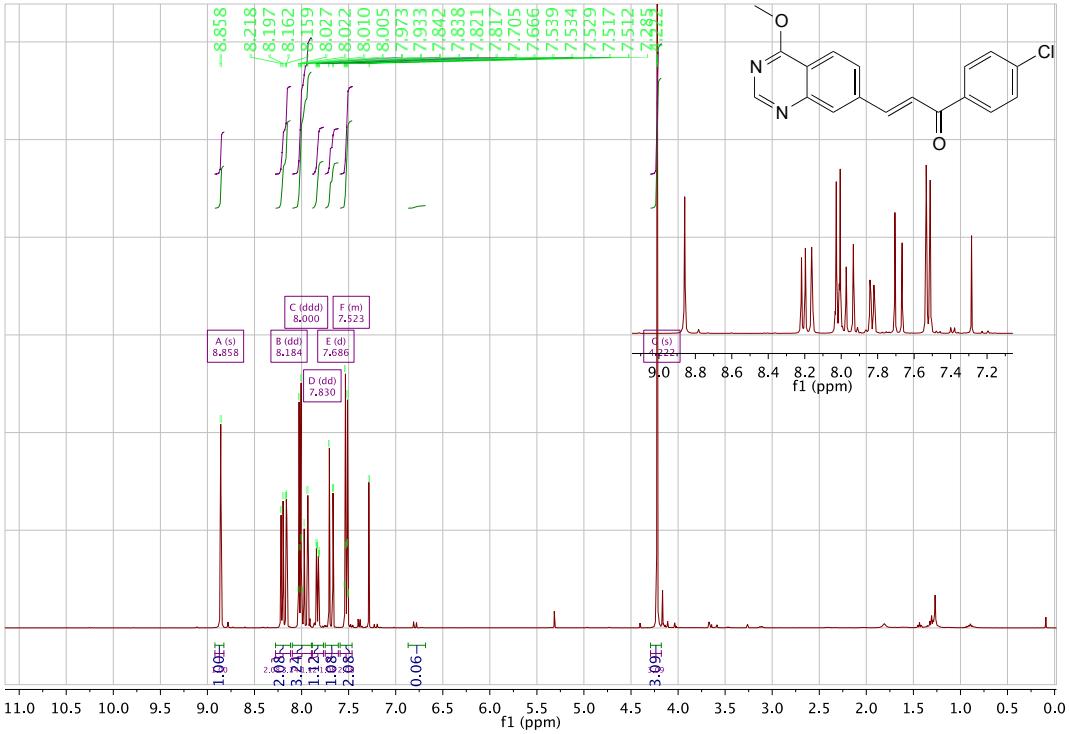


**Figure S101**. $^{1}$H NMR spectrum of **10k** in $CDCl_3$, 400 MHz, 298 K.

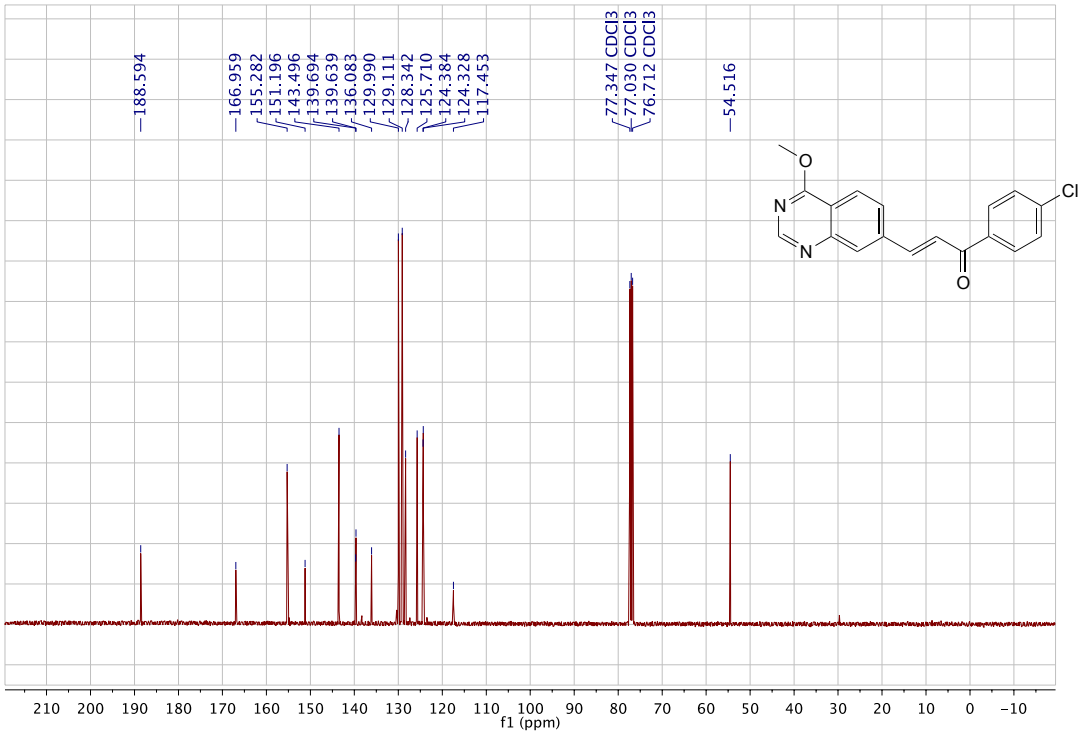


**Figure S102**. $^{13}$C NMR spectrum of **10k** in $CDCl_3$, 100 MHz, 298 K.

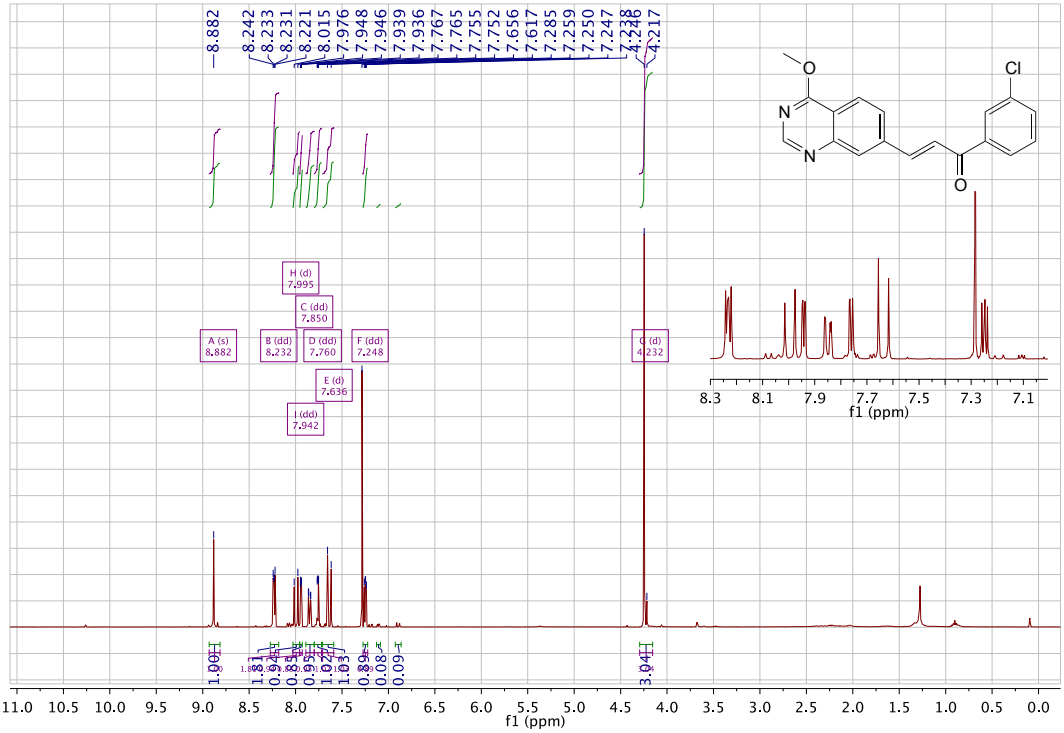

**Figure S103**. $^{1}$H NMR spectrum of **10n** in $CDCl_3$, 400 MHz, 298 K.

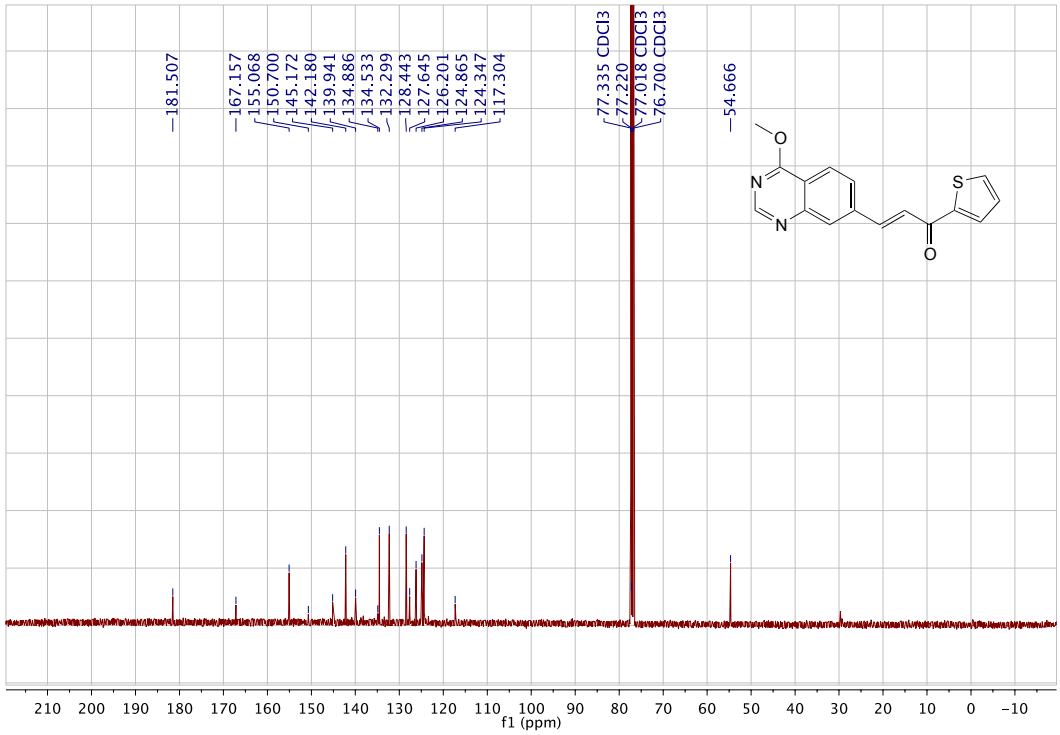

**Figure S104**. $^{13}$C NMR spectrum of **10n** in $CDCl_3$, 100 MHz, 298 K.

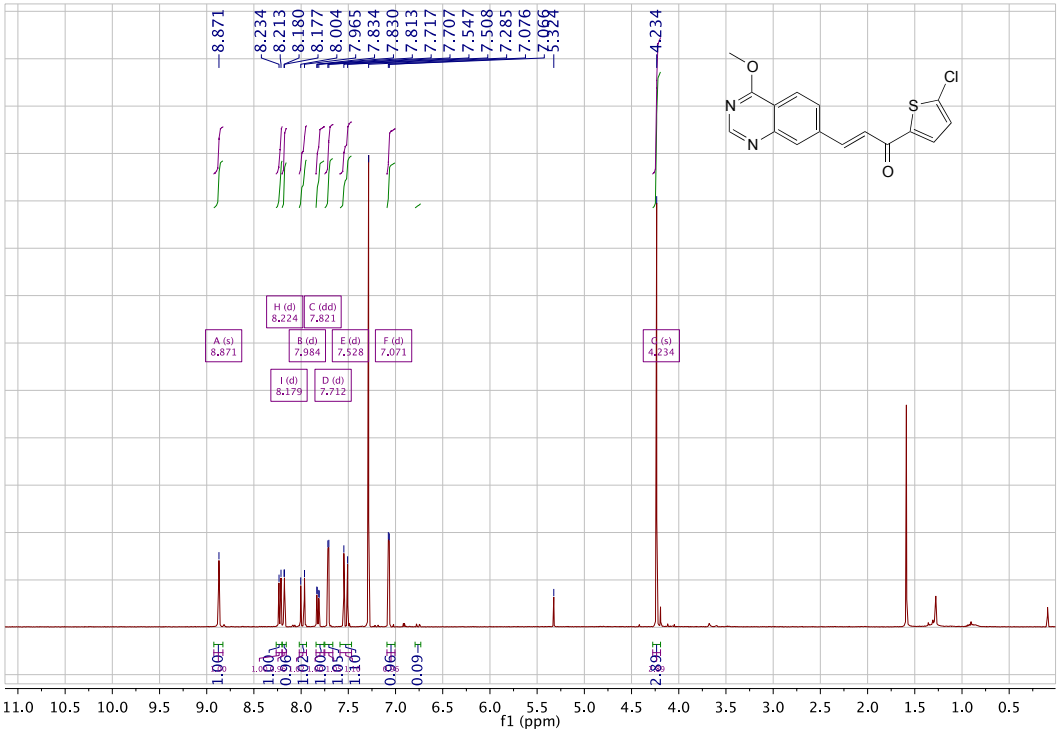


**Figure S105**. $^{1}$H NMR spectrum of **10o** in $CDCl_3$, 400 MHz, 298 K.

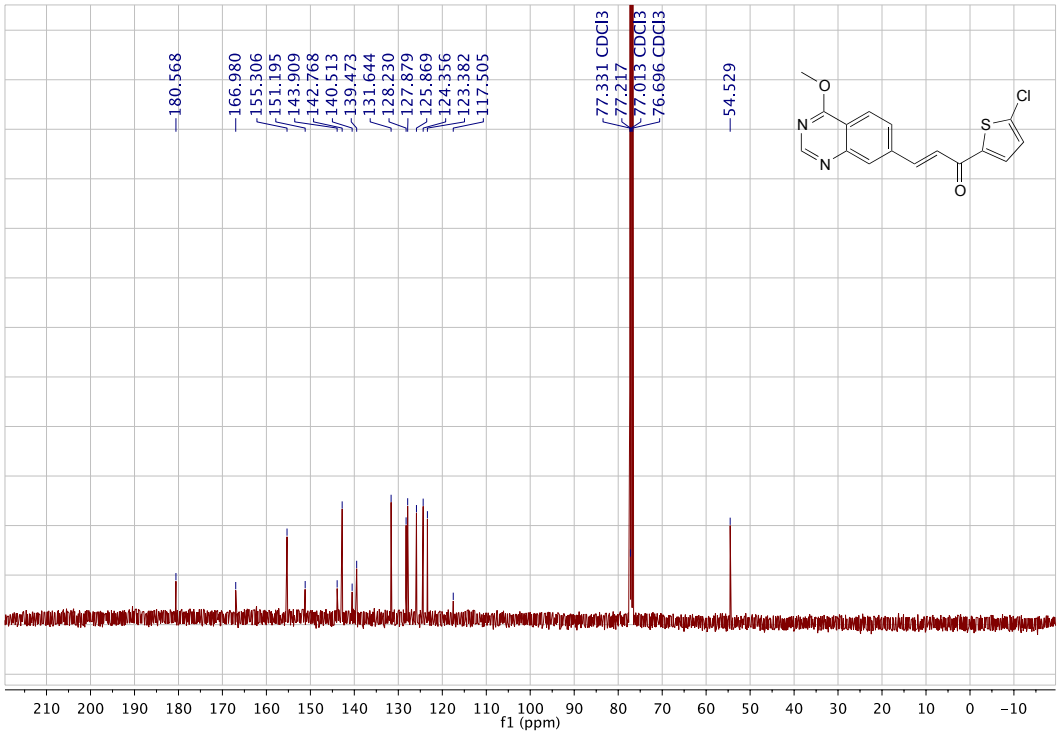


**Figure S106**. $^{13}$C NMR spectrum of **10o** in $CDCl_3$, 100 MHz, 298 K.

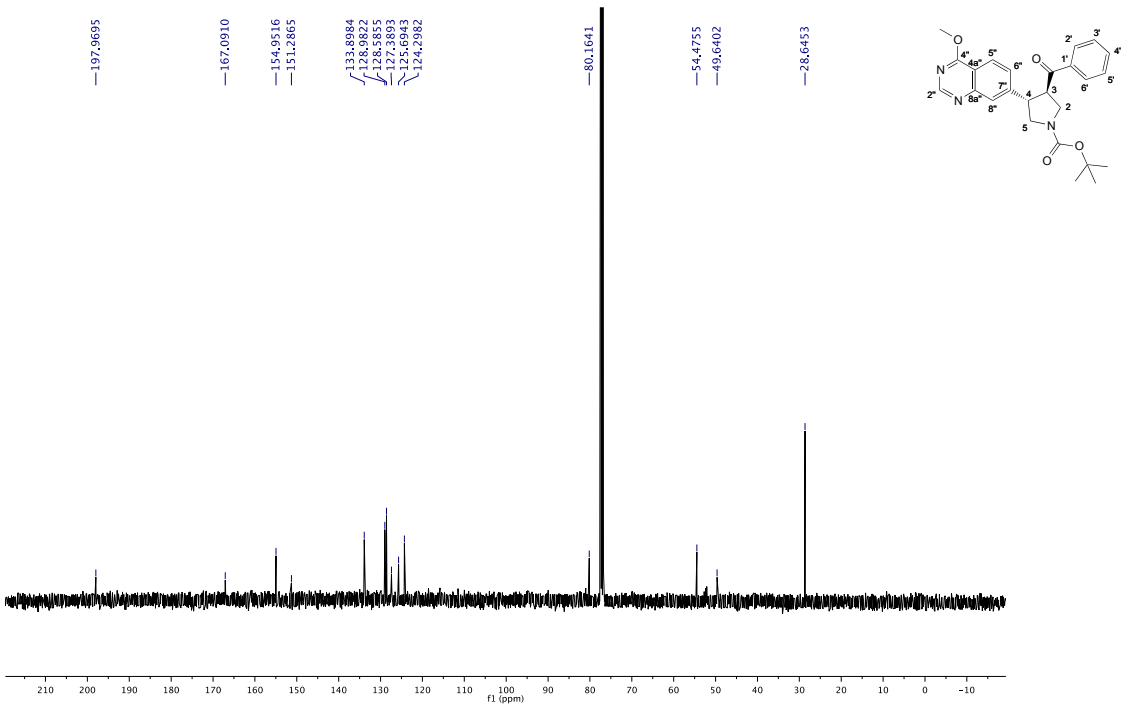


**Figure S107**. $^{13}C$ NMR spectrum of **13a** in $CDCl_3$, 400 MHz, 298 K.

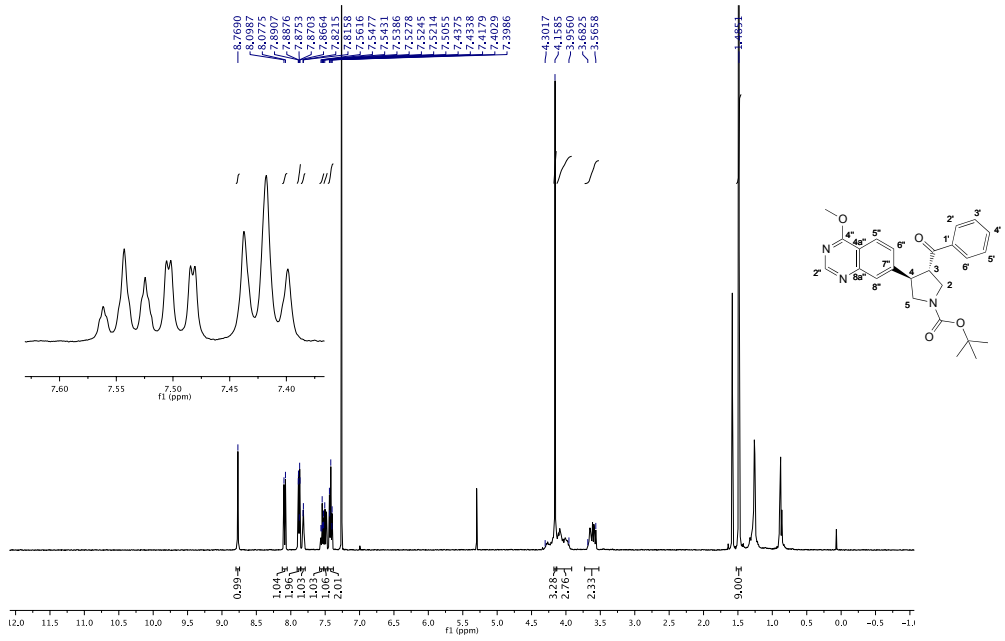


**Figure S108**. $^{1}H$ NMR spectrum of (–)-**13a** in $CDCl_3$, 100 MHz, 298 K.

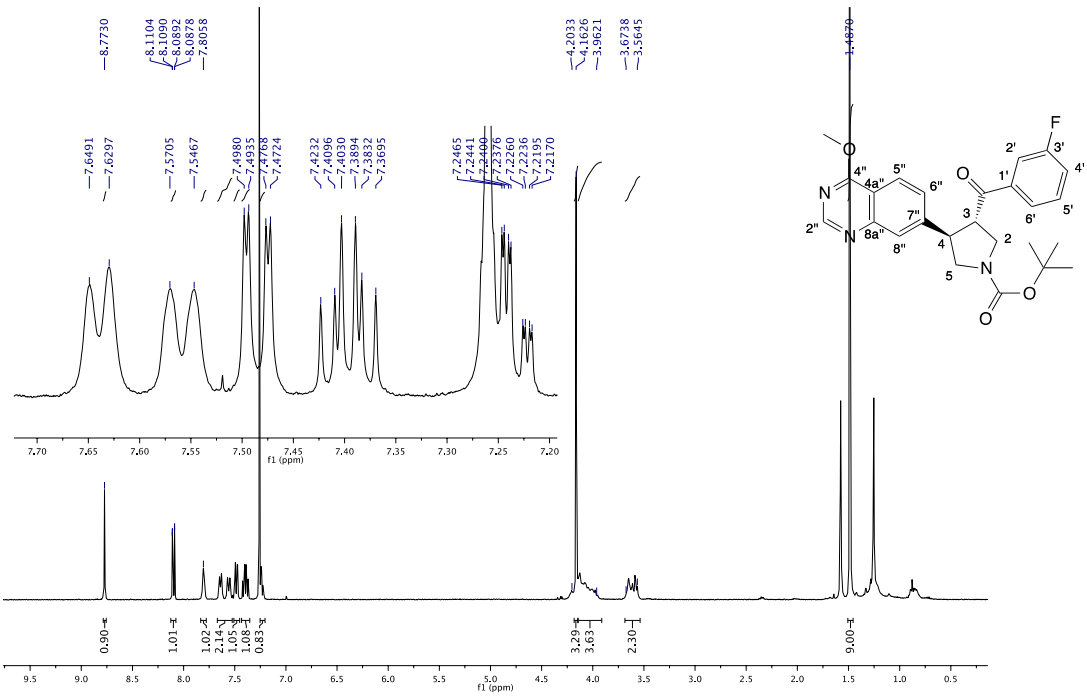

**Figure S109**. $^{1}$H NMR spectrum of (+)-**13b** in $CDCl_3$, 400 MHz, 298 K.

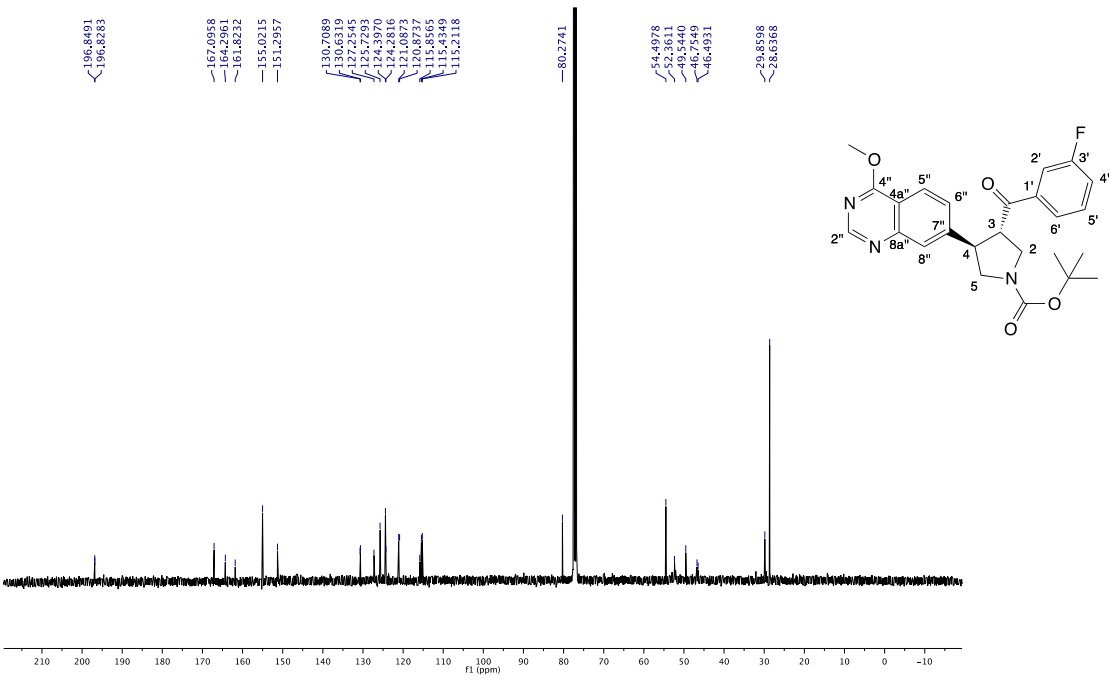

**Figure S110**. $^{13}$C NMR spectrum of (+)-**13b** in $CDCl_3$, 100 MHz, 298 K.

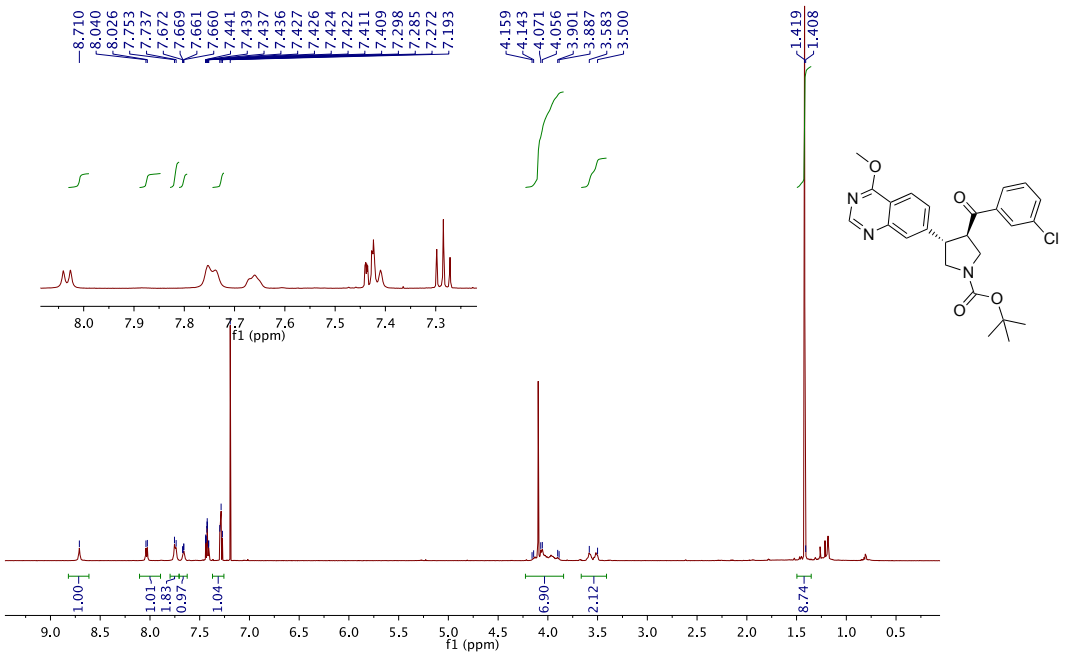


**Figure S111**. $^{1}$H NMR spectrum of **13c** in $CDCl_3$, 400 MHz, 298 K.

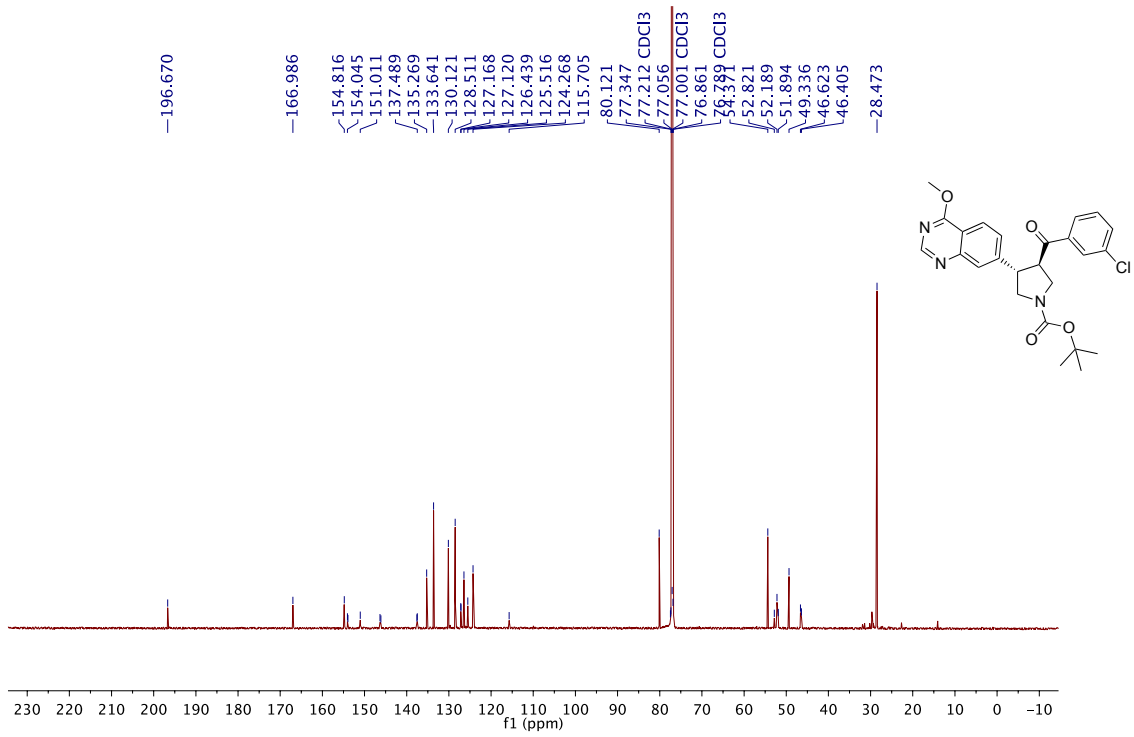


**Figure S112**. $^{13}$C NMR spectrum of **13c** in $CDCl_3$, 100 MHz, 298 K.

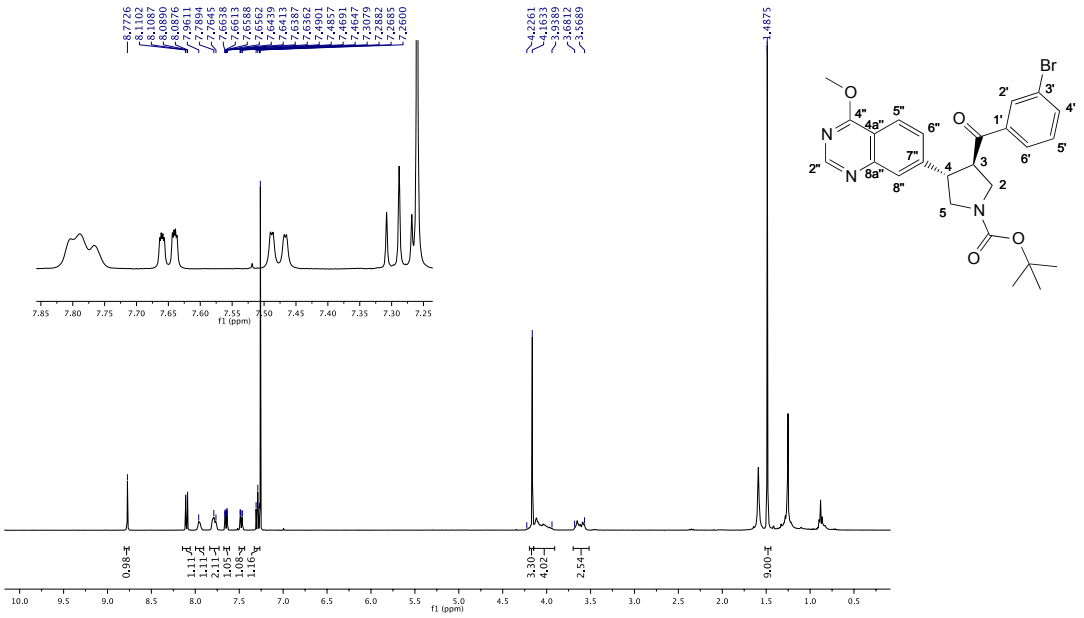

**Figure S113**. $^{1}$H NMR spectrum of (+)-**13d** in $CDCl_3$, 400 MHz, 298 K.

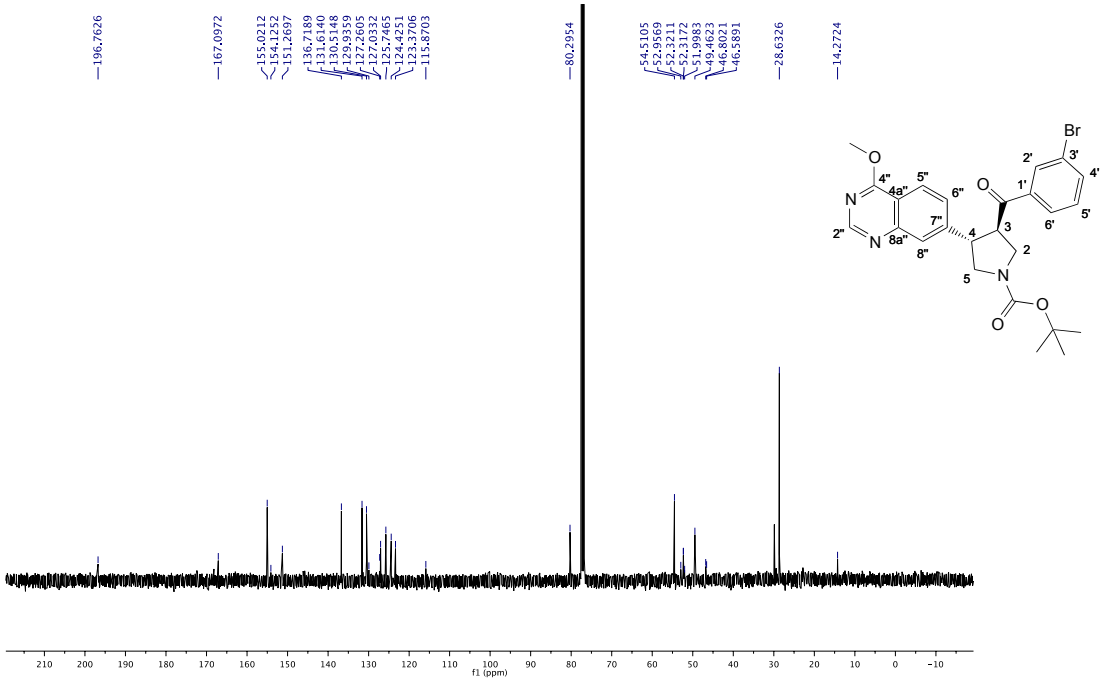

**Figure S114**. $^{13}$C NMR spectrum of (+)-**13d** in $CDCl_3$, 100 MHz, 298 K.

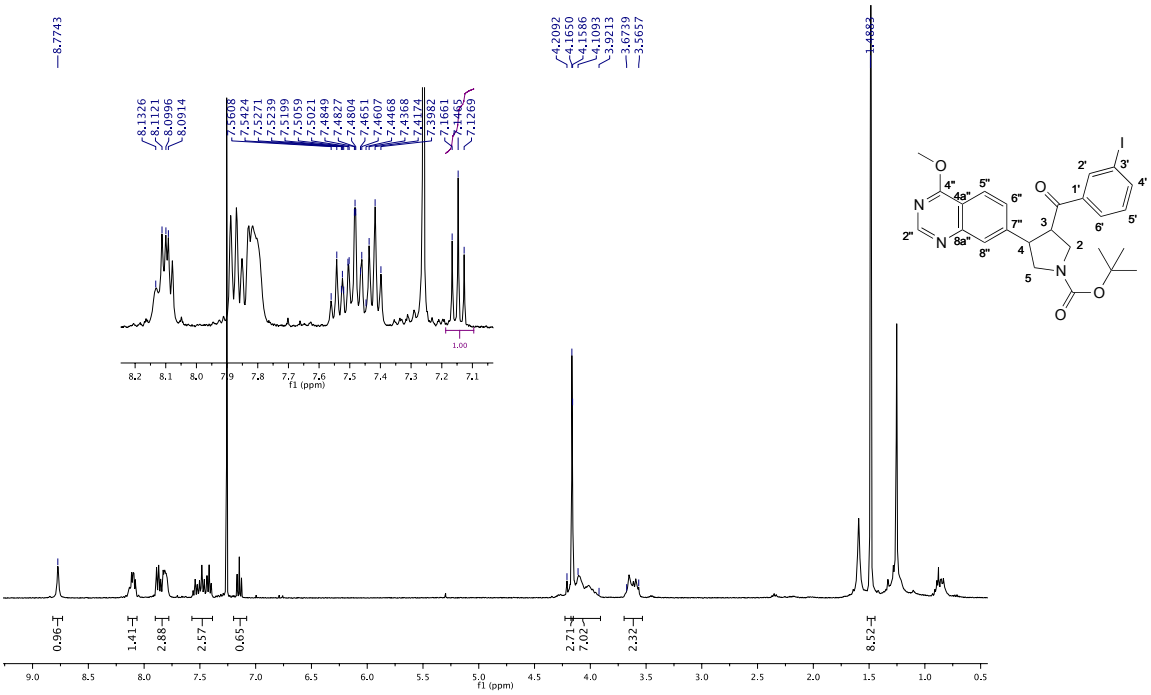

**Figure S115**. $^{1}$H NMR spectrum of instable (+)-**13e** in $CDCl_3$, 400 MHz, 298 K.

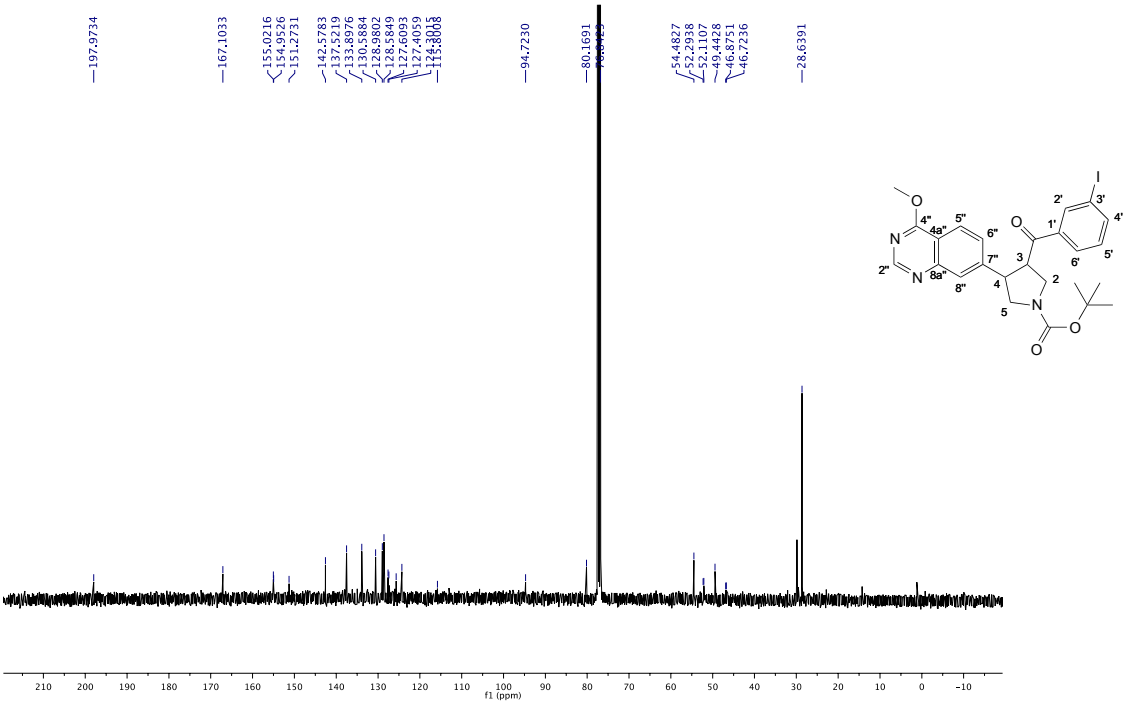

**Figure S116**. $^{13}$C NMR spectrum of instable (+)-**13e** in $CDCl_3$, 100 MHz, 298 K.

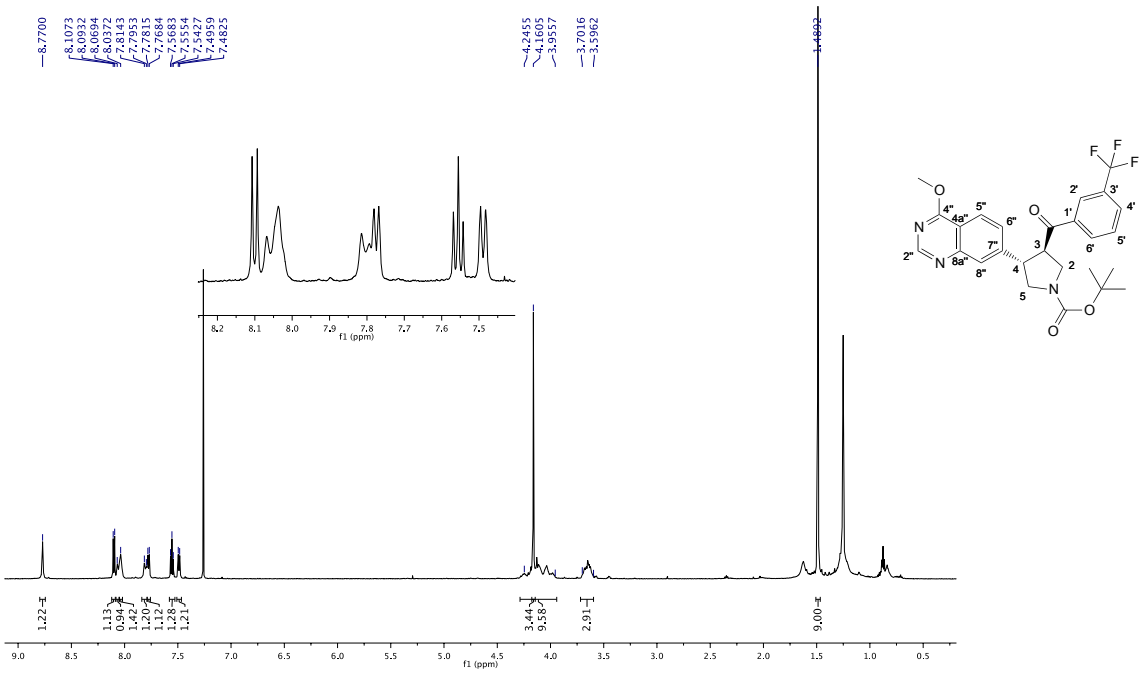

**Figure S117**. $^{1}$H NMR spectrum of (+)-**13f** in $CDCl_3$, 600 MHz, 298 K.

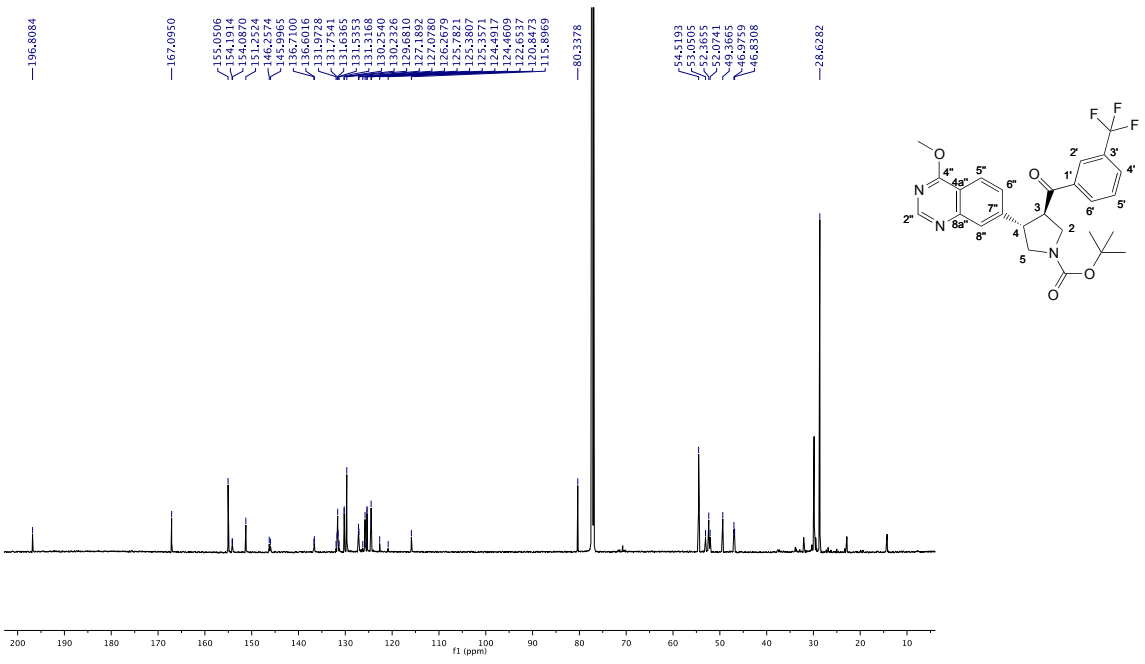

**Figure S118**. $^{13}$C NMR spectrum of (–)-**13f** in $CDCl_3$, 150 MHz, 298 K.

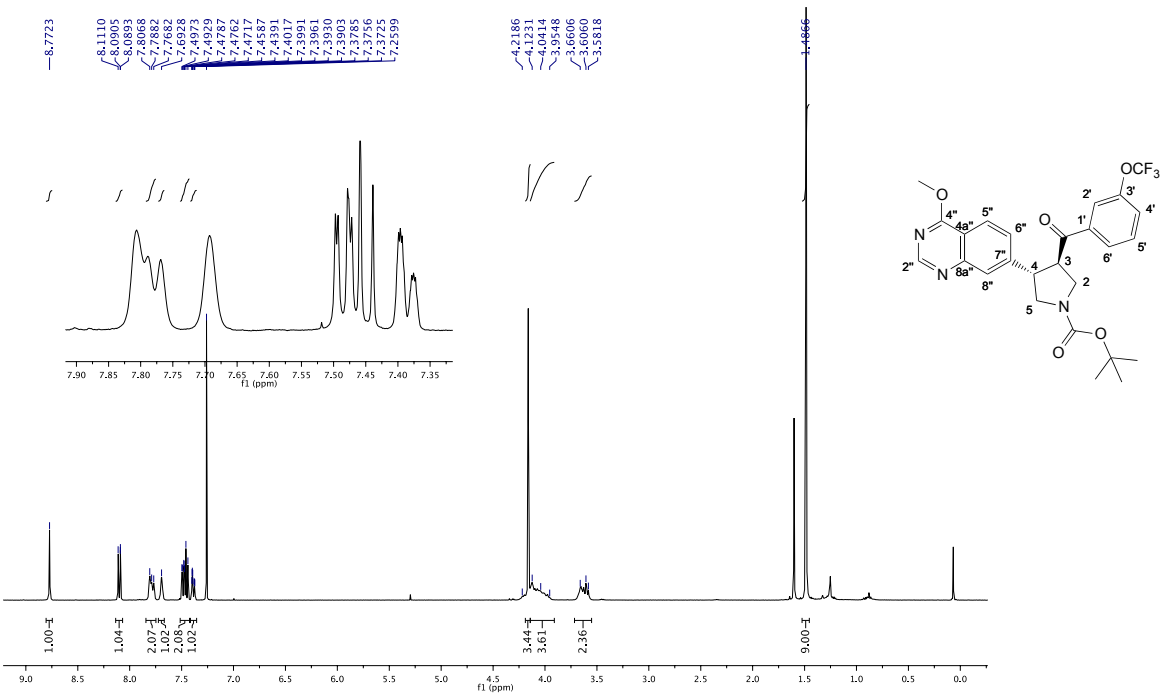

**Figure S119**. $^{13}C$ NMR spectrum of (+)-**13g** in $CDCl_3$, 400 MHz, 298 K.

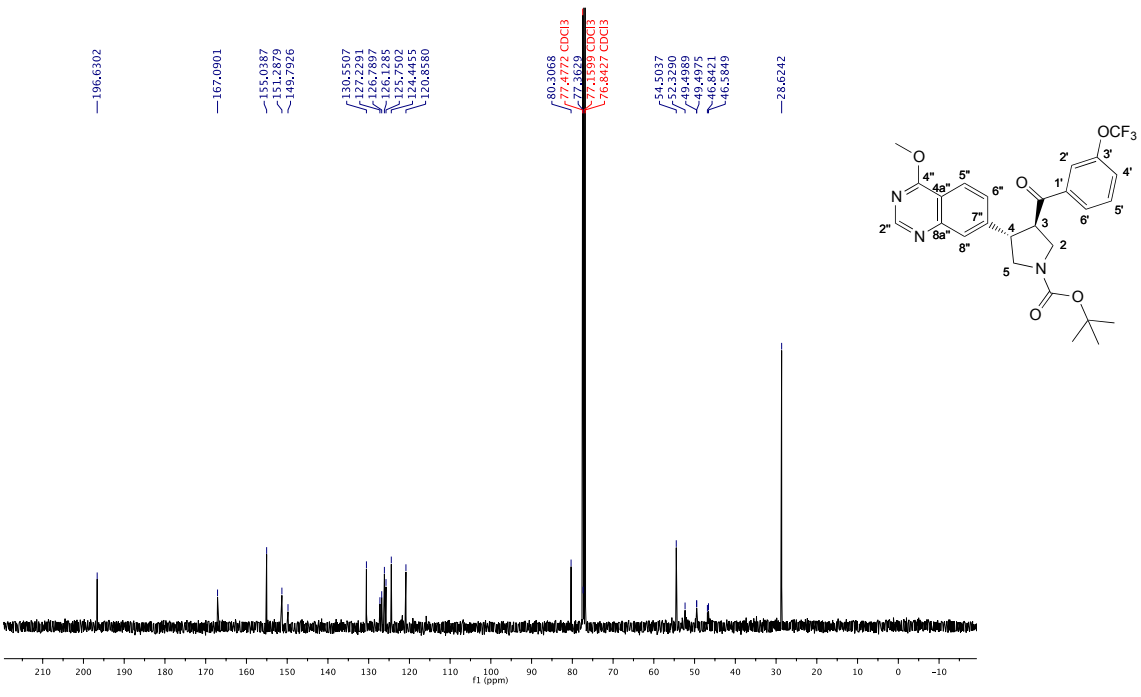

**Figure S120**. $^{13}C$ NMR spectrum of (+)-**13g** in $CDCl_3$, 100 MHz, 298 K.

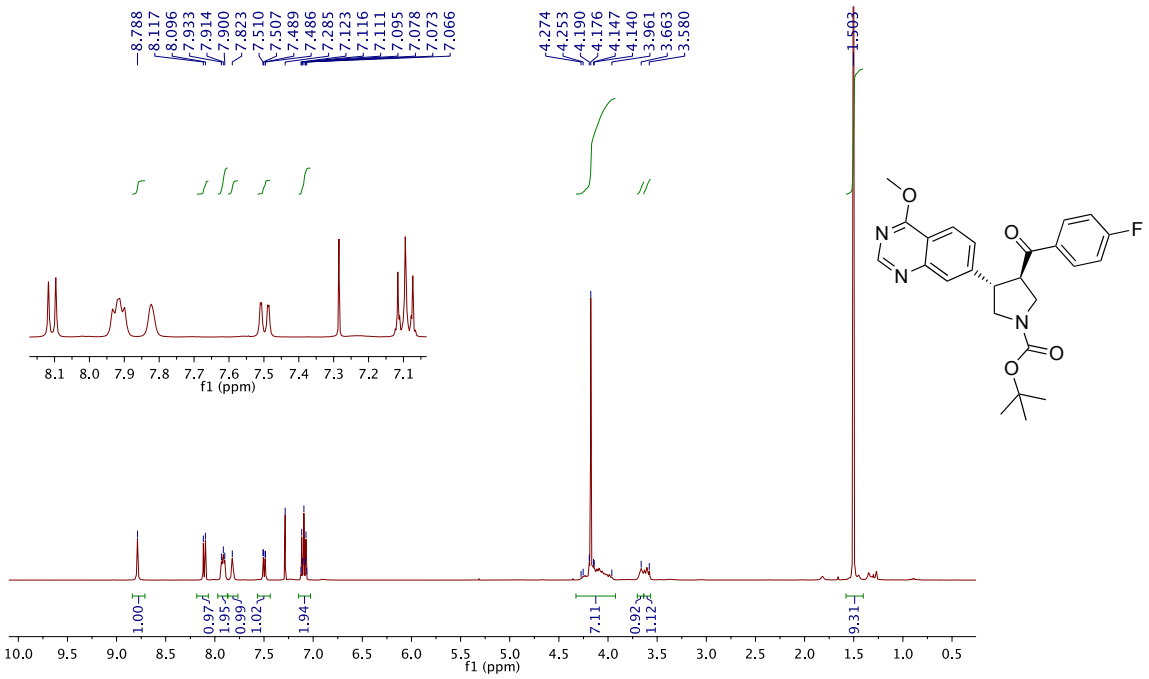

**Figure S121**. $^{1}$H NMR spectrum of **13h** in $CDCl_3$, 400 MHz, 298 K.

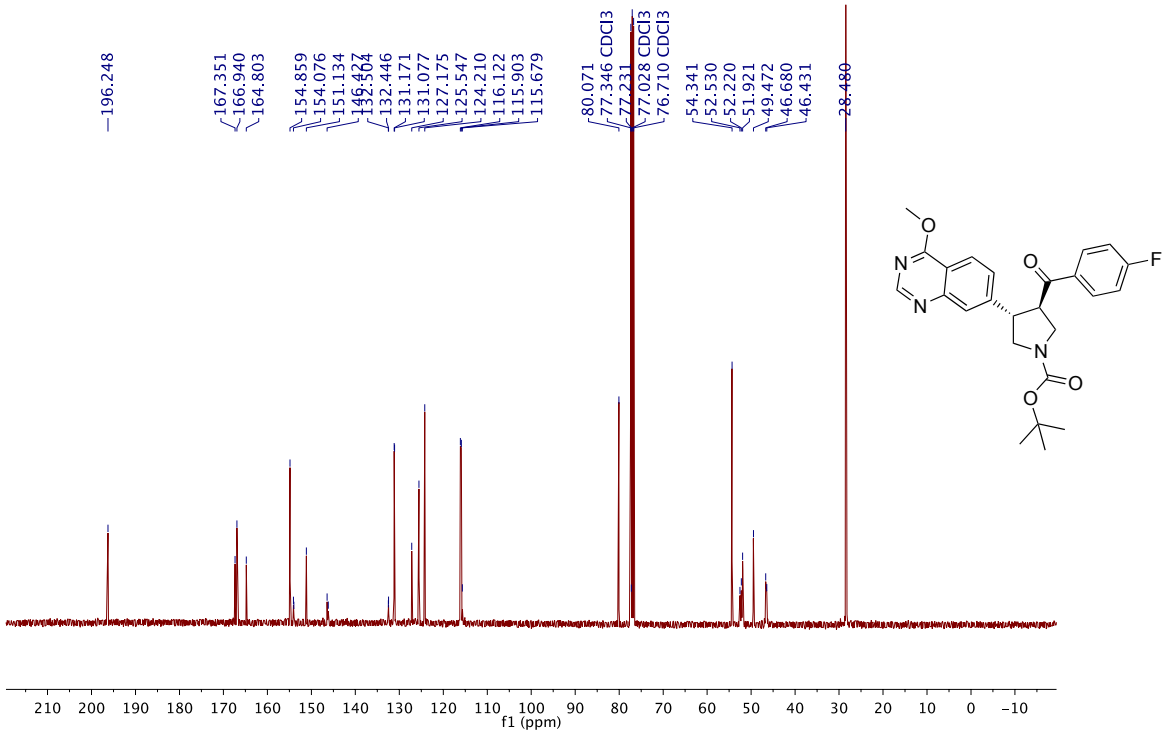

**Figure S122**. $^{13}$C NMR spectrum of **13h** in $CDCl_3$, 100 MHz, 298 K.

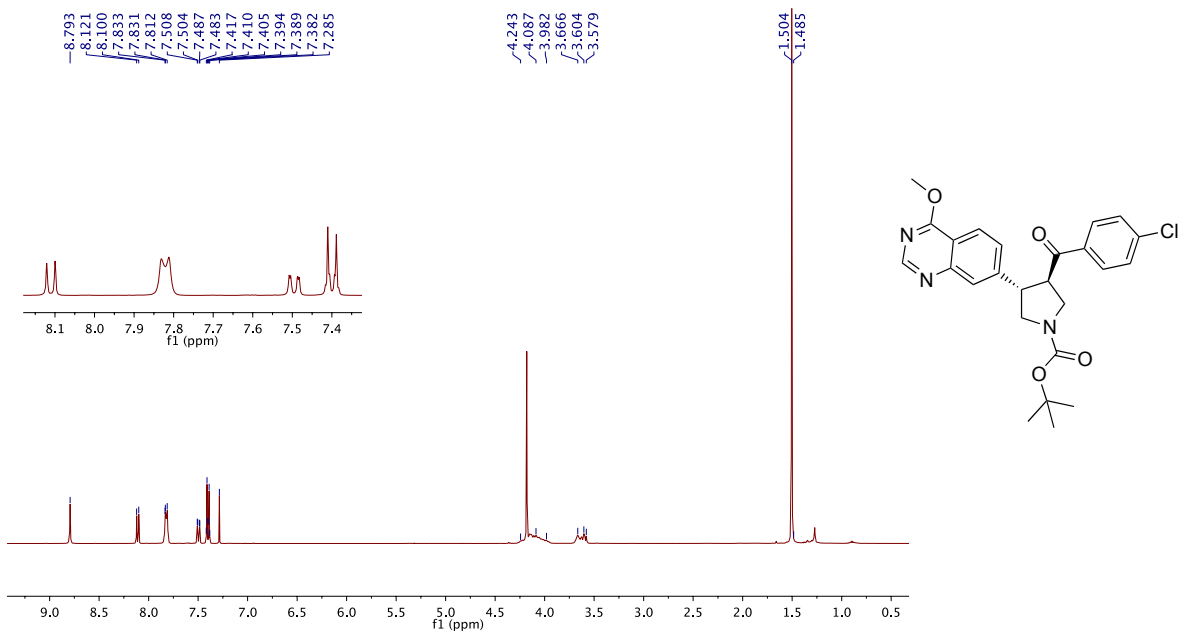


**Figure S123**. $^{1}$H NMR spectrum of (+)-**13i** in $CDCl_3$, 400 MHz, 298 K.

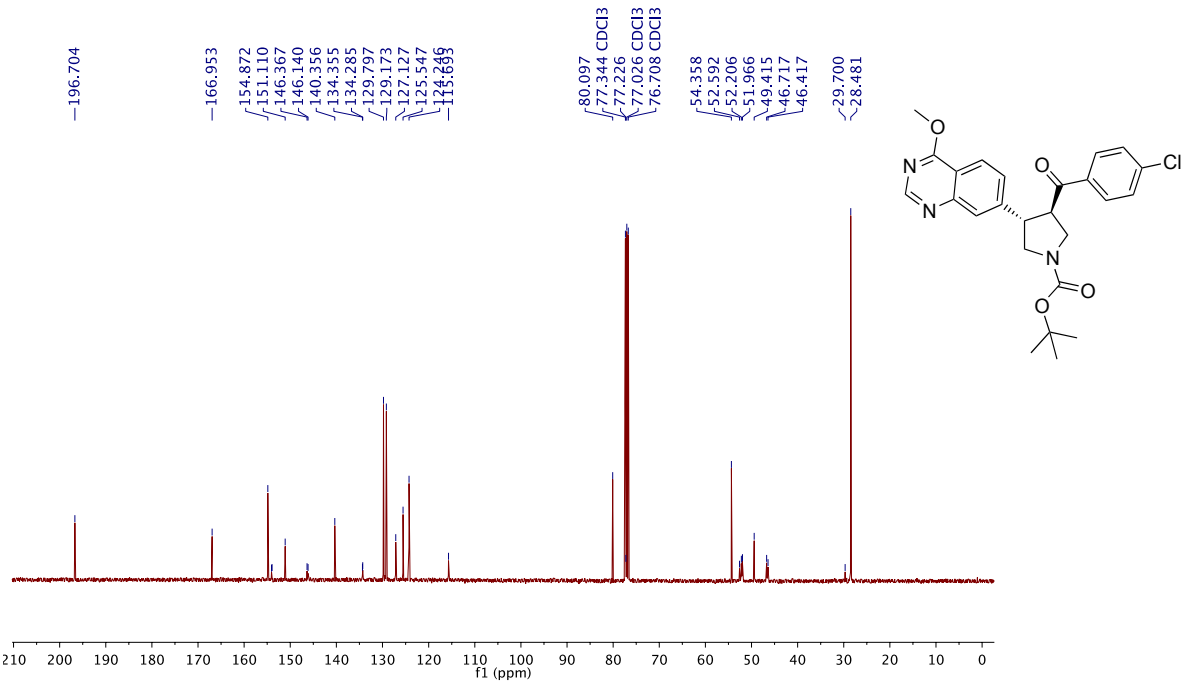


**Figure S124**. $^{13}$C NMR spectrum of (+)-**13i** in $CDCl_3$, 100 MHz, 298 K.

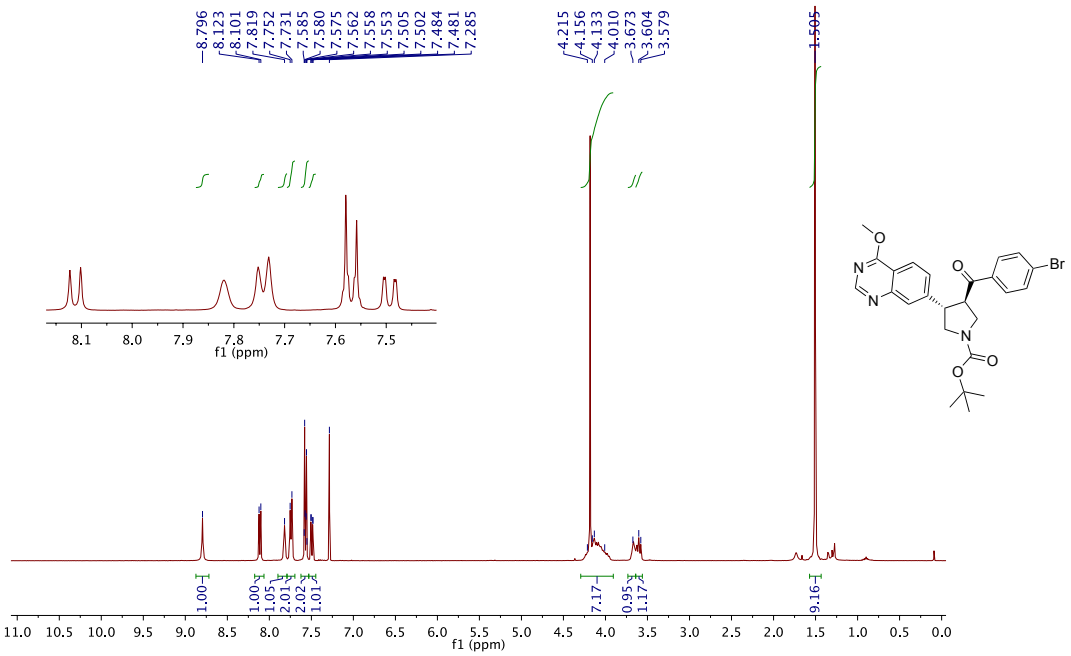


**Figure S125**. $^{1}$H NMR spectrum of (+)-**13j** in $CDCl_3$, 400 MHz, 298 K.

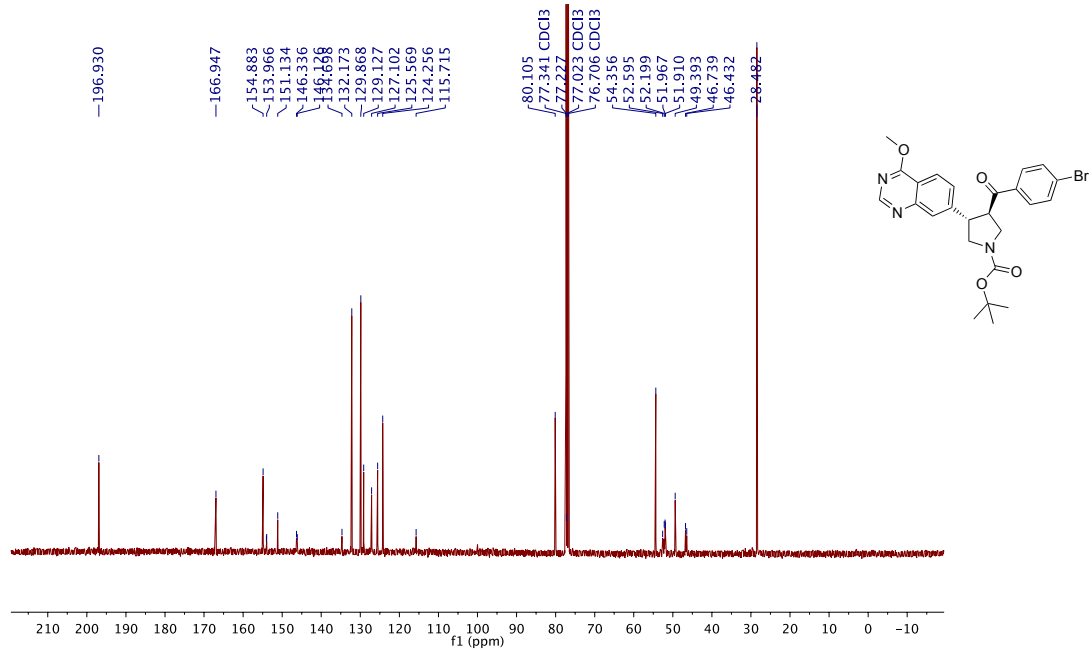


**Figure S126**. $^{13}$C NMR spectrum of (+)-**13j** in $CDCl_3$, 100 MHz, 298 K.

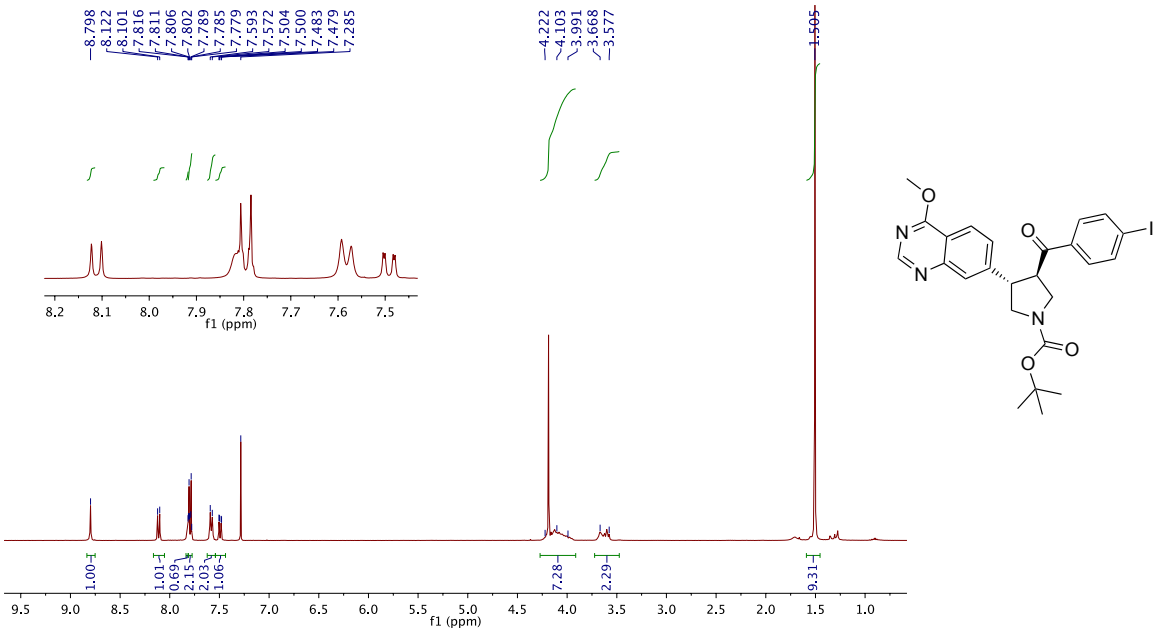

**Figure S127**. $^{1}$HNMR spectrum of (+)-**13k** in $CDCl_3$, 400 MHz, 298 K.

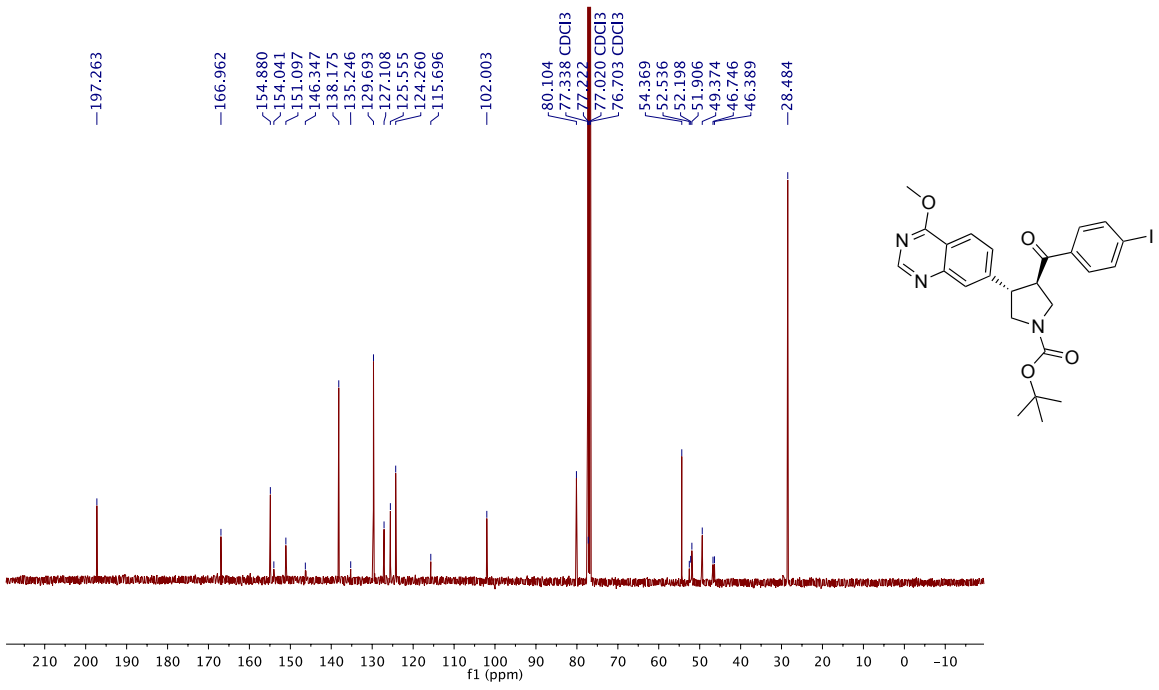

**Figure S128**. $^{13}$C NMR spectrum of (+)-**13k** in $CDCl_3$, 100 MHz, 298 K.

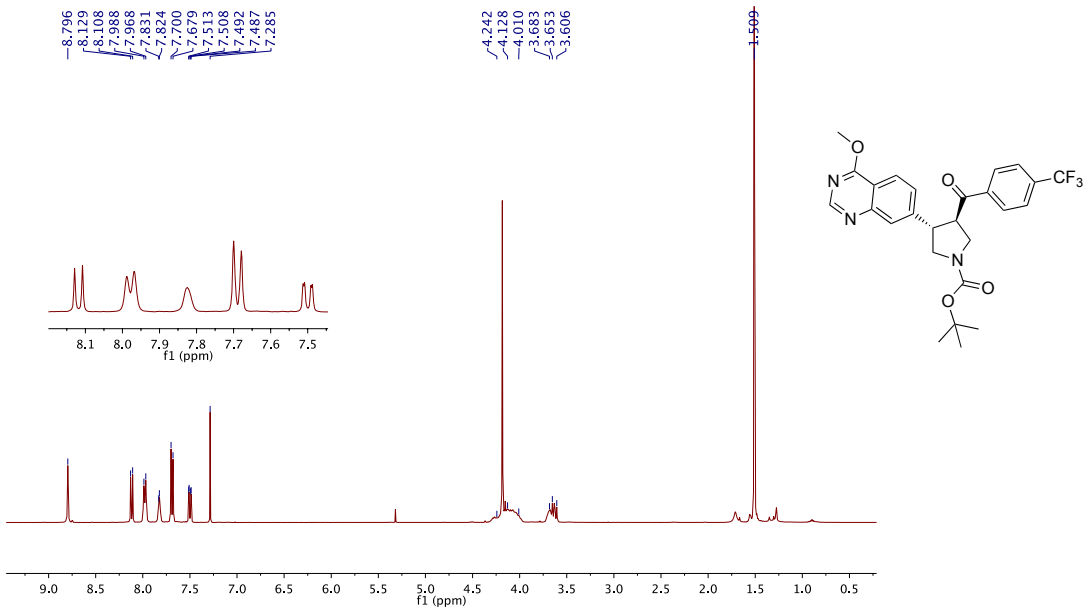


**Figure S129**. $^{1}$H NMR spectrum of (+)-**13l** in $CDCl_3$, 400 MHz, 298 K.

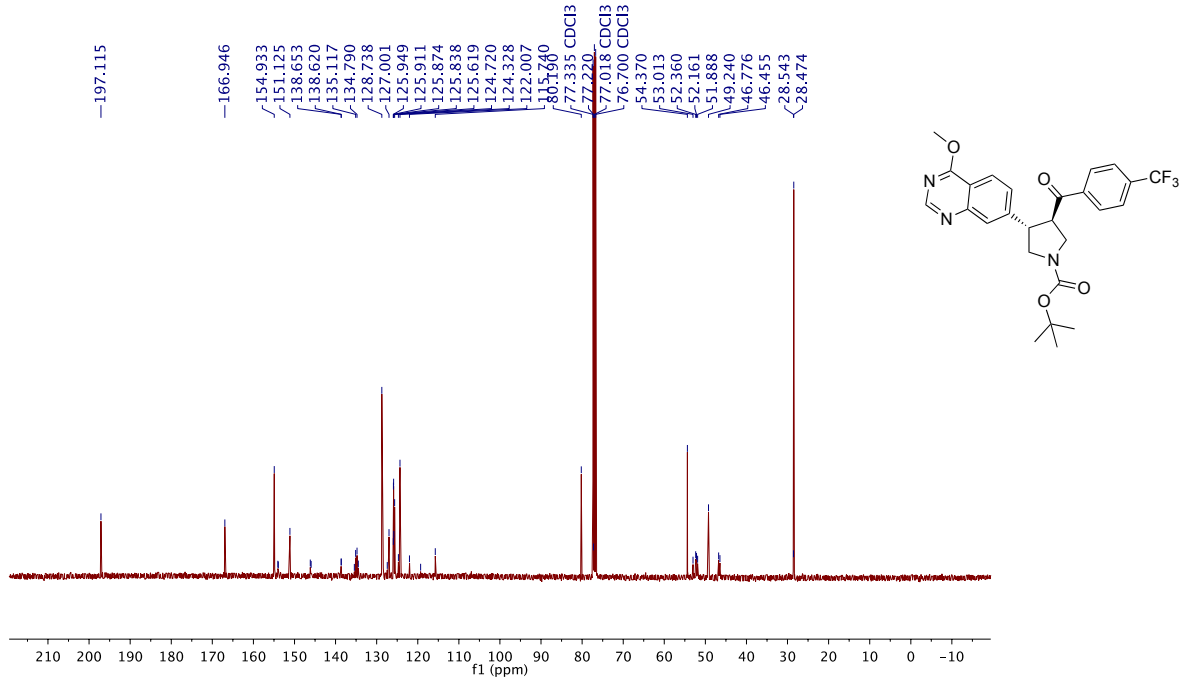


**Figure S130**. $^{13}$C NMR spectrum of (+)-**13l** in $CDCl_3$, 100 MHz, 298 K.

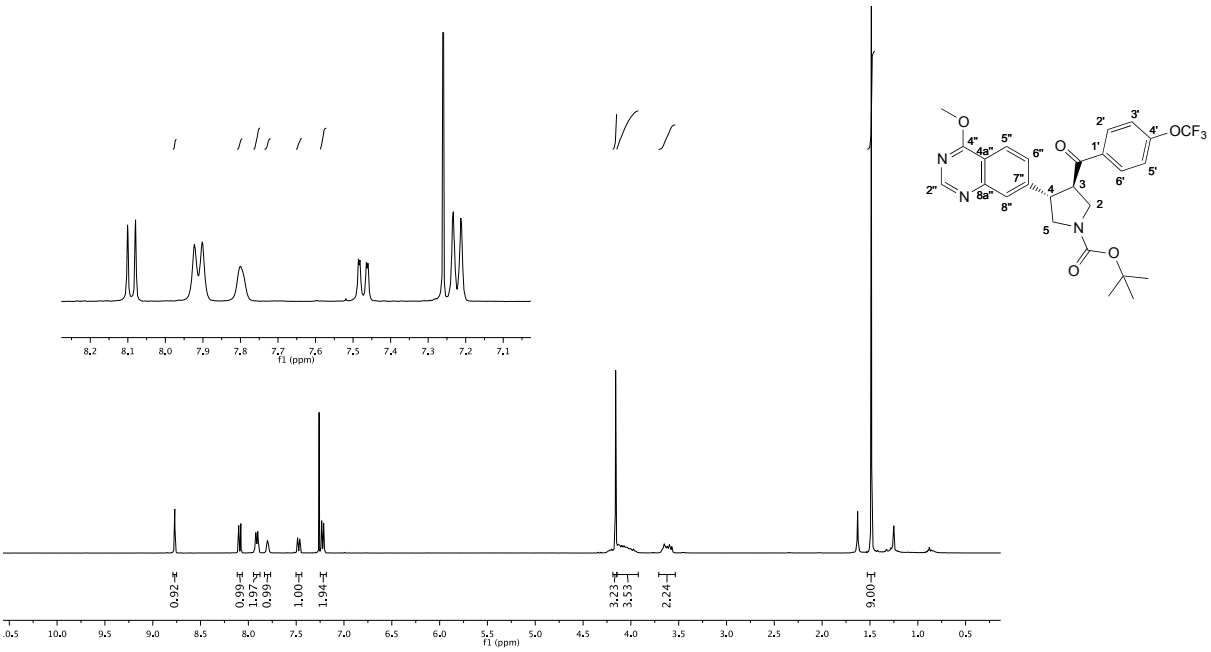

**Figure S131**. $^{1}$H NMR spectrum of (+)-**13m** in $CDCl_3$, 400 MHz, 298 K.

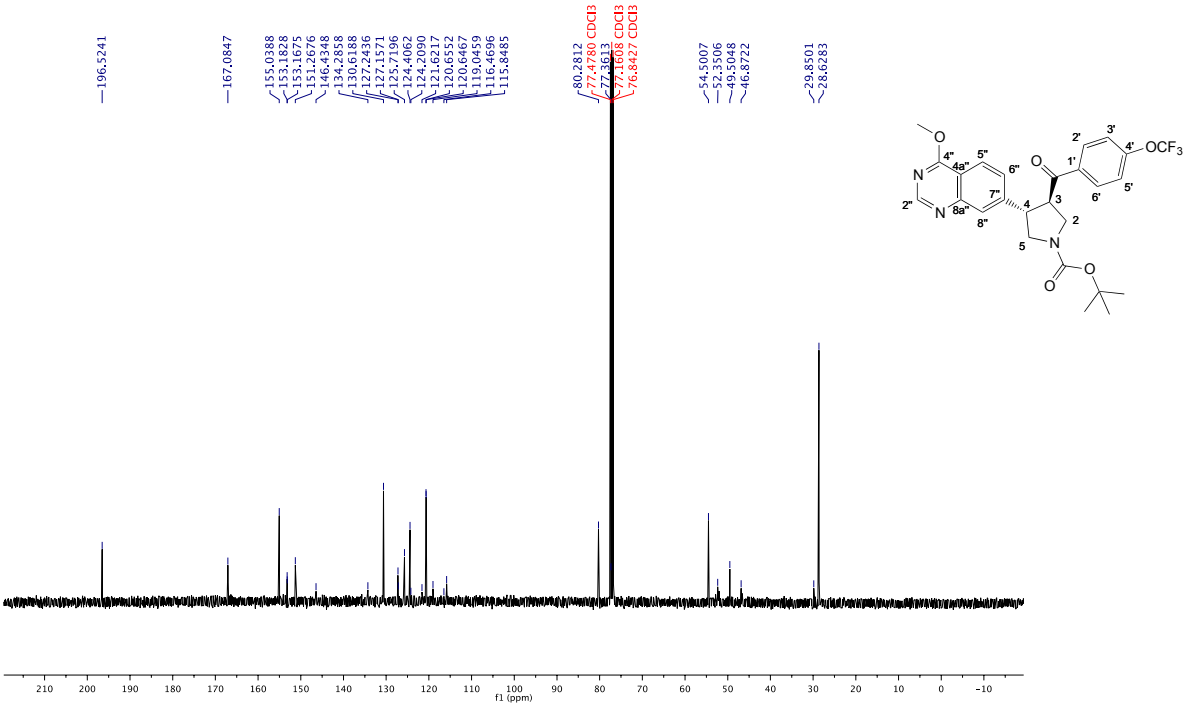

**Figure S131**. $^{13}$C NMR spectrum of (+)-**13m** in $CDCl_3$, 100 MHz, 298 K.

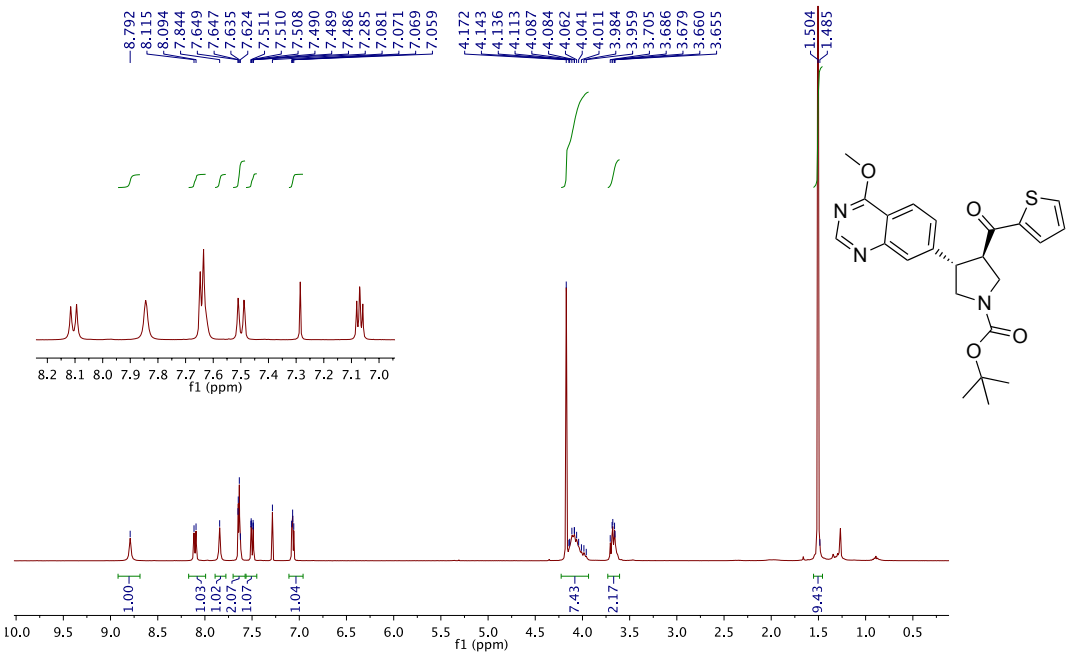

**Figure S132**. $^{1}$H NMR spectrum of (+)-**13n** in $CDCl_3$, 400 MHz, 298 K.

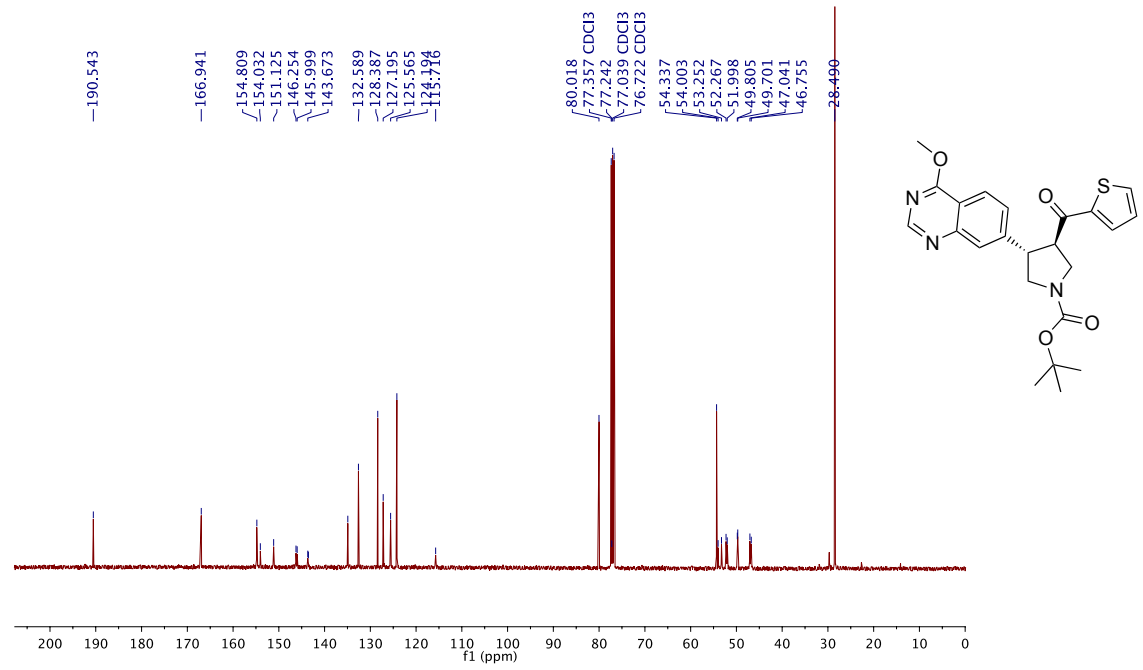

**Figure S133**. $^{13}$C NMR spectrum of (+)-**13n** in $CDCl_3$, 100 MHz, 298 K.

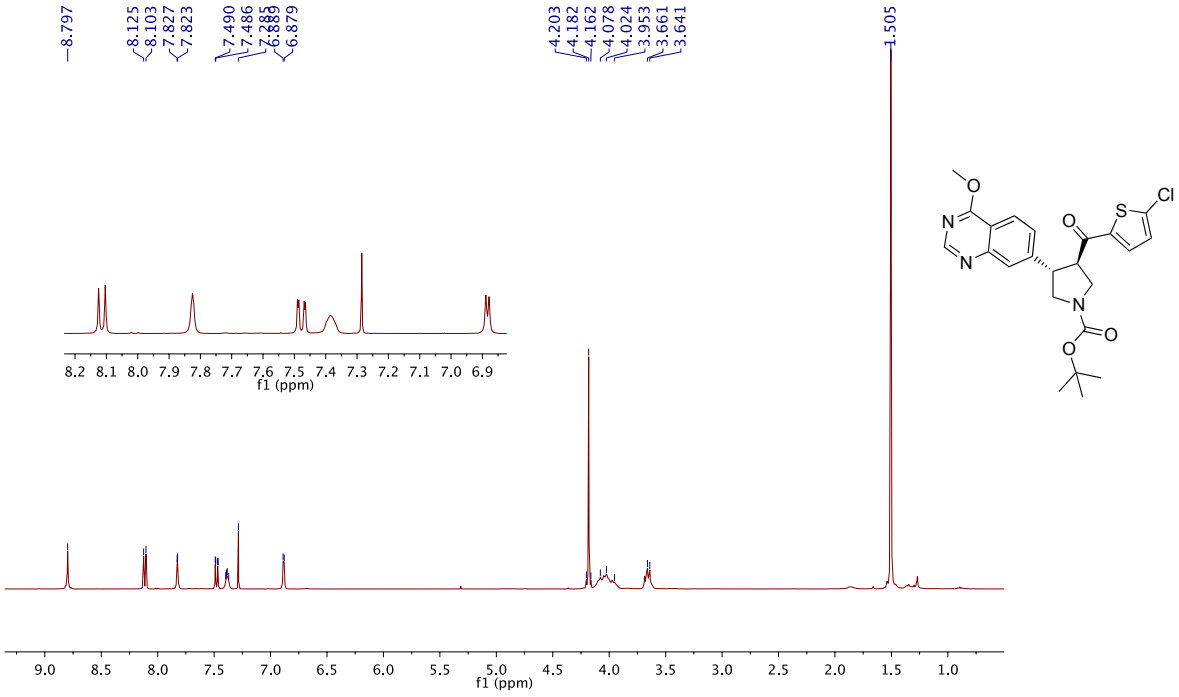


**Figure S134**. $^{1}$H NMR spectrum of (+)-**13o** in $CDCl_3$, 400 MHz, 298 K.

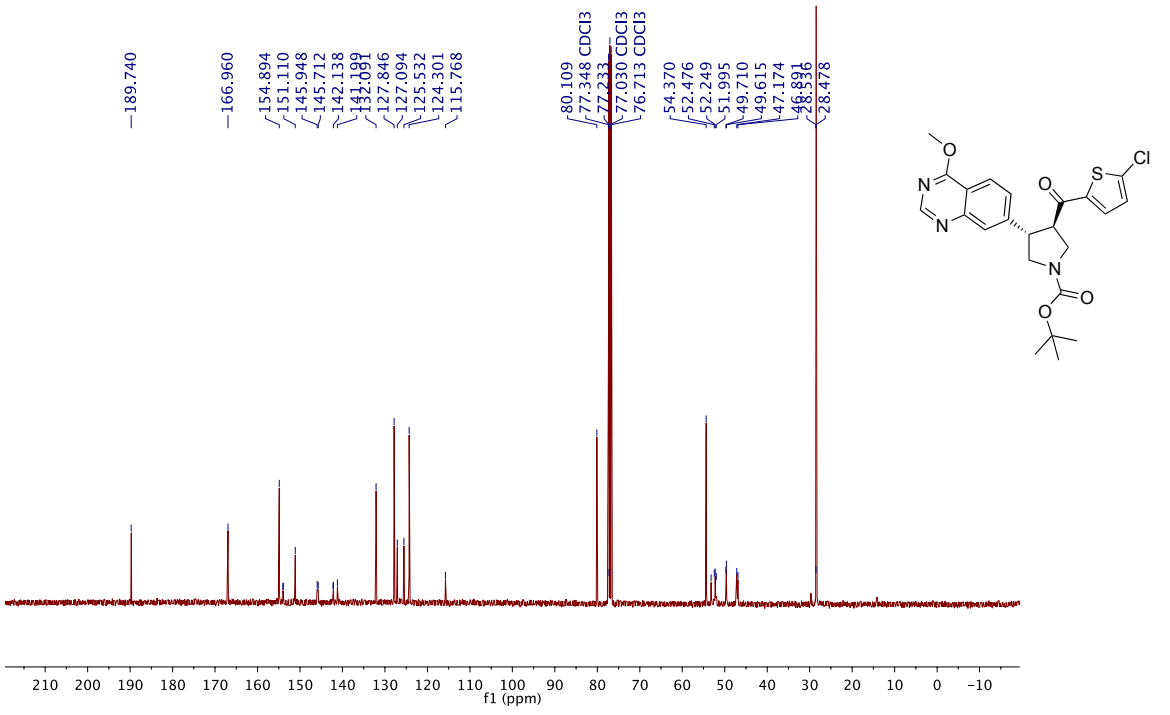


**Figure S135**. $^{13}$C NMR spectrum of (+)-**13o** in $CDCl_3$, 100 MHz, 298 K.

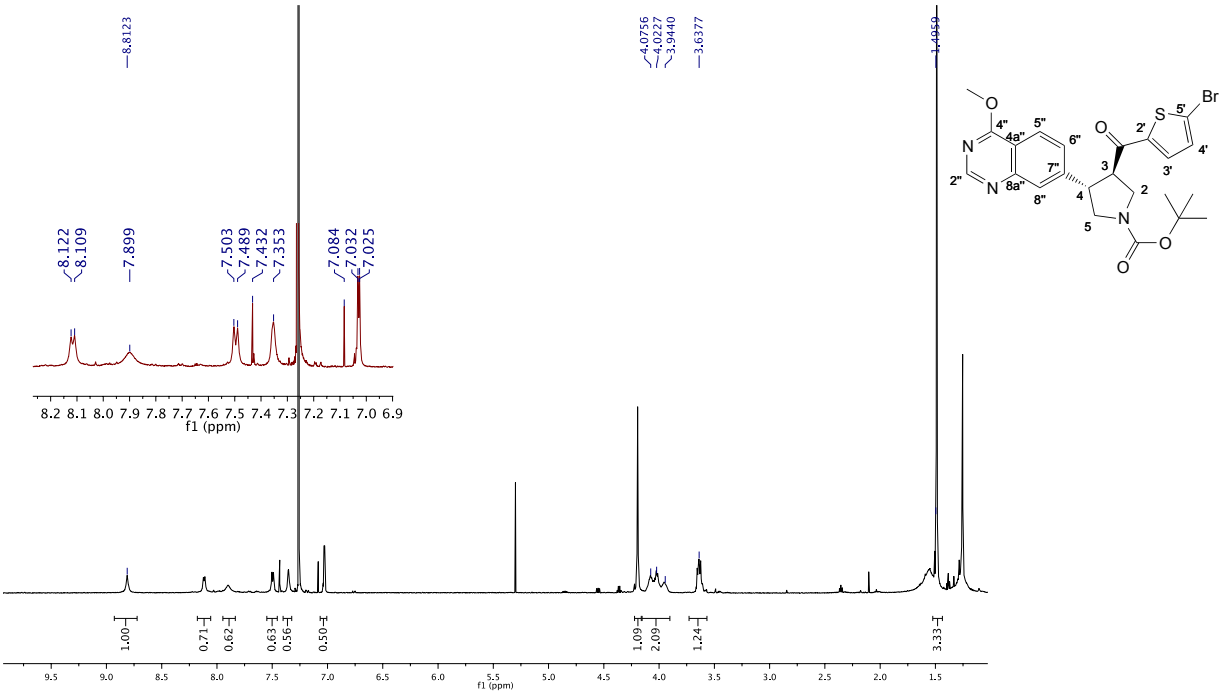


**Figure S136**. $^{1}$H NMR spectrum of (+)-**13p** in $CDCl_3$, 600 MHz, 298 K.

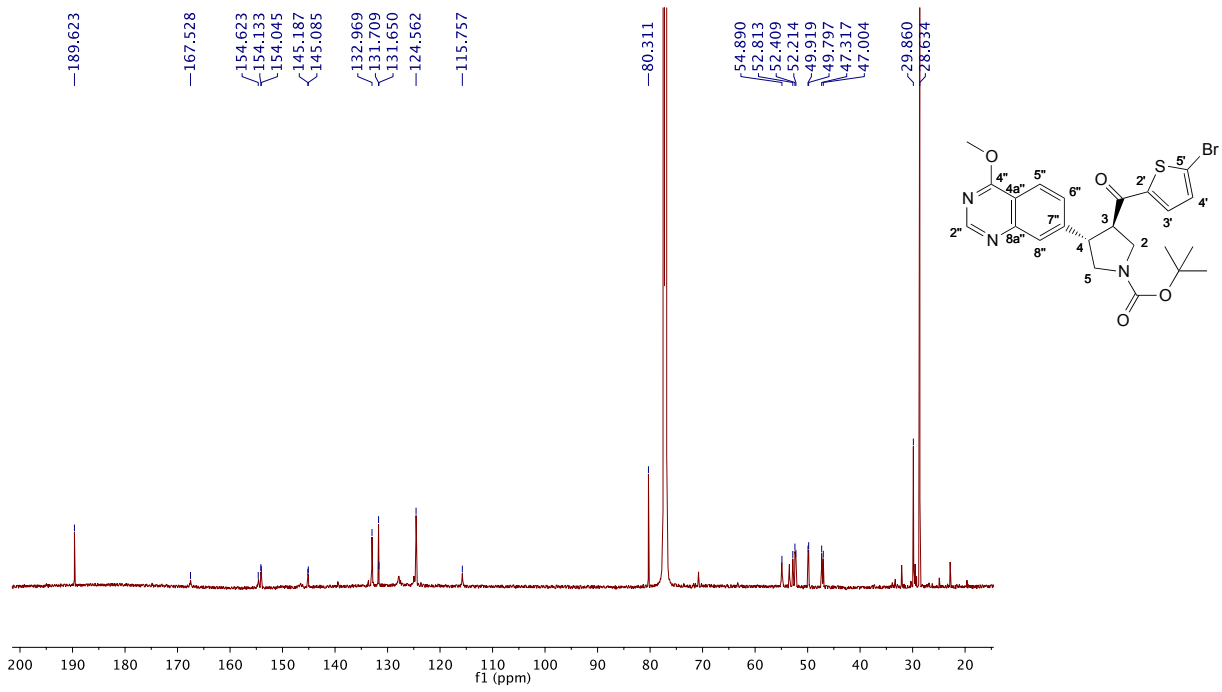


**Figure S137**. $^{13}$C NMR spectrum of (+)-**13p** in $CDCl_3$, 150 MHz, 298 K.

## S7. References


[1] E. Åberg, B. Lund, A. Pflug, O. A. B. S. M. Gani, U. Rothweiler, T. M. de Oliveria, R. A. Engh, *Biol. Chem*. **2012**, *393*, 1121–1129.

[2] D. Bossmeyer, R. A. Engh, V. Kinzel, H. Ponstingl, R. Huber, *EMBO J.* **1993**, *12*, 849–859.

[3] Macromodel, Version 9.7, Schrödinger, LLC, New York, NJ, **2009**.

[4] M. J. Frisch, G. W. Trucks, H. B. Schlegel, G. E. Scuseria, M. A. Robb, J. R. Cheeseman, G. Scalmani, V. Barone, B. Mennucci, G. A. Petersson, H. Nakatsuji, M. Caricato, X. Li, H. P. Hratchian, A. F. Izmaylov, J. Bloino, G. Zheng, J. L. Sonnenberg, M. Hada, M. Ehara, K. Toyota, R. Fukuda, J. Hasegawa, M. Ishida, T. Nakajima, Y. Honda, O. Kitao, H. Nakai, T. Vreven, J. A. Montgomery, Jr., J. E. Peralta, F. Ogliaro, M. Bearpark, J. J. Heyd, E. Brothers, K. N. Kudin, V. N. Staroverov, R. Kobayashi, J. Normand, K. Raghavachari, A. Rendell, J. C. Burant, S. S. Iyengar, J. Tomasi, M. Cossi, N. Rega, J. M. Millam, M. Klene, J. E. Knox, J. B. Cross, V. Bakken, C. Adamo, J. Jaramillo, R. Gomperts, R. E. Stratmann, O. Yazyev, A. J. Austin, R. Cammi, C. Pomelli, J. W. Ochterski, R. L. Martin, K. Morokuma, V. G. Zakrzewski, G. A. Voth, P. Salvador, J. J. Dannenberg, S. Dapprich, A. D. Daniels, Ö. Farkas, J. B. Foresman, J. V. Ortiz, J. Cioslowski, and D. J. Fox, Gaussian 09, Revision A.1; Gaussian, Inc.: Wallingford, CT, **2009**.

[5] S. Grimme, J. Antony, S. Ehrlich, H. Krieg, *J. Chem. Phys*. **2010**, *132,* 154104-01–154104-19.

[6] B. Kuhn, J. E. Fuchs, M. Reutlinger, M. Stahl, N. R. Taylor, *J. Chem. Inf. Model.* **2011**, *51*, 3180–3198.

[7] Madhusudan, E. A. Trafny, N.-H. Xuong, J. A. Adams, L. F. Ten Eyck, S. S. Taylor, J. M. Sowadski, *Protein Science* **1994**, *3*, 176–187.

[8] C. Breitenlechner, M. Gassel, H. Hidaka, V. Kinzel, R. Huber, R. A. Engh, D. Bossemeyer, *Structure* **2003**, *11*, 1595–1607.

[9] R. A. Engh, A. Girod, V. Kinzel, R. Huber, D. Bossemeyer, *J. Biol. Chem.* **1996**, *271*, 26157–26164.

[10] I. Collins, J. Caldwell, T. Fonseca, A. Donald, V. Bavetsias, L.-J. K. Hunter, M. D. Garrett, M. G. Rowlands, G. W. Aherne, T. G. Davies, V. Berdini, S. J. Woodhead, D. Davis, L. C. A. Seavers, P. G. Wyatt, P. Workman, E. McDonald, *Bioorg. Med. Chem*. **2006**, *14*, 1255–1273.

[11] A. Donald, T. McHardy, M. G. Rowlands, L.-J. K. Hunter, T. G. Davies, V. Berdini, R. G. Boyle, G. W. Aherne, M. D. Garrett, I. Collins, *J. Med. Chem*. **2007**, *50*, 2289–2292.

[12] G. Saxty, S. J. Woodhead, V. Berdini, T. G. Davies, M. L. Verdonk, P. G. Wyatt, R. G. Boyle, D. Barford, R. Downham, M. D. Garrett, R. A. Carr, *J. Med. Chem*. **2007**, *50*, 2293–2296.

[13] J. S. Ahn, M. L. Radhakrishnan, M. Mapelli, S. Choi, B. Tidor, G. D. Cuny, A. Musacchio, L.-A. Yeh, K. S. Kosik, *Chem. & Biol*. **2005**, *12*, 811–823.

[14] J. J. Caldwell, T. G. Davies, A. Donald, T. McHardy, M. G. Rowlands, G. W. Aherne, L. K. Hunter, K. Taylor, R. Ruddle, F. I. Raynaud, M. Verdonk, P. Workman, M. D. Garrett, I. Collins, *J. Med. Chem.* **2008**, *51*, 2147–2157.

[15] T. A. Yap, M. I. Walton, K. M. Grimshaw, R. H. te Poele, P. D. Eve, M. R. Valenti, A. K. de Haven Brandon, V. Martins, A. Zetterlund, S. P. Heaton, K. Heinzmann, P. S. Jones, R. E. Feltell, M. Reule, S. J. Woodhead, T. G. Davies, J. F. Lyons, F. I. Raynaud, S. A. Eccles, P. Workman, N. T. Thompson, M. D. Garrett, *Clin. Cancer. Res*. **2012**, *18*, 3912–3923.

[16] P. F. Cook, M. E. Neville Jr., K. E. Vrana, E. Kent, F. T. Hartl, R. Roskoski Jr., *Biochemistry* **1982**, *21*, 5794–5799.

[17] Y.-C Cheng, W. H Prusoff, *Biochem. Pharmacol.* **1973**, *22*, 3099–3108.

[18] M. Gaßel, C. B. Breitenlechner, P. Rüger, U. Jucknischke, T. Schneider, R. Huber, D. Bossemeyer, R. A. Engh, *J. Mol. Biol.* **2003**, 329, 1021–1034.

[19] W. Kabsch, *J. Appl. Crystallogr.* **1993**, *26*, 795–800.

[20] A. G. W. Leslie, *Protein Crystallogr.* **1992**, *26*, 27–33.

[21] P. D. Adams, P. V. Afonine, G. Bunkoczi, V. B. Chen, I. W. Davis, N. Echols, J. J. Headd, L. W. Hung, G. J. Kapral, R. W. Grosse-Kunstleve, A. J. McCoy, N. W. Moriarty, R. Oeffner, R. J. Read, D. C. Richardson, J. S. Richardson, T. C. Terwilliger, P.H. Zwart. *Acta Cryst.* **2010**, *D66*, 213–221.

[22] A. W. Schüttelkopf, D. M. F van Aalten, *Acta Crystallogr. Sect. D: Biol. Crystallogr*. **2004**, *60*, 1355–1363.

[23] B. R. Baker, R. E. Schaub, J. P. Joseph, F. J. McEvoy, J. H. Williams, *J. Org. Chem.* **1952**, *17*, 149–156.